CARDE TECHNICAL LETTER 1122/58

DSI Release No. 1077

Copy No. 21

SIXTH PROGRESS REPORT

ON

CF-105 WEAPON SYSTEM ASSESSMENT

Compiled by C. J. Wilson

DEFENCE RESEARCH BOARD

CANADIAN ARMAMENT RESEARCH AND DEVELOPMENT ESTABLISHMENT

VALCARTIER, QUEBEC

APRIL, 1958

58-06948
#303331

Technical Letter No. 1122/58

P.C.C. No. D46-97-36-21

UNCLASSIFIED

PROJECT
CF-105 ASSESSMENT

SIXTH PROGRESS REPORT

Period 1 Jan. 1958 to 31 March 1958

Compiled by

C.J. Wilson

CANADIAN ARMAMENT RESEARCH AND DEVELOPMENT ESTABLISHMENT

VALCARTIER, QUE.

APRIL, 1958.

SUMMARY

This technical letter is a progress report on work at CARDE in connection with the CF-105 Weapon System Assessment, recording work done in the final period of the study, January to March 1958.

Further REAC computation has produced placement charts for the interceptor when using infra-red guidance and when carrying infra-red guided missiles. More effort has been directed to methods of homing when the A.I. is jammed. The results of these studies are given in undigested form.

Less detailed work on some other topics is included here for completeness in reporting.

The final report on the complete study is being actively prepared.

<u>TABLE OF CONTENTS</u>

<u>APPENDICES</u>

SIXTH PROGRESS REPORT

on

CF 105 WEAPON SYSTEM ASSESSMENT

1.0 INTRODUCTION

The engagement of high speed targets by supersonic interceptors armed with air-to-air missiles introduces a variety of new problems which cannot be assessed by extrapolation of data arising from experience with conventionally armed subsonic aircraft.

For this reason, CARDE has been requested by the RCAF to carry out an evaluation study of the effectiveness of a supersonic interceptor weapon system based on the AVRO CF-105 aircraft armed with Sparrow II or Sparrow III air-to-air missiles.

The primary objectives of the study as stated by the RCAF are:

(i) To evaluate the combat effectiveness of the system with different types of armament, beginning with the Sparrow series, for probable bomber threats including the Bison, Badger and Bear.

(ii) To investigate the effect of variation in fire control parameters such as A.I. radar range and look angle.

(iii) To establish the minimum acceptable level of aerodynamic performance and to investigate the effect of possible design changes in the aircraft and engine parameters, insofar as these changes affect combat performance.

(iv) To determine the effect of variations in G.C.I. placement accuracy.

(v) To explore possible tactics and suggest optimum modes of attack.

In order to arrive at an accurate assessment of the overall combat effectiveness of this weapon system, the many inter-dependent sub-systems of which it is composed require analysis, first individually and then collectively, so that the relative importance of the principal parameters can be established. Naturally, an exploratory study of this nature is quite involved and certainly time-consuming, if it is to be sufficiently exhaustive to achieve the above-stated objectives. Further, the task is rendered difficult in that very little primary information is available on which to base investigations, as it is evident that the establishment of such data is perhaps the primary object of the study.

The general approach then has been to adopt a range of parameters which should encompass final characteristics, then to conduct an analysis based on these and thus establish their validity and importance in the particular sub-system, as well as their influence on the effectiveness of the system as a whole. In this way overall effectiveness can be established as a function of the parameters of individual sub-systems and optimum design values indicated.

Although this method is elongated and somewhat tedious, an important compensatory feature lies in the fact that the most critical areas requiring further study are highlighted.

2.0 PROGRESS OF STUDY

CARDE Technical Letter N-47-3, May 1956, gives a review of the general interceptor-weapon problem with particular reference to the proposed CF-105 system, and sets out in some detail a proposal for the prosecution of studies to attain the objectives enumerated by the RCAF. Progress of the work is detailed in CARDE Technical Letters N-47-8, N-47-12, N-47-18, 1012/57 and 1091/58. Digests of the results, written at the ends of the first and second years respectively, are contained in CARDE Technical Memoranda 150/57 and 183/58.

The work has now been terminated and only a final report remains to be completed. This is the last progress report and it is published in order to include a full record of the work up to the end of the study. More raw data on placement studies and minimum information studies are included together with some reviews of particular problems which have been considered.

3.0 EFFORT ALLOTTED TO THE STUDY

The work has been carried out by specialist sections within the Wings of CARDE, under the coordination and direction of the Systems Group, which has been generally responsible for the task.

During the period under review, a total of eight professional personnel have been engaged in the programme. The degree of participation, including contractors' personnel, was as follows:-

	Full Time	Part Time
Systems Group	1	2
"G" Wing	5	3
TOTAL	6	5

The number of contractors' personnel employed on the project has been diminishing since 1st. January. All but one had left by 1st April; he will leave by 1st. May.

4.0 **ACTIVITIES** - January - March 1958.

4.1 General

The placement study work has been continued. Study of the interceptor in an E.C.M. free environment with A.I. radar and radar guided missiles fully effective had been completed in the previous quarter. The work reported here has its emphasis almost completely on methods of overcoming E.C.M., including infra-red guidance for both the interceptor and its missiles and a number of homing-on-the-jammer navigational modes.

4.2 Placement Studies

The kinematic aspects of interceptor placement and fire control have been covered by a series of placement studies. Appendix 'A' includes the basic information on all those studies not previously reported and forms an extension of the programme outlined on pages 14 and 15 of CARDE Technical Letter 1012/57. The extension was suggested by the earlier results. It is now possible to comment on the supplementary infra-red guidance for the CF-105, on placement limitations which might occur with infra-red guided missiles and on the look-angle limitations with both radar and infra-red interceptor guidance.

Appendix 'F' reports on improvements in placement probabilities which might be achieved with coordinated interceptors attacking one target. There appears to be an advantage when a high-speed target manoeuvres to evade interceptions but this may be counter-balanced by the difficulties of interceptor coordination in practice.

4.3 Minimum Information Studies

Navigational methods proposed for homing against jamming were described in CARDE Technical Letter 1091/58, Appendix 'B'. Results obtained from study of these methods are published in Appendix 'B' of this report and indicate how successful the various modes can be.

Appendix 'G' describes additional studies of methods of range finding in jamming designed to be accurate enough for launching guided missiles.

4.4 Other Fire Control Studies.

Some fire control problems were detailed in Appendix 'B', page 39, of Technical Letter 1012/57. Three of these problems have received some consideration and reports are given here, viz. Appendix 'C' on Launch Zones, Appendix 'D' on Snap-up Attacks and Appendix 'E' on Navigation Towards a Favoured Aspect.

5.0 CONCLUSIONS FROM THE STUDY

No attempt has been made to draw conclusions here. The reader is referred to CARDE Technical Memorandum 183/58 "The CF-105 Assessment Study, Summary Report II", published in March 1958, for conclusions made from the study and to the forthcoming final report on the study.

APPENDIX 'A'

FURTHER RESULTS OF THE THREE DIMENSIONAL PLACEMENT STUDY

by D.R. Tait

1.0 INTRODUCTION

The scheduled work on the three dimensional REAC simulation of the CF 105 Interceptions was completed in 1957. (refs. 1, 2, 3, 4, 5) The results of this study indicated that further work should be done if time was available and it was felt that some side issues not included in the original study should be investigated. The report describes some of the additional work which was done.

In conducting the REAC study some factors which influence the success of the Weapon System were observed. Some of these which have not been discussed in previous progress reports are included below.

2.0 SOME SYSTEM RECOMMENDATIONS

2.1 The IR Subsystem

The infrared subsystem has been incorporated into the Arrow fire control system to overcome ECM and possible failure of the AI radar or computer. The primary performance requirement is the long range detection and subsequent interception of enemy targets from frontal aspects. (ref. 6) In the forward hemisphere supersonic targets (M2.0) may be expected to yield acquisition ranges comparable with the radar except for a small range of aspects within 10° of the nose of the target. Subsonic targets such as the Bison (type 37), may give acquisition ranges of the order of 1/4 of this. (see fig. 1).

The arbitrary situation of the IR seeker on the tail of the fighter makes the IR subsystem quite ineffective against a moderately intelligent target.

Consider the case where the CF 105 has established lock-on and is homing onto the target flying a lead collision course. If the target commences to evade with a given load factor turn, the CF 105 must maneuver with the same load factor turn to keep on course. A target having similar aerodynamic characteristics to the CF 105 will be able to sustain a 3 g turn at 40,000 feet without deceleration. If it maneuvers to reduce the fighter aspect - i.e. turns away from the fighter, the target will be obscured by the interceptor wings as soon as the lead angle reaches 8°. For a 2 g target turn, the interceptor loses the target as soon as the lead angle reaches 21°. (see fig. 2). The target has 100% probability of escape.

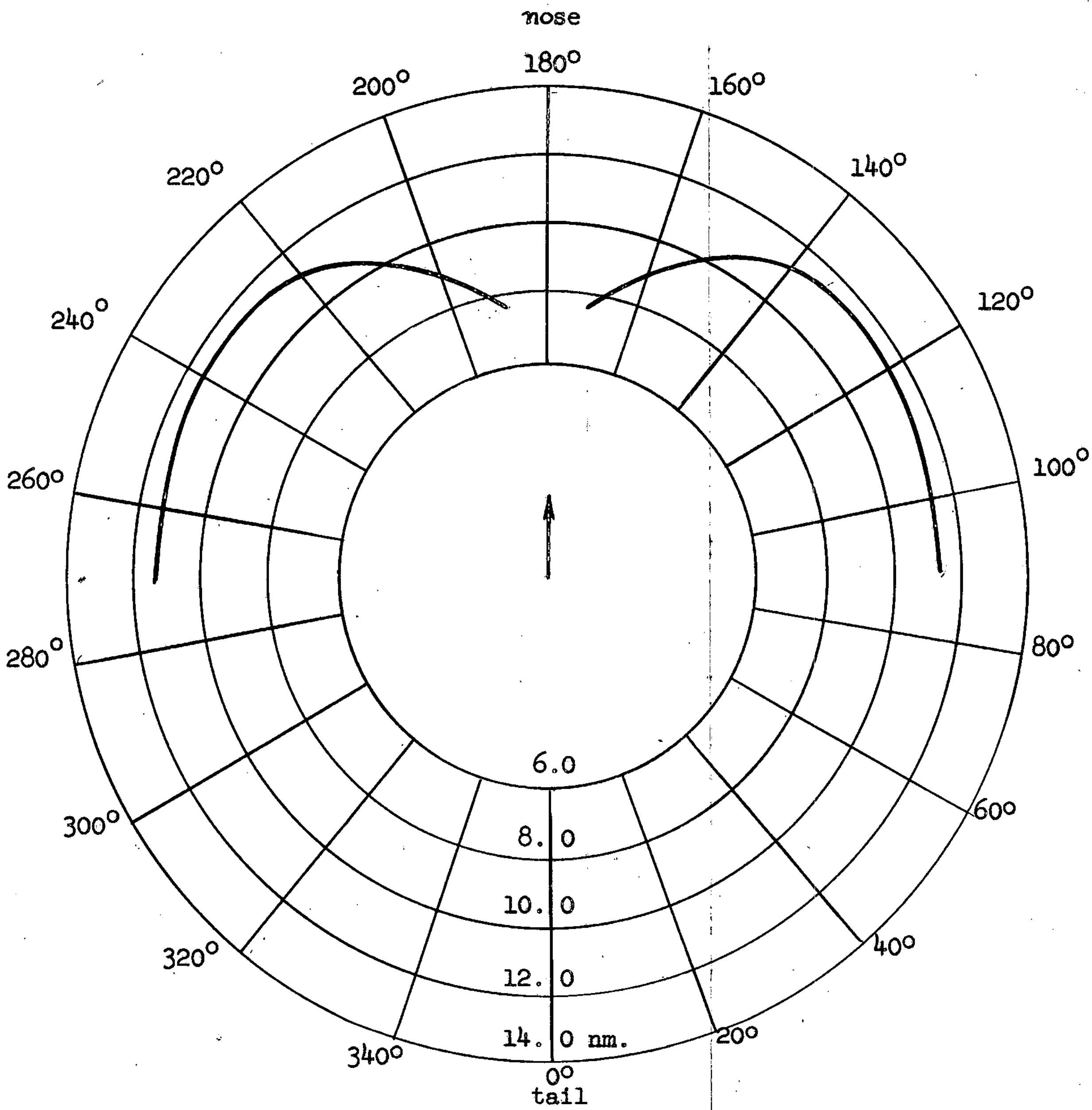

IR DETECTION CONTOUR FOR B-52

FORWARD HEMISPHERE

Figure 1

Figure 2

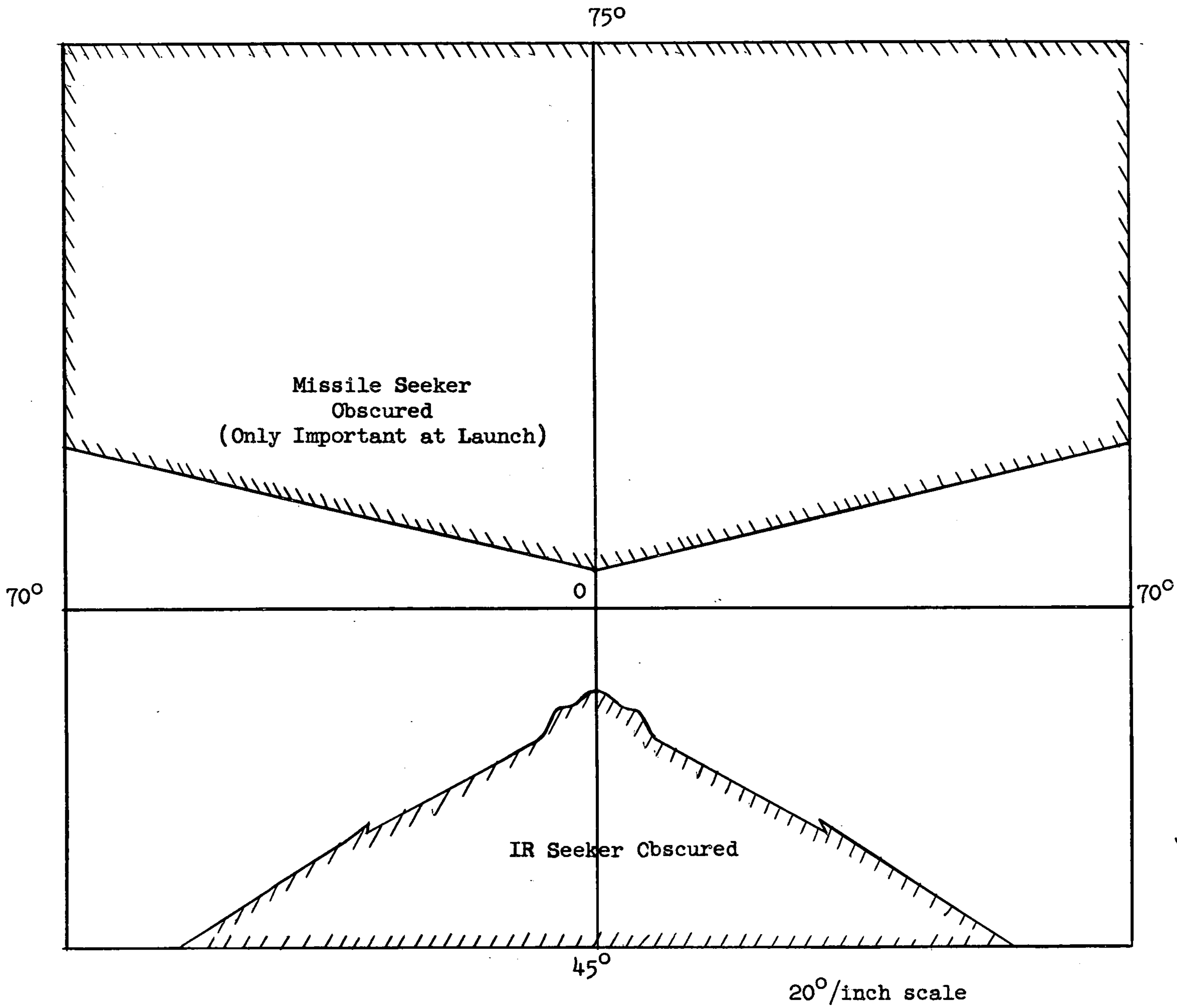

APPROXIMATE FIELD OF VIEW FOR IR AI - TAIL INSTALLATION

The same objection applies to the retractible chin installation except that here the interceptor will also be unable to detect targets more than 12^{o} above the boresight - a height difference of some 10 K feet for an acquisition range of 50 K feet.

In this case the optimum target maneuver is to turn towards the interceptor. For a 2 g turn the target escapes if the lead angle equals 30^{o}. However, the lead angle will be decreasing so that the interceptor tactics can be modified to make this interception successful. A suitable technique would be to restrict the interceptor bank angle temporarily so that the interceptor drifts off course until the lead angle is sufficiently small that it can bank steeply without losing the target. This maneuver sequence unfortunately assists the target in another direction by maneuvering the interceptor into a region of minimum acquisition range. The chin installation would probably be less effective in a close combat, than the tail situation.

If the IR subsystem is to function efficiently the location of the seeker must be altered or else two coordinated seeker heads should be employed.

2.2 The AI Radar

In the study using the AI radar the arbitrary division of the available elevation gimbal deflection into -45^{o} and $+75^{o}$ is the largest single cause of reduced placement probability in the interception of supersonic targets. For initial course differences near 180^{o} this reduction is slight but for smaller course differences it is significant.

The illustrative example which RCA use to justify the system when analysed in greater detail demonstrates the way in which the probability is reduced.

The situation is postulated where ideal lead angle $= 50^{o}$ and actual lead angle $= 30^{o}$. Suppose it refers to a M2.0 fighter intercepting a target at an altitude 50,000 feet from an initial range of 100 K feet. Detailed point by point calculation of the trajectories shows that the interceptor loses the target 2 seconds after lock-on. In this time the lead angle increases to 37.3^{o}, bank angle $= 75^{o}$ and angle of attack $= 10.73^{o}$ and the velocity has dropped to 1892 ft/sec (assuming the aircraft turns at a rate corresponding to maximum lift or at $1/3^{o}$/sec/degree of error whichever is less). Fig. 3 shows the variation of the required elevation gimbal deflection with time.

For zero climb angle the elevation gimbal deflection ϵ is given by,

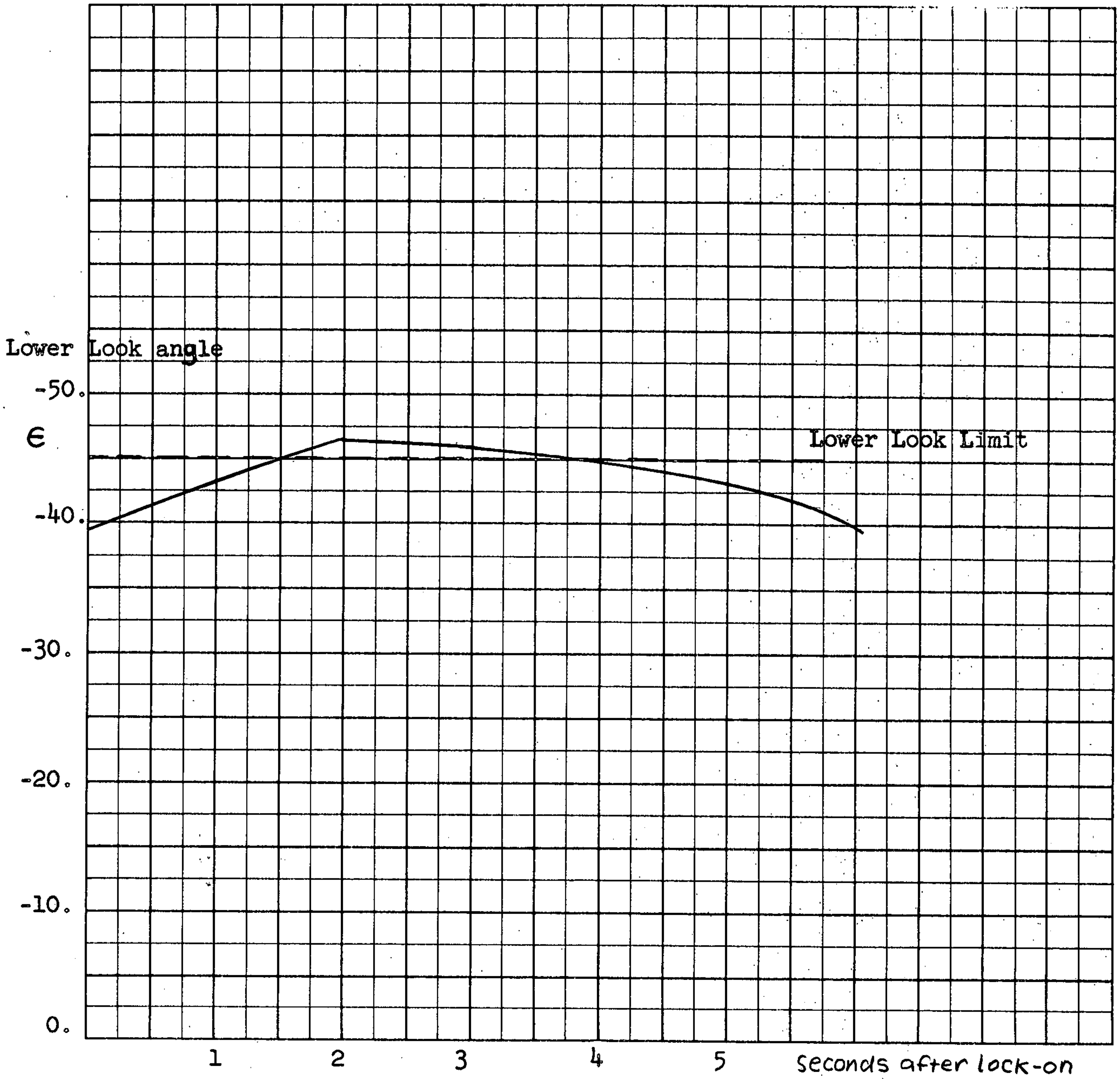

Initial Aspect = 90°
Initial Lead Angle = 30°
Ideal Lead Angle (for Lead Collision Course) = 50°

Accurate Calculation for CF 105 Flying at 50 K With Initial Speed of M2.0

RADAR ELEVATION GIMBAL DEFLECTION

Figure 3

$$\sin(\epsilon + \alpha) = \sin L_a \sin \phi$$

α = angle of attack

ϕ = bank angle

L_a = lead angle

If in the above example the heading error is 10° i.e. lead angle = 40° or 60°, bank angle = 74.1° and angle of attack = 9.8°.

upper look angle = 46.6
lower look angle = -48.0

As soon as the interceptor banks to attack, the target is lost when heading error is negative. The corresponding upper look angle is 28.4° within the limit.

When the heading error is 5° the interception is just successful. Essentially only positive look angle errors result in successful interceptions and placement probability would be around 50%.

It should be appreciated that when the CF 105 is flying at M2.0 at 50 K feet and turns at its maximum rate, it has an angle of attack of 10° so that the effective look angle limits in elevation with respect to the fighter velocity vector are -35° and 85°.

Since the interceptor presumably detects it's target in level flight and then banks, it cannot intercept a target when the lead angle is greater than 70°. Hence in this attack situation more than 15° of useless deflection is available in the positive direction while inadequate deflection is available in the negative direction. At lower altitudes angles of attack will be smaller but, as has been stated by RCA, the high altitude performance is the first consideration.

Tactical situations using the 75° upper look angle are extremely rare in the preferred frontal attacks at high altitude. However, cases which fail owing to insufficient available negative deflection are common.

It is suggested that + 65° and -55° would produce a significant improvement in placement probability.

2.3 Loop Gain (Demanded rate of turn of interceptor per degree of heading error).

When the REAC simulation of the 3 D interception problem was first instrumented it was felt that since high gain implies maximum utilisation of the fighter's maneuver capabilities, it would also give optimistic placement zones. The study would then provide an ideal which the real aircraft would approach. It was realised that this would introduce stability problems and in solving these spurious dynamic lags would be introduced. It was assumed that the fighter navigation computer would have the highest gain consistent with its stable operation.

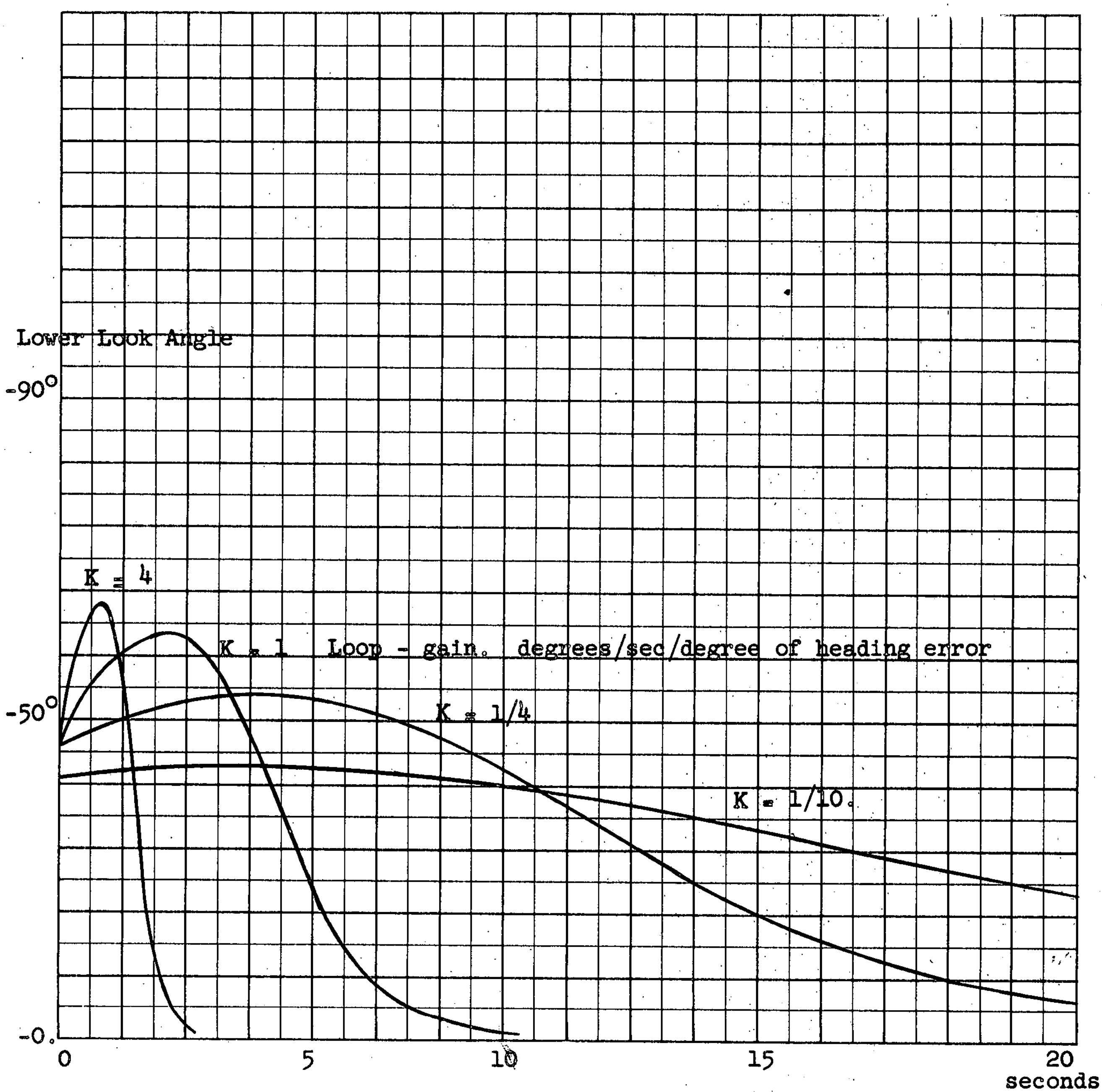

Initial Lead Angle = 46°
Final Lead Angle = 70° (θ limit)
M_f = 1.5 (constant speed)

Time from lock-on

Effect of Varying Look Gain Approximate Calculation Neglecting Angle of Attack and "g" Limit

RADAR ELEVATION GIMBAL DEFLECTION

Figure 4

The constant speed investigation which was carried out in the early stages of the CF 105 study gave results which confirmed this theory.

Unfortunately in a real fighter, sustained high "g" turns produce serious deceleration. In addition, high gain means that a high bank angle is maintained until the fighter is almost on course. With the small permissible negative deflection of the radar elevation gimbal, this causes serious encroachment of look angle barriers. Fig. 4 shows how the required negative gimbal deflection varies for different values of loop gain, starting from the same situation in each case.

A study was carried out to determine the effects of varying the loop gain. As a result the following facts emerged. Where placement probability is limited by look-angle, fall-back or minimum velocity barriers the placement zone increases as the gain and hence the turn rate is reduced. Where the placement zone is bounded by a maneuver barrier, probability is reduced when the gain is reduced but only after a threshold value is passed. This value corresponds to the interceptor turning at maximum rate when the heading error is equal to the maximum tolerated by the missile and it is the maximum value of loop gain which need be considered. There may be a case for using a smaller value because of the increase in probability due to improved look angle boundaries but there is nothing to be said for a larger value, since by definition a larger value does not improve maneuver barriers and it reduces the zone at other boundaries. If the allowable heading error is 15° at 50 K feet, the maximum value of loop gain is given by $K_{max} = 0.29^{\circ}$/sec per degree of heading error. A slightly higher value is optimum at 60 K feet.

The value of K = 4 which was used in the REAC simulation will give pessimistic placement probabilities. The value of K = 1/3 used by RCA seems much more suitable.

Inter-relation of the effects on placement probability of changes in loop gain, maximum load factor and look-angle limits are discussed below.

2.4 Inter-Relation of Look Angle Limits, Load Factor Limits and Loop Gain.

Increasing the look-angle limits, reducing the load factor to the power limit and reducing the loop gain all increase the placement probability against a non-maneuvering target in regions where probability is not limited by missile heading error.

However, once the radar azimuth deflection limits have been set, for a given maximum bank angle and angle of attack there is a value beyond which the elevation look angle limits need not be increased. This value decreases with decreasing maximum load factor. As the loop gain is reduced the lower look angle allowance may be further decreased because the lead angle for a given bank angle will be less.

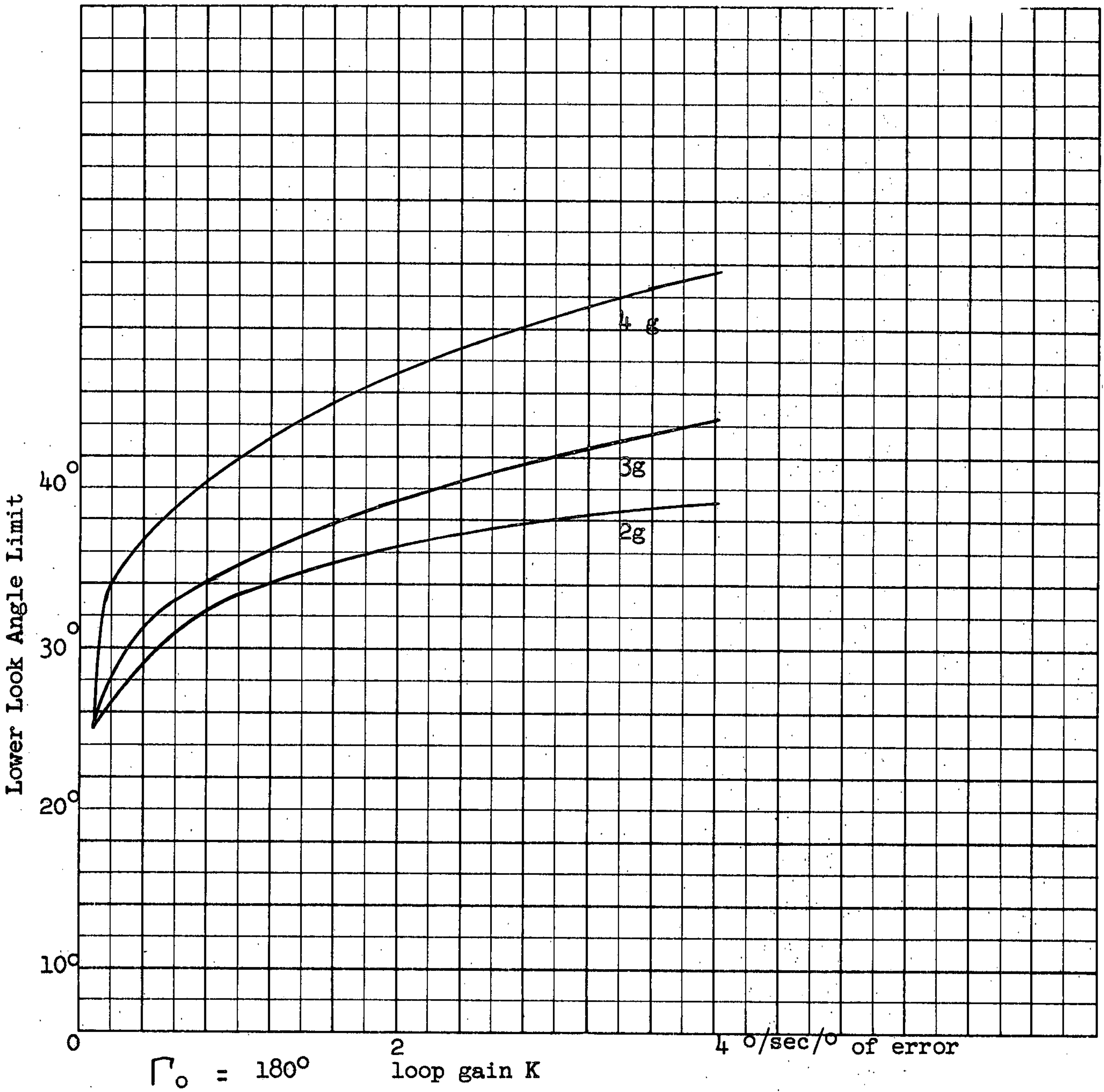

Γ_o = 180°

Δh = 20 K

M_t = M_f = 2.0

h_t = 60 K

A case of Interrelation between Lower Look Angle Limit Maximum Load Factor and Loop Gain.

CONSTANT PROBABILITY CURVES

Figure 5

If K = 1/4 and maximum bank angle = 60° (2 g load factor) 55° lower look angle limit is sufficient. However if the lower look angle limit is 45° maximum load factor should be less than 1.5 g.

Fig. 5 shows an example of the way these factors may be changed to yield the same placement probability.

3.0 SOME TACTICAL RECOMMENDATIONS FROM THE CF 105 STUDY

3.1 Subsonic Target

The CF 105 by suitable choice of tactics invariably has a high probability of success against a subsonic target. Cases studied were; constant speed target, maneuvering target and simple ECM. In the latter case it was assumed that cross-over occurred i.e. jamming was ineffective at close range.

The success of the CF 105 against more refined countermeasures or in cases where cross-over does not occur was not evaluated (see Appendix 'B' of this report, however, for some consideration these cases).

The recommended procedure is to maintain maximum speed until at close range. Hence maneuvers at long and medium range should be power limited.

3.2 Supersonic Non-Maneuvering Target

If the heading error is negative - that is the interceptor has to turn away from the target to get on course - it should fly with reduced g's at long and medium ranges. The basis of this recommendation is that the most important factor in the early stages of the attack is the maintenance of maximum speed. Besides the possibility of being outdistanced, the performance of the CF 105 deteriorates quickly as the speed falls.

(1) deceleration for a given g turn increases

(2) thrust available for level flight is reduced

(3) Power limited g's are reduced
- at 50 K M2.0 power-limited load-factor = 2.0
- at 50 K M1.2 power-limited load-factor = 1.4

(4) maximum allowable lift is reduced, (buffet limited g's)

3.3 Snap-Up Attacks

Snap-up attacks should not be used if another mode of attack has a high probability of success. Snap-up attacks are susceptible to late jamming and late evasion. Where the interceptor has good aerodynamic capabilities at target altitude coaltitude attacks are preferable. The pursuit-style modes of navigation which are available under jammed conditions may lead to awkward maneuvers in the vertical plane.

In a snap-up attack, if the target is not maneuvering initially the interceptor g's should be limited so that the interceptor goes into snap-up with maximum velocity.

3.4 Attack Under Jammed Conditions

If cross-over is anticipated outside the launch zone - say in sufficient time to correct some heading error, pure collision navigation has many advantages especially for course differences less than 135° against a supersonic target.

Some of the navigation systems which look promising under jammed condition are pursuit modes which tend to become tail chases at close range. This sort of maneuver which can be accomplished in the horizontal plane will in general be less successful in the vertical plane.

Therefore coaltitude attacks are preferable.

4.0 SOME FURTHER WORK IN THE CF 105 3 D INTERCEPTION STUDY

4.1 Supersonic Target

When the target is not jamming and the missile has a microwave seeker placement probability is high for head-on attacks.

(a) When the missile has an infrared system, head-on climbing or coaltitude attacks are not successful because of the low IR emission from the target. Beam attacks (initial course difference near 110°) are quite successful for high GCI accuracy. The snap-up mode of attack in which the interceptor flies level until at close range and then climbs steeply produces a spectacular improvement for head on attacks. Results are as good as those for the standard microwave missile.

(b) When the infrared AI is used several deteriorating factors are introduced. No range information is obtained so the available navigation systems are limited - the usual lead collision mode is not possible.

The situation of the infra-red detector on the tail of the interceptor causes the target to be obscured by the wings of the interceptor in many situations. This trouble can be overcome by restricting the interceptor bank angle to 45° in attacks against a non-maneuvering target.

Placement probability may be limited by the low acquisition ranges when the interceptor is directly ahead of the target.

(c) Fixed range lead pursuit is a promising navigation system which may be used when the target is jamming the AI radar or when IR AI is being used. In this system the interceptor flies so that the lead angle (angle between the interceptor's course and the line of sight) is proportional to the rate at which the line of sight rotates. The system has the advantage that over a wide region the fighter is headed in the correct direction for successful launch of its missiles. By chosing the proportionality factor correctly this region of success can be made to lie within the launch zone of the missile.

Some other information must be available to decide when to launch the missiles.

In this study it was assumed that at some short range the jamming would cease to be effective and launch information would be available. The system gave high placement probabilities for head-on attacks. Probability falls quickly for initial course differences less than 135°. If the infrared system is used, the interceptor bank angle should be limited to 45°.

The choice of a navigation mode must depend on the range at which cross-over is expected. If cross-over was expected at 60 K feet say, some heading error could be corrected before launching the missile. In this case a pure collision course in the early phases of the attack would lead to the highest placement probabilities and give the most direct interceptor course.

(d) If the target is not maneuvering or jamming, an unguided missile gives a high placement probability. The kill probability is limited by the accuracy of the open loop system. Probably the main virtue of a guided missile is in that the requirements of the navigation and fire control computer are not so critical and the precise knowledge of the trajectory which the missile would fly if unguided is not required.

(e) The effects of restricting the interceptor maneuver rates have been studied. For a given initial course difference between target and interceptor there is line relative to the target along which the interceptor may approach without maneuvering because it is already on the required lead collision course. This is the "ideal approach line". From any other initial position the interceptor has to turn either toward the target or away from it until it is on course. If the interceptor has to turn away from the target highest placement probability corresponds to a power limited turn and if it has to turn towards the target placement probability corresponds to a fast turn.

4.2 Subsonic Target

Against a subsonic target the tactics which produce success are simpler. In the standard situation where the missile has a microwave seeker and the AI radar may be used, placement probability is very high even against a rapidly maneuvering target. The interceptor's success is ensured if the initial interceptor speed is high and if it restricts itself to low load-factor maneuvers at long and medium ranges.

(a) As a subsonic target is a much weaker IR source than the supersonic target discussed above, the success of the IR missile in frontal attacks is even less. However, since the interceptor has a speed advantage small initial course differences give high placement probability. Course differences of 110° and less are successful. Again snap-up attacks may be successful from head-on.

(b) Infrared AI suffers most from the low I.R. emission of a subsonic target. By reducing the bank angles which are used in the attack the interceptor may keep lock-on without the wings obscuring the target, but attacks should be restricted to the beam and tail to ensure lock-on at sufficient range to launch the missiles.

(c) Most modes of navigation are successful against a slow target provided the missile may be launched satisfactorily. Again by using fixed range lead pursuit the interceptor may ensure that the missile is correctly headed in the launch zone.

(d) The unguided missile is subject to the same limitations as in the case of a supersonic target. In general, the slower the target, the more chance an unguided missile will have of success.

4.3 Cases Studied

For ease in reference the cases which were studied are given problem numbers following on from the studies described in the 5th progress report (ref. 5).

Problem Number	Problem Description	Target
X	IR missile study	(
XI	IR AI study	(
XII	Fixed range lead pursuit study	(supersonic
XIII	Unguided missile study	(
XIV	Interceptor maximum load factor study	(
XV	Subsonic interceptor study	(
XVI	IR missile and subsonic interceptor	(subsonic
XVII	Unguided missile and subsonic interceptor	(
XVIII	IR AI fixed range lead pursuit study	(
XIX	Maneuvering target study	(

Tables giving the parameter values and graphs showing the placement zones and corresponding placement probabilities are to be found on the following pages:-

Problem No.	Parameters Studied Page No.	Placement Zones and Prob. Curves Page No.
X	21	22 to 40
XI	41	42 to 53
XII	54	55 to 60
XIII	61	62 to 73
XIV	74, 83, 91	75 to 82, 84 to 90 92 to 94
XV	95	96 to 97, 99 to 100
XVI	102	103 to 106
XVII	95	96, 98 to 99, 101
XVIII	121	107 to 120
XIX	121 and 136	122 to 135

4.4.0 Infrared Missile Studies - Problem X

Among the differences between the missile with infrared seeker system and the conventional radar seeker the most significant is the variation of maximum seeker range with interceptor aspect. At the ranges corresponding to attacks at M2.0 this is equivalent to a failure zone for aspects ± 30° from the nose of the target in the vertical and horizontal planes. Several interceptions were carried out for a variety of initial course differences. Attacks which concluded with the missile being launched within 30° of the nose of the target were classed as failures.

The results are shown as placement charts and probability curves.

4.4.0.1 Infrared Missile Study Conditions

Problem conditions are the same as Prob. II (ref. 4)

Missile incremental velocity = 875 ft/sec.
Target velocity M2.0 Not evading.
Target angle of attack 7°
Fighter maximum velocity M2.0
Target altitude 60K

PROBLEM X - IR MISSILE STUDY

	A	B	C	D	E	F	G	H
h_{fo}	60K	40K	60K	40K	60K	40K	60K	40K
T_s	-	20 sec	-	20 sec	-	20 sec	-	20 sec
Γ_o	180		135°		110°		75°	

h_{fo} = initial height of fighter

T_s = time-to-go for the initiation of snap-up

Γ_o = initial course difference

4.4.0.2 Conclusions

Coaltitude Attacks

Placement probability is very low for initial course differences from 180° to 135° and rises quite abruptly at 110°. For course differences less than 110° the probability falls again because of encroachment of look angle barriers - as in the case of the microwave missile.

IR Missile

Prob. X A

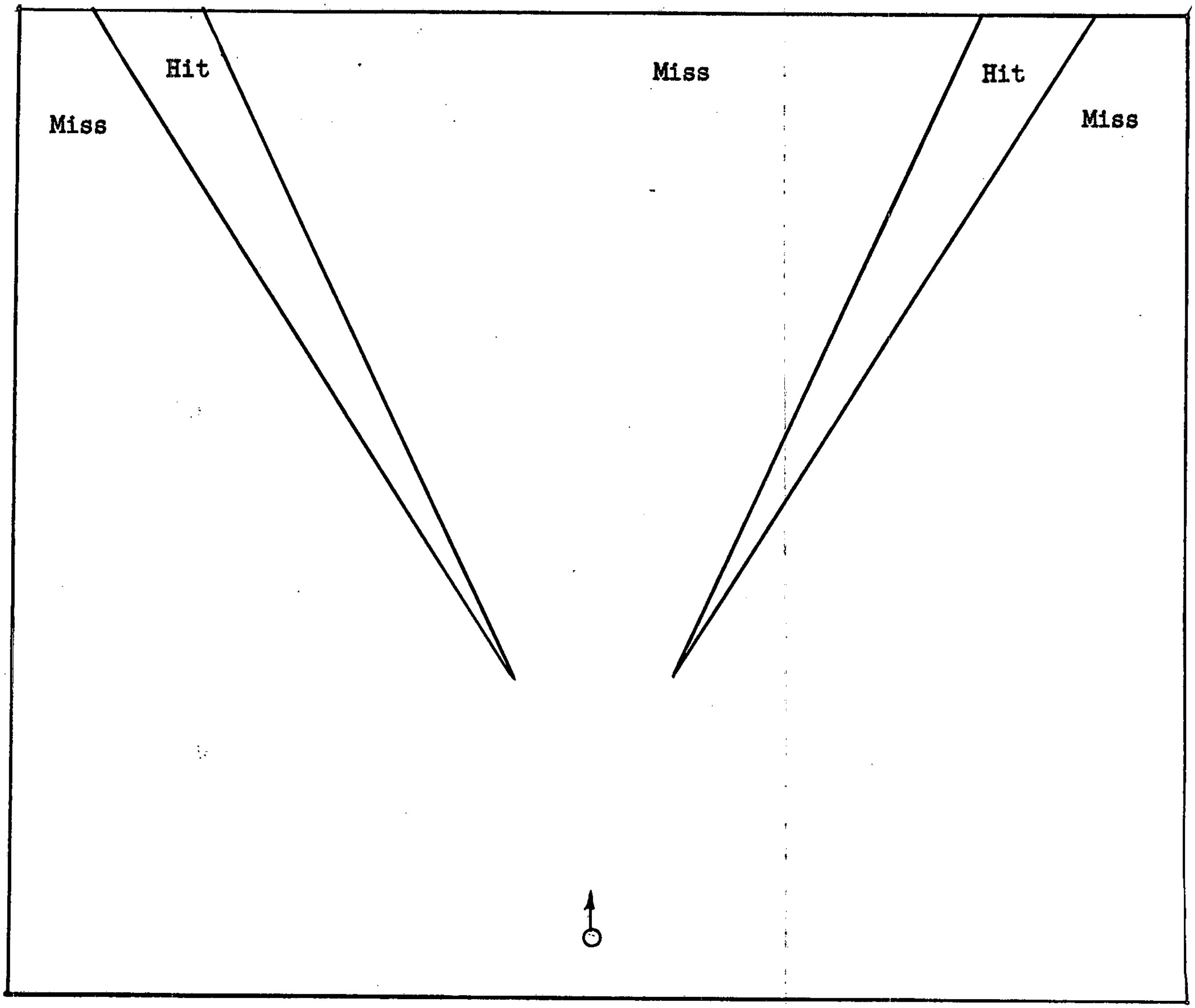

$M_t = 2.0$ $h_t = 60$ K Scale 25,000 ft/cm

$M_f = 2.0$ $h_{fo} = 60$ K

$\Gamma_o = 180°$

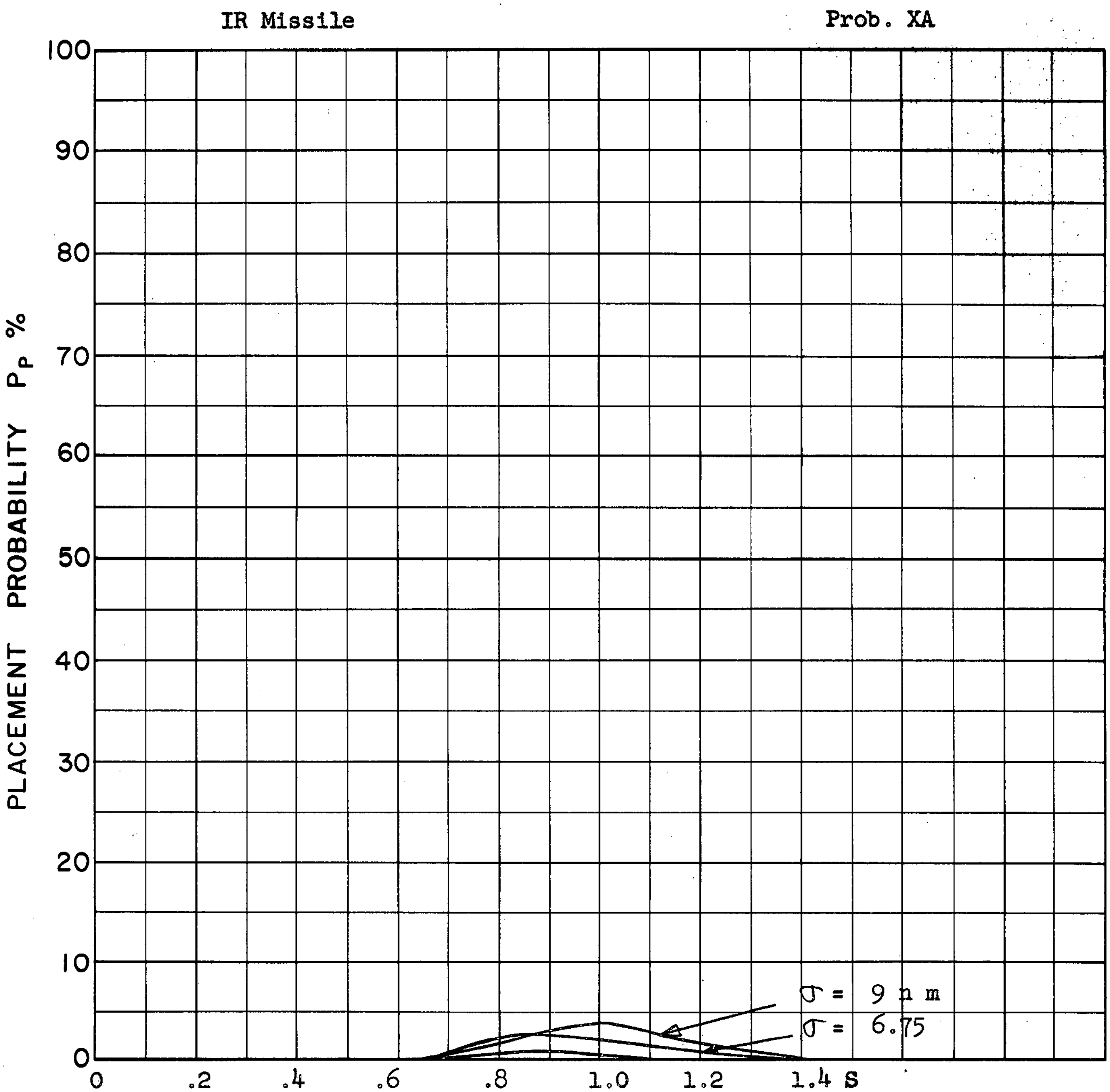

COURSE DIFFERENCE: 180°
TARGET EVASION: 0
TARGET MACH NO.: 2.0
INTERCEPTOR LATERAL G's: Avro 3.3
INTERCEPTOR MACH NO.: 2.0
σ OF G.C.I. ACCURACY: 5 Values
A.I. DETECTION RANGE AS FRACTION OF SPECIFICATION RANGE, S: Abscissa
A.I. DETECTION RANGE CONTOUR: Delta
ALTITUDE: H_t 60 K
H_{fo} 60 K

IR Missile Prob. X B

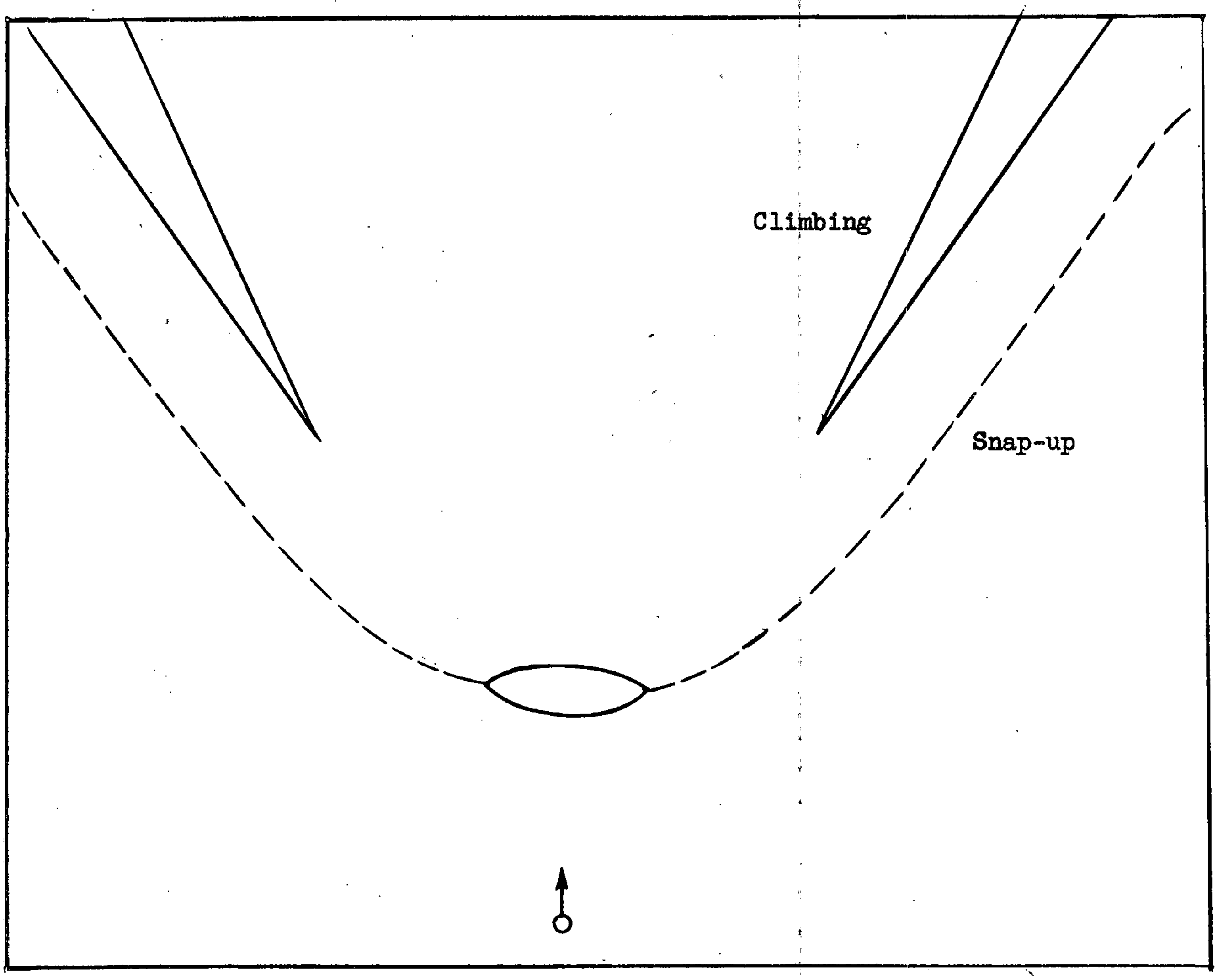

M_t = 2.0 h_t = 60 K Scale = 25,000 ft/cm

M_{fo} = 2.0 h_{fo} = 40 K

Γ_o = 180°

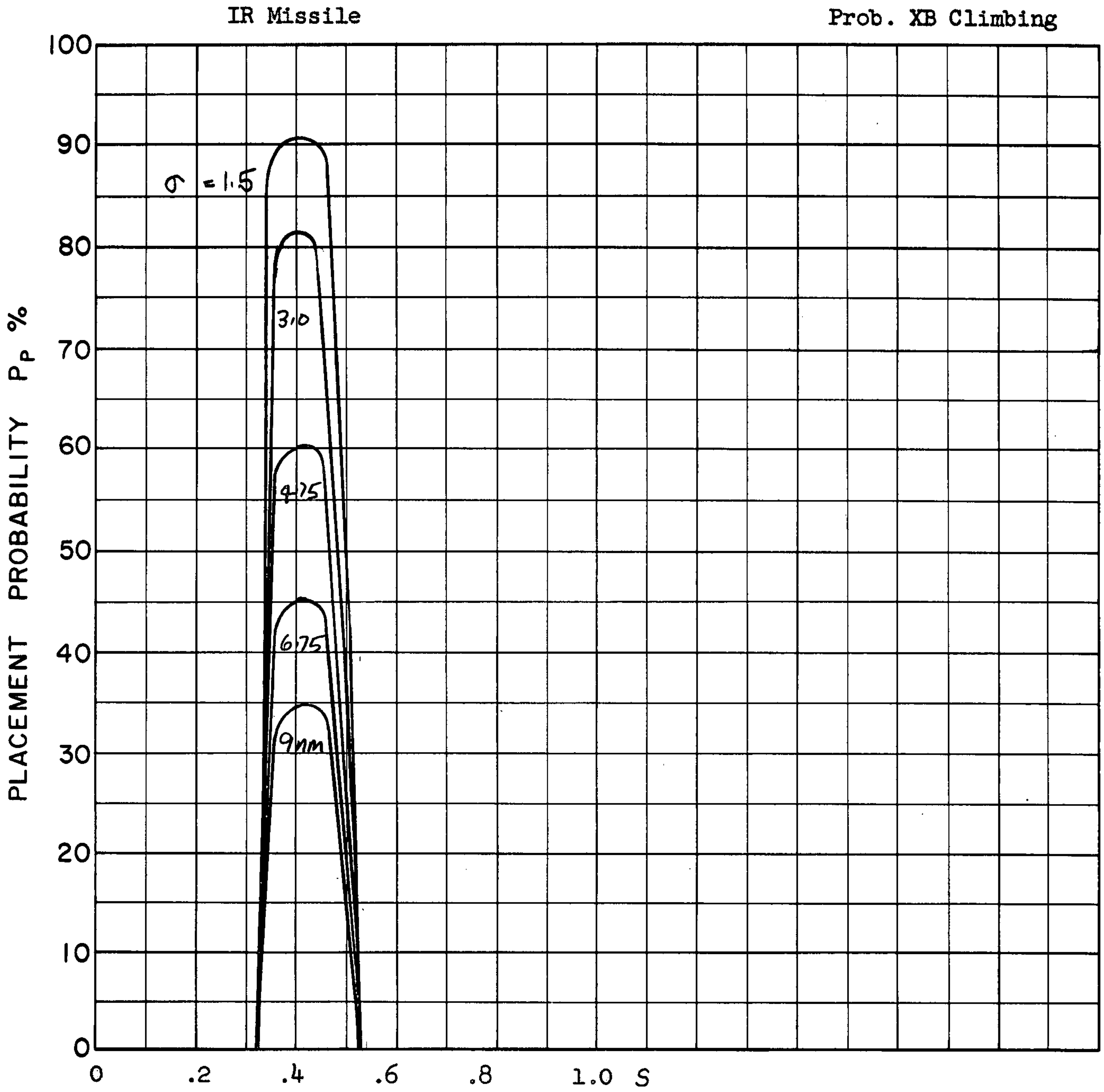

COURSE DIFFERENCE: 180°
TARGET EVASION: 0
TARGET MACH NO.: 2.0
INTERCEPTOR LATERAL G's: Avro 3.3
INTERCEPTOR MACH NO.: 2.0
σ OF G.C.I. ACCURACY: 5 Values
A.I. DETECTION RANGE AS FRACTION OF SPECIFICATION RANGE, S: Abscissa
A.I. DETECTION RANGE CONTOUR: Delta
ALTITUDE: H_t = 60 K

H_{fo} = 40 K

IR Missile

Prob XB Snap-up

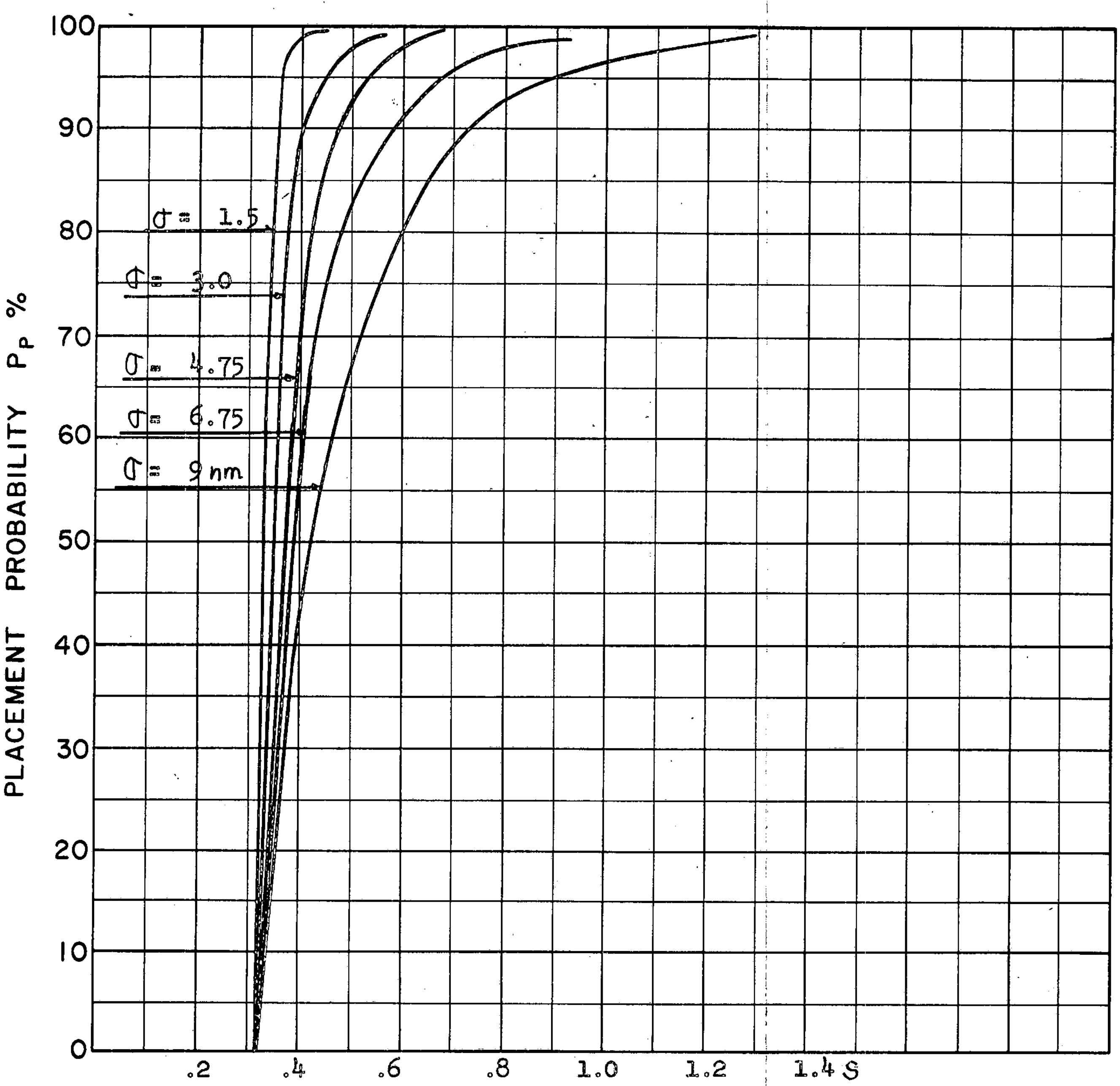

COURSE DIFFERENCE: 180°
TARGET EVASION: 0
TARGET MACH NO.: 2.0
INTERCEPTOR LATERAL G's: Avro
INTERCEPTOR MACH NO.: 2.0
σ OF G.C.I. ACCURACY: 5 Values
A.I. DETECTION RANGE AS FRACTION OF SPECIFICATION RANGE, S: Abscissa
A.I. DETECTION RANGE CONTOUR: Delta
ALTITUDE: H_t = 60 K
H_{fo} = 40 K
T_s = 20 sec.

IR Missile

Prob. X C

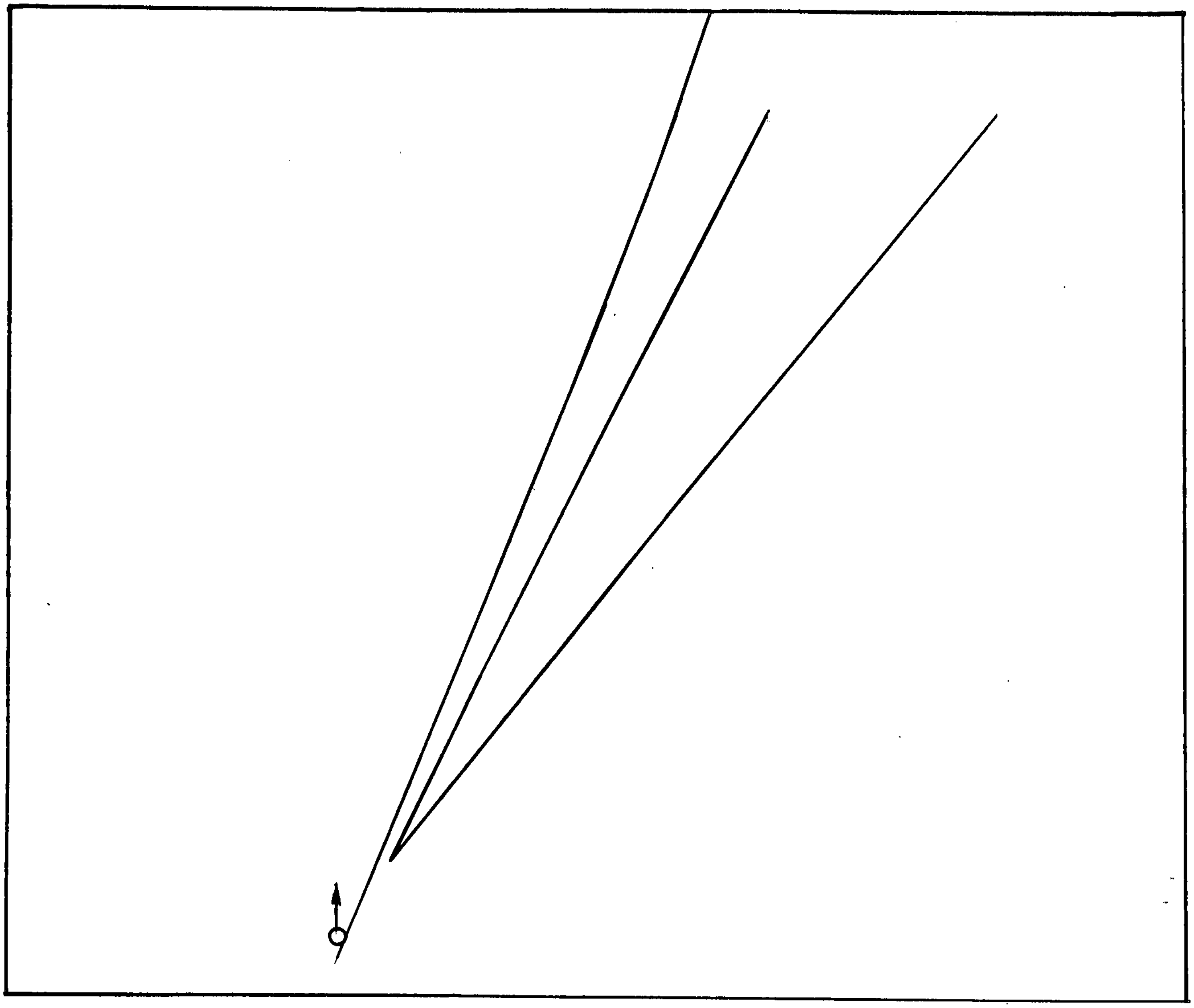

M_t = 2.0 h_t = 60 K Scale 25,000 ft/cm

M_{fo} = 2.0 h_f = 60 K

Γ_o = 135°

IR Missile Prob. XC

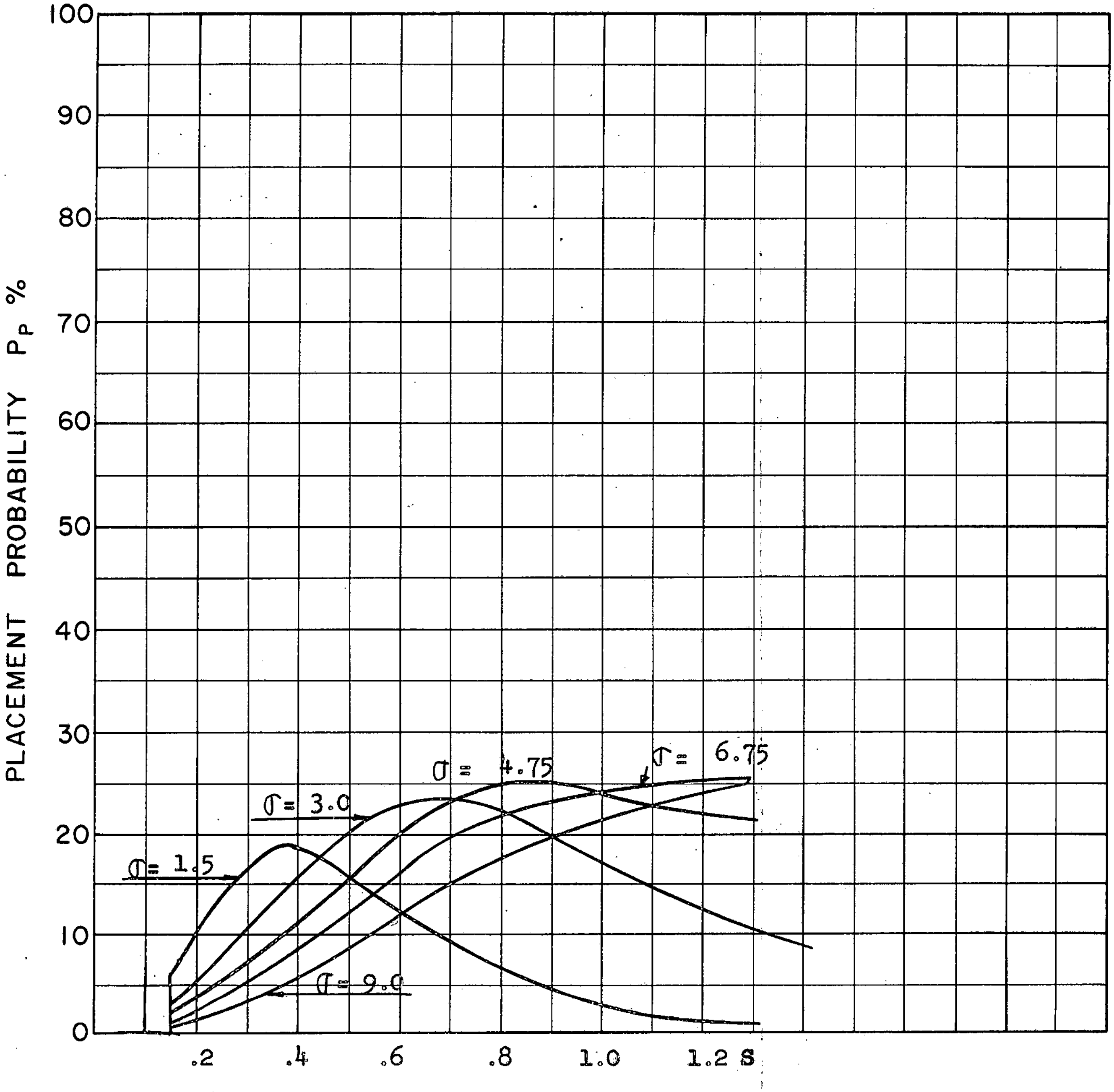

COURSE DIFFERENCE: 135°
TARGET EVASION: 0
TARGET MACH NO.: 2.0
INTERCEPTOR LATERAL G's: Avro 3.3
INTERCEPTOR MACH NO.: 2.0
σ OF G.C.I. ACCURACY: 5 Values
A.I. DETECTION RANGE AS FRACTION OF SPECIFICATION RANGE, S: Abscissa
A.I. DETECTION RANGE CONTOUR: Delta
ALTITUDE: H_t = 60 K
H_f = 60 K

IR Missile

Prob. X D

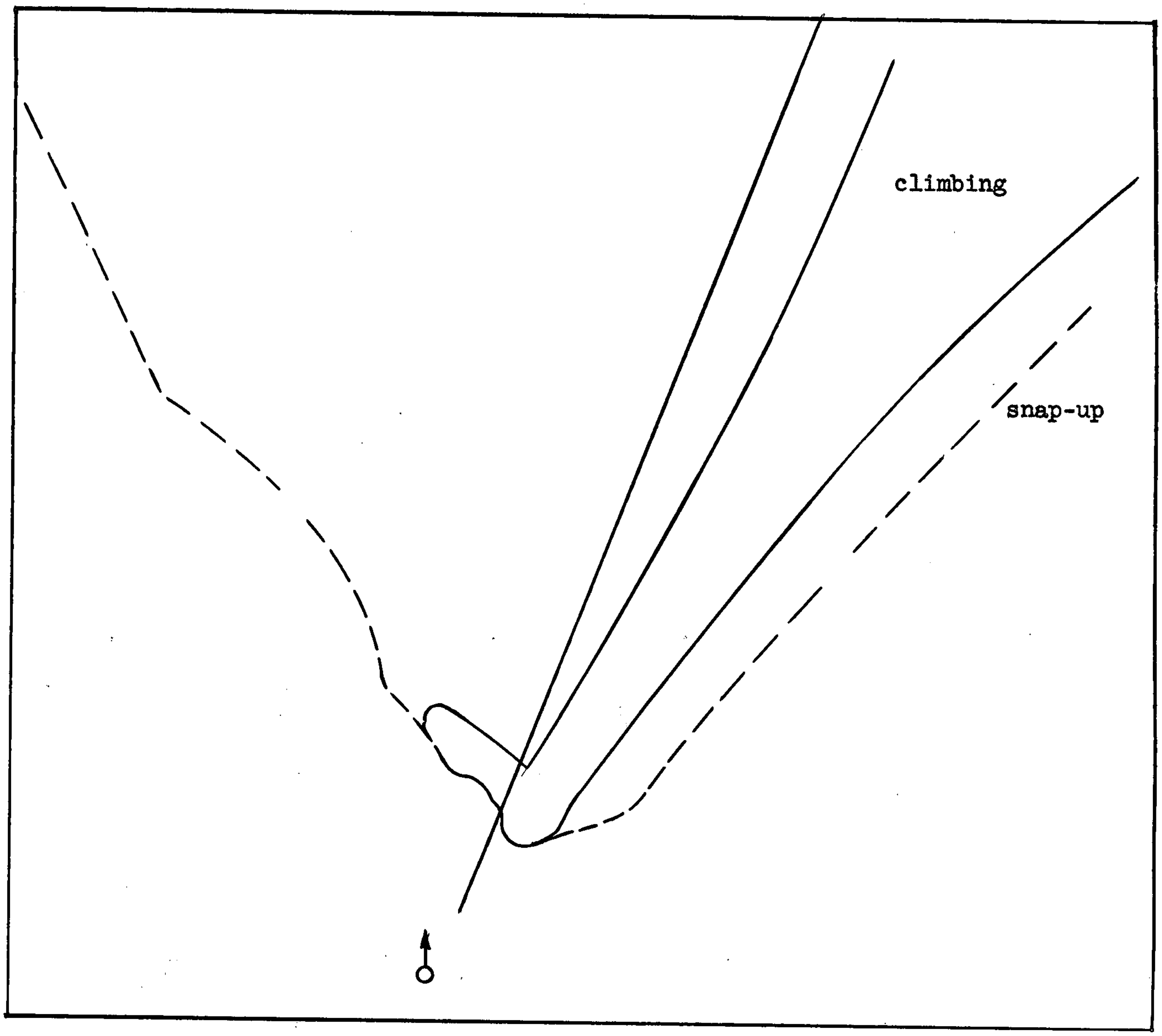

$M_t = 2.0 \qquad h_t = 60\text{ K}$

$M_{fo} = 2.0 \qquad h_{fo} = 40\text{ K}$

$\Gamma_o = 135^\circ$

IR Missile Prob. XD Climbing

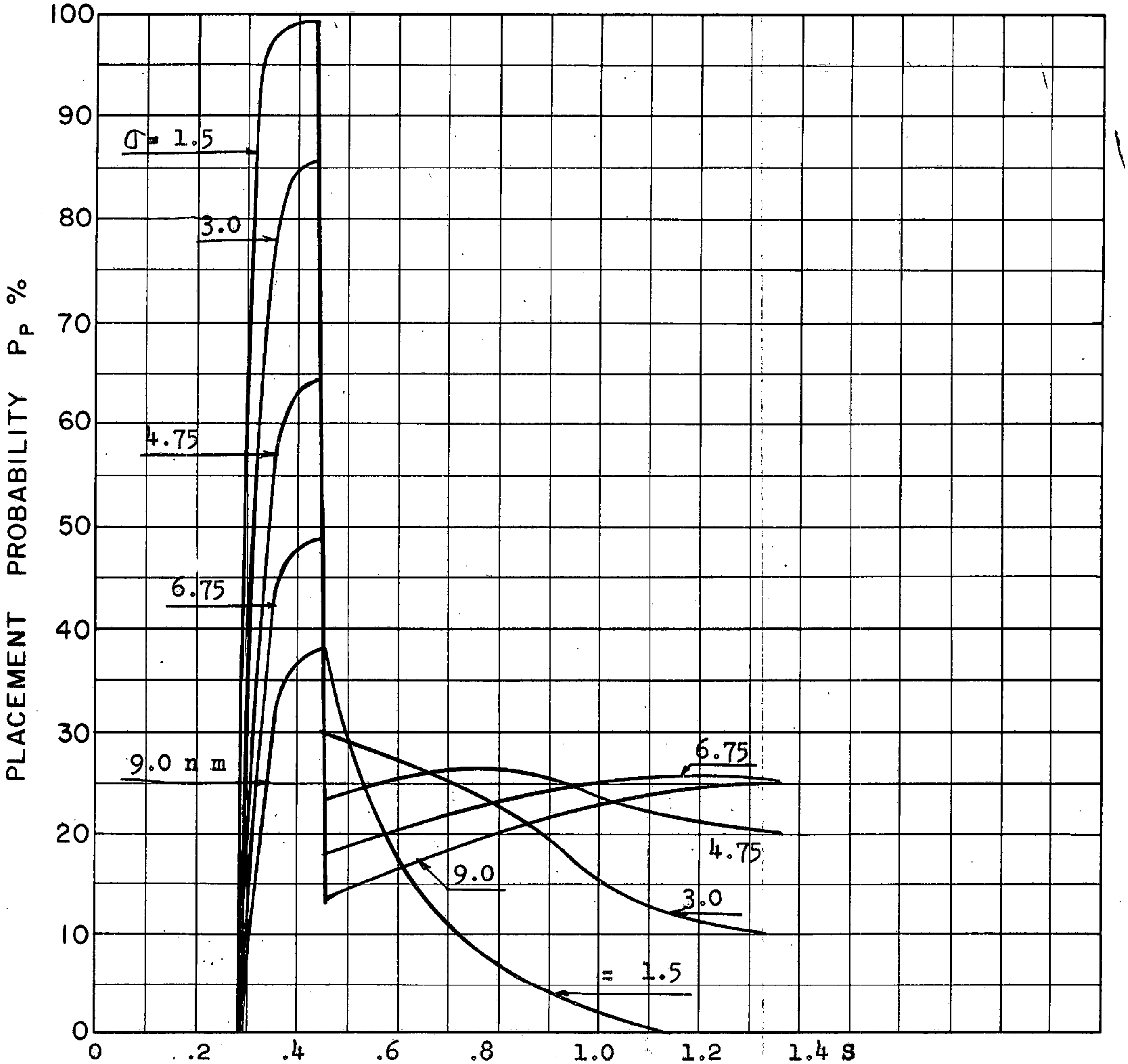

COURSE DIFFERENCE: 135°
TARGET EVASION: 0
TARGET MACH NO.: 2.0
INTERCEPTOR LATERAL G's: Avro 3.3
INTERCEPTOR MACH NO.: 2.0
σ OF G.C.I. ACCURACY: 5 Values
A.I. DETECTION RANGE AS FRACTION OF SPECIFICATION RANGE, S: Abscissa
A.I. DETECTION RANGE CONTOUR: Delta
ALTITUDE: H_f = 60 K
H_{fo} = 40 K

IR Missile

Prob. XD Snap-up

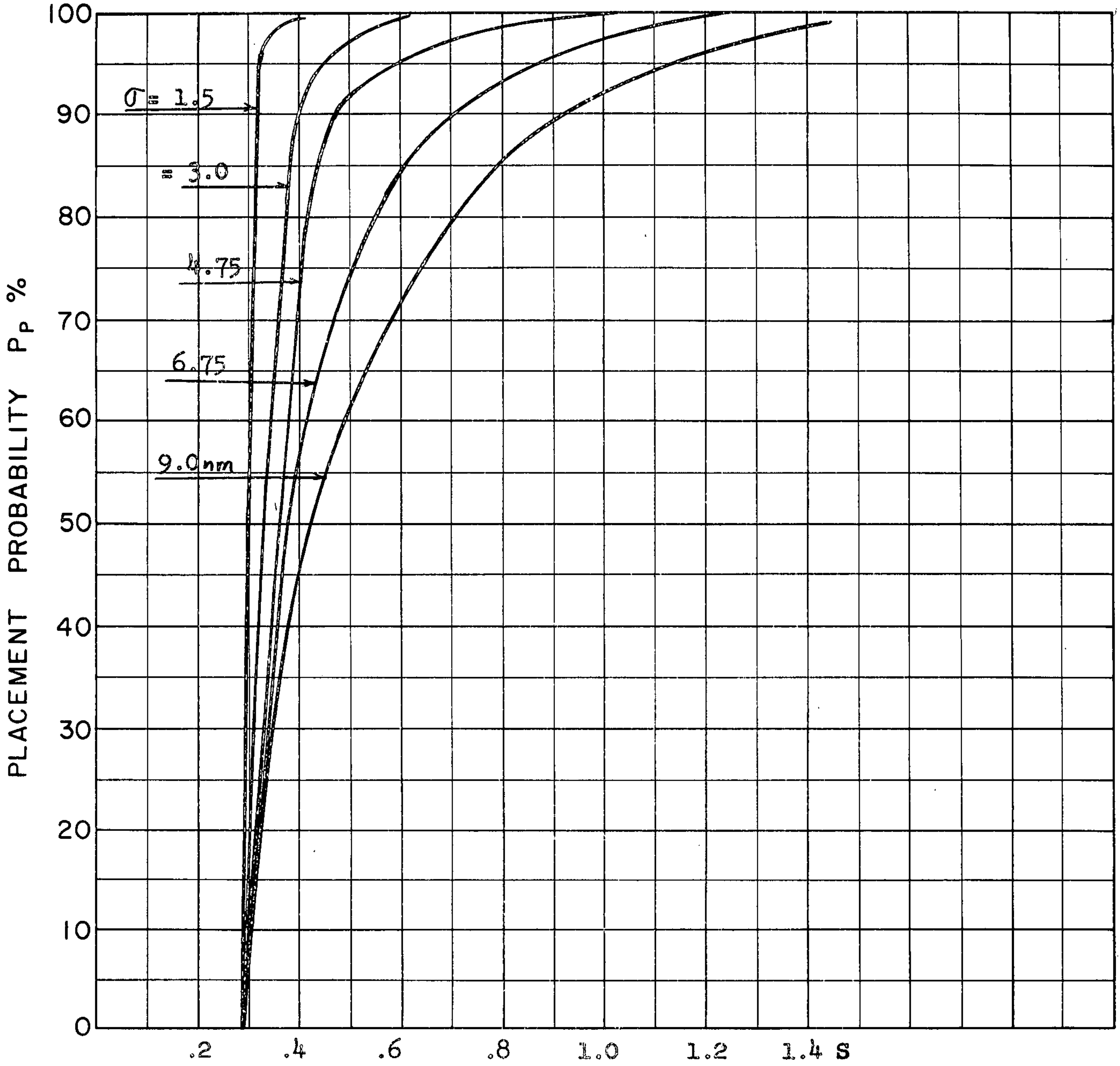

COURSE DIFFERENCE: 135°
TARGET EVASION: 0
TARGET MACH NO.: 2.0
INTERCEPTOR LATERAL G's: Avro 3.3
INTERCEPTOR MACH NO.: 2.0
σ OF G.C.I. ACCURACY: 5 Values
A.I. DETECTION RANGE AS FRACTION OF SPECIFICATION RANGE, S: Abscissa
A.I. DETECTION RANGE CONTOUR: Delta
ALTITUDE: H_t = 60 K
H_{fo} = 40 K

IR Missile   Prob. X E

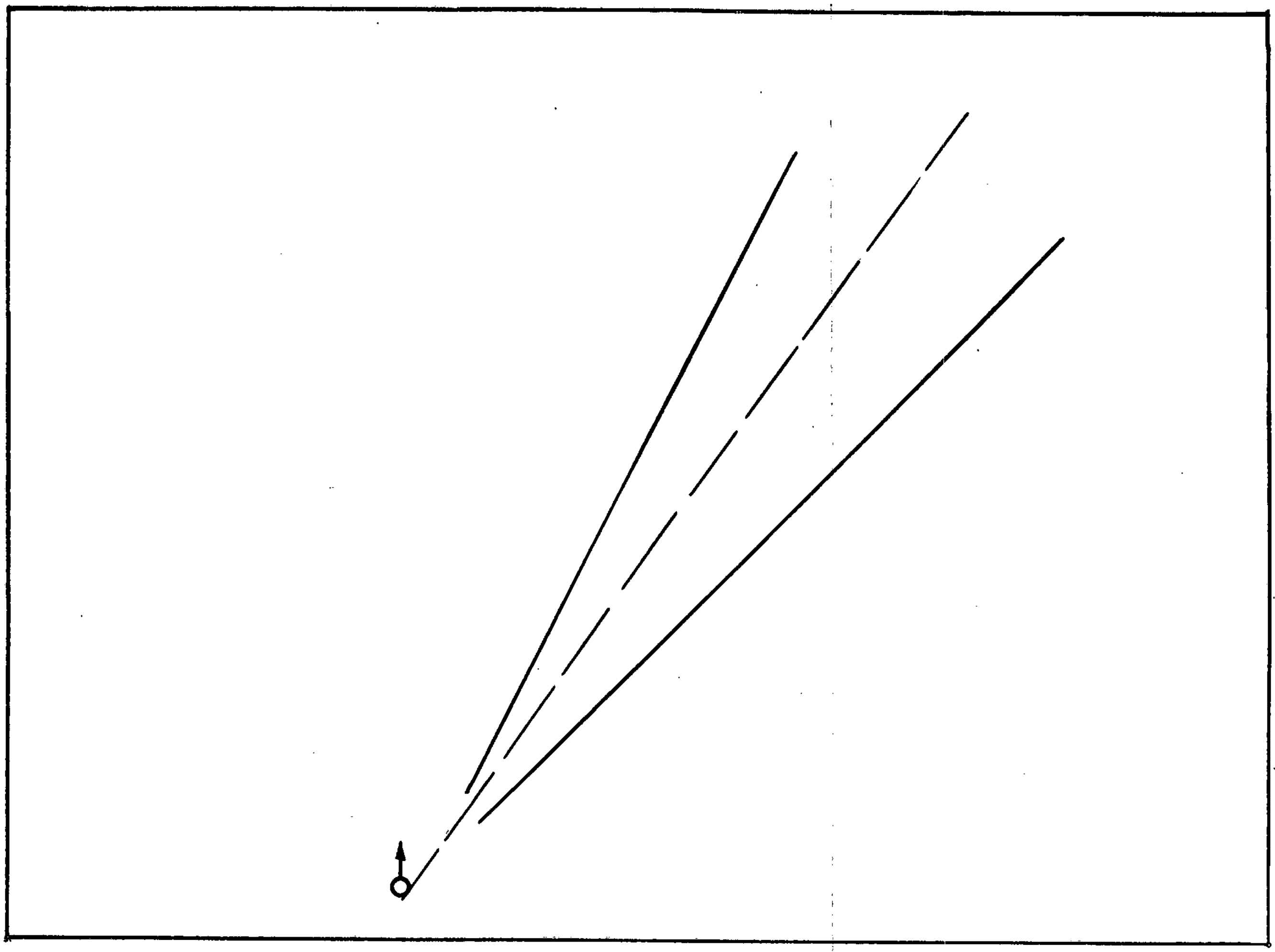

$M_t = 2.0$ $h_t = 60$ K   Scale = 25,000 ft/cm

$M_{fo} = 2.0$ $h_f = 60$ K

$\Gamma_o = 110^\circ$

IR Missile Prob. XE

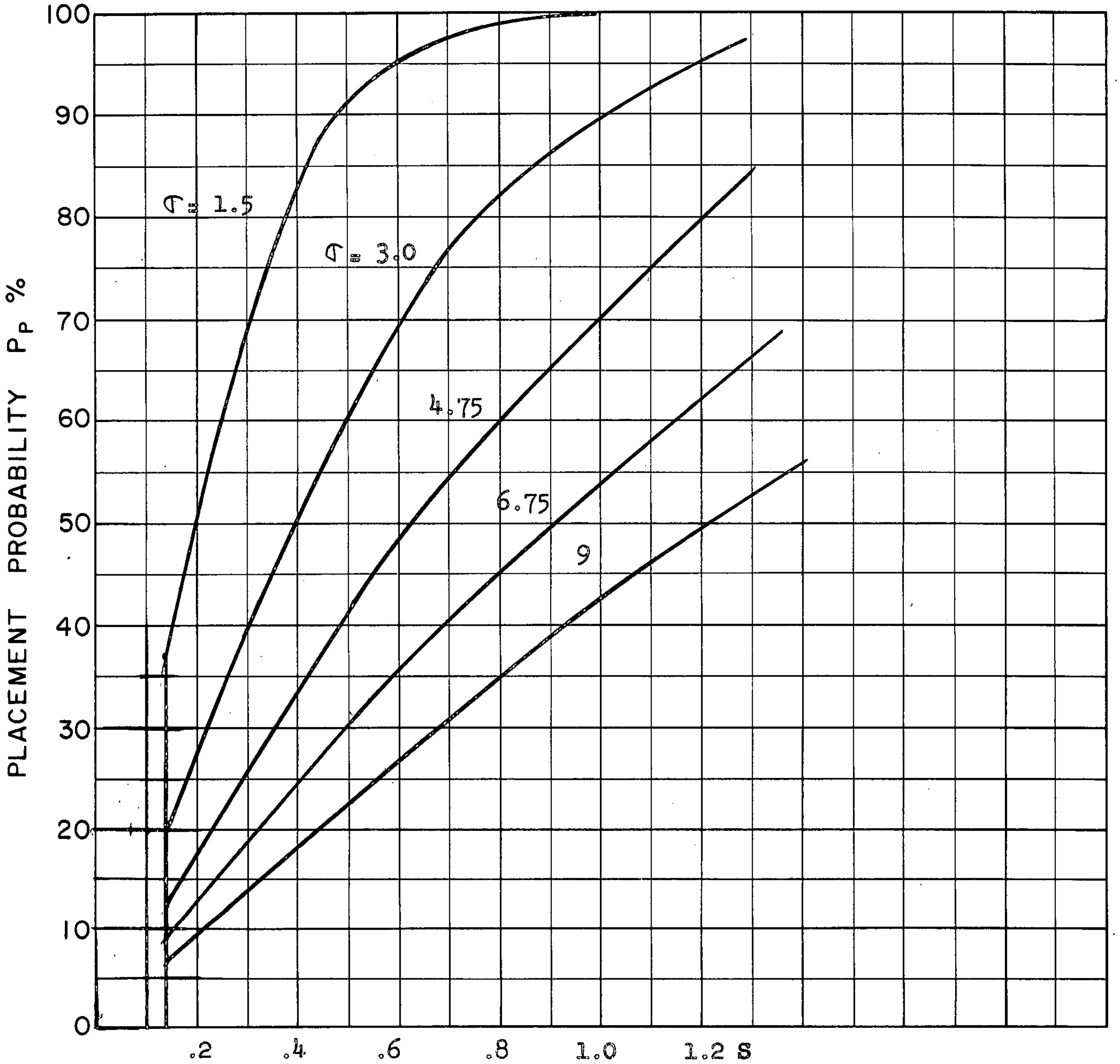

COURSE DIFFERENCE: 110°
TARGET EVASION: 0
TARGET MACH NO.: 2.0
INTERCEPTOR LATERAL G's: Avro 3.3
INTERCEPTOR MACH NO.: 2.0
σ OF G.C.I. ACCURACY: 5 Values
A.I. DETECTION RANGE AS FRACTION OF SPECIFICATION RANGE, S: Abscissa
A.I. DETECTION RANGE CONTOUR: Delta
ALTITUDE: H_{fo} = 60 K
H_t = 60 K

IR Missile

Prob. X F

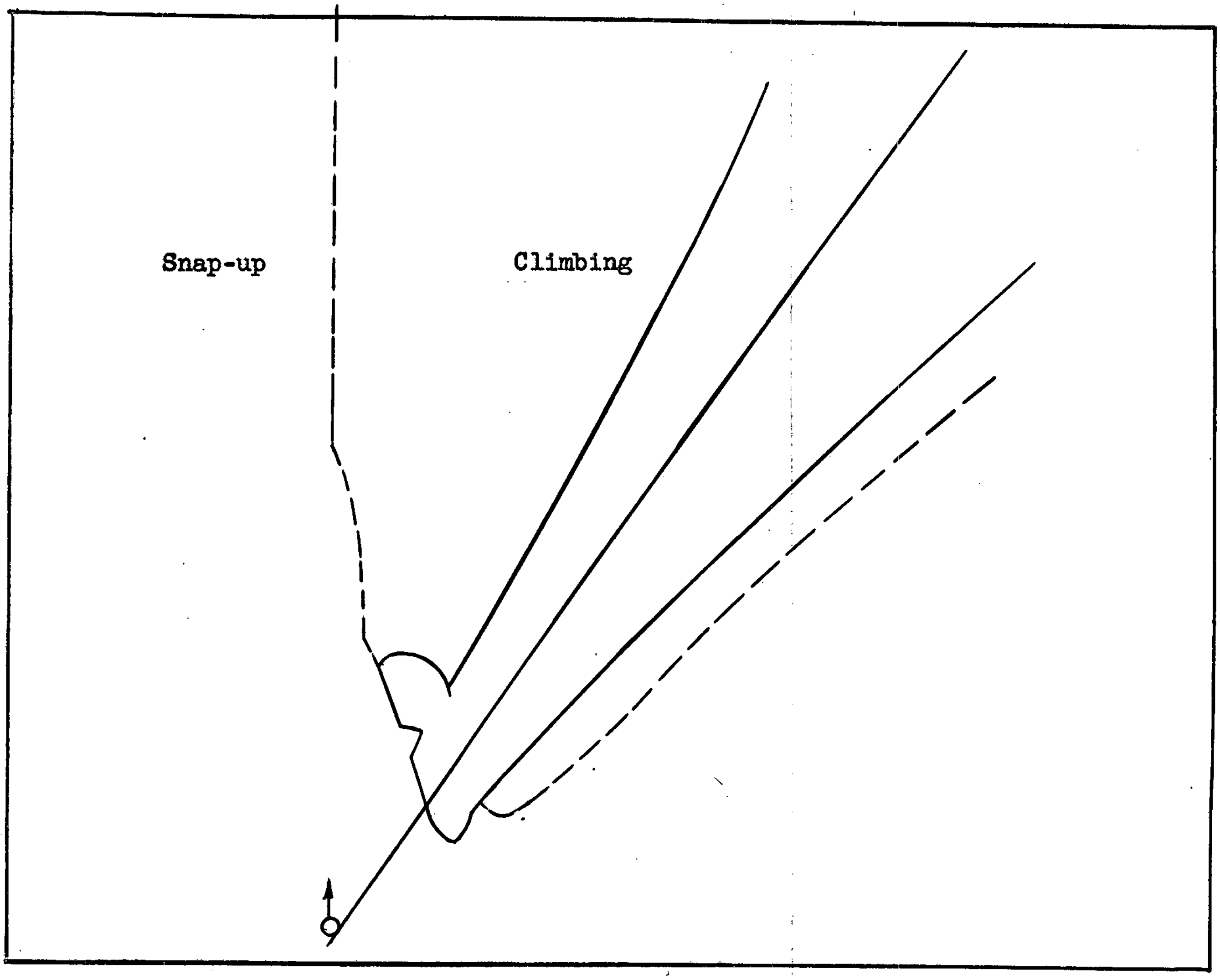

M_t = 2.0 h_t = 60 K

M_{fo} = 2.0 h_{fo} = 40 K

Γ_o = 110°

Scale = 25,000 ft/cm

IR Missile

Prob. XF Climbing

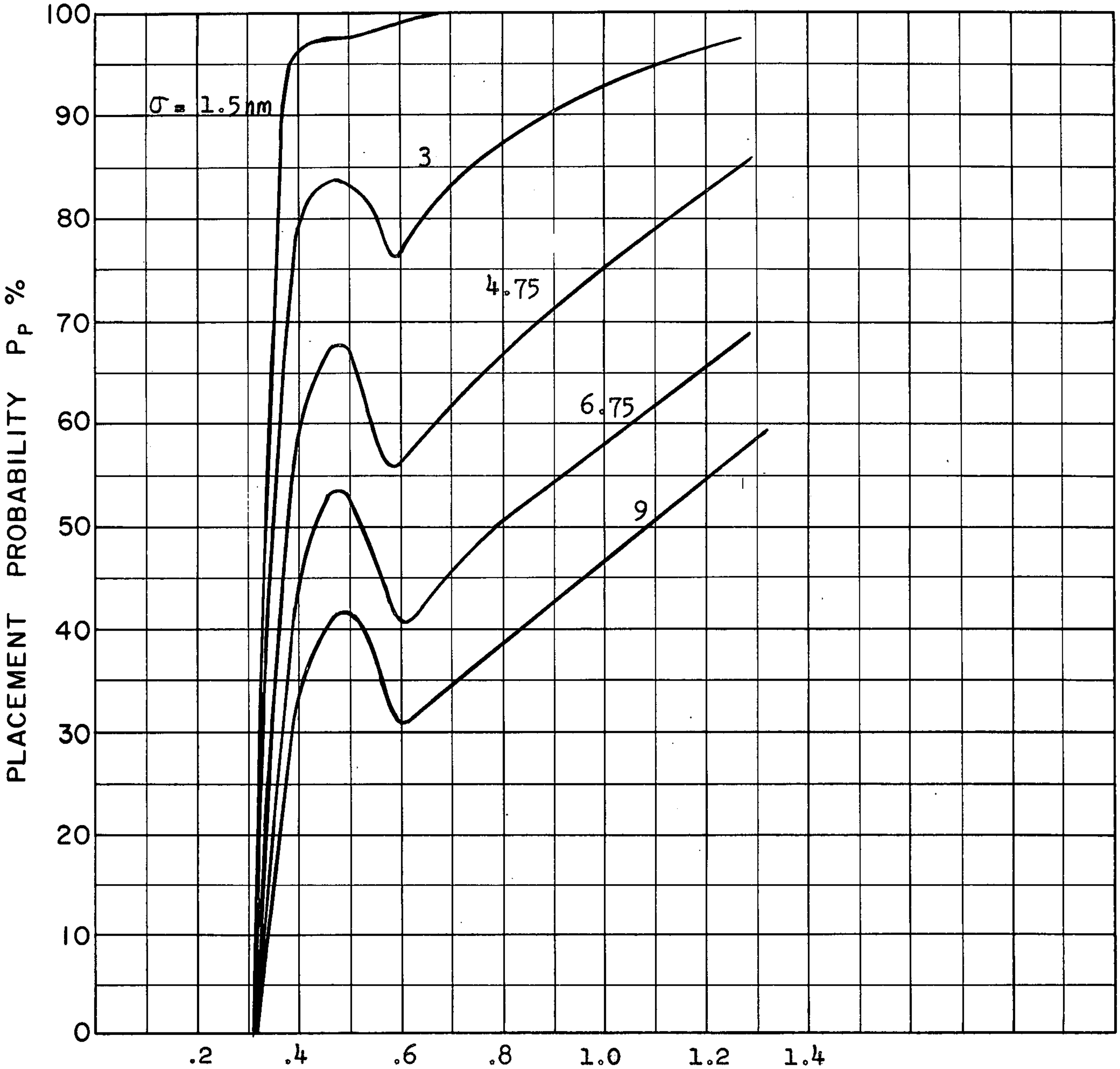

COURSE DIFFERENCE: 110°
TARGET EVASION: 0
TARGET MACH NO.: 2.0
INTERCEPTOR LATERAL G's: Avro 3.3
INTERCEPTOR MACH NO.: 2.0
σ OF G.C.I. ACCURACY:
A.I. DETECTION RANGE AS FRACTION OF SPECIFICATION RANGE, S:
A.I. DETECTION RANGE CONTOUR: Delta
ALTITUDE: H_{fo} = 40 K
H_t = 60 K

IR Missile

Prob. XF Snap-up

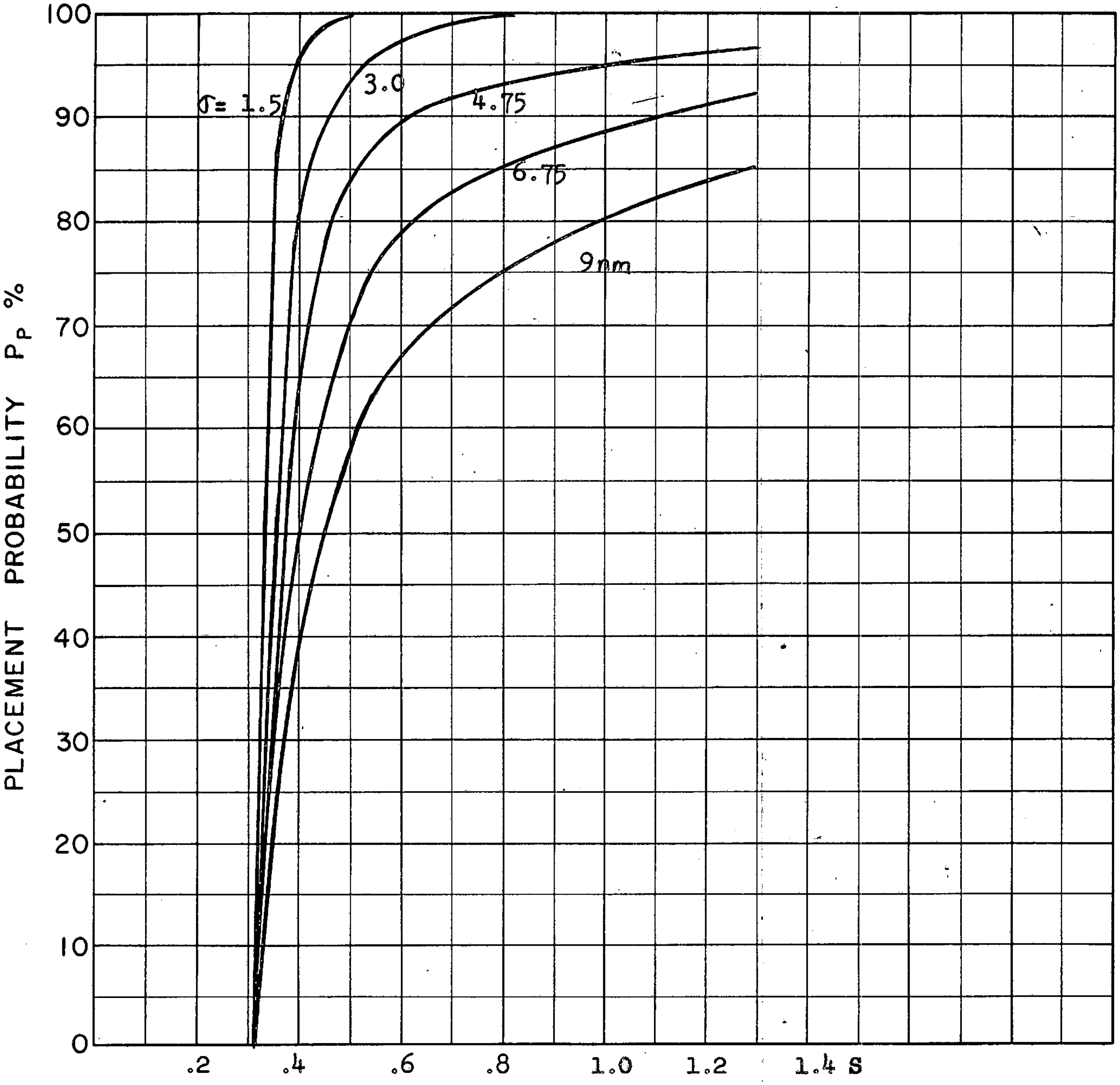

COURSE DIFFERENCE: 110°
TARGET EVASION: 0
TARGET MACH NO.: 2.0
INTERCEPTOR LATERAL G's: Avro 3.3
INTERCEPTOR MACH NO.: 2.0
σ OF G.C.I. ACCURACY: 5 Values
A.I. DETECTION RANGE AS FRACTION OF SPECIFICATION RANGE, S: Abscissa
A.I. DETECTION RANGE CONTOUR: Delta
ALTITUDE: H_t = 60 K
H_{fo} = 40 K

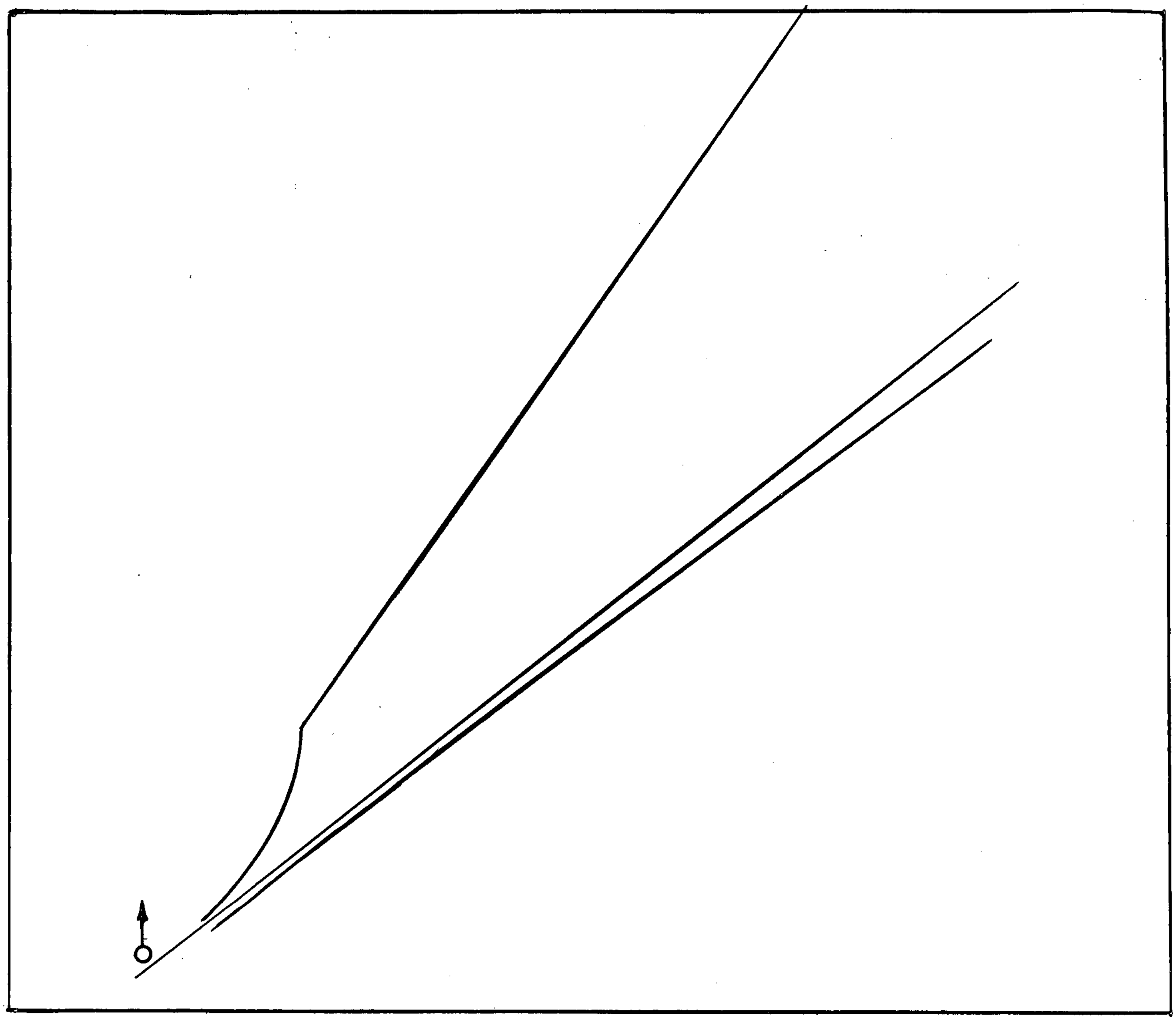

M_t = 2.0 h_t = 60 K Scale = 25,000 ft/cm

M_{fo} = 2.0 h_f = 60 K

Γ_o = 75°

IR Missile

Prob. XG

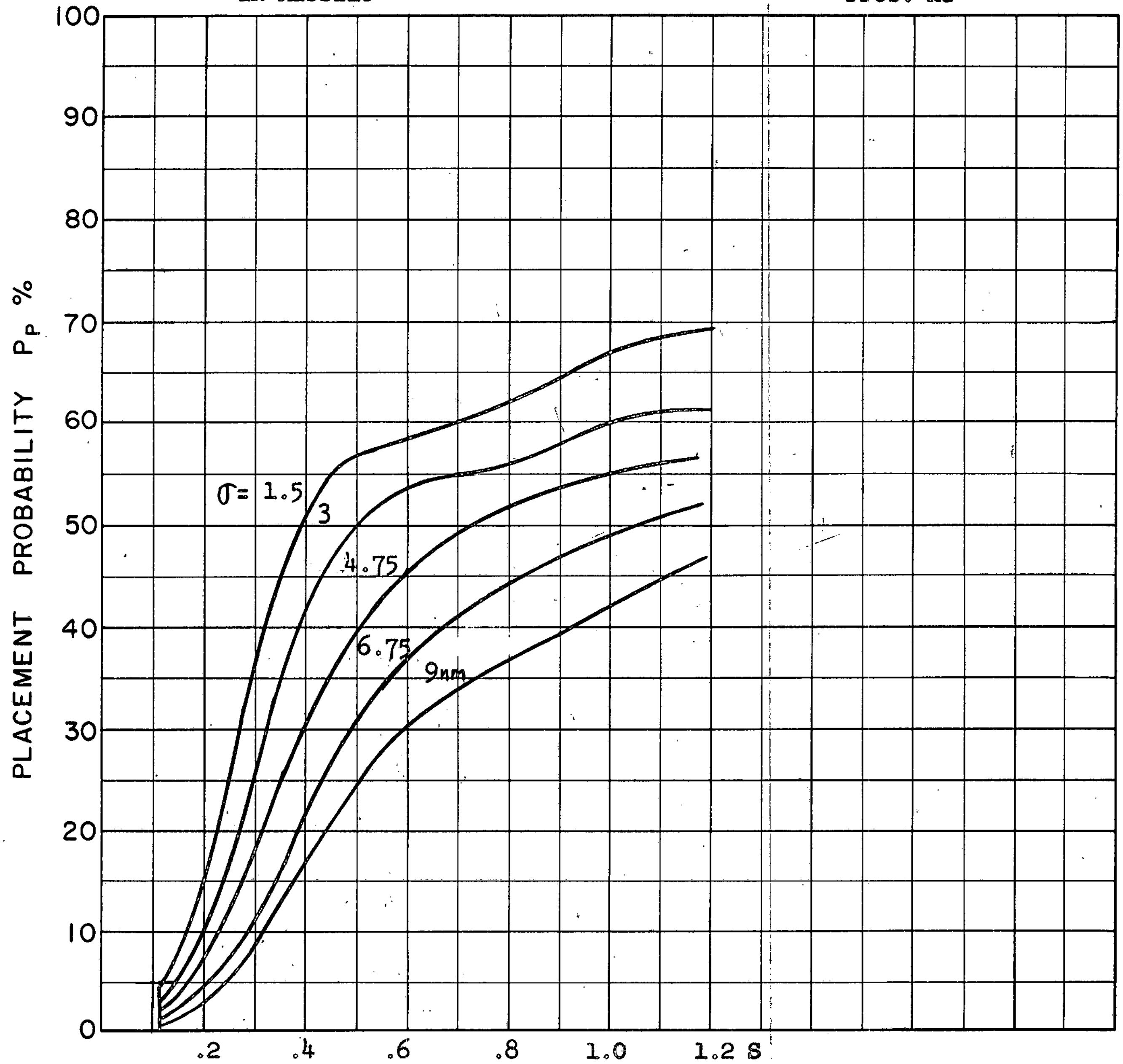

COURSE DIFFERENCE: 75°
TARGET EVASION: 0
TARGET MACH NO.: 2.0
INTERCEPTOR LATERAL G's: Avro 3.3
INTERCEPTOR MACH NO.: 2.0
σ OF G.C.I. ACCURACY: 5 Values
A.I. DETECTION RANGE AS FRACTION OF SPECIFICATION RANGE, S: Abscissa
A.I. DETECTION RANGE CONTOUR: Delta
ALTITUDE: H_{fo} = 60 K

H_t = 60 K

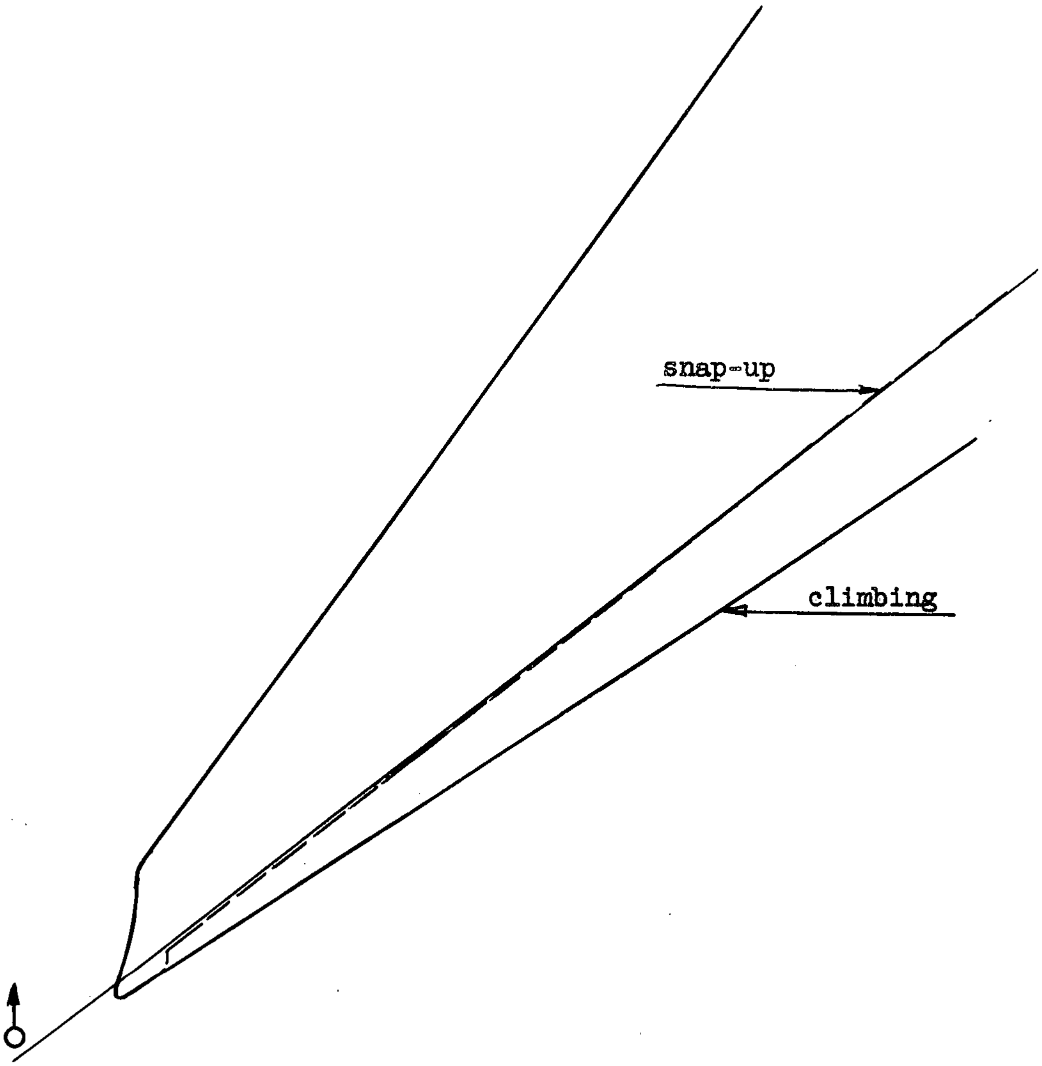

M_t = 2.0 h_t = 60 K Scale 25,000 ft/cm

M_{fo} = 2.0 h_{fo} = 40 K

Γ_o = 75°

IR Missile Prob. XH Snap-Up

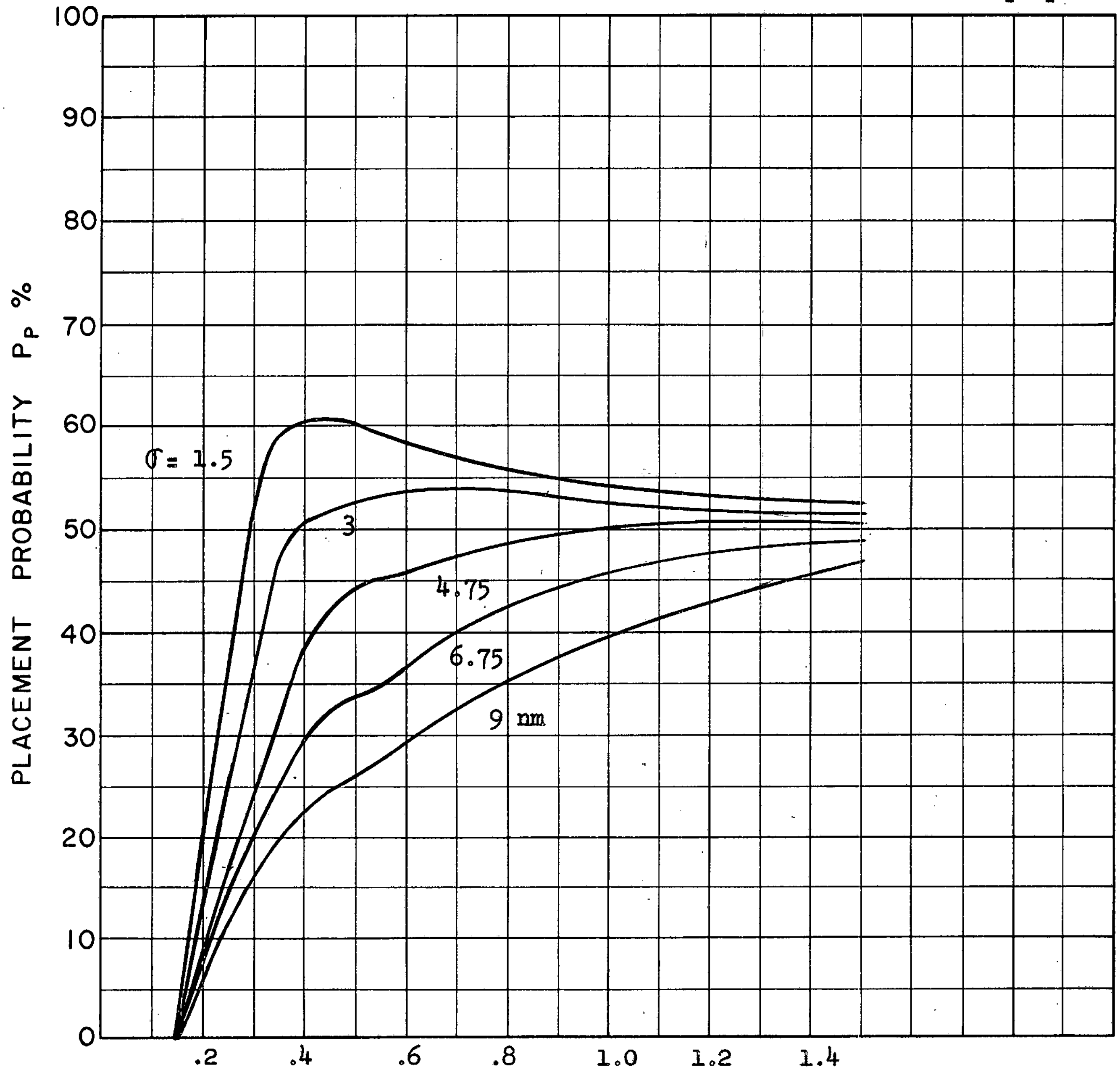

COURSE DIFFERENCE: 75°
TARGET EVASION: 0
TARGET MACH NO.: 2.0
INTERCEPTOR LATERAL G's: Avro 3.3
INTERCEPTOR MACH NO.: 2.0
σ OF G.C.I. ACCURACY: 5 Values
A.I. DETECTION RANGE AS FRACTION OF SPECIFICATION RANGE, S: Abscissa
A.I. DETECTION RANGE CONTOUR: Delta
ALTITUDE: H_t = 60 K
H_{fo} = 40 K

Climbing Attacks

The results are generally the same as for coaltitude attacks but at short ranges a high probability region appears as with the high interceptor climb angles involved the exhaust plumes become visible from below.

Snap-Up Attacks

Are very successful for course difference greater than 110°. The technique is to fly level until at close range and snap-up. The exhaust plumes are visible from below when the missile is launched. The precise configuration of the region from which the fighter must climb for a successful attack depends on data which is only known approximately. The results must be accepted as qualitatively correct but may be subject to numerical changes due to seeker characteristics, target IR emission contour and angle of attack.

4.4.1.0 Infra-Red A.I. Studies - Problem XI

Under jammed conditions or in the event of failure of the microwave radar, the infra-red A.I. system may be used.

If the infra-red detector is housed in the tail of the fighter (ref. 6) the wings and fuselage may obscure its view of the target while maneuvering into position to launch the missiles. The new look angle limits resulting from this situation have a significant effect on placement probability. The study is broken up into several sections to show which parameters are significant in going from microwave AI to IR AI with its corresponding look angle limits.

4.4.1.2 Problem XI Conditions

IR LOOK ANGLE LIMIT STUDY

	A	B	C	D	E	F
h_{fo}	60K	40K	60K	40K	60K	40K
Γ_o	180°		135°		110°	

$F = 7K$, $t_f = 8$ sec, $h_t = 60$ K,

$V_t = M2.0$ $V_{fo} = M2.0$

IR AI Phase

Prob. XI A

(IR Providing Angle Data)

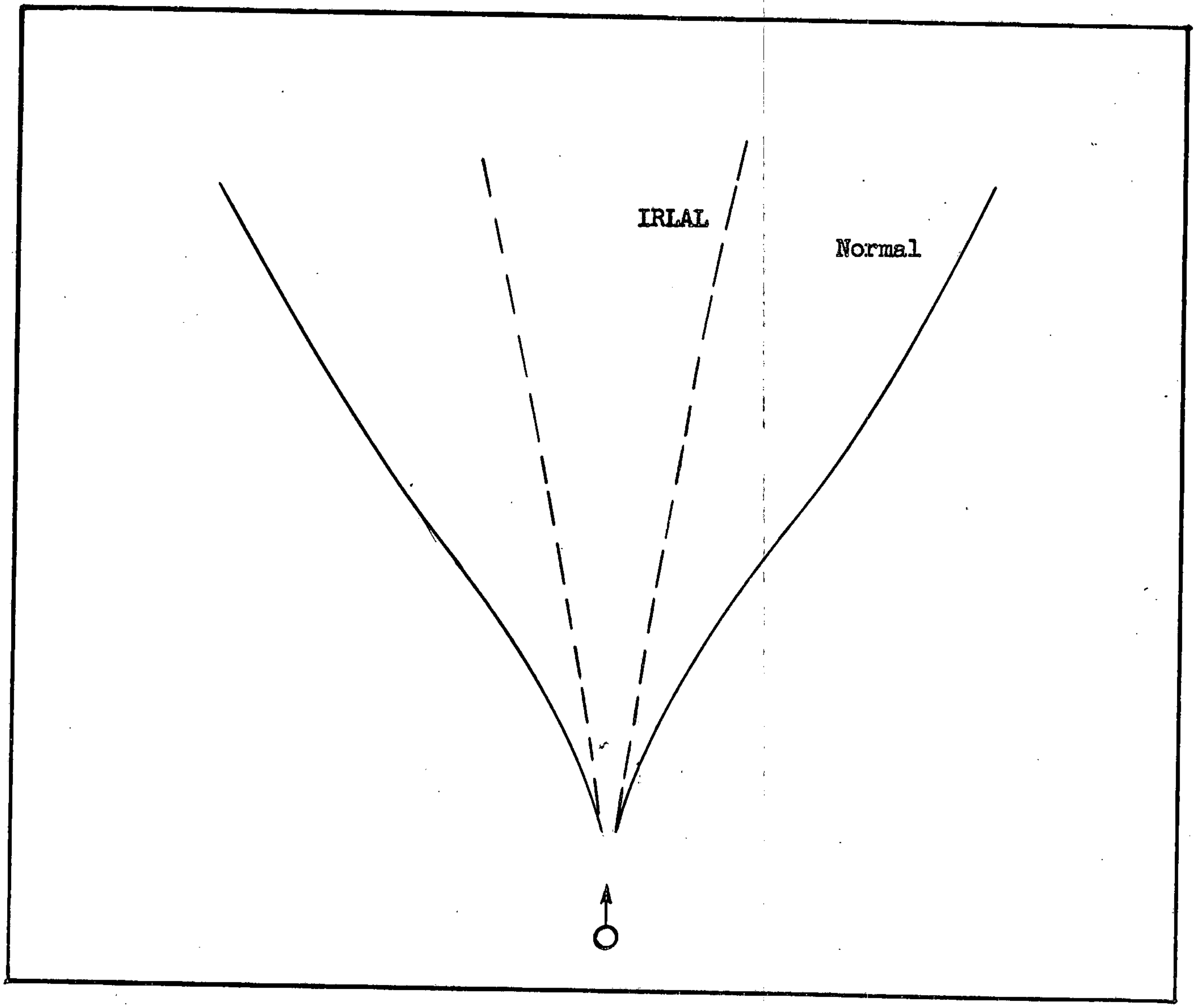

M_t = 2.0 h_t = 60 K

$M_{f\delta}$ = 2.0 h_f = 60 K

Γ_o = 180°

Scale 25,000 ft/cm

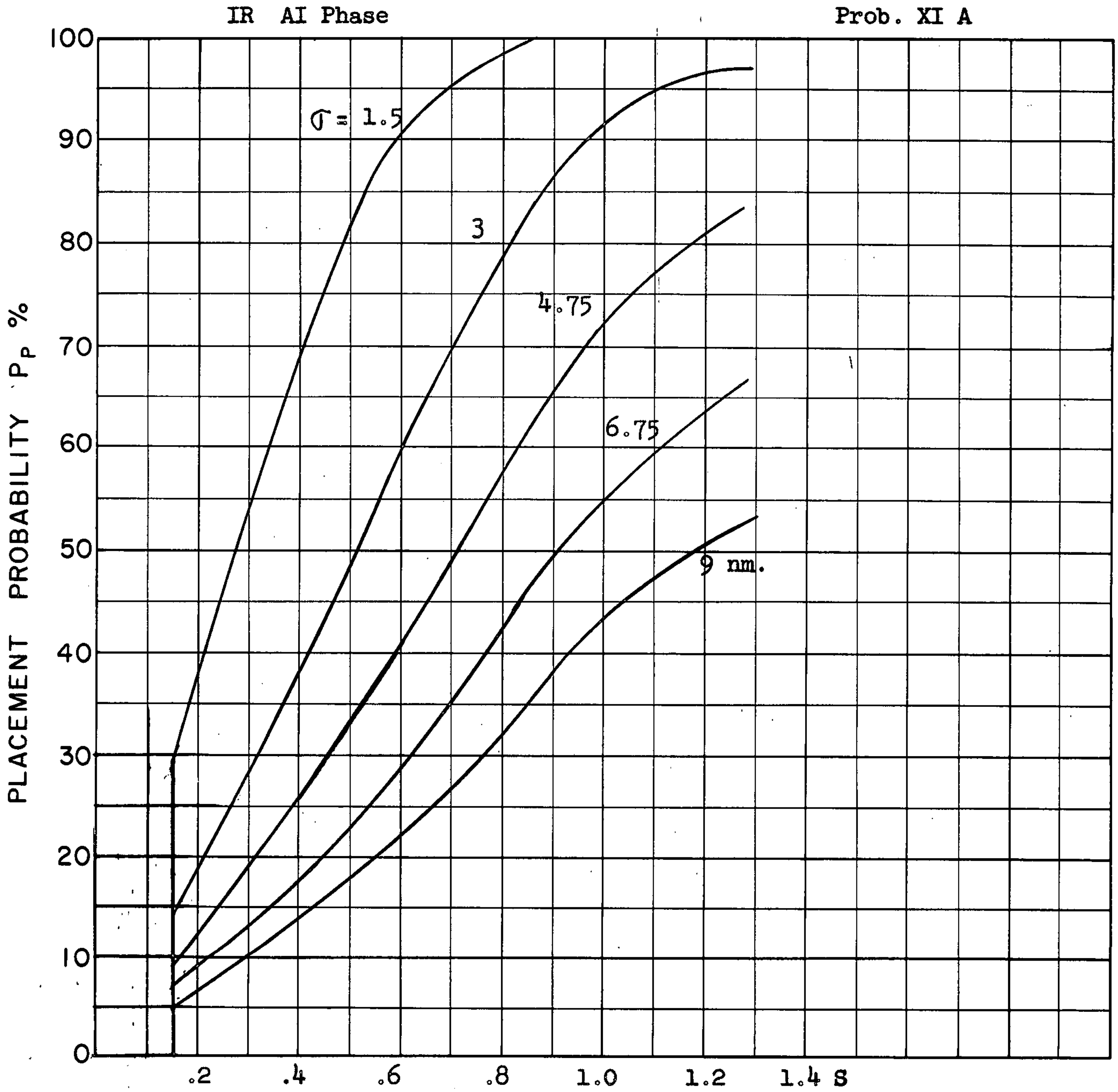

COURSE DIFFERENCE: 180°
TARGET EVASION: 0
TARGET MACH NO.: 2.0
INTERCEPTOR LATERAL G's: Avro 3.3
INTERCEPTOR MACH NO.: 2.0
σ OF G.C.I. ACCURACY: 5 Values
A.I. DETECTION RANGE AS FRACTION OF SPECIFICATION RANGE, S: Abscissa
A.I. DETECTION RANGE CONTOUR: Delta
ALTITUDE: 60 K

IR AI Phase Prob. XI B

(IR Providing Angle Data)

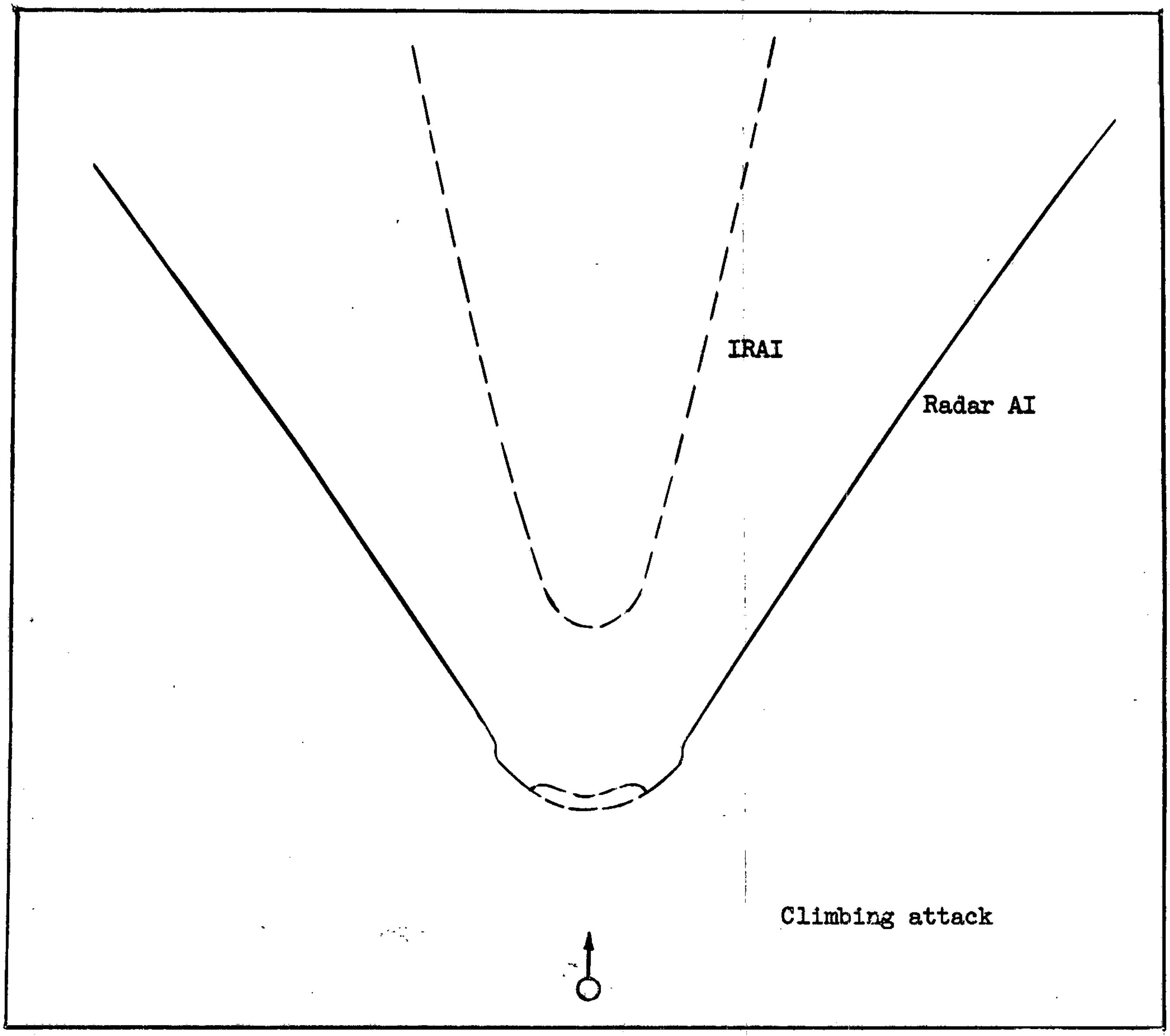

M_t = 2.0 h_t = 60 K Scale 25,000 ft/cm

M_{fo} = 2.0 h_{fo} = 40 K

$_o$ = 180^o

IR AI Phase

Prob. XI B

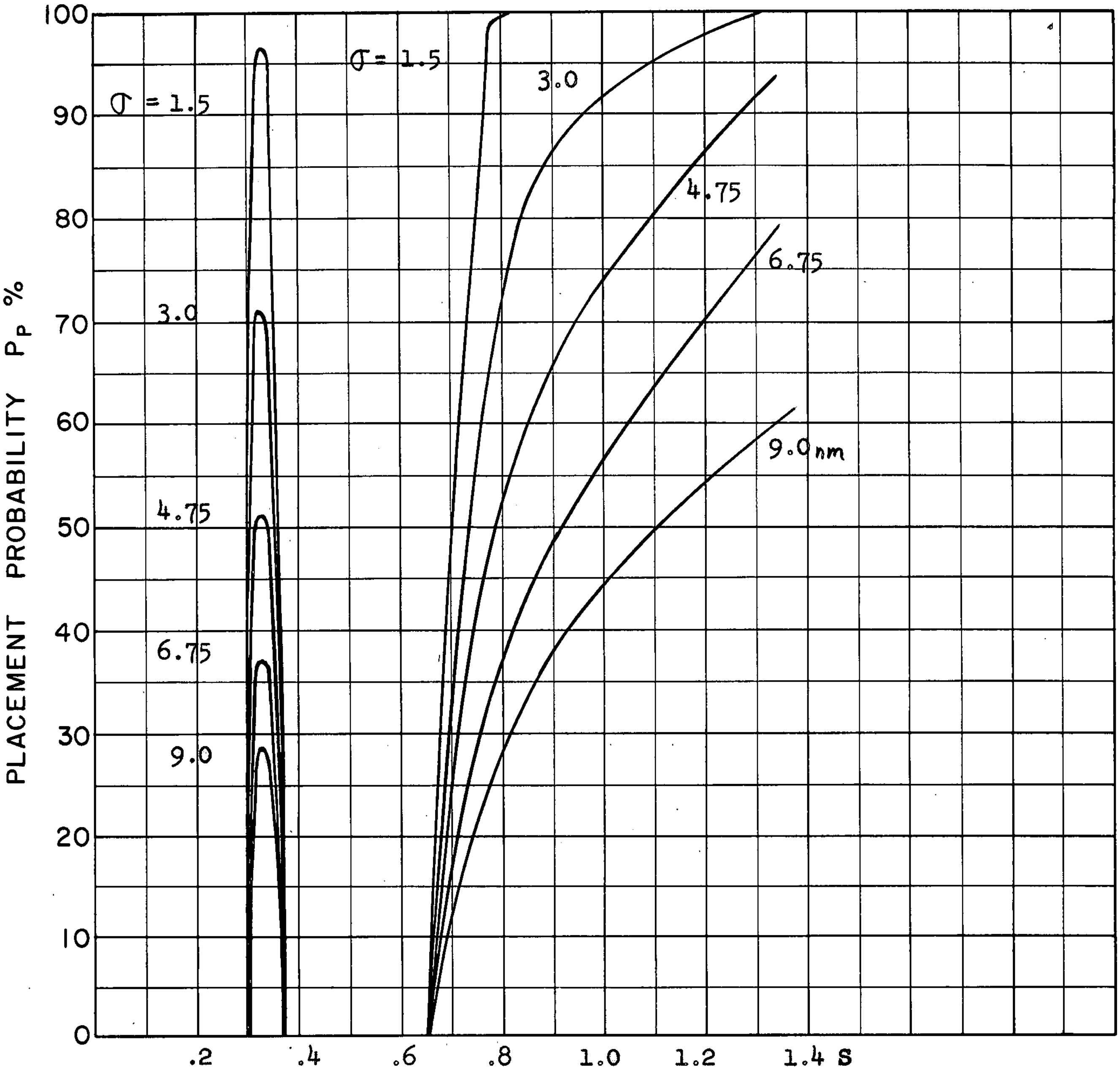

COURSE DIFFERENCE: 180°
TARGET EVASION: 0
TARGET MACH NO.: 2.0
INTERCEPTOR LATERAL G's: Avro 3.3
INTERCEPTOR MACH NO.: 2.0
σ OF G.C.I. ACCURACY: 5 Values
A.I. DETECTION RANGE AS FRACTION OF SPECIFICATION RANGE, S: Abscissa
A.I. DETECTION RANGE CONTOUR: Delta
ALTITUDE: H_t = 60 K
H_{fo} = 40 K

IR AI Phase

(IR providing angle data)

Prob. XI C

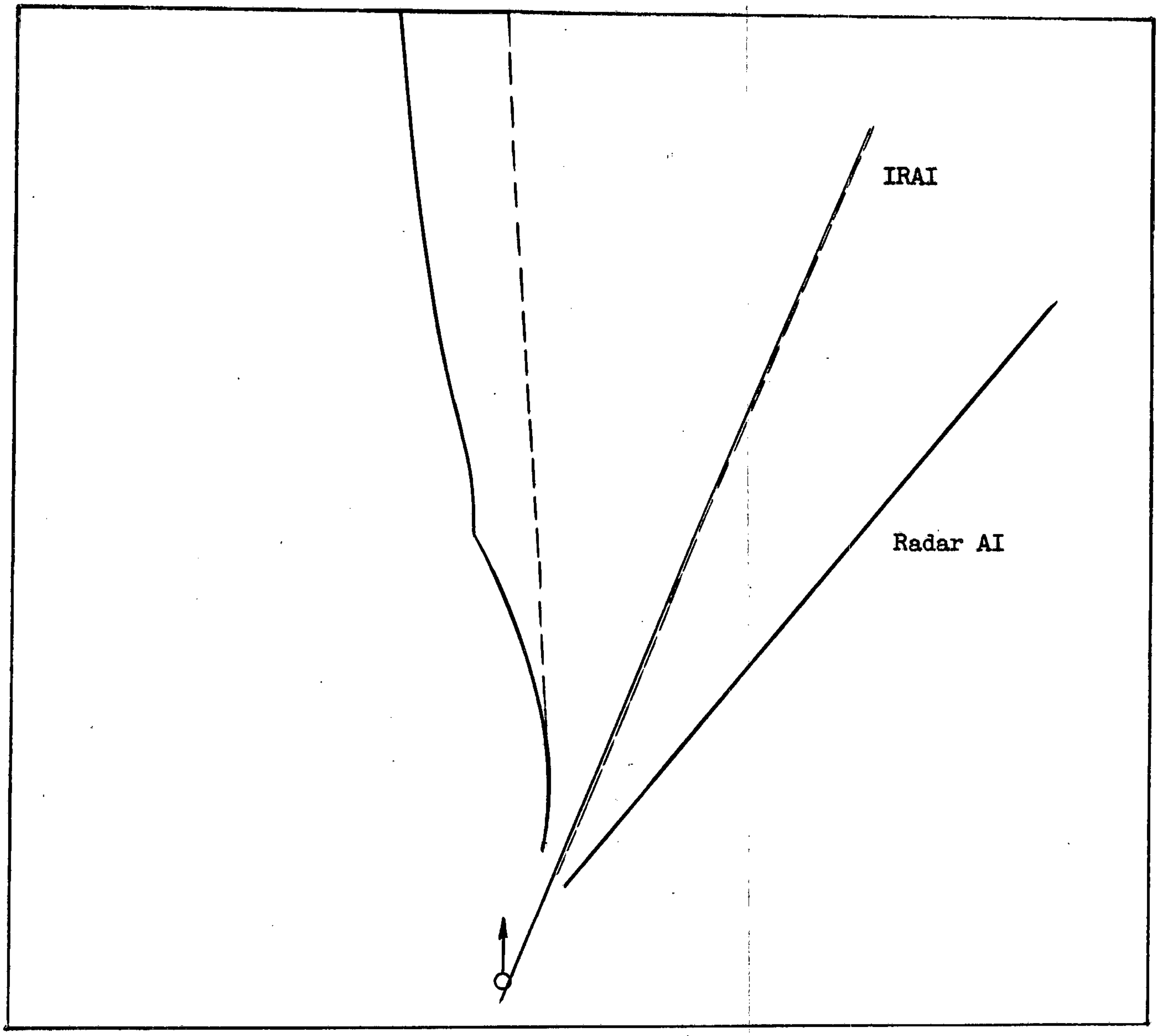

M_t = 2.0 h_t = 60 K

M_{fo} = 2.0 h_f = 60 K

Γ_o = 135°

Scale 25,000 ft/cm

IR AI Phase

Prob. XI C

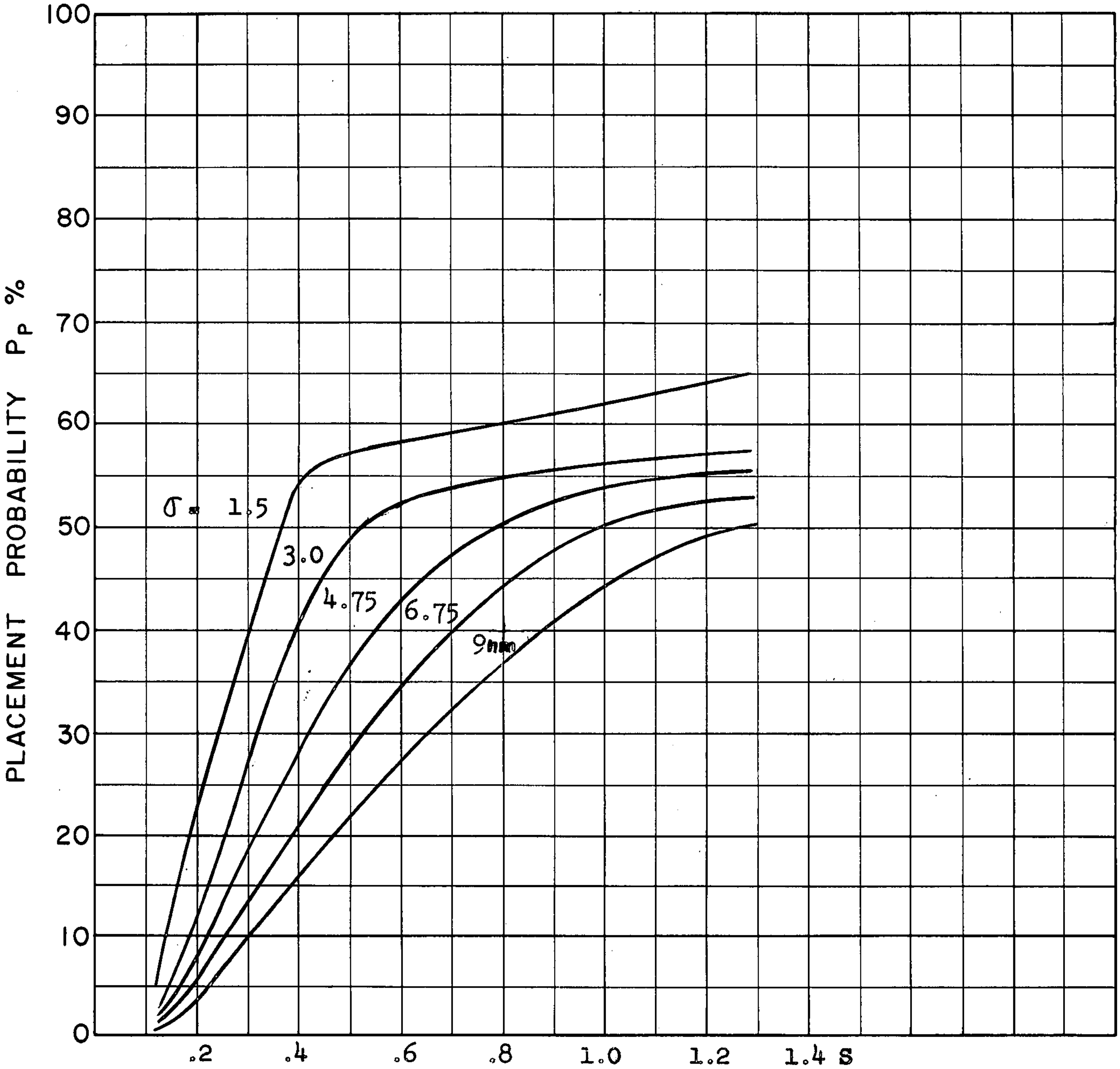

COURSE DIFFERENCE: 135°
TARGET EVASION: 0
TARGET MACH NO.: 2.0
INTERCEPTOR LATERAL G's: Avro 3.3
INTERCEPTOR MACH NO.: 2.0
σ OF G.C.I. ACCURACY: 5 Values
A.I. DETECTION RANGE AS FRACTION OF SPECIFICATION RANGE, S: Abscissa
A.I. DETECTION RANGE CONTOUR: Delta
ALTITUDE: H_f = 60K
H_t = 60 K

IR AI Phase

(IR providing angle data)

Prob. XI D

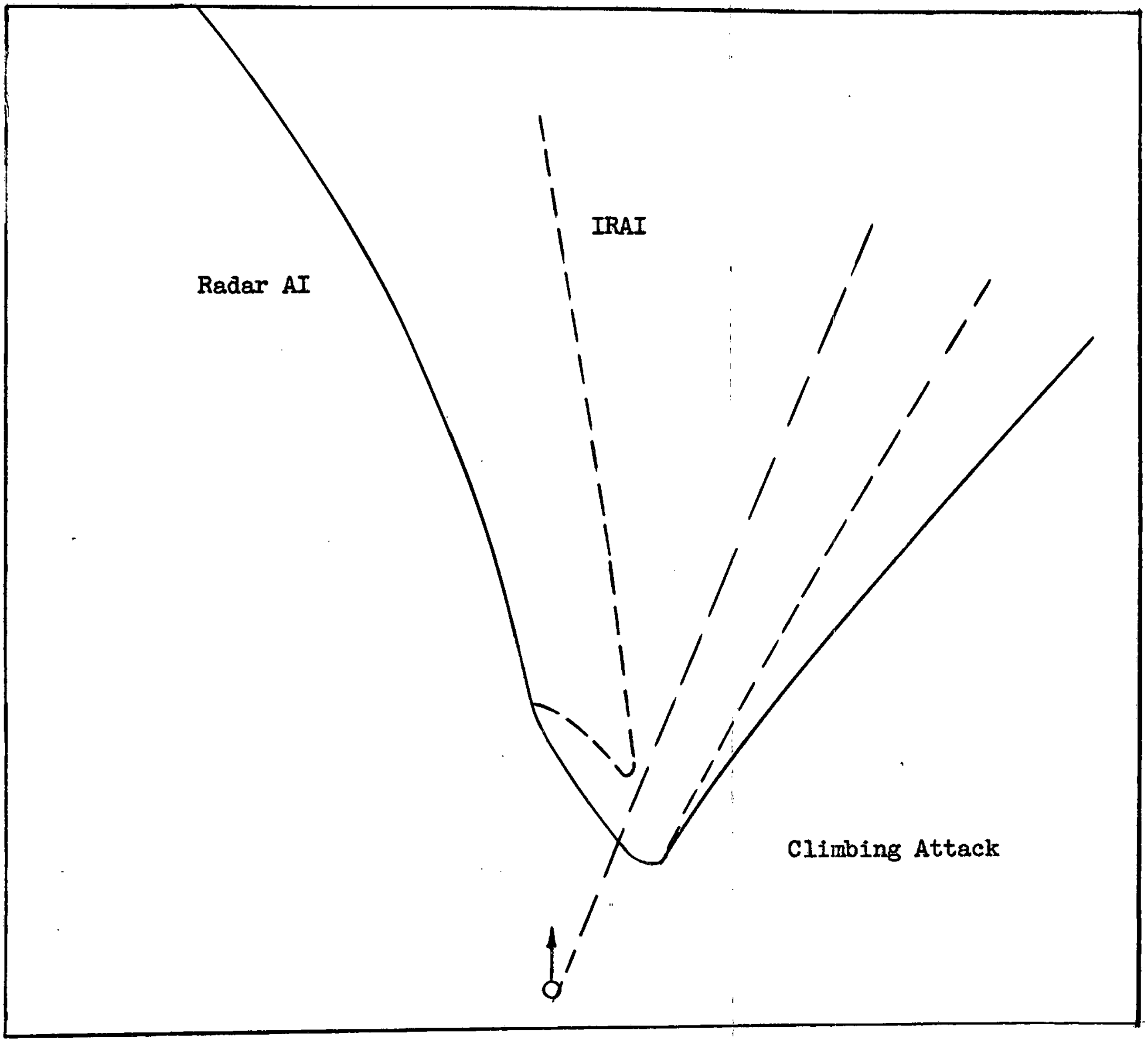

M_t = 2.0 h_t = 60 K

M_{fo} = 2.0 h_{fo} = 40 K

Γ_o = 135°

Scale 25,000 ft/cm

IR AI Phase

Prob. XI D

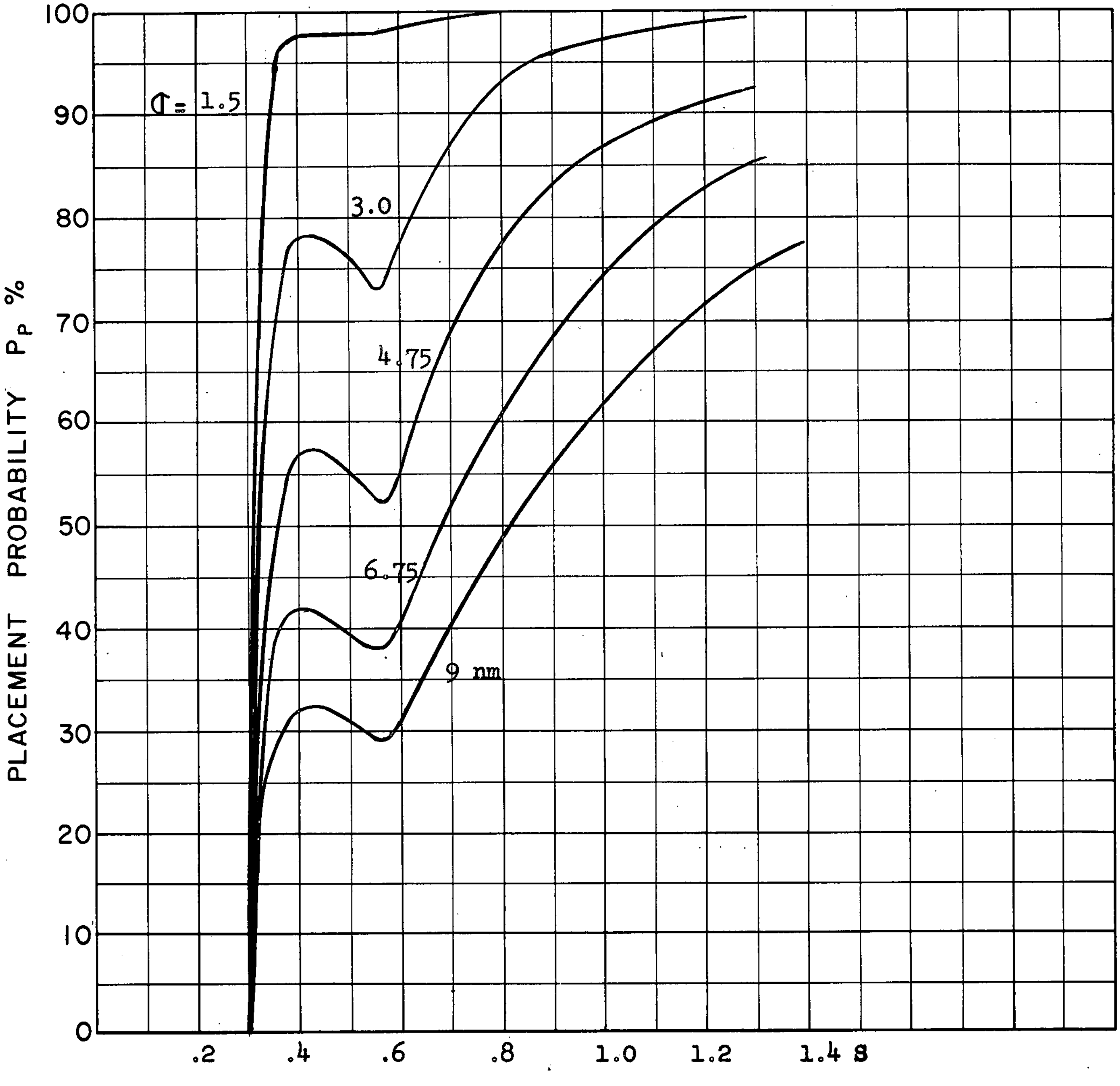

COURSE DIFFERENCE: 135^{o}
TARGET EVASION: 0
TARGET MACH NO.: 2.0
INTERCEPTOR LATERAL G's: Avro 3.3
INTERCEPTOR MACH NO.: 2.0
σ OF G.C.I. ACCURACY: 5 Values
A.I. DETECTION RANGE AS FRACTION OF SPECIFICATION RANGE, S: Abscissa
A.I. DETECTION RANGE CONTOUR: Delta
ALTITUDE: H_{fo} = 40 K

H_t = 60 K

IR AI Phase

Prob. XI E

(IR providing angle data)

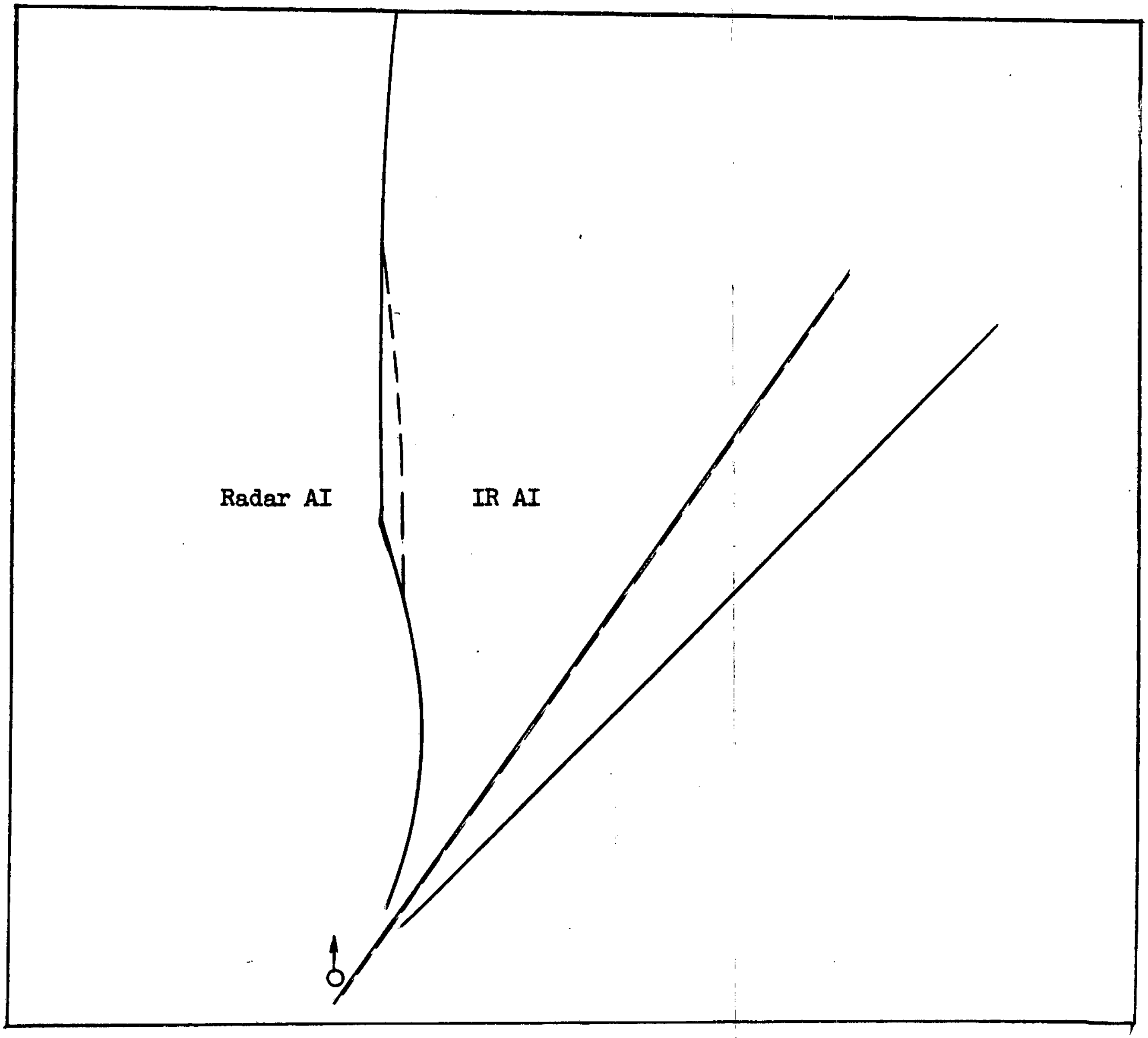

M_t = 2.0 h_t = 60 K Scale 25,000 ft/cm

M_{fo} = 2.0 h_{fo} = 60 K

Γ_o = 110°

IR AI Phase Prob. XI E

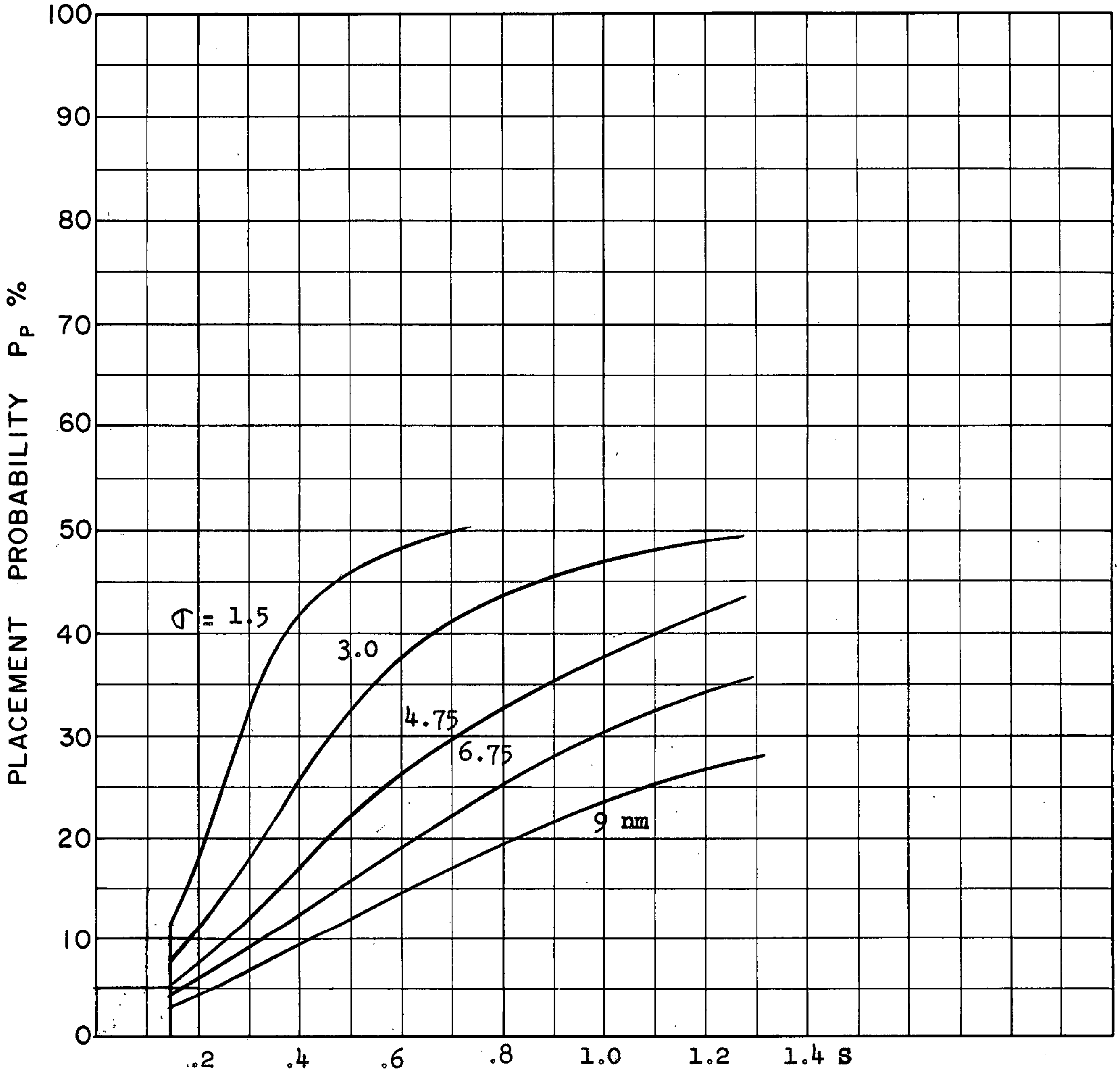

COURSE DIFFERENCE: 110°
TARGET EVASION: 0
TARGET MACH NO.: 2.0
INTERCEPTOR LATERAL G's: Avro 3.3
INTERCEPTOR MACH NO.: 2.0
σ OF G.C.I. ACCURACY: 5 Values
A.I. DETECTION RANGE AS FRACTION OF SPECIFICATION RANGE, S: Abscissa
A.I. DETECTION RANGE CONTOUR: Delta
ALTITUDE: $H_{fo} = H_t = 60$ K

IR AI Phase

(IR providing angle data)

Prob. XI F

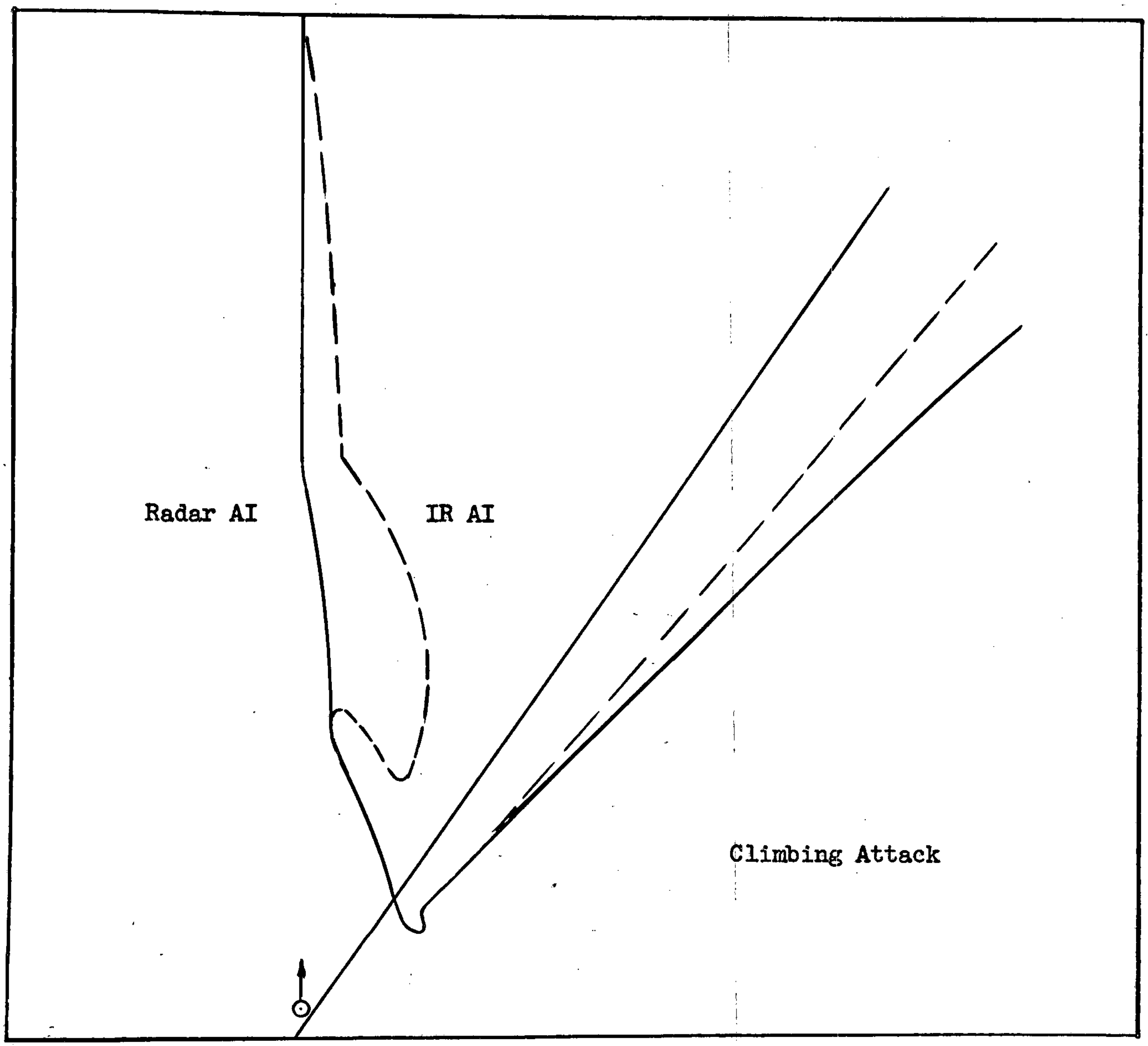

M_t = 2.0 h_t = 60 K

M_{fo} = 2.0 h_{fo} = 40 K

Γ_o = 110°

Scale 25,000 ft/cm

IR AI Phase

Prob. XI F

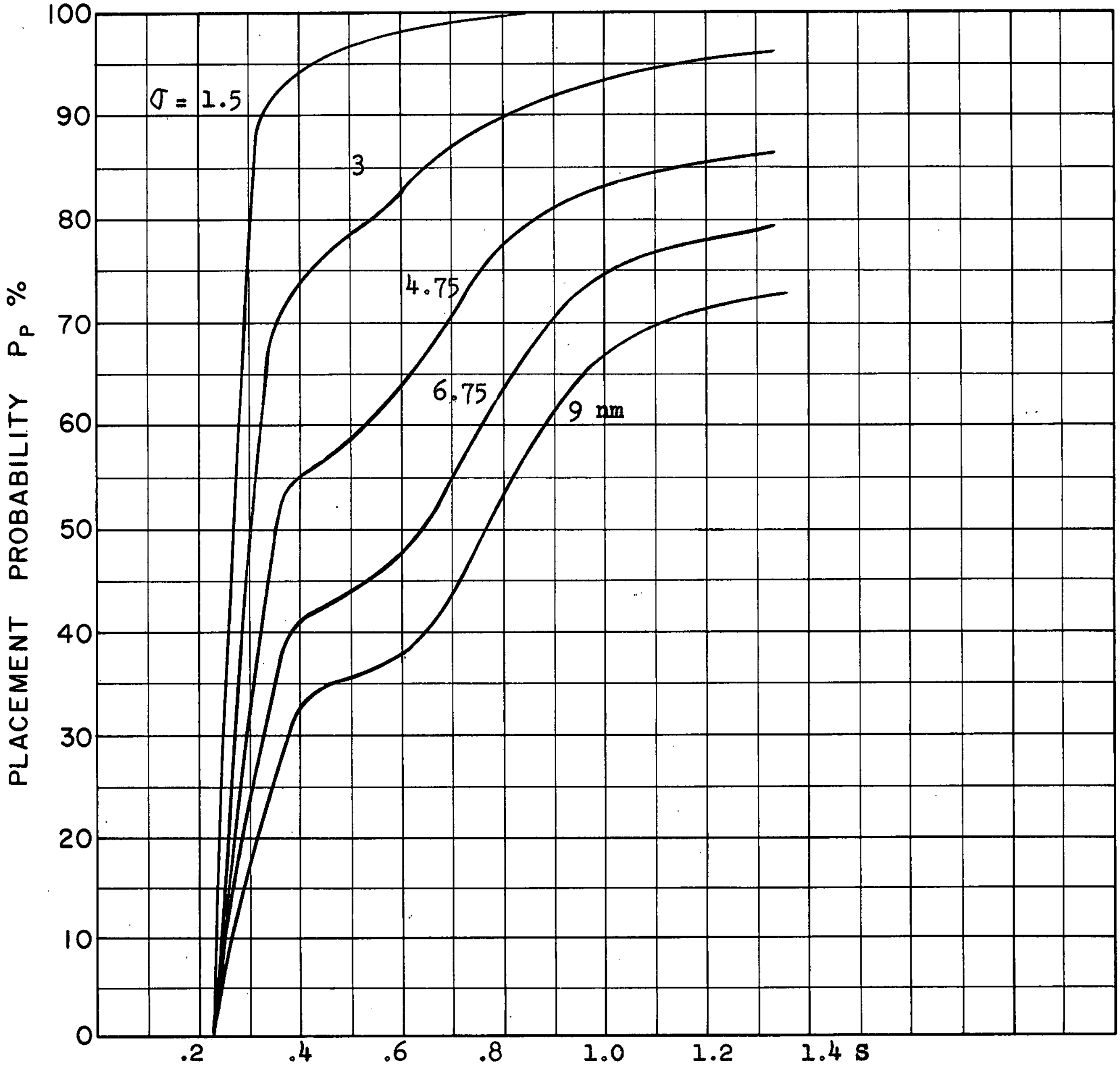

COURSE DIFFERENCE: 110°
TARGET EVASION: 0
TARGET MACH NO.: 2.0
INTERCEPTOR LATERAL G's: Avro 3.3
INTERCEPTOR MACH NO.: 2.0
σ OF G.C.I. ACCURACY: 5 Values
A.I. DETECTION RANGE AS FRACTION OF SPECIFICATION RANGE, S: Abscissa
A.I. DETECTION RANGE CONTOUR: Delta
ALTITUDE: H_t = 60 K

H_{fo} = 40 K

4.4.1.3 In this situation the placement probability is reduced to 50% for course differences less than 180° because maneuvers in one direction only are permitted.

4.4.2.0 Study of Fixed Range Lead Pursuit Navigation with Cross-Over (called "Fixed R & T" in ref. 7) - Problem XII

For IR AI controlled navigation some system which relies on angular information only is used. This study used fixed range lead pursuit. (refs.7 & 8) As jamming intensity varies as $\frac{1}{R^2}$ and microwave radar return signal varies as $\frac{1}{R^4}$, a cross-over may occur, the range becoming sufficiently short for jamming to be no longer effective. In this study it was assumed that when the missiles were launched, range information would be available and the launch zone could be defined by time-to-go equals a constant.

The time-to-go which was selected was 8 secs. This figure corresponds fairly closely to the minimum time to lower, to lock on and to launch the missile.

4.4.2.1 Conditions for Fixed Parameter Study with Cross-Over

$V_{fo} = V_t = M1.5 \qquad h_f = h_t = 50\ K$

$\Delta V = M1.0 \qquad t_f = 8$ secs.

$\Gamma_o = 180^\circ \quad 135^\circ \quad 110^\circ$

This problem was run for normal and IR look angle limits. This is a practical problem and the comparison shows what is sacrificed by reducing the look angle limits. The case with normal L.A. limits corresponds to radar homing under jammed conditions and is dealt with in detail in reference 8.

The AI detector range contour which is appropriate is the IR emission contour of the target.

4.4.2.2 Conclusions

The placement zones show the effect of changing the look angle limits. These differences have been reduced to probabilities (see below)

For initial course differences of 180° there is a high placement probability. Two factors are in conflict in this problem:-

(1) Fixed R & T navigation is most effective for course differences near 180°

Fixed Range Lead Pursuit with Cross-over

Prob. XII A

Effect of IR LOOK ANGLE LIMITS

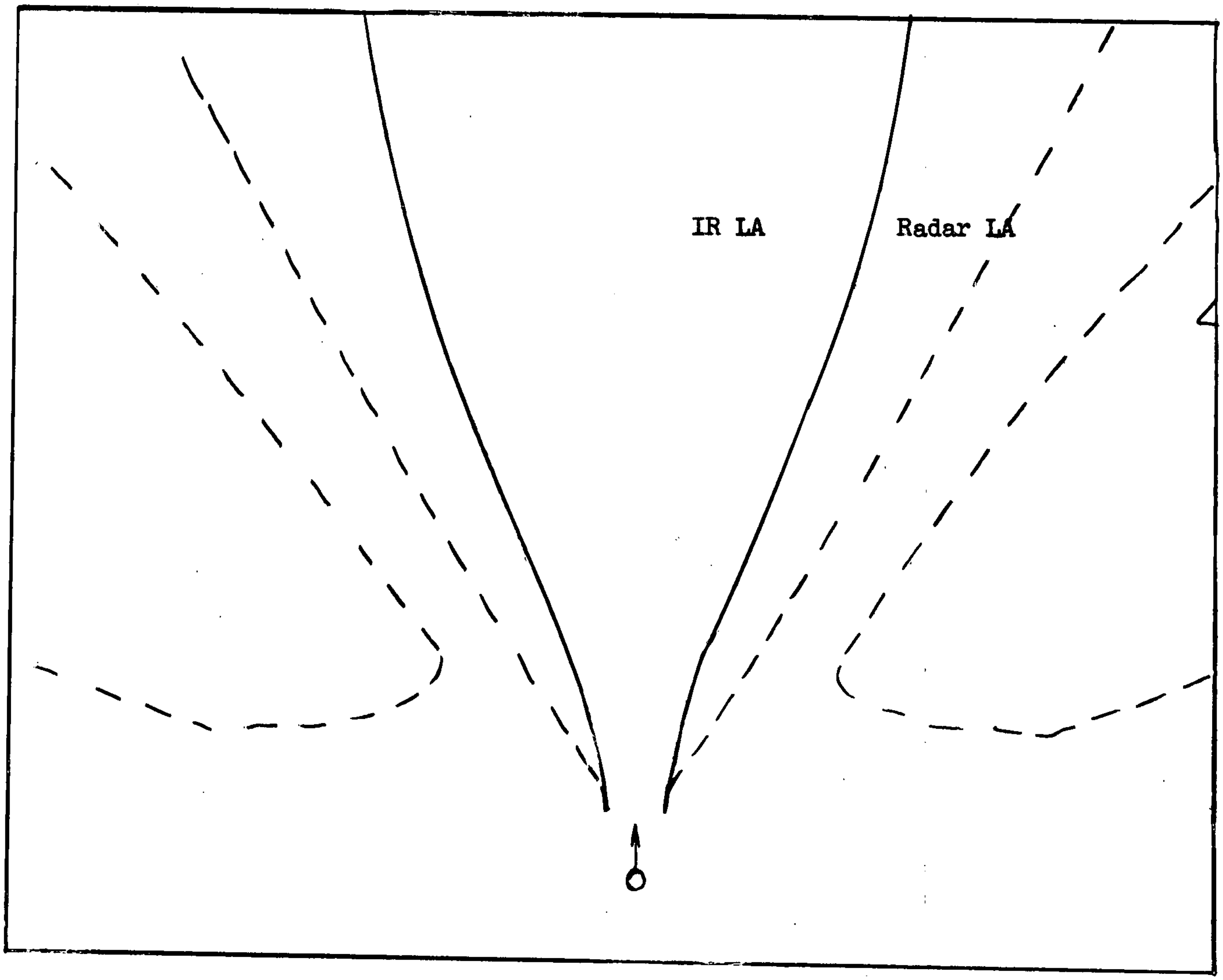

M_t = 1.5 h_t = 50 K

M_{fo} = 1.5 h_{fo} = 50 K

Γ_o = 180°

Scale 25,000 ft/cm

Fixed Range Lead Pursuit with Cross-over   Prob. XII A

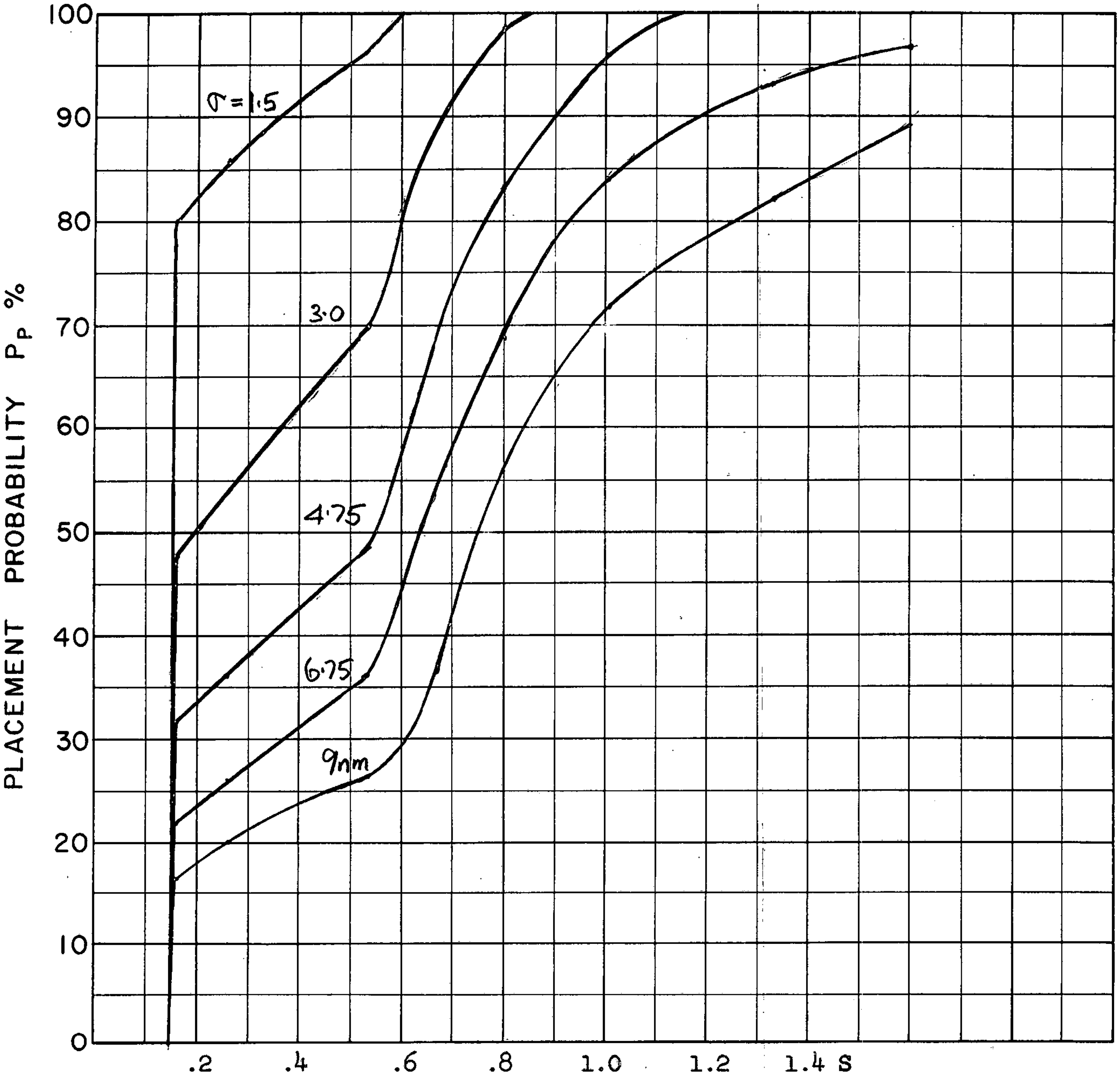

COURSE DIFFERENCE: 180°
TARGET EVASION: 0
TARGET MACH NO.: 1.5
INTERCEPTOR LATERAL G's: Avro 3.3
INTERCEPTOR MACH NO.: 1.5
σ OF G.C.I. ACCURACY: 5 Values
A.I. DETECTION RANGE AS FRACTION OF SPECIFICATION RANGE, S: Abscissa
A.I. DETECTION RANGE CONTOUR: 3 x B 52 IR Contour *
ALTITUDE: 50 K

* This can be expected from a M1.5 target but if IR emission is less, abscissa should be rescaled accordingly.

Fixed Range Lead Pursuit with Cross-over | Prob. XII B

Effect of IR LOOK ANGLE LIMITS

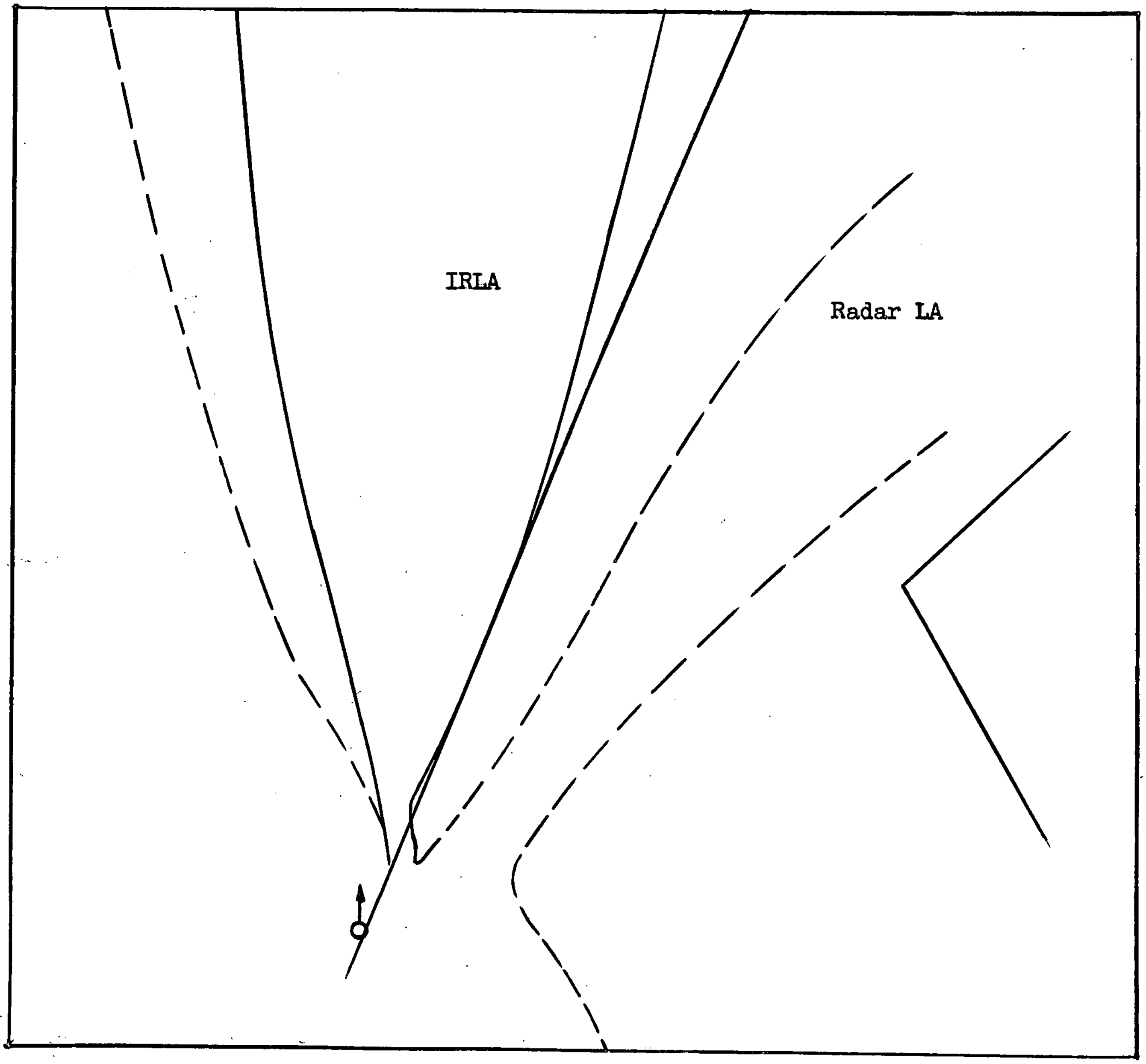

M_t = 1.5 h_t = 50 K Scale 25,000 ft/cm

M_{fo} = 1.5 h_{fo} = 50 K

Γ_o = 135°

Fixed Range Lead Pursuit with Cross-over   Prob. XII B

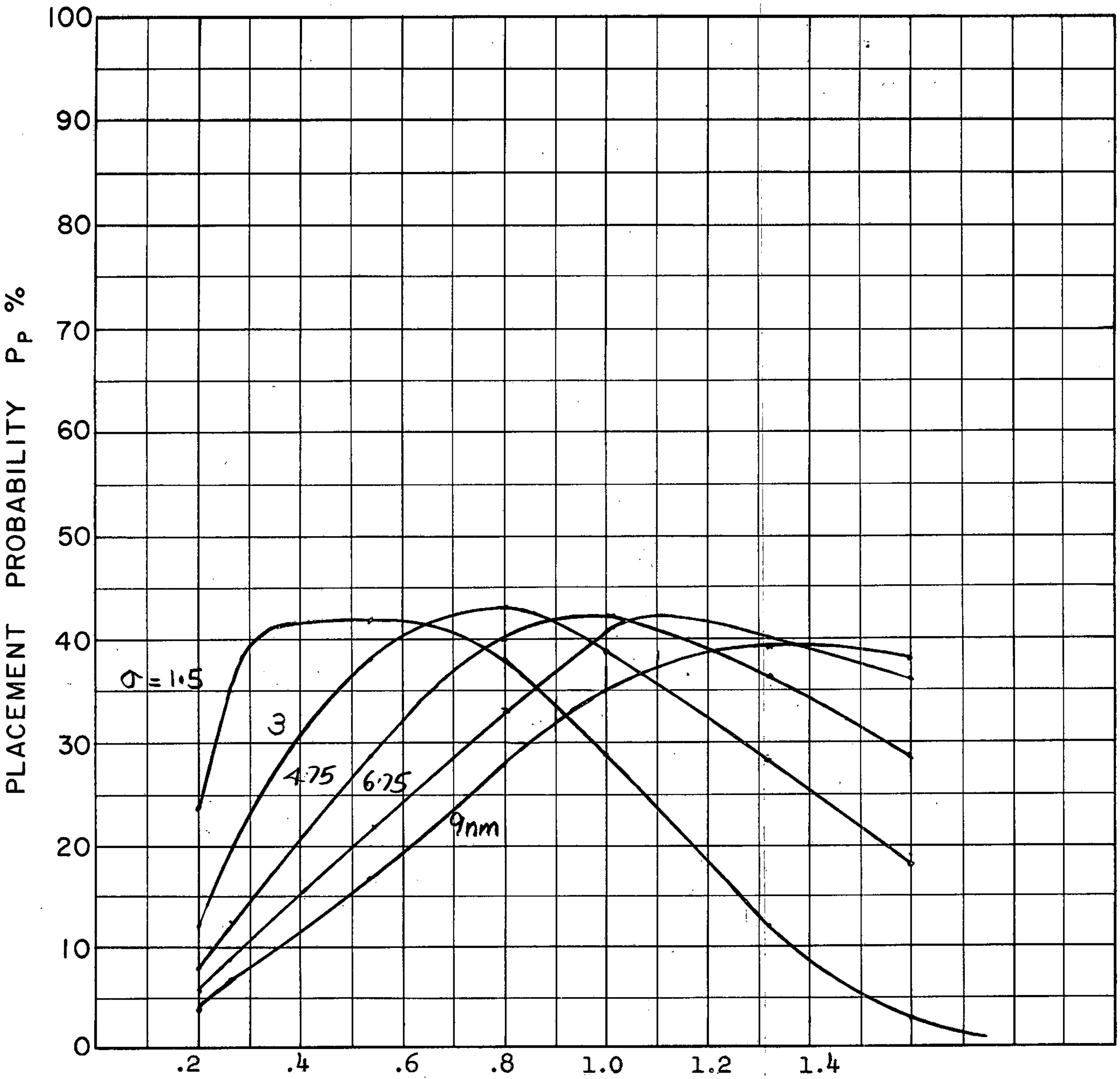

COURSE DIFFERENCE: 135°
TARGET EVASION: 0
TARGET MACH NO.: 1.5
INTERCEPTOR LATERAL G's: Avro 3.3
INTERCEPTOR MACH NO.: 1.5
σ OF G.C.I. ACCURACY: 5 Values
A.I. DETECTION RANGE AS FRACTION OF SPECIFICATION RANGE, S: Abscissa
A.I. DETECTION RANGE CONTOUR: = 3 x B 52 * IR contour
ALTITUDE: 50 K ft.

* This can be expected from a M1.5 target but if IR emission is less abscissa should be rescaled accordingly.

Fixed Range Lead Pursuit with Cross-over

Prob. XII C

Effect of IR LOOK ANGLE LIMITS

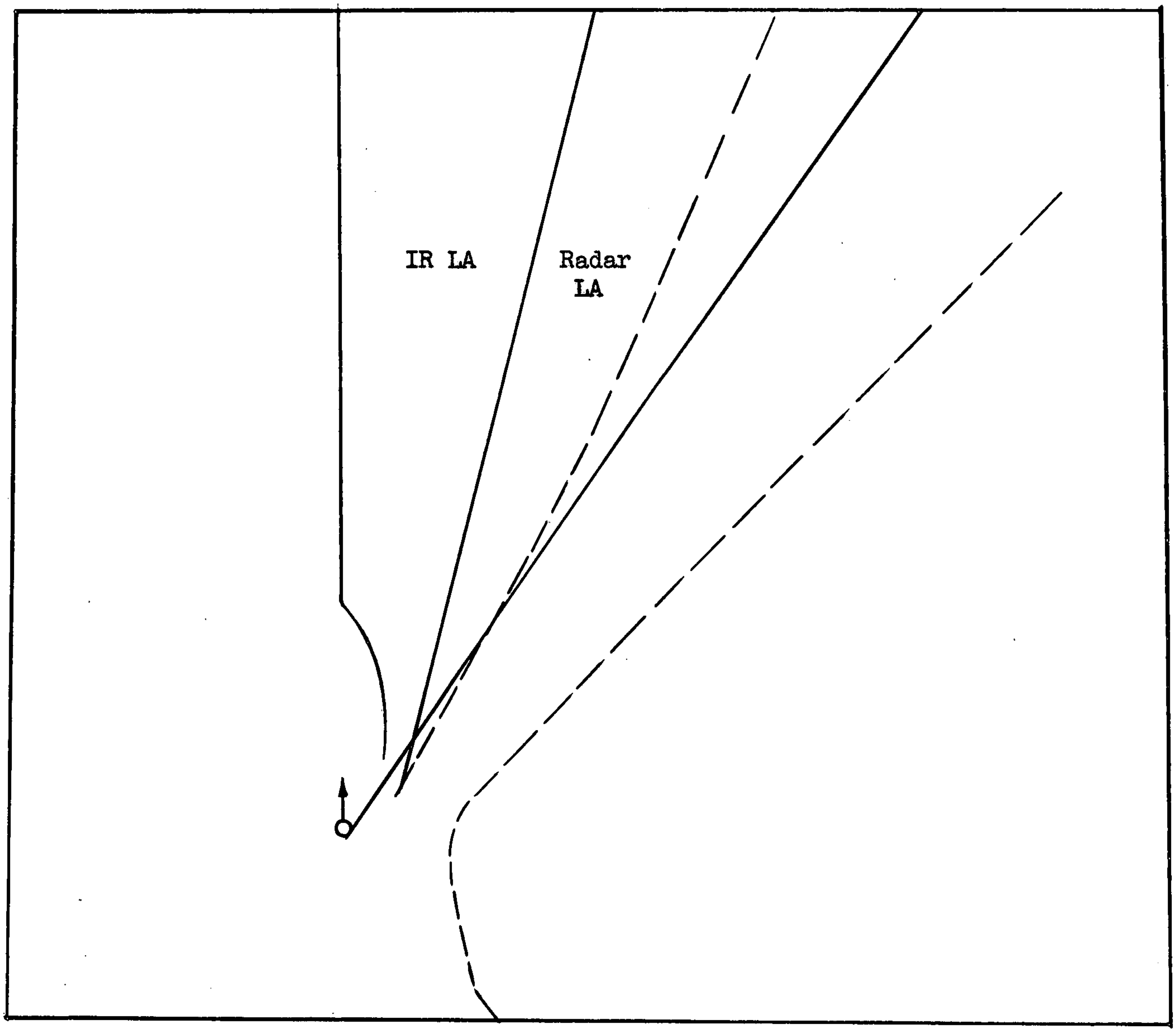

M_t = 1.5 h_t = 50 K

M_{fo} = 1.5 h_f = 50 K

Γ_o = 110°

Scale 25,000 ft/cm

Fixed Range Lead Pursuit Prob. XII C

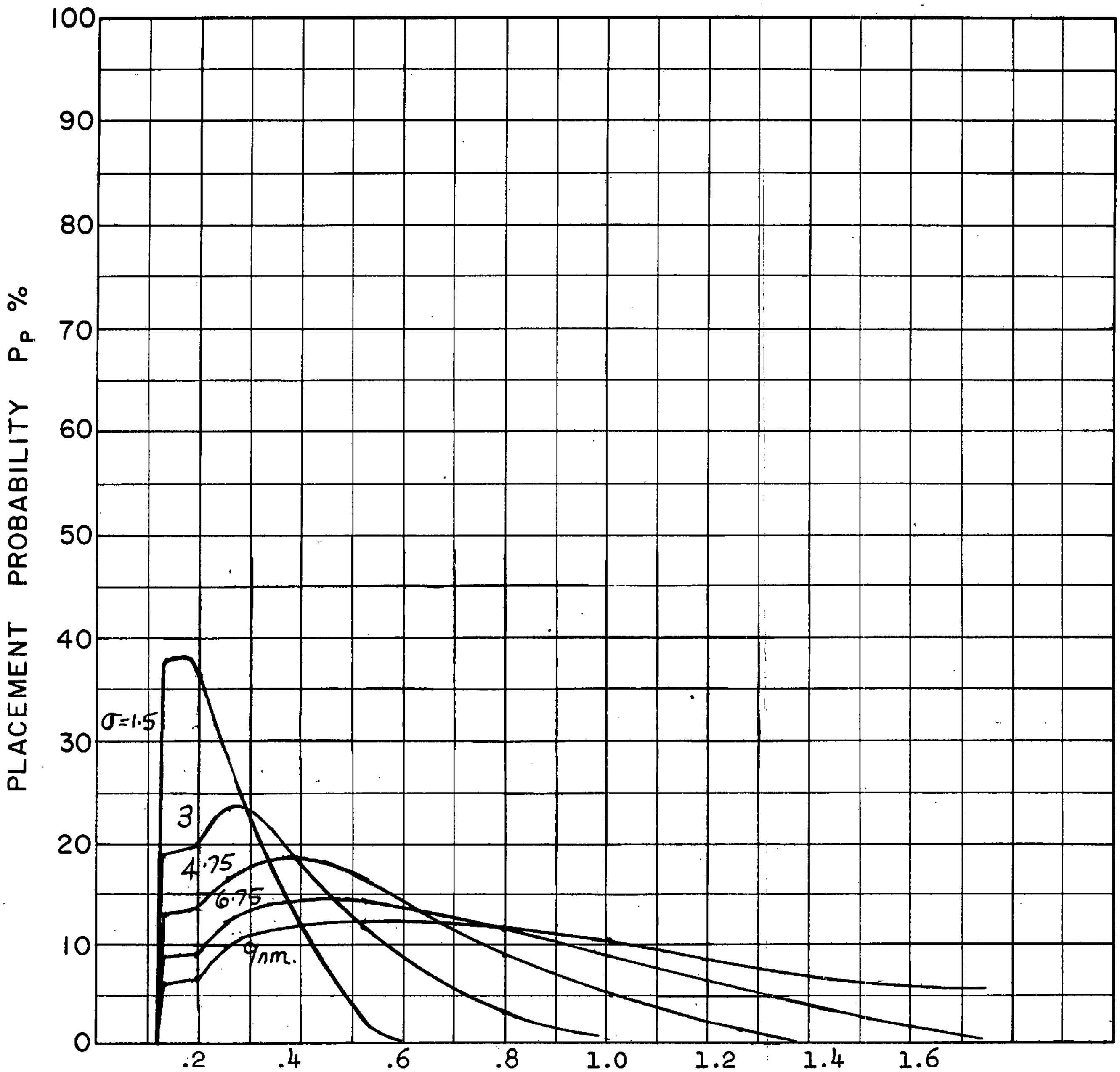

COURSE DIFFERENCE: 110°
TARGET EVASION: 0
TARGET MACH NO.: 1.5
INTERCEPTOR LATERAL G's: Avro 3.3
INTERCEPTOR MACH NO.: 1.5
σ OF G.C.I. ACCURACY: 5 Values
A.I. DETECTION RANGE AS FRACTION OF SPECIFICATION RANGE, S: Abscissa
A.I. DETECTION RANGE CONTOUR: (B 52 IR x 3) *
ALTITUDE: 50 K

* This is an estimate for a Mach 1.5 target.

(2) Course differences near 180° imply final aspects near 180° where IR detection range is low. The minimum range limitation is due to the intersection of the IR seeker range contour and the minimum successful time-to-go to launch the missile.

For a supersonic target (M1.5) acquisition ranges are expected to be of the order of 3 times those corresponding to a subsonic target.

4.4.3.0 Problem XIII - Unguided Missile Study

If the aircraft is armed with rockets instead of guided missiles, the allowable heading error at launch is very small compared with the allowable heading error in the guided missile.

The aircraft navigation system is designed to reduce the heading error to zero. The accuracy to which it achieves this was not considered in this study although of course it would be a critical factor in the actual interceptor. The attack is called a success if the heading error at launch is of the same order as the noise of the system.

4.4.3.1 Problem XIII

h_t = 60 K V_t = M2.0 V_{fo} = M2.0

F = 7 K t_f = 8 secs.

	A	B	C	D	E	F
h_{fo}	60 K	50 K	40 K	60 K	50 K	40 K
Γ_o		180°			110°	

4.4.3.2 Conclusions

The effect of permitting zero heading error has a small effect on placement probability as it merely shifts the maneuver barrier at short detection ranges. Hence the limitation is not placement probability but rather computer accuracy and system stability.

Prob. XIII A

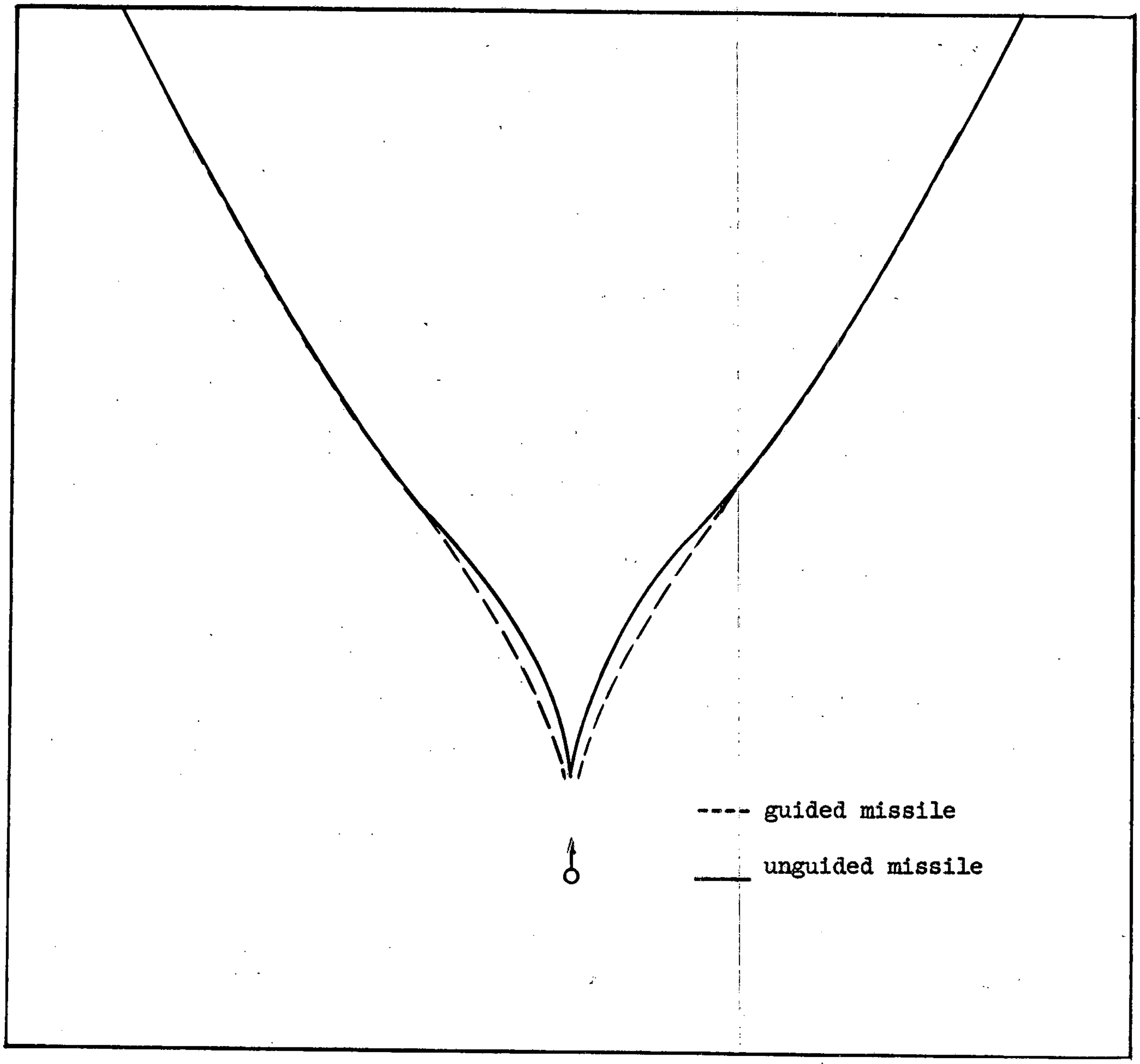

M_t = 2.0 h_t = 60 K

M_{fo} = 2.0 h_{fo} = 60 K

Γ_o = 180°

Scale 25,000 ft/cm

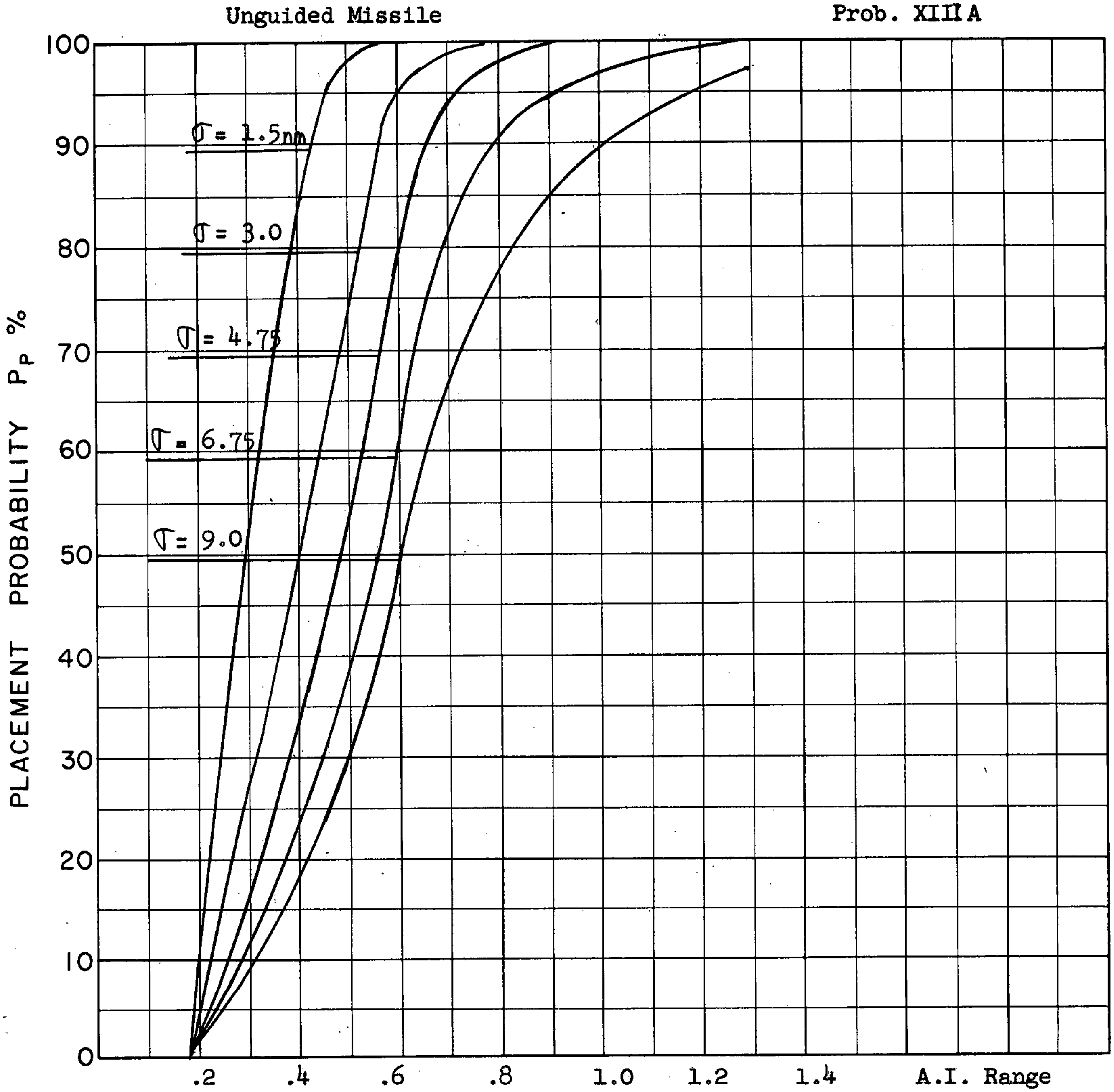

COURSE DIFFERENCE: 180°
TARGET EVASION: 0
TARGET MACH NO.: 2.0
INTERCEPTOR LATERAL G's: Avro 3.3
INTERCEPTOR MACH NO.: 2.0
σ OF G.C.I. ACCURACY: 5 Values
A.I. DETECTION RANGE AS FRACTION OF SPECIFICATION RANGE, S: Abscissa
A.I. DETECTION RANGE CONTOUR: Delta
ALTITUDE: H_t = 60 K
H_f = 60 K

Prob. XIII B

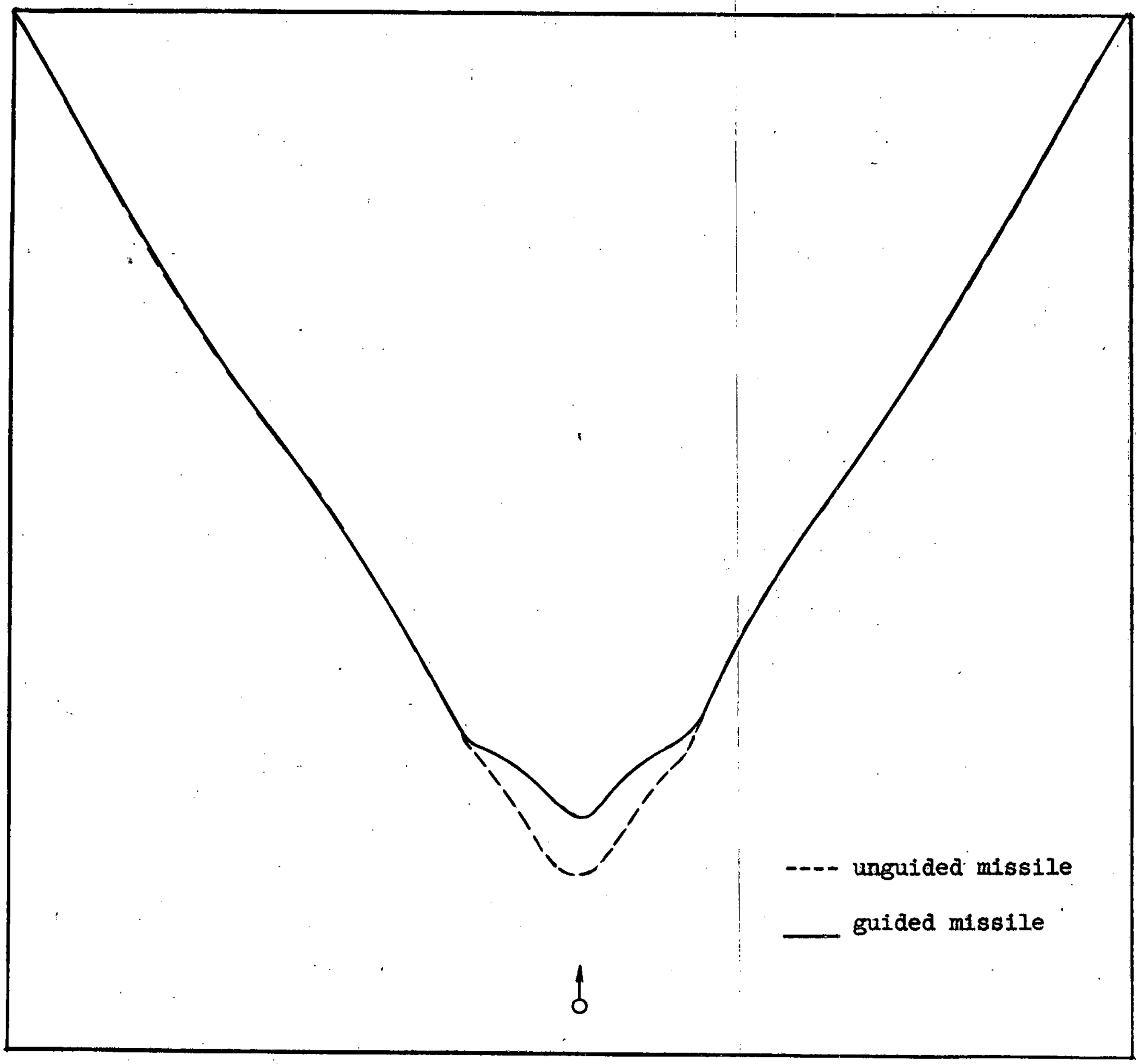

$M_t = 2.0 \quad h_t = 60$ K

$M_{fo} = 2.0 \quad h_{fo} = 50$ K

$\Gamma_o = 180°$

Scale 25,000 ft/cm

Unguided Missile | Prob. XIII B

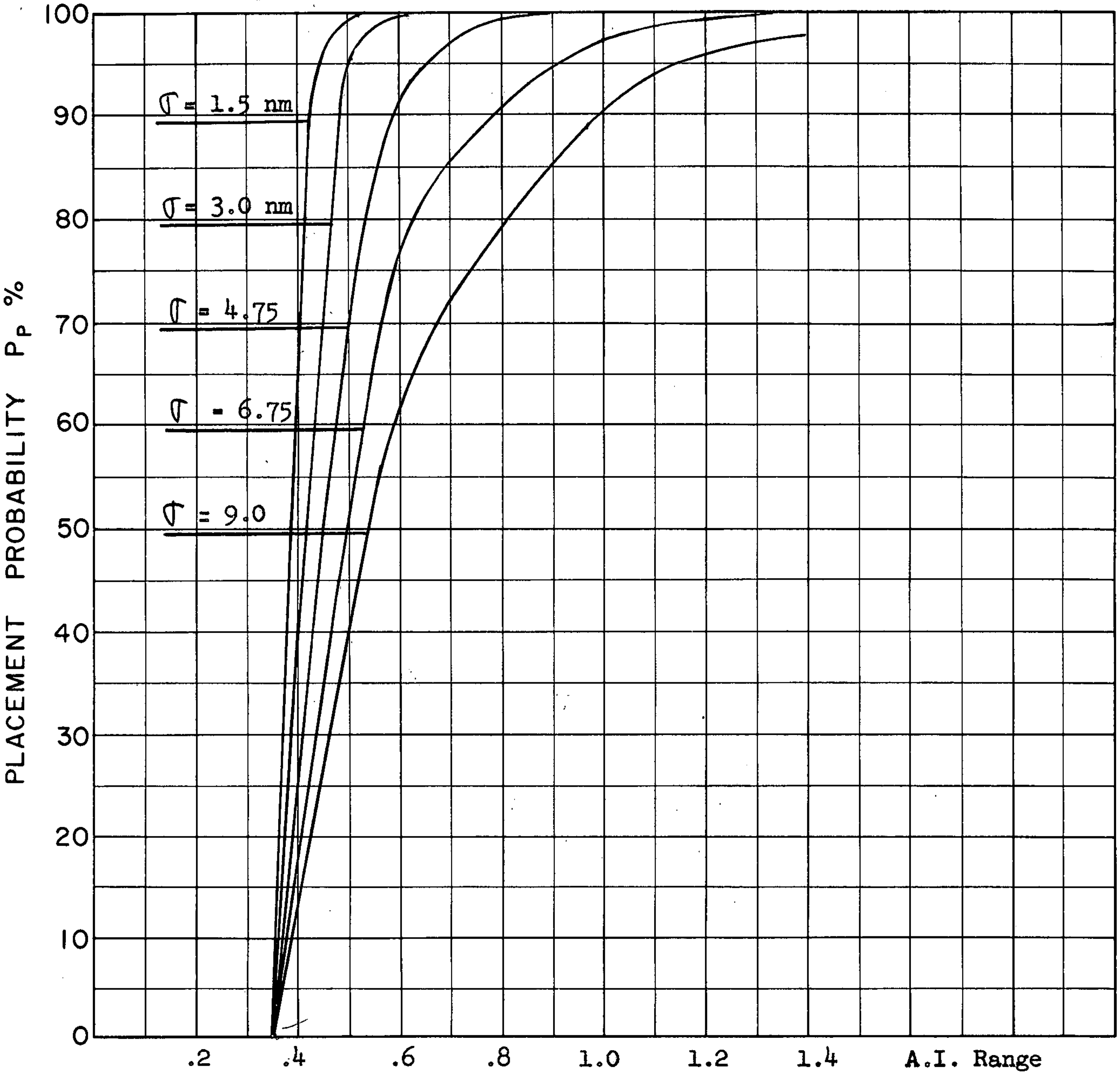

COURSE DIFFERENCE: 180°
TARGET EVASION: 0
TARGET MACH NO.: 2.0
INTERCEPTOR LATERAL G's: Avro 3.3
INTERCEPTOR MACH NO.: 2.0
σ OF G.C.I. ACCURACY: 5 Values
A.I. DETECTION RANGE AS FRACTION OF SPECIFICATION RANGE, S: Abscissa
A.I. DETECTION RANGE CONTOUR: Delta
ALTITUDE: H_t = 60 K
H_f = 50 K

Prob. XIII C

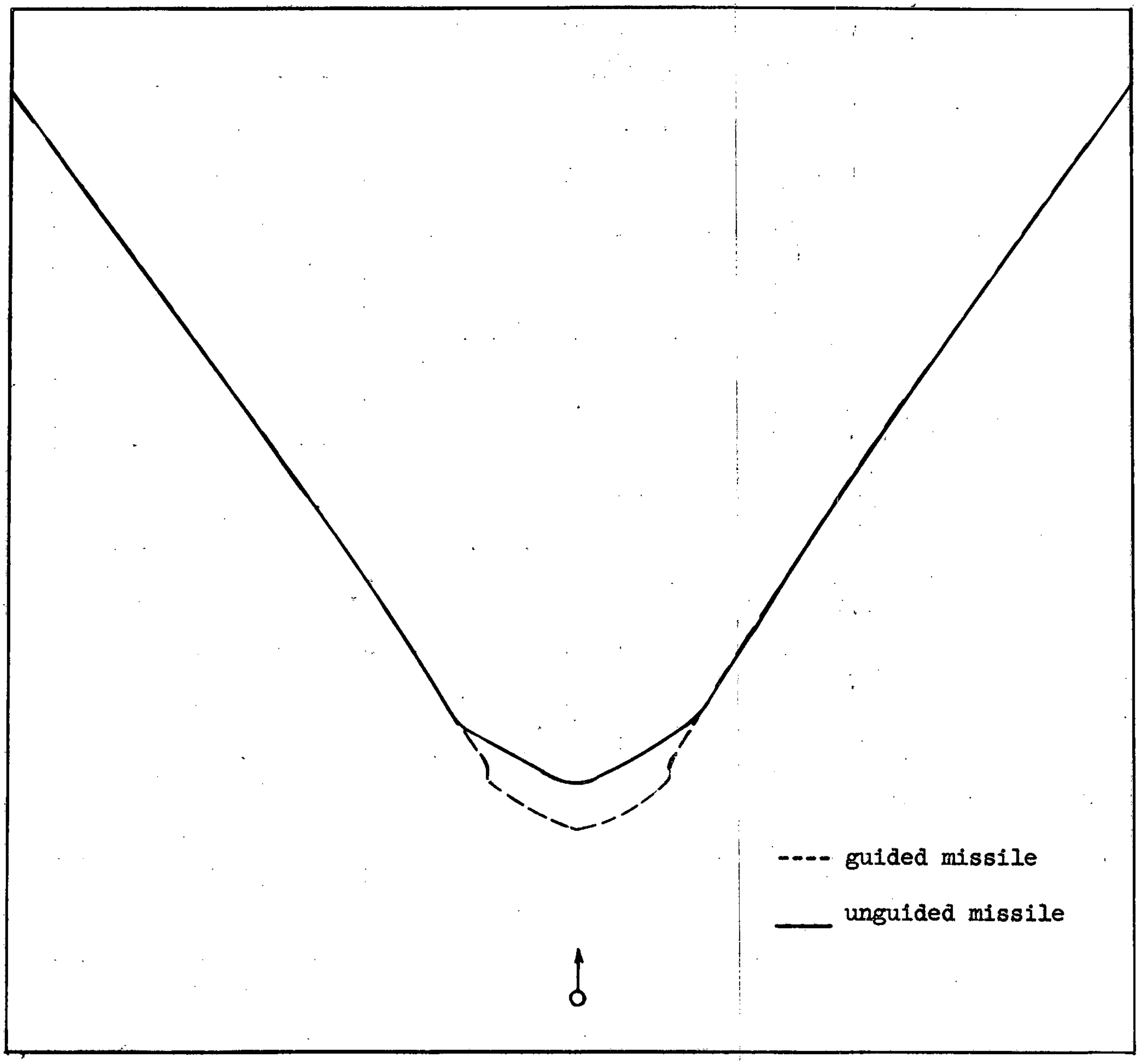

$M_t = 2.0$ $h_t = 60$ K

$M_{fo} = 2.0$ $h_{fo} = 40$ K

$\Gamma_o = 180^\circ$

Scale 25,000 ft/cm

Unguided Missile

Prob. XIII C

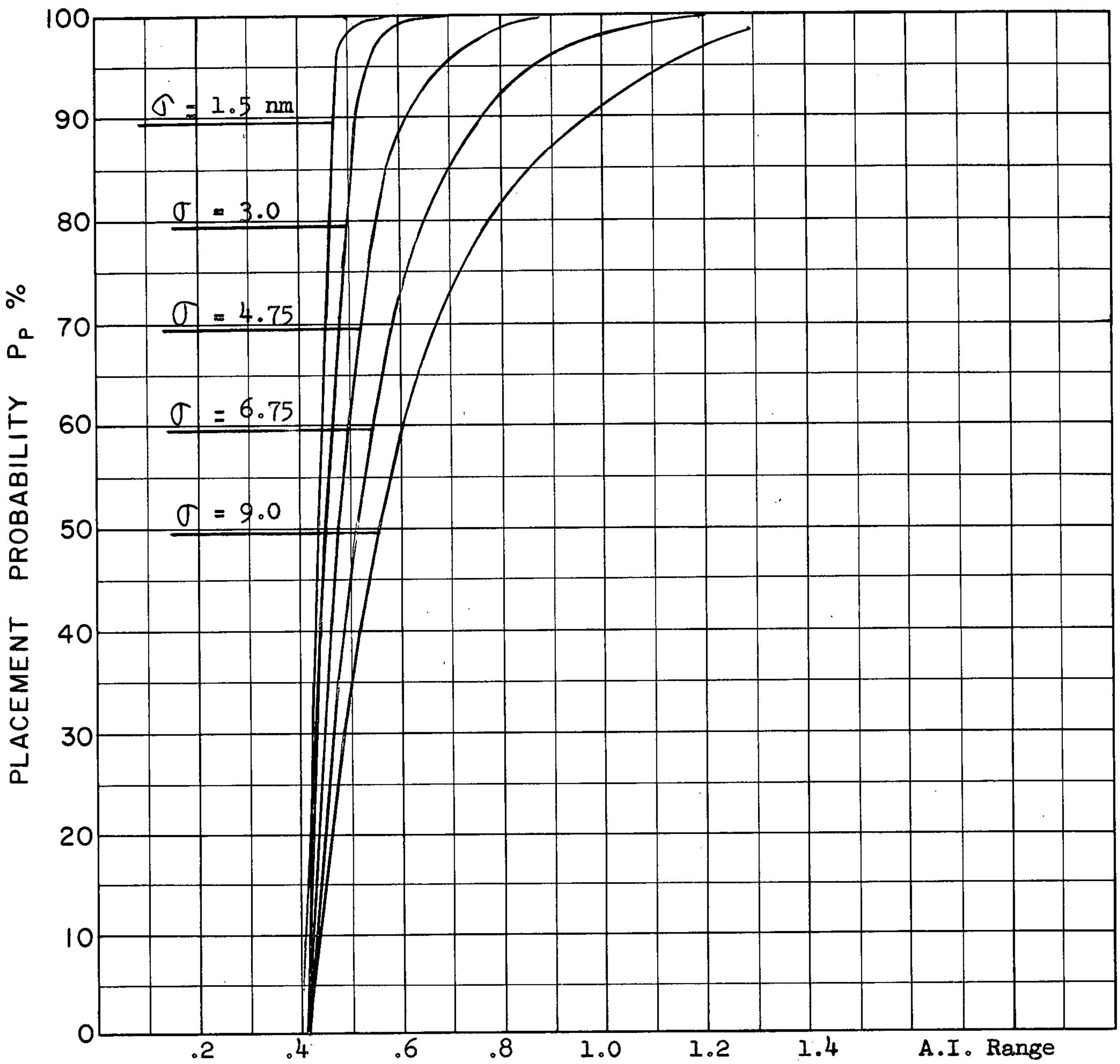

COURSE DIFFERENCE: 180°
TARGET EVASION: 0
TARGET MACH NO.: 2.0
INTERCEPTOR LATERAL G's: Avro 3.3
INTERCEPTOR MACH NO.: 2.0
σ OF G.C.I. ACCURACY: 5 Values
A.I. DETECTION RANGE AS FRACTION OF SPECIFICATION RANGE, S: Abscissa
A.I. DETECTION RANGE CONTOUR: Delta
ALTITUDE: H_t = 60 K
H_f = 40 K

Prob. XIII D

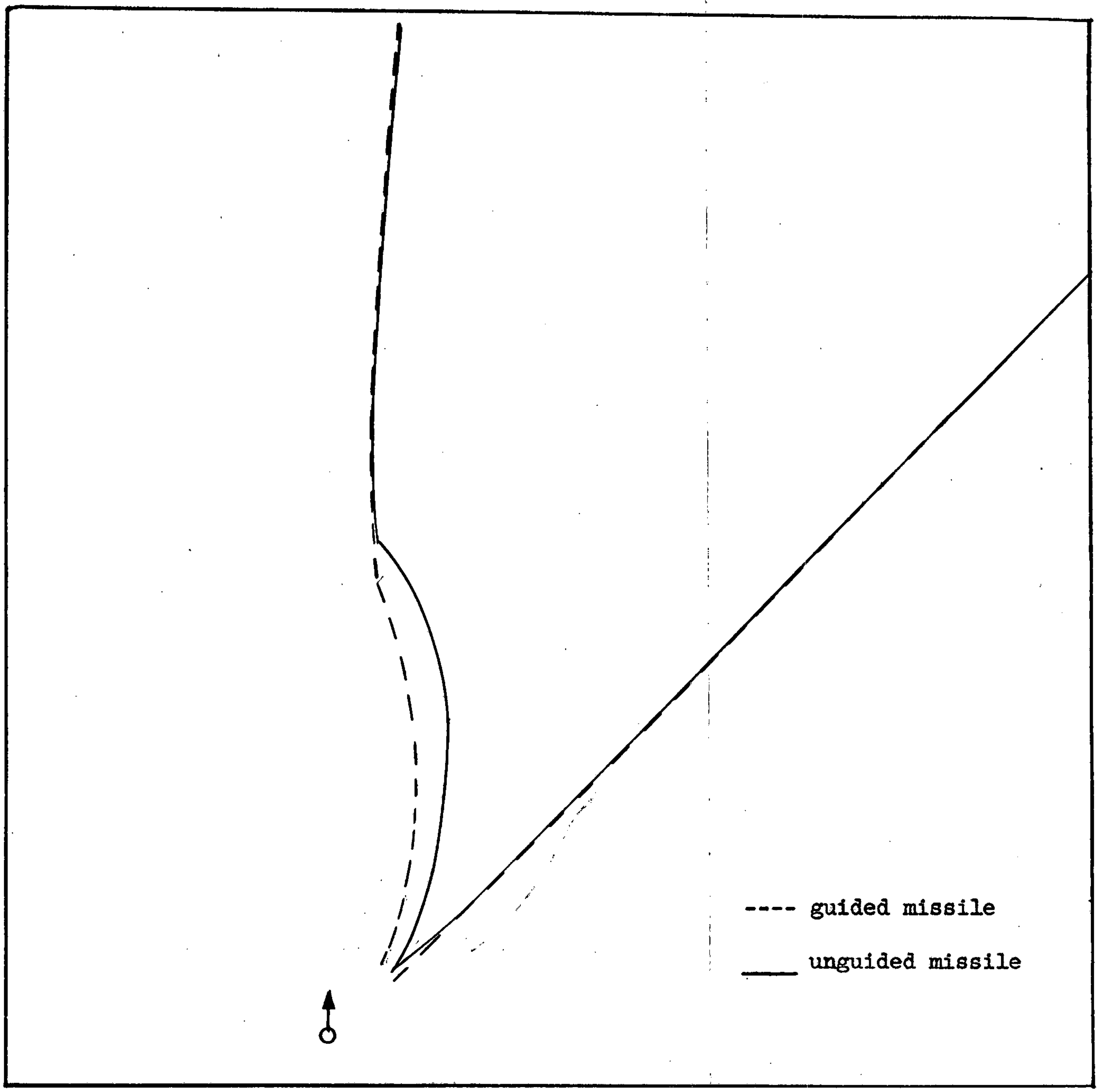

M_t = 2.0 h_t = 60 K

M_{fo} = 2.0 h_{fo} = 60 K

Γ_o = 110°

Scale 25,000 ft/cm

Unguided Missile

Prob. XIII D

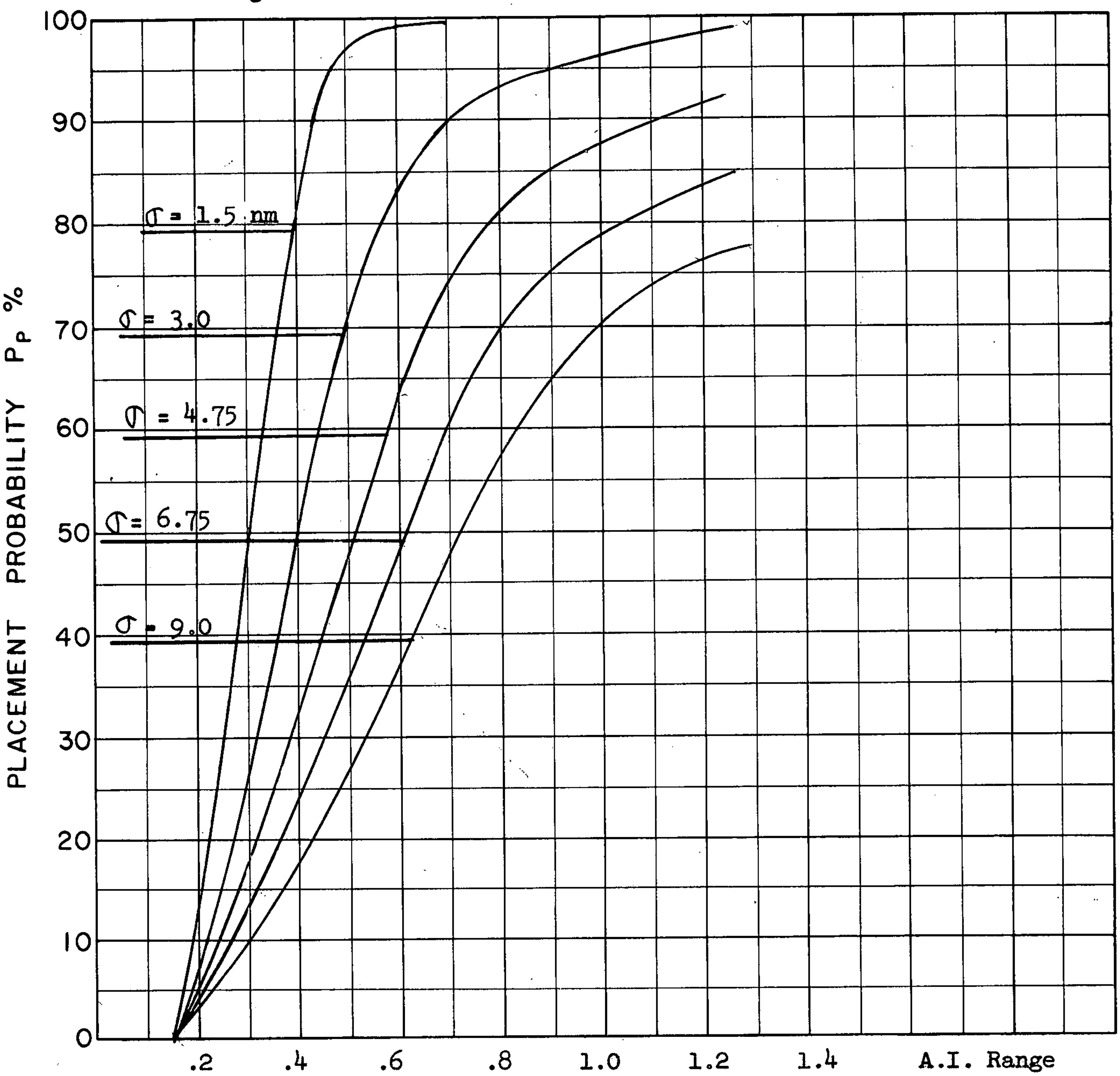

COURSE DIFFERENCE: 110°
TARGET EVASION: 0
TARGET MACH NO.: 2.0
INTERCEPTOR LATERAL G's: Avro 3.3
INTERCEPTOR MACH NO.: 2.0
σ OF G.C.I. ACCURACY: 5 Values
A.I. DETECTION RANGE AS FRACTION OF SPECIFICATION RANGE, S: Abscissa
A.I. DETECTION RANGE CONTOUR: Delta
ALTITUDE: H_f = 60K
H_t = 60 K

Prob. XIII E

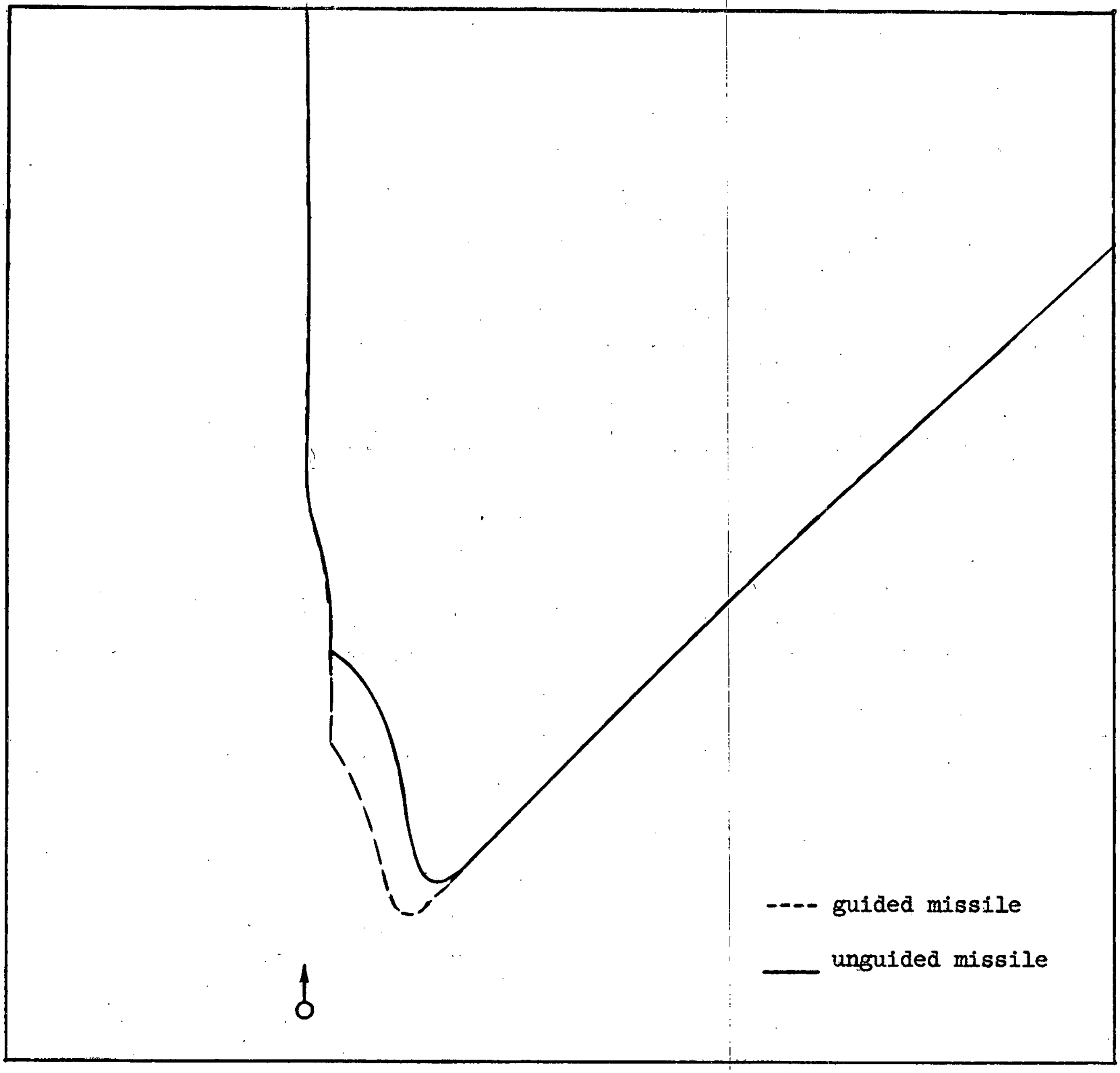

M_t = 2.0 h_t = 60 K

M_{fo} = 2.0 h_{fo} = 40 K

Γ_o = 110°

Scale 25,000 ft/cm

Unguided Missile | Prob. XIII E

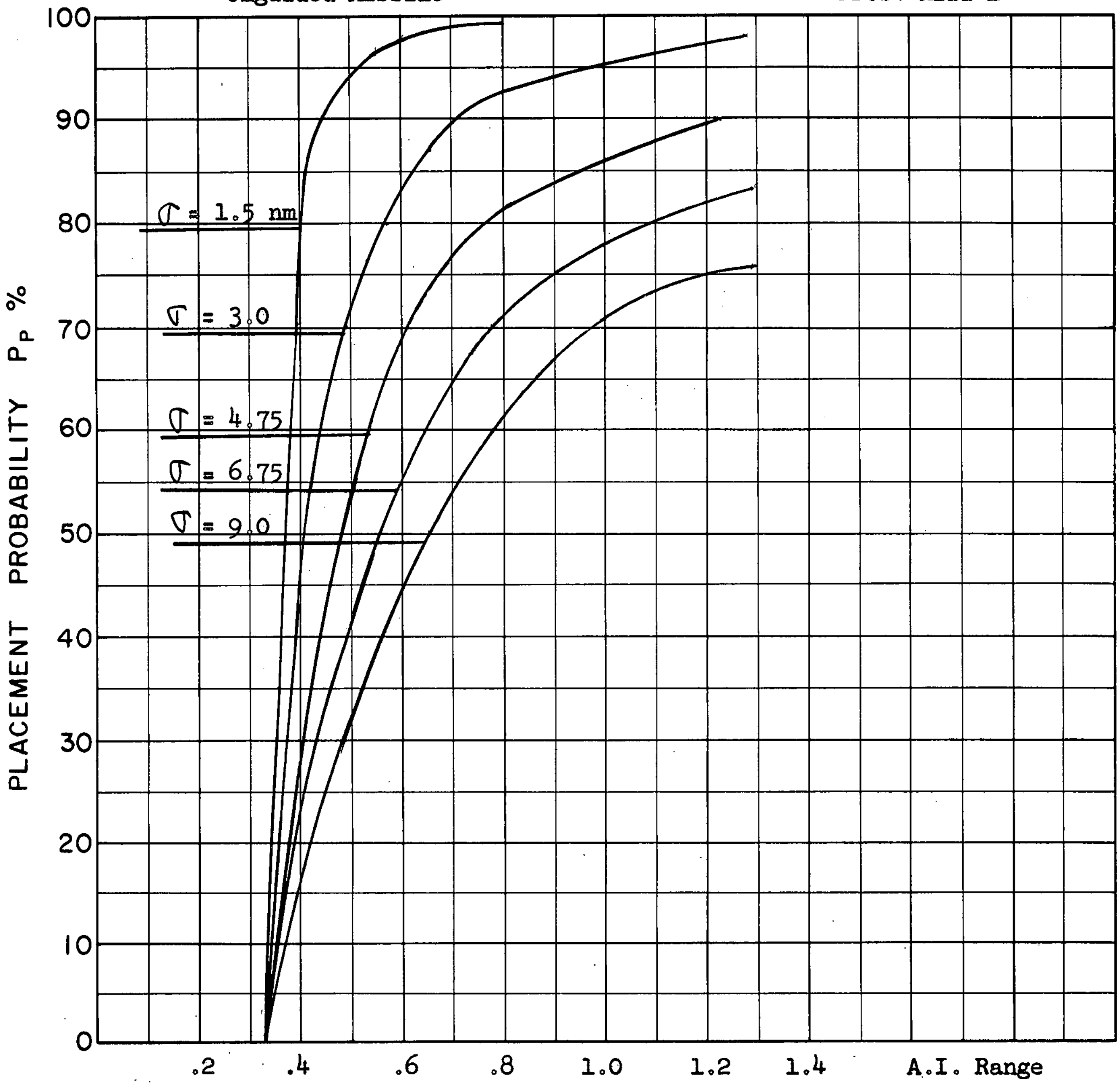

COURSE DIFFERENCE: 110°
TARGET EVASION: 0
TARGET MACH NO.: 2.0
INTERCEPTOR LATERAL G's: Avro 3.3
INTERCEPTOR MACH NO.: 2.0
σ OF G.C.I. ACCURACY: 5 Values
A.I. DETECTION RANGE AS FRACTION OF SPECIFICATION RANGE, S: Abscissa
A.I. DETECTION RANGE CONTOUR: Delta
ALTITUDE: H_{f_o} = 50 K
H_t = 60 K

Prob. XIII F

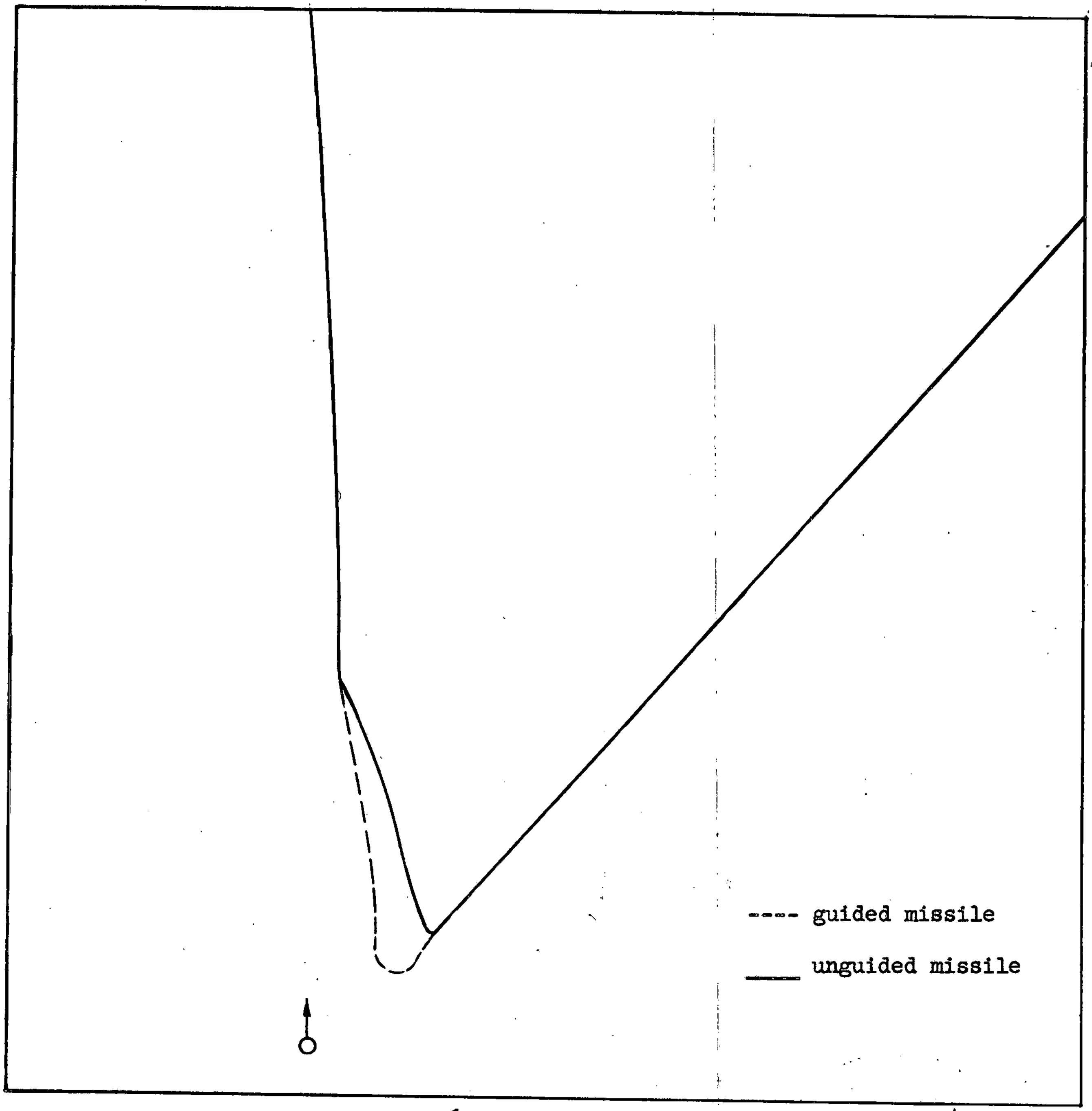

M_t = 2.0 h_t = 60 K

M_{fo} = 2.0 h_{fo} = 50 K

Γ_o = 110°

Scale 25,000 ft/cm

Unguided Missile

Prob. XIII F

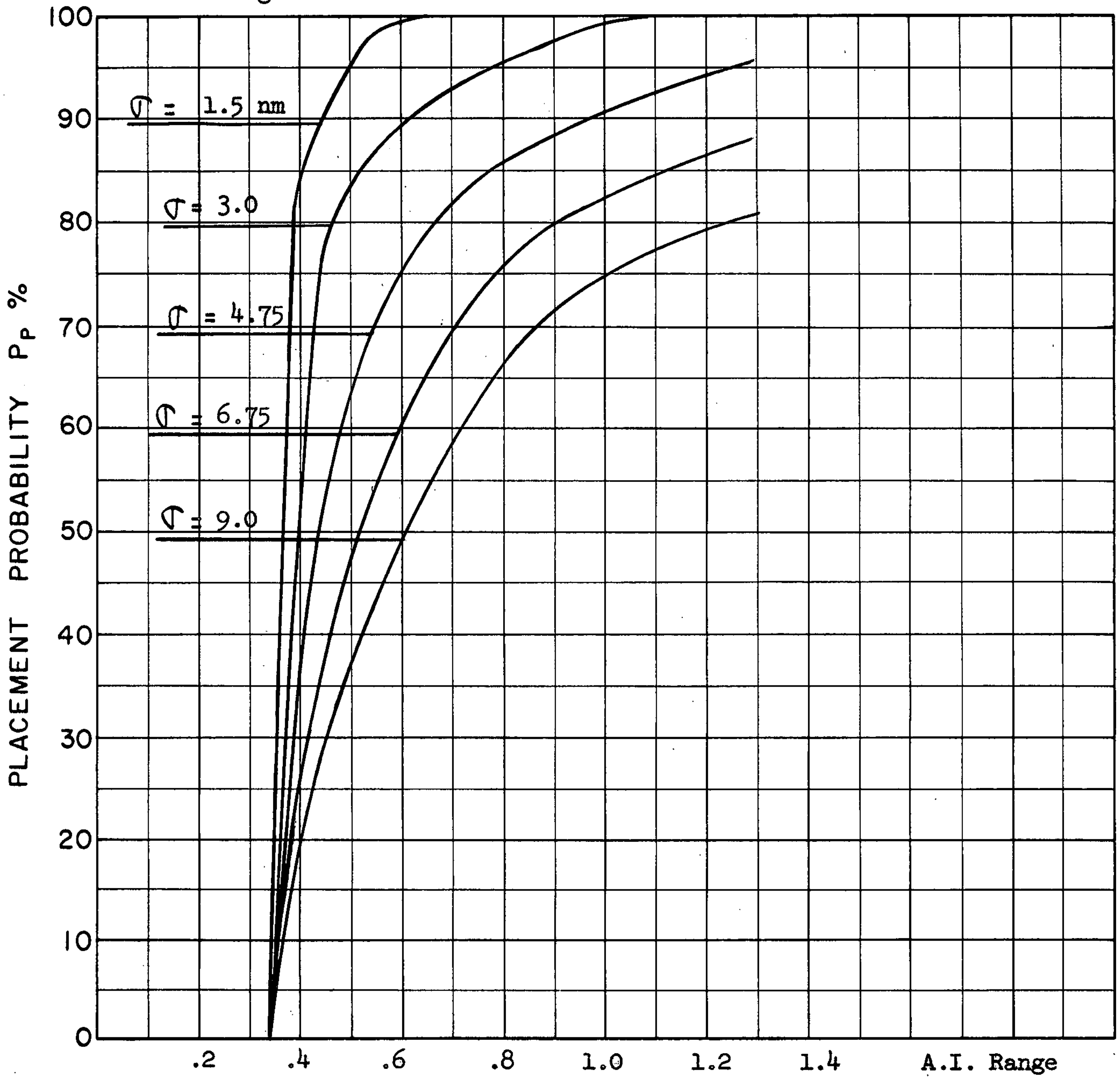

COURSE DIFFERENCE: 110°
TARGET EVASION: 0
TARGET MACH NO.: 2.0
INTERCEPTOR LATERAL G's: Avro 3.3
INTERCEPTOR MACH NO.: 2.0
σ OF G.C.I. ACCURACY: 5 Values
A.I. DETECTION RANGE AS FRACTION OF SPECIFICATION RANGE, S: Abscissa
A.I. DETECTION RANGE CONTOUR: Delta
ALTITUDE: H_f = 40 K
H_t = 60 K

4.4.4.0 Problem XIV - Maximum Interceptor Load Factor Studies

In previous studies the interceptor was assumed to turn with maximum load factor until on the demand course. In many situations this does not give the largest placement zone.

In some cases against a non-maneuvering or a slowly maneuvering target use of its full g capability causes the fighter to fall back because of the velocity which is lost in turning or to lose the target on its AI radar because of banking to too steep an angle.

In this study the effects of varying the maximum g's were studied.

4.4.4.1 2 g Limit Study

This problem considered the interception of a M2.0 target at 60,000 ft; maximum interceptor load factor of 2.

Problem Conditions

$V_{fo} = V_t = M2.0 \quad F = 7\text{ K} \quad t_f = 8\text{ secs}$

$h_t = 60\text{ K}$

XIV	A	B	C	D
h_{fo}	60 K	40 K	60 K	40 K
Γ_o	180°		110°	

4.4.4.2 Conclusions

The placement probability may be appreciably improved in some regions by reducing the maximum turn rate of the fighter.

Against a non-maneuvering target at long range it is advantageous to turn with less than maximum g's. At short ranges where heading error at launch is the limiting factor it is of course necessary to turn at the maximum rate.

A simple rule for attacks from 40 K to 60 K against a non-maneuvering target at 60 K feet for course differences less than 160° could be

Interceptor Load Factor Study

Prob. XIV A

Effect of 2 g limit

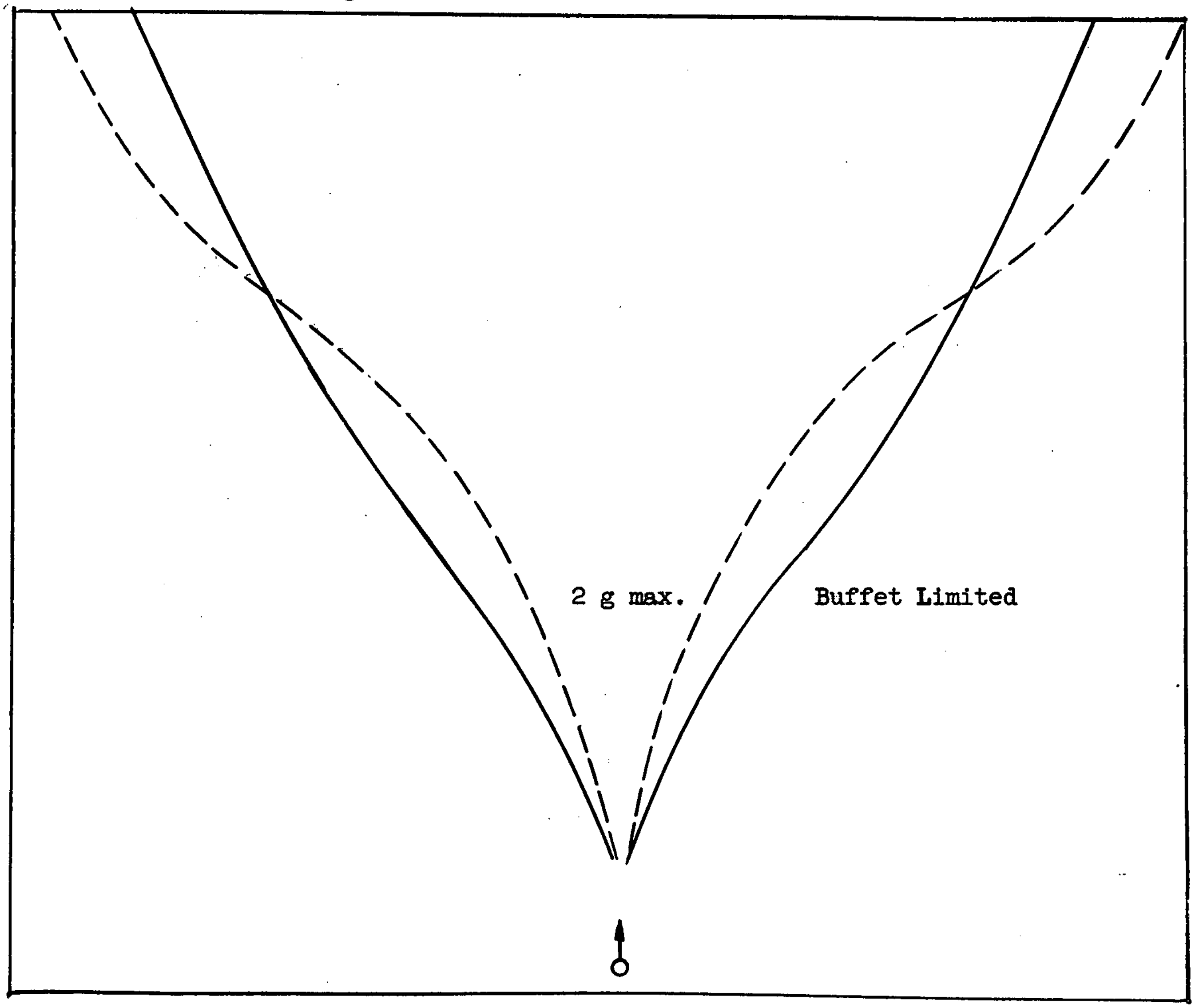

$M_t = 2.0$ $h_t = 60$ K

$M_{fo} = 2.0$ $h_{fo} = 60$ K

$\Gamma_o = 180°$

Scale 25,000 ft/cm

Interceptor Load Factor Study
2 g limit

Prob. XIV A

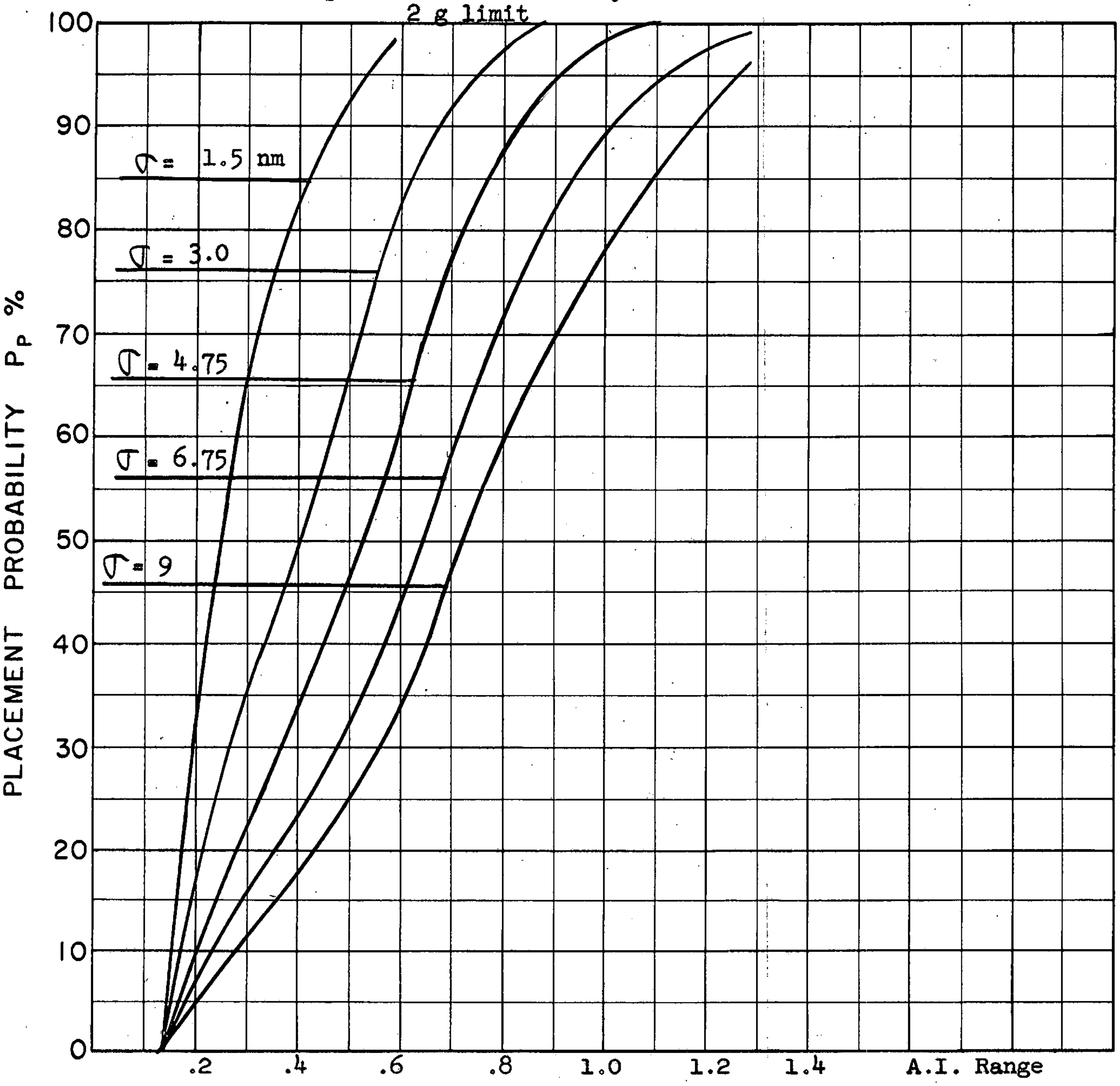

COURSE DIFFERENCE: 180°
TARGET EVASION: 0
TARGET MACH NO.: 2.0
INTERCEPTOR LATERAL G's: Avro 3.3 2 g Limit (Load Factor)
INTERCEPTOR MACH NO.: 2.0
σ OF G.C.I. ACCURACY: 5 Values
A.I. DETECTION RANGE AS FRACTION OF SPECIFICATION RANGE, S: Abscissa
A.I. DETECTION RANGE CONTOUR: Delta
ALTITUDE: 60K

Interceptor Load Factor Study

Prob. XIV B

Effect of 2 g limit

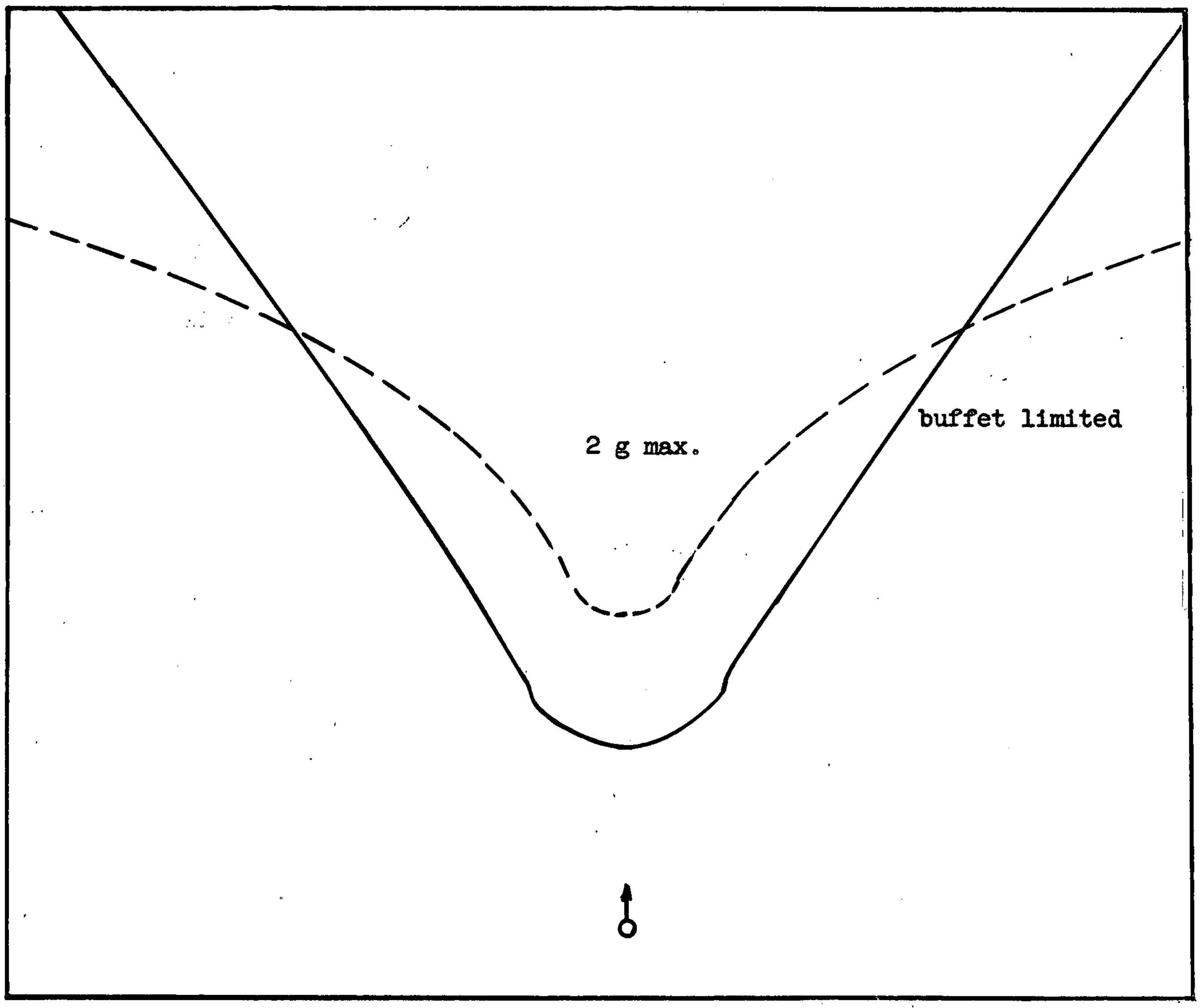

M_t = 2.0 h_t = 60 K

M_{fo} = 2.0 h_{fo} = 40 K

Γ_o = 180°

Scale 25,000 ft/cm

Interceptor Load Factor Study

2 g Limit

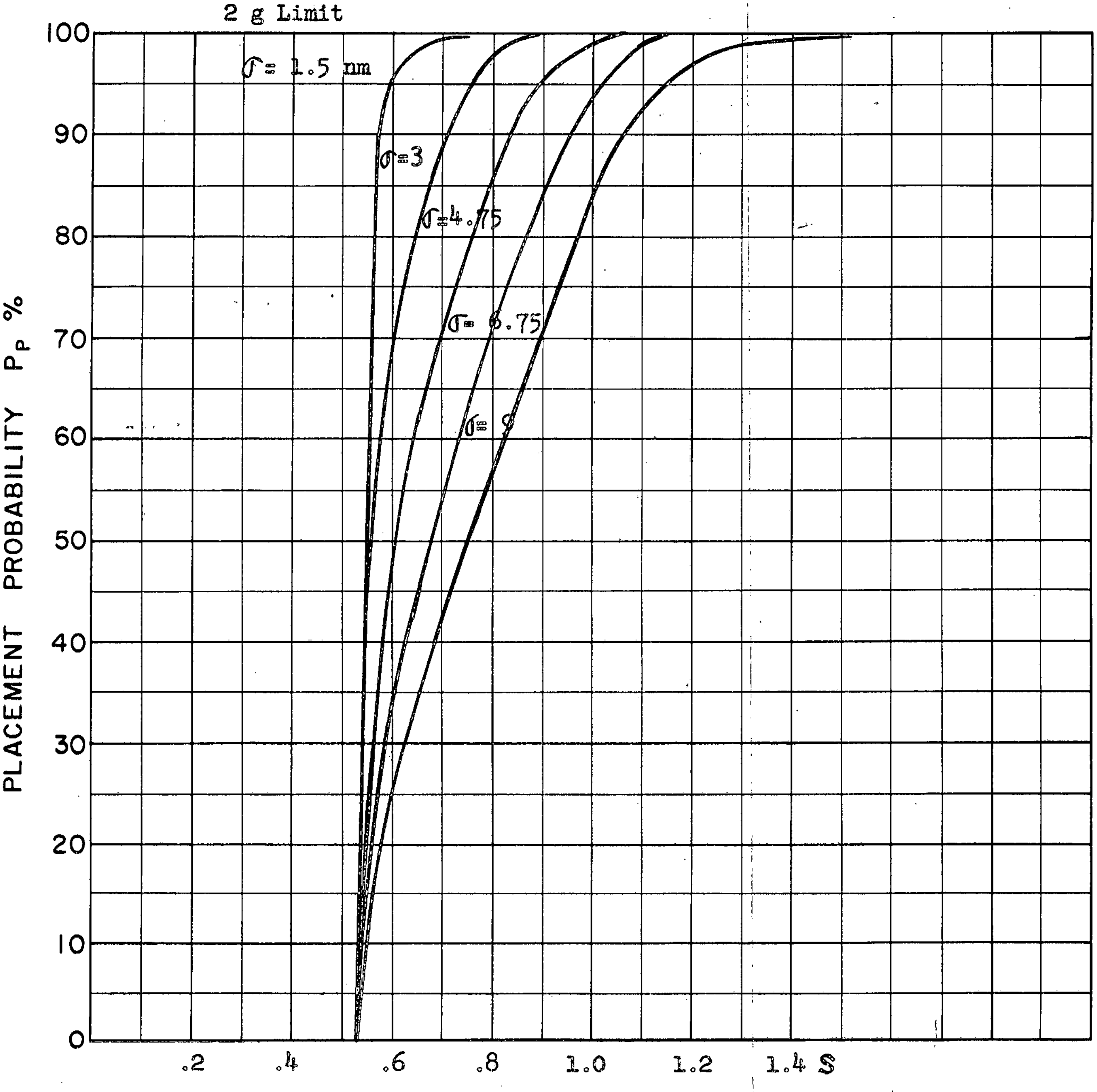

COURSE DIFFERENCE: 180°
TARGET EVASION: 0
TARGET MACH NO.: 2.0
INTERCEPTOR LATERAL G's: Avro 3.3 with 2 g Limit (Load-Factor)
INTERCEPTOR MACH NO.: 2.0
σ OF G.C.I. ACCURACY: 5 Values
A.I. DETECTION RANGE AS FRACTION OF SPECIFICATION RANGE, S: Abscissa
A.I. DETECTION RANGE CONTOUR: Delta
ALTITUDE: H_t = 60 K H_{fo} = 40 K

Interceptor Load Factor Study   Prob. XIV C

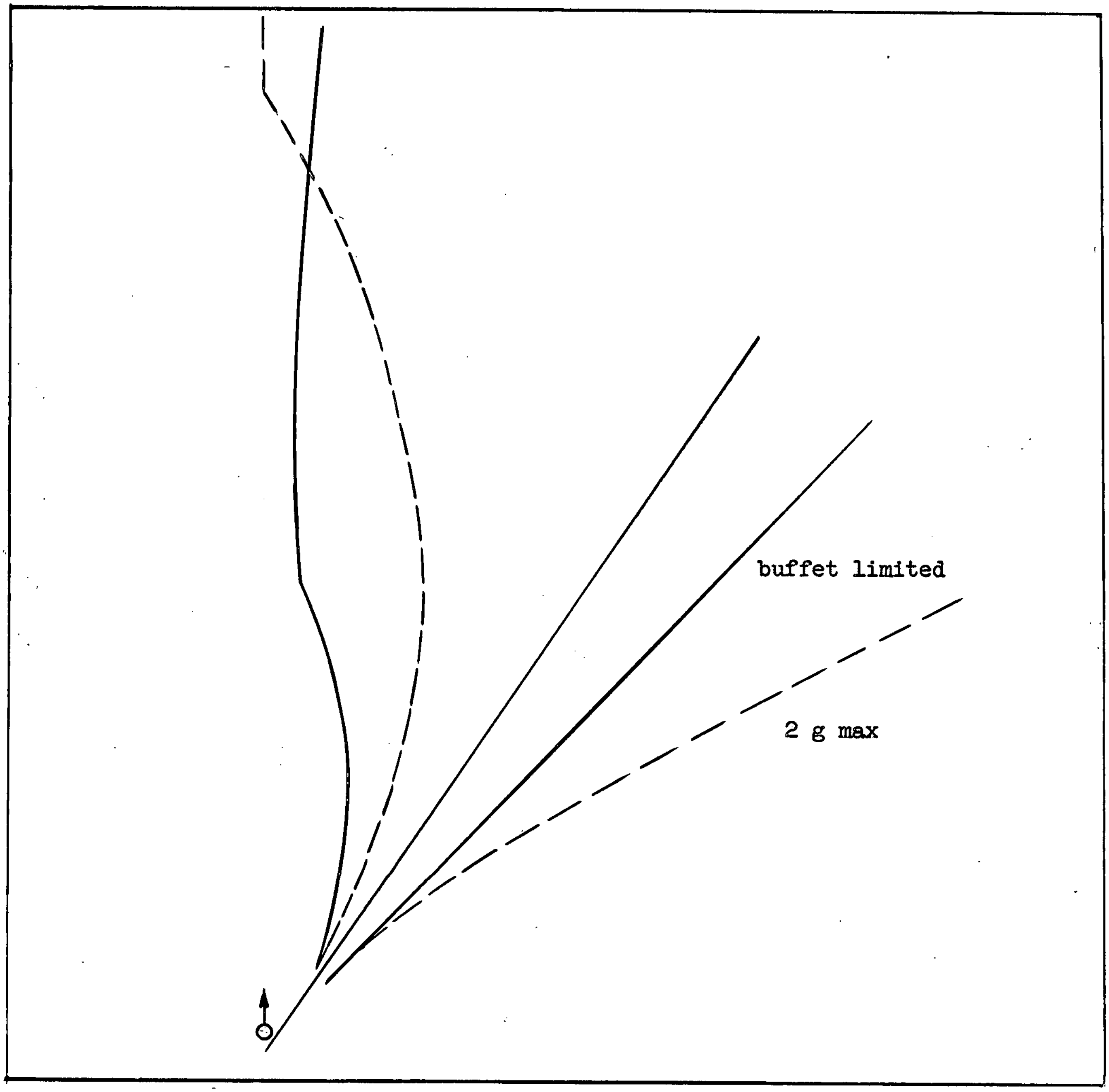

M_t = 2.0 h_t = 60 K   Scale 25,000 ft/cm

M_{fo} = 2.0 h_{fo} = 60 K

Γ_o = 110°

2 g Limit

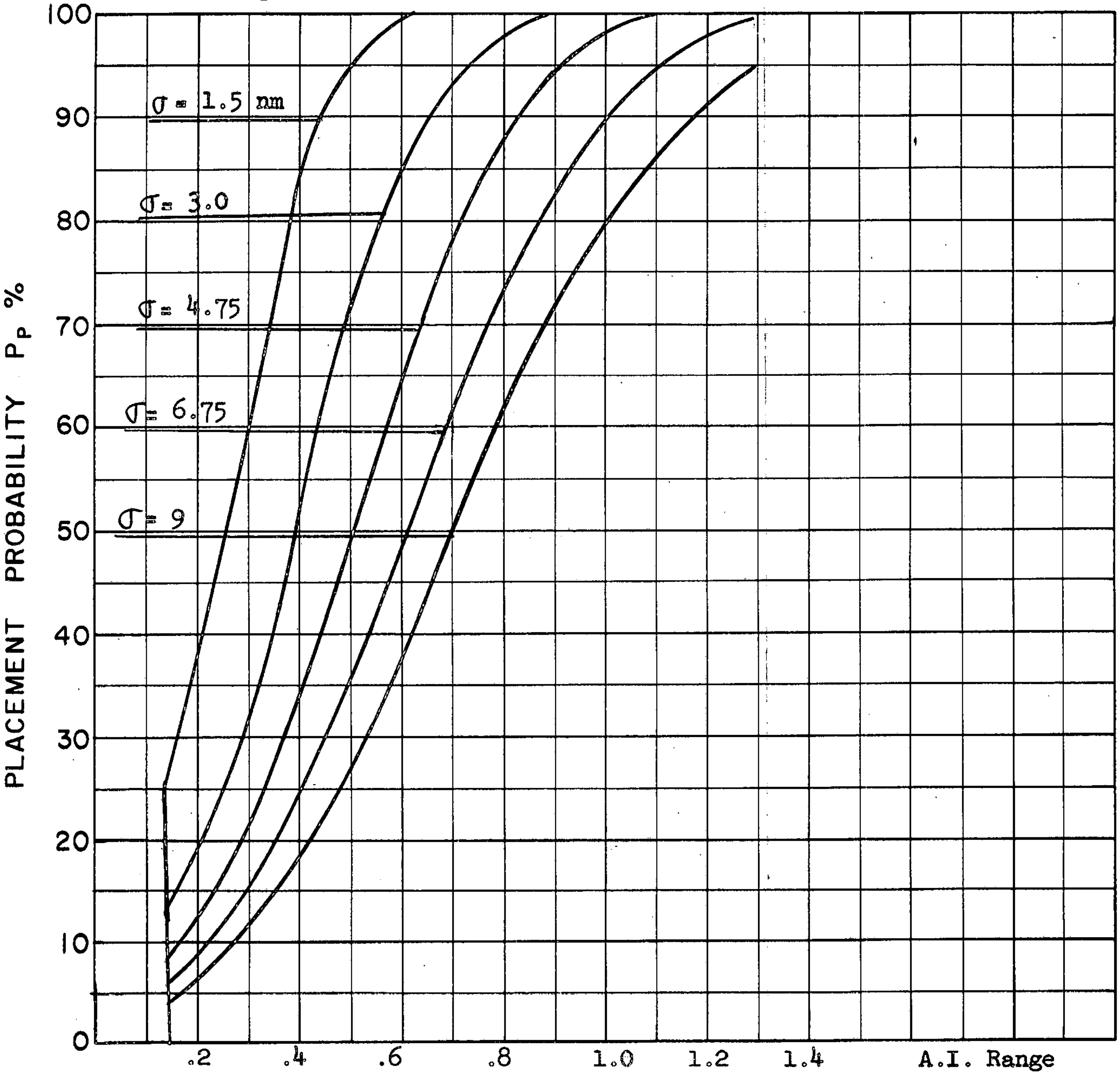

COURSE DIFFERENCE: 110°
TARGET EVASION: 0
TARGET MACH NO.: 2.0
INTERCEPTOR LATERAL G's: Avro 3.3 2 g Limit (Lift)
INTERCEPTOR MACH NO.: 2.0
σ OF G.C.I. ACCURACY: 5 Values
A.I. DETECTION RANGE AS FRACTION OF SPECIFICATION RANGE, S: Abscissa
A.I. DETECTION RANGE CONTOUR: Delta
ALTITUDE: 60 K

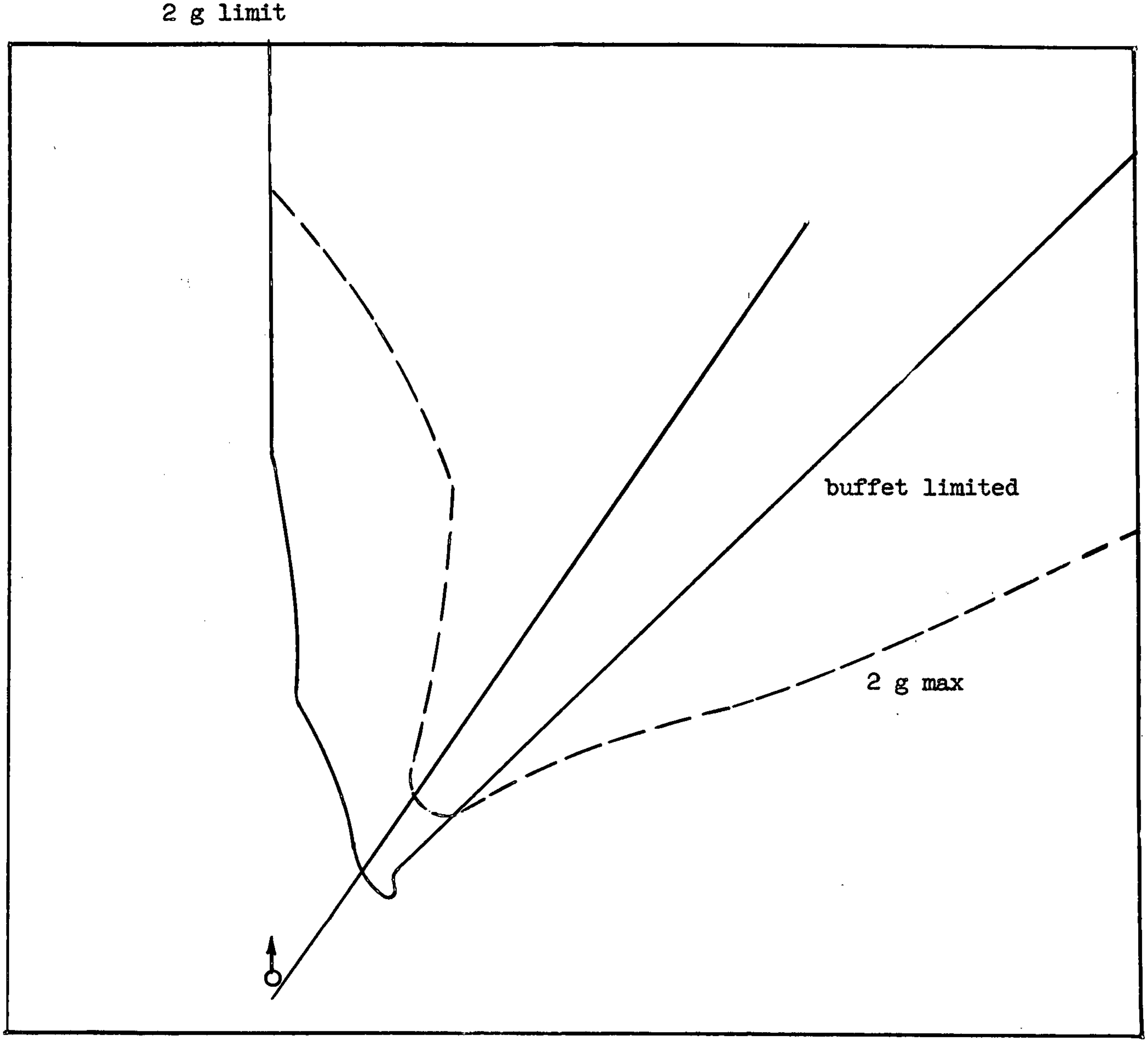

M_t = 2.0 h_t = 60 K Scale 25,000 ft/cm

M_{fo} = 2.0 h_{fo} = 40 K

Γ_o = 110°

Interceptor Load Factor Study
2 g Limit

Prob. XIV D

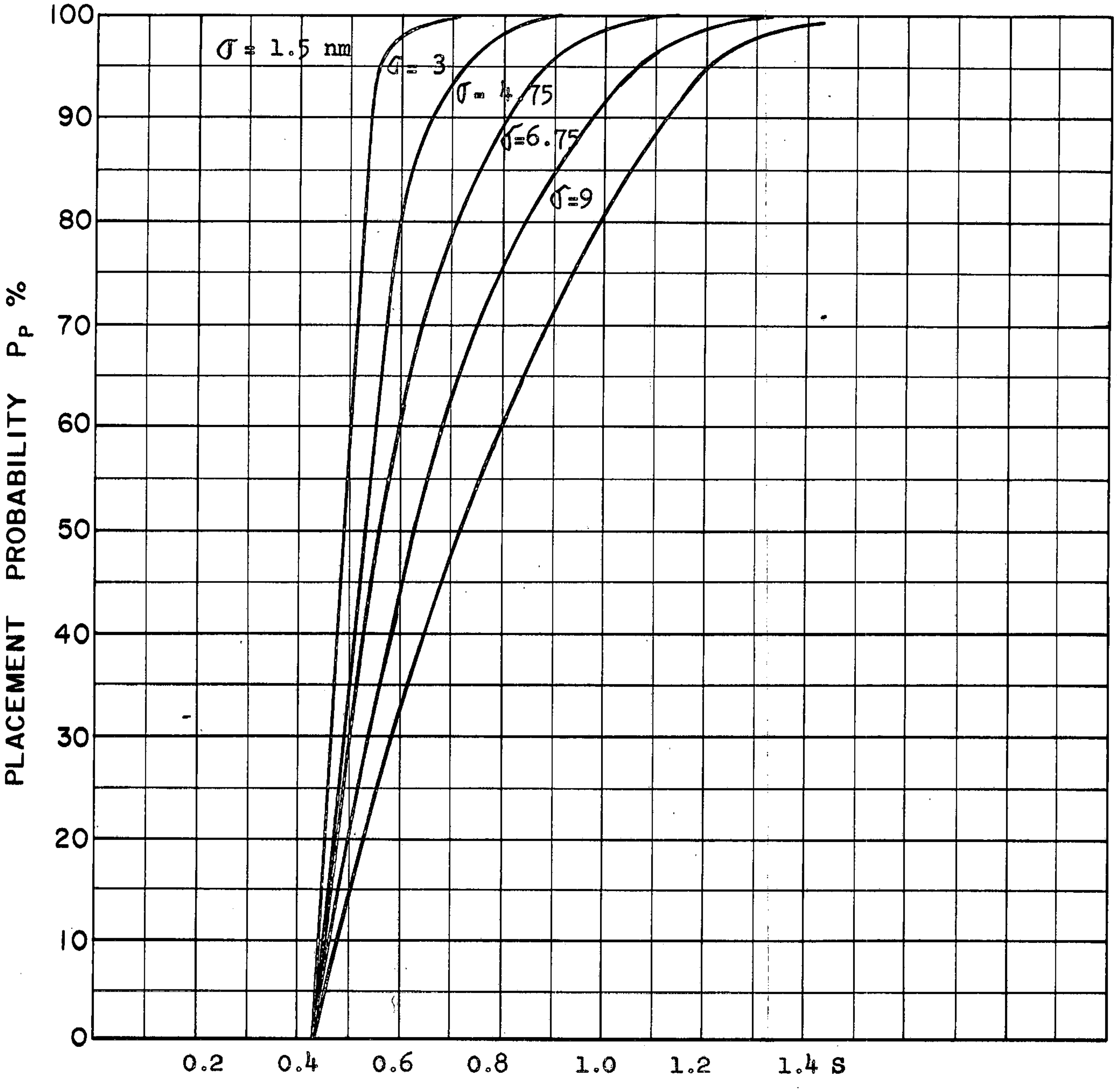

COURSE DIFFERENCE: 110°
TARGET EVASION: 0
TARGET MACH NO.: 2.0
INTERCEPTOR LATERAL G's: Avro 3.3 with 2 g Limit
INTERCEPTOR MACH NO.: 2.0
σ OF G.C.I. ACCURACY: 5 Values
A.I. DETECTION RANGE AS FRACTION OF SPECIFICATION RANGE, S: Abscissa
A.I. DETECTION RANGE CONTOUR: Delta
ALTITUDE: H_t = 60 K H_{fo} = 40 K

1. <u>Interceptor Initially Ahead of the Ideal Approach Line (Has to Turn Towards the Target)</u>

   Turn with maximum load factor = 4 g's

2. <u>Interceptor Initially Behind the Ideal Approach Line (Has to Turn Away to get on a Lead Collision Course)</u>

   Turn with maximum load factor = 2 g's for long ranges (greater than 100 K feet)

   Turn with maximum load factor = 4 g's for short ranges (less than 100 K ft.)

   For course differences of 160° to 180° turn with maximum g's.

4.4.4.3 <u>Maximum g's Study for 90° Course Difference</u>

For course differences of 90° and less the maximum probability in coaltitude attacks falls to near 50% because the AI look angle barrier is near the ideal approach line. This is because the initial lead angle is large and if the aircraft banks steeply, the target is lost on the -45° AI limit. Reduction of the bank angle may be achieved by reducing the maximum load factor, permitting a much larger lead angle.

In this problem two cases were studied, coaltitude attacks at 60 K and climbing attacks from 40 K

$M_{fo} = M_t = 2.0 \quad F = 7\text{ K} \quad t_f = 8$ secs.

Placement zones and probabilities are shown for various values of maximum load factor. If the rule stated in section 4.4.4.2 above were used, a substantial improvement in placement probability would result.

Problem	h_{fo}	Interceptor Max g's
XIV E	60 K	2.5 g (buffet)
XIV F	60 K	2 g
XIV G	60 K	1.5 g
XIV H	40 K	4 g
XIV J	40 K	2 g

Interceptor Maximum Load Factor Study — Prob. XIV EFG

Effect of "g" Limit on a Coaltitude Attack

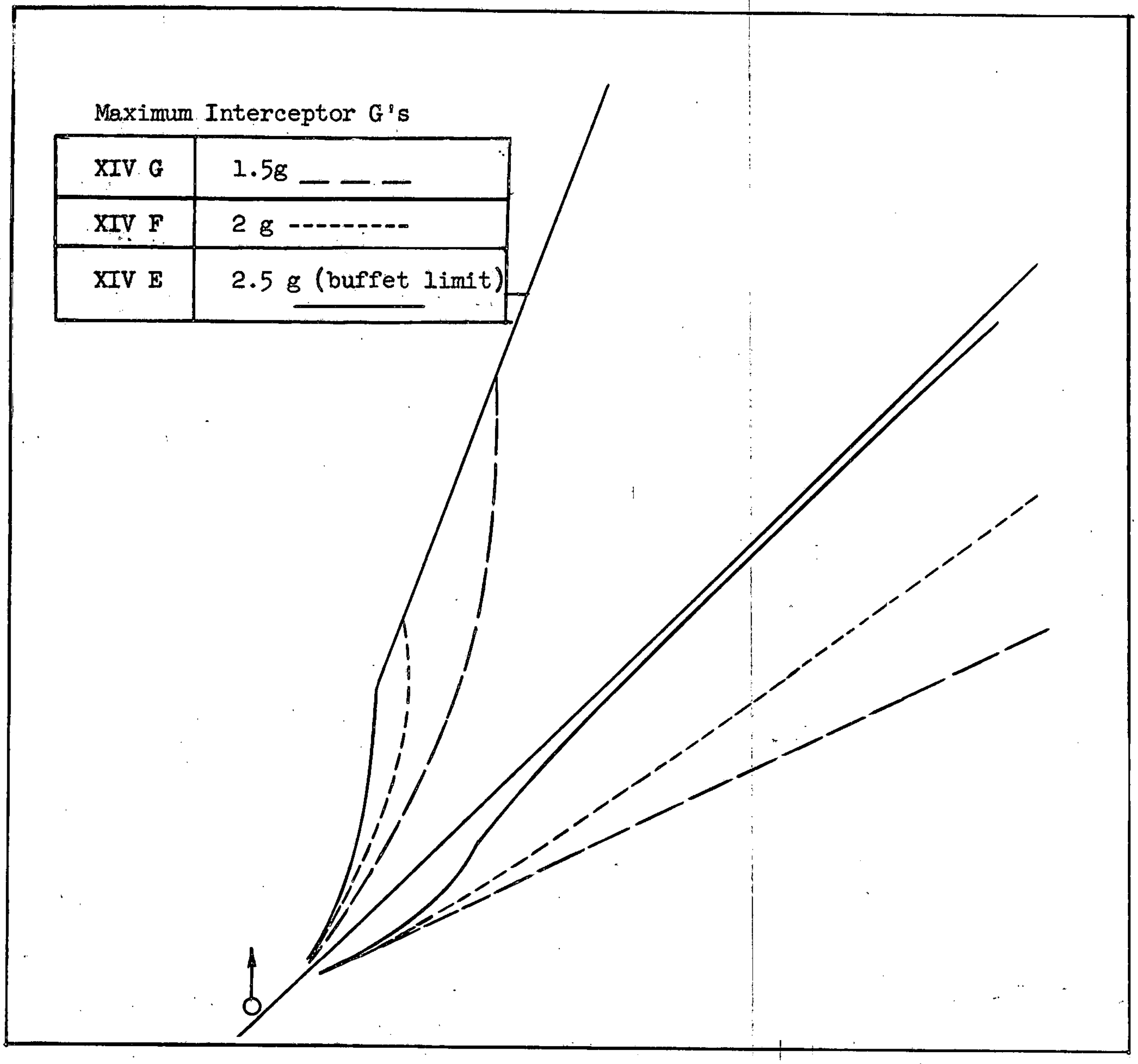

$M_t = 2.0 \quad h_t = 60$ K

$M_{fo} = 2.0 \quad h_f = 60$ K

$\Gamma_o = 90^\circ$

Scale 25,000 ft/cm

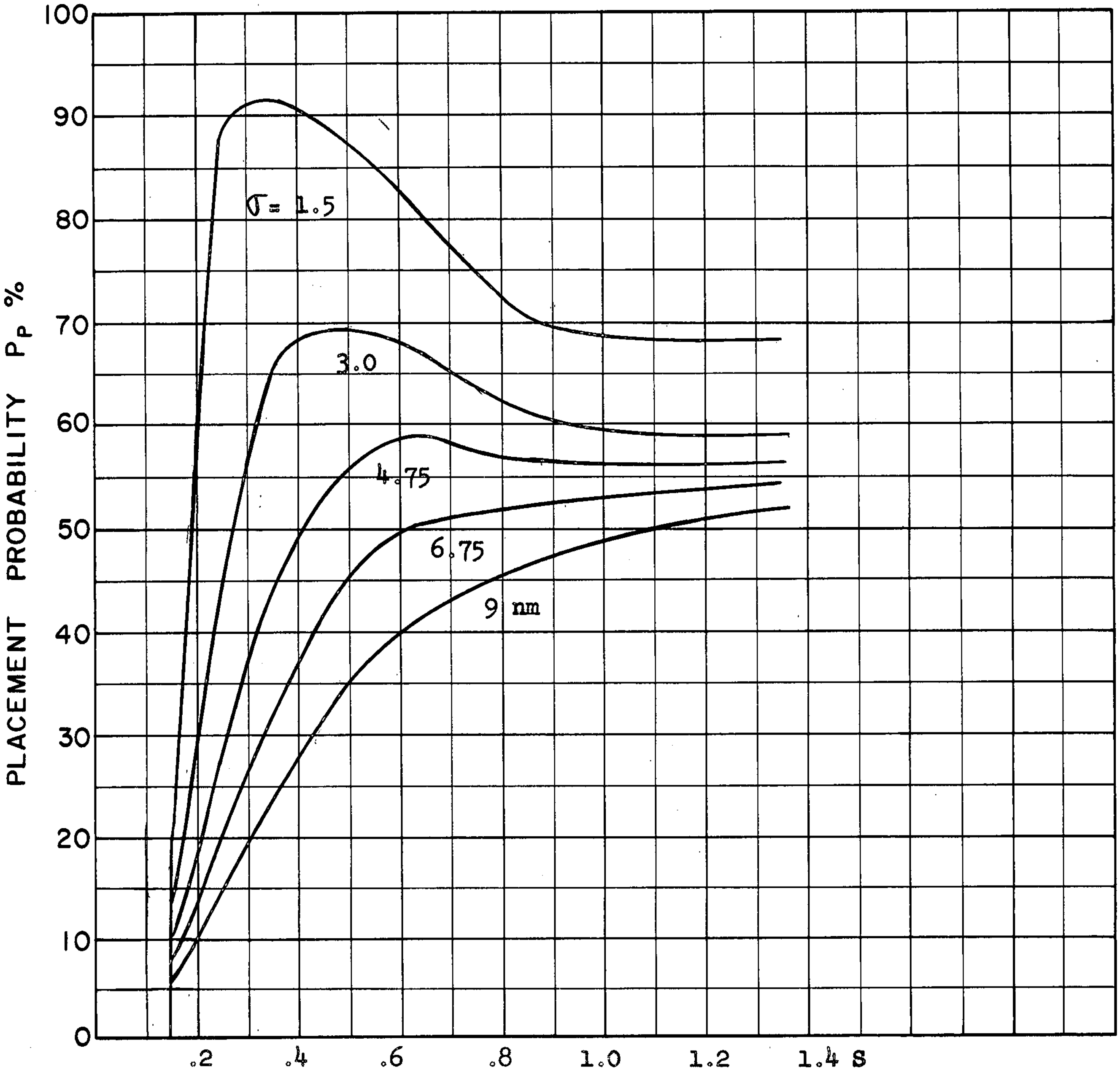

COURSE DIFFERENCE: 90°
TARGET EVASION: 0
TARGET MACH NO.: 2.0
INTERCEPTOR LATERAL G's: Avro 3.3
INTERCEPTOR MACH NO.: 2.0
σ OF G.C.I. ACCURACY: 5 Values
A.I. DETECTION RANGE AS FRACTION OF SPECIFICATION RANGE, S: Abscissa
A.I. DETECTION RANGE CONTOUR: Delta
ALTITUDE: 60 K

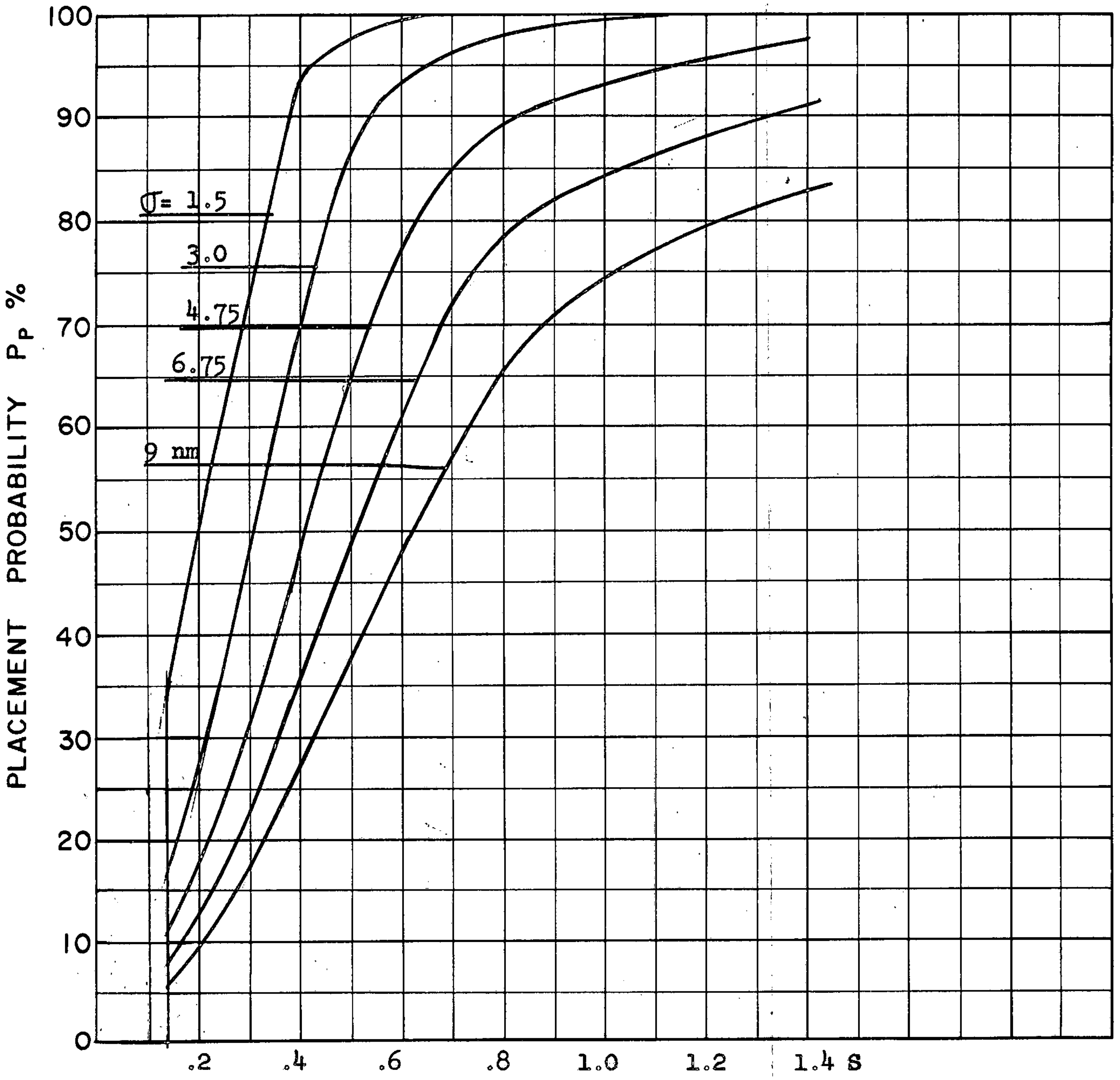

COURSE DIFFERENCE: 90°
TARGET EVASION: 0
TARGET MACH NO.: 2.0
INTERCEPTOR LATERAL G's: Avro 3.3 with 2.0 g max. (Load Factor)
INTERCEPTOR MACH NO.: 2.0
σ OF G.C.I. ACCURACY: 5 Values
A.I. DETECTION RANGE AS FRACTION OF SPECIFICATION RANGE, S: Abscissa
A.I. DETECTION RANGE CONTOUR: Delta
ALTITUDE: 60 K

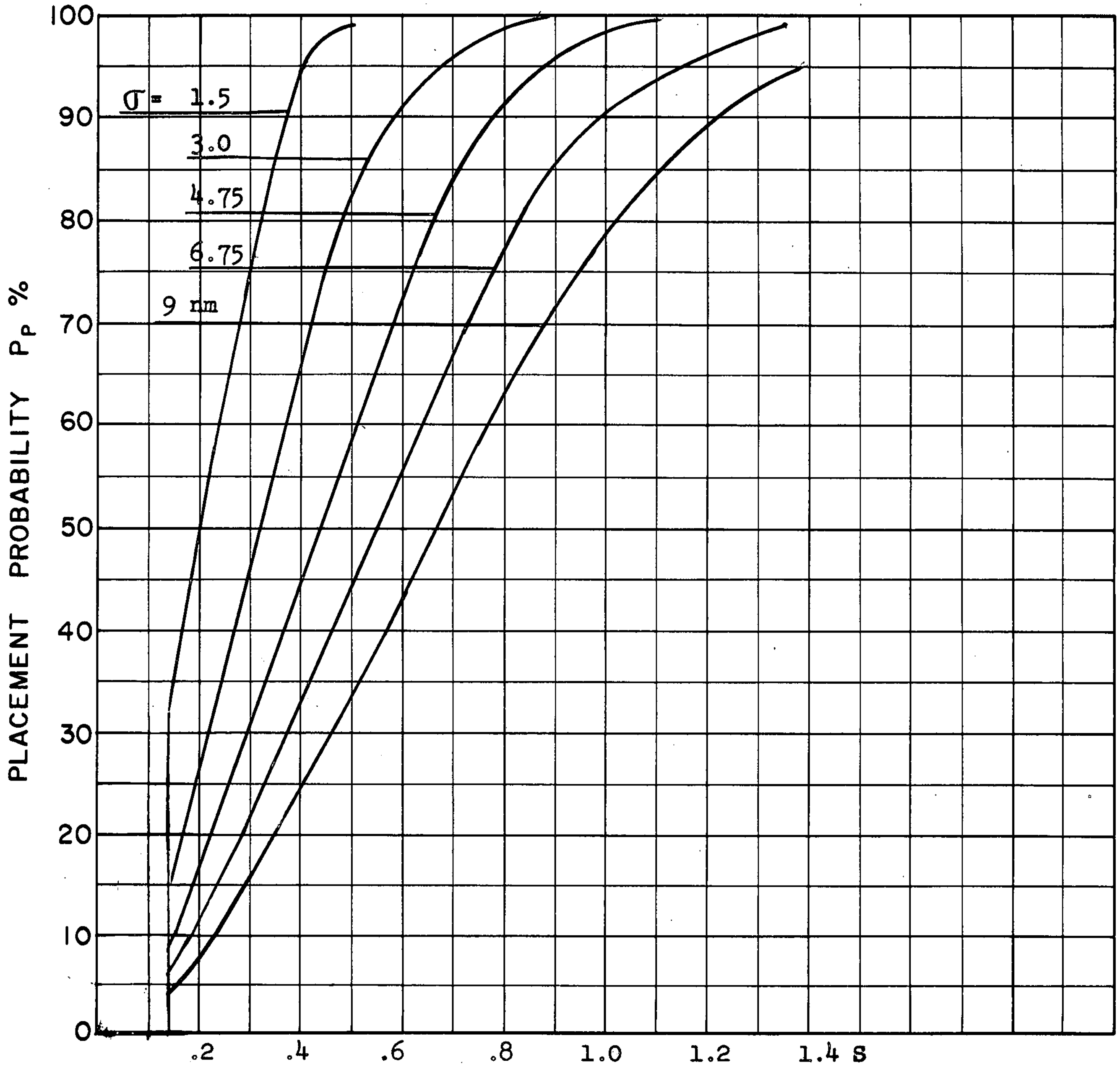

COURSE DIFFERENCE: 90°
TARGET EVASION: 0
TARGET MACH NO.: 2.0
INTERCEPTOR LATERAL G's: Avro 3.3 with 1.5 g max Load-Factor
INTERCEPTOR MACH NO.: 2.0
σ OF G.C.I. ACCURACY: 5 Values
A.I. DETECTION RANGE AS FRACTION OF SPECIFICATION RANGE, S: Abscissa
A.I. DETECTION RANGE CONTOUR: Delta
ALTITUDE: 60 K

Interceptor Maximum Load Factor Study

Prob. XIV H J

Effect of "g" Limit on a Climbing Attack

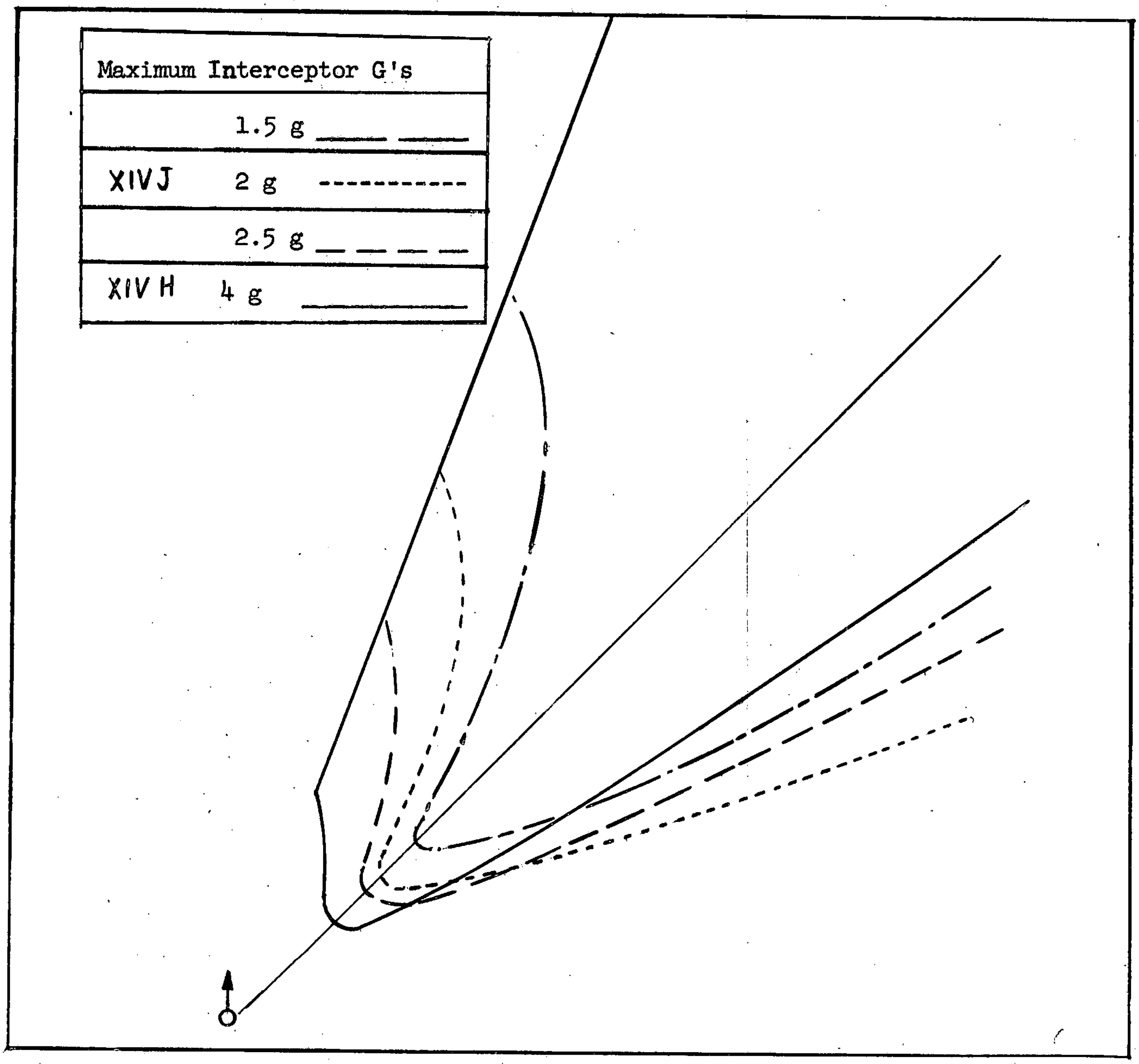

M_t = 2.0 h_t = 60 K

M_{fo} = 2.0 h_{fo} = 40 K

Γ_o = 90°

Scale 25,000 ft/cm

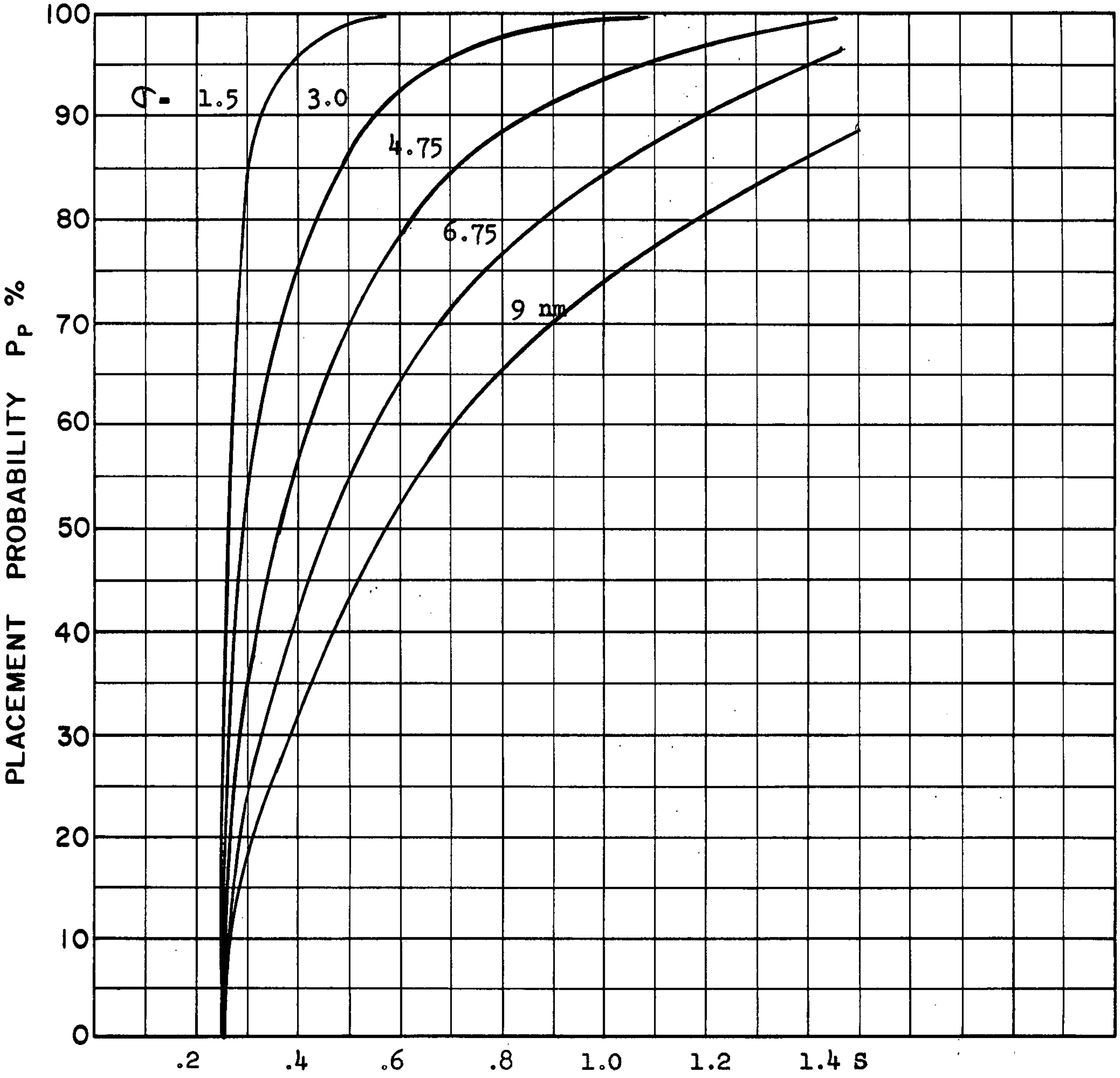

COURSE DIFFERENCE: 90°
TARGET EVASION: 0
TARGET MACH NO.: 2.0
INTERCEPTOR LATERAL G's: Avro 3.3 4 g limit
INTERCEPTOR MACH NO.: 2.0
σ OF G.C.I. ACCURACY: 5 Values
A.I. DETECTION RANGE AS FRACTION OF SPECIFICATION RANGE, S: Abscissa
A.I. DETECTION RANGE CONTOUR: Delta
ALTITUDE: H_t = 60 K

H_{fo} = 40 K

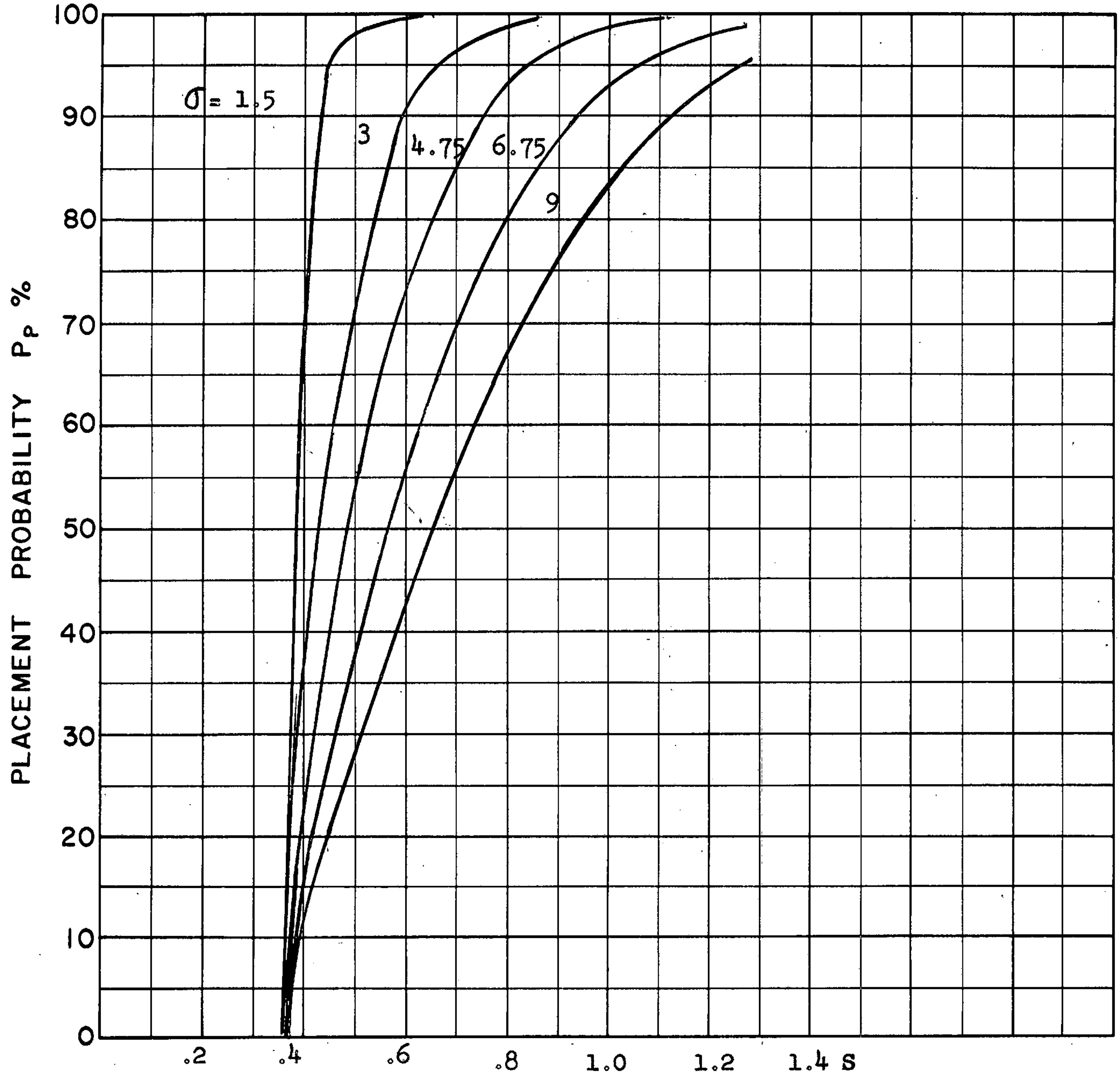

COURSE DIFFERENCE: 90°
TARGET EVASION: 0
TARGET MACH NO.: 2.0
INTERCEPTOR LATERAL G's: Avro 3.3   2 g Load-Factor Limit
INTERCEPTOR MACH NO.: 2.0
σ OF G.C.I. ACCURACY: 5 Values
A.I. DETECTION RANGE AS FRACTION OF SPECIFICATION RANGE, S: Abscissa
A.I. DETECTION RANGE CONTOUR: Delta
ALTITUDE: H_t = 60 K

H_{fo} = 40 K

4.4.4.4 Optimum Maximum Load Factor Studies

In flying from a point in space to intercept a non-maneuvering target, the navigation computer instructs the fighter to turn until it is flying in a straight line towards the collision point.

If the interceptor turns at maximum rate two adverse effects occur

(1) it banks too steeply and tends to lose the target from the -45° AI radar elevation gimbal deflection limit.

(2) it decelerates and the fall-back barriers close in on the ideal approach line.

These two effects combine because the final lead angle increases as the speed falls, thus increasing the possibility of a look-angle failure.

If the interceptor turns too slowly it may either reach the launch zone with a heading error greater than the missile can correct or it may overshoot the target.

Hence it is expected that there should be a range of values of maximum load factor which result in a successful interception. As the initial aspect changes this range of successful values of maximum load factor may change.

On a boundary which arises from conditions occurring during the interception (as opposed to initial look angle say), the range of values will generally converge to a single value. These have been found for three cases.

$M_{fo} = M_t = 2.0 \quad F = 7\text{ K} \quad t_f = 8\text{ secs.} \quad h_f = 60\text{ K}$

	XIV K	XIV L	XIV M
Γ_o	180°	110°	110°
h_{fo}	40 K	60 K	40 K

In cases L and M the optimum value falls to a steady value at medium ranges.

Interceptor Maximum Load Factor Study — Prob. XIV K

Optimum Load Factor Limit

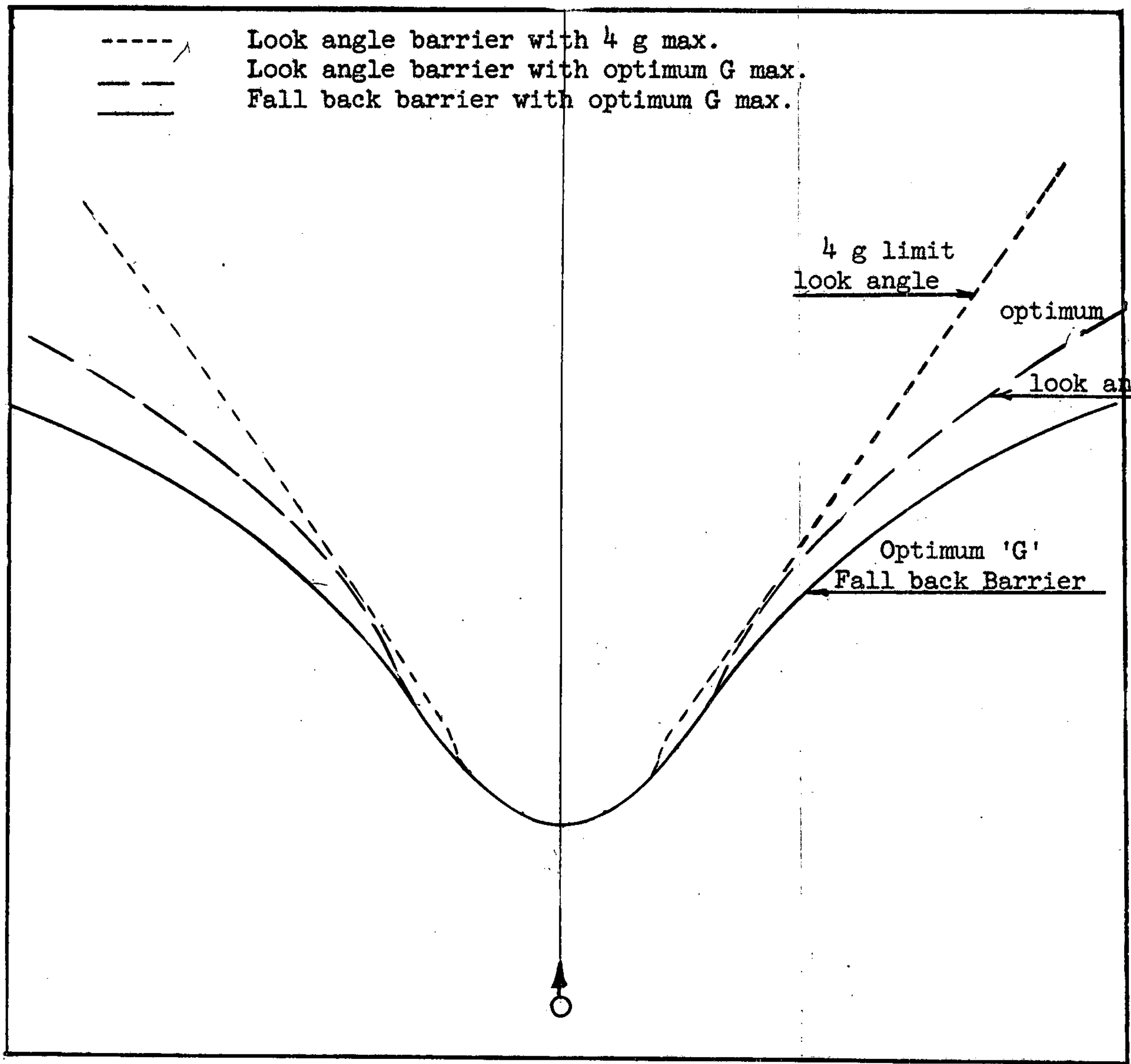

$M_t = 2.0$ $h_t = 60$ K

$M_{fo} = 2.0$ $h_{fo} = 40$ K

$\Gamma_o = 180^\circ$

Scale 25,000 ft/cm

Interceptor Maximum Load Factor Study

Optimum Load Factor Limit

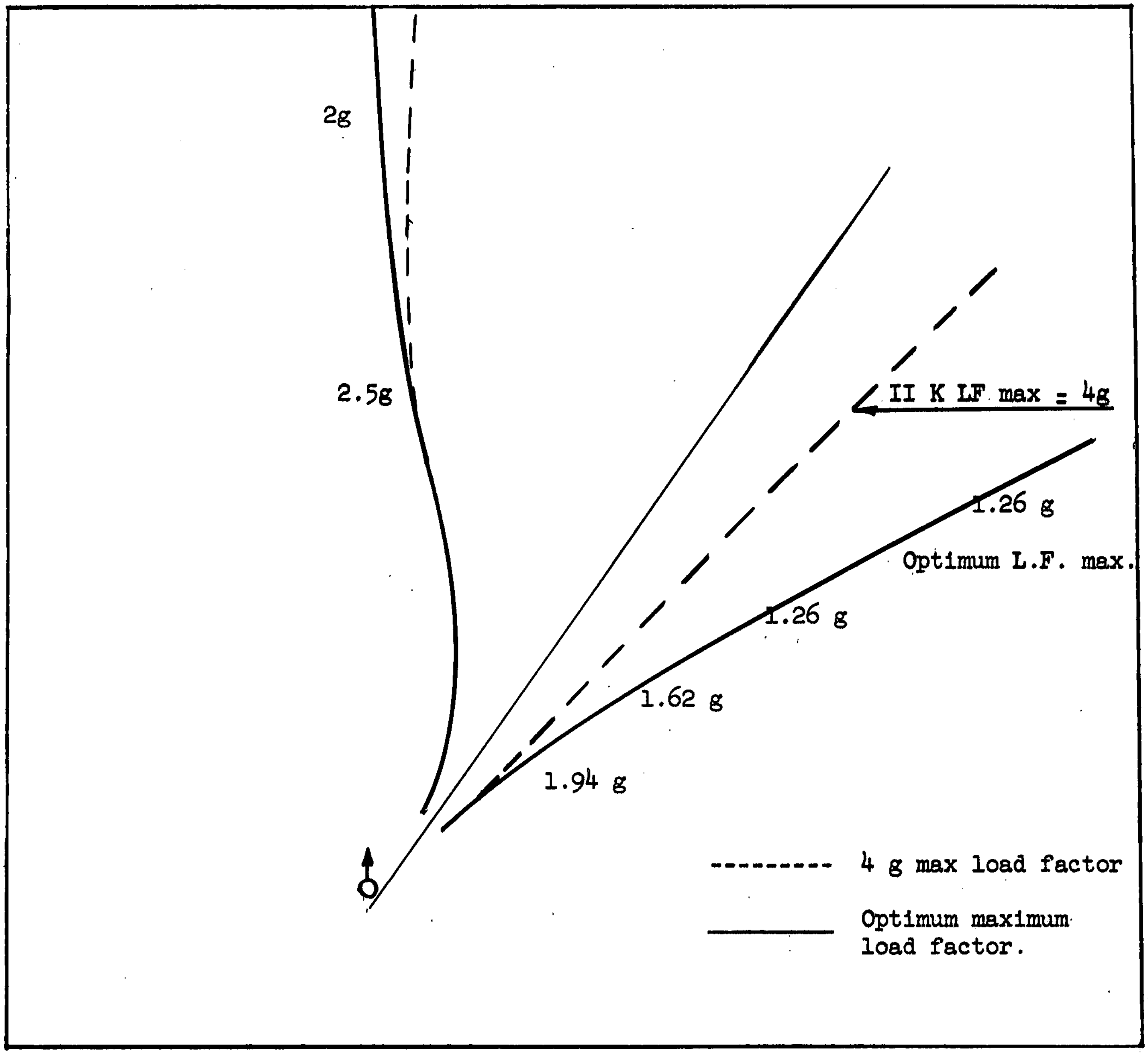

M_t = 2.0 h_t = 60 K Scale 25,000 ft/cm

M_{fo} = 2.0 h_{fo} = 60 K

Γ_o = 110°

Interceptor Maximum Load Factor Study — Prob. XIV M

Optimum Load Factor Limit

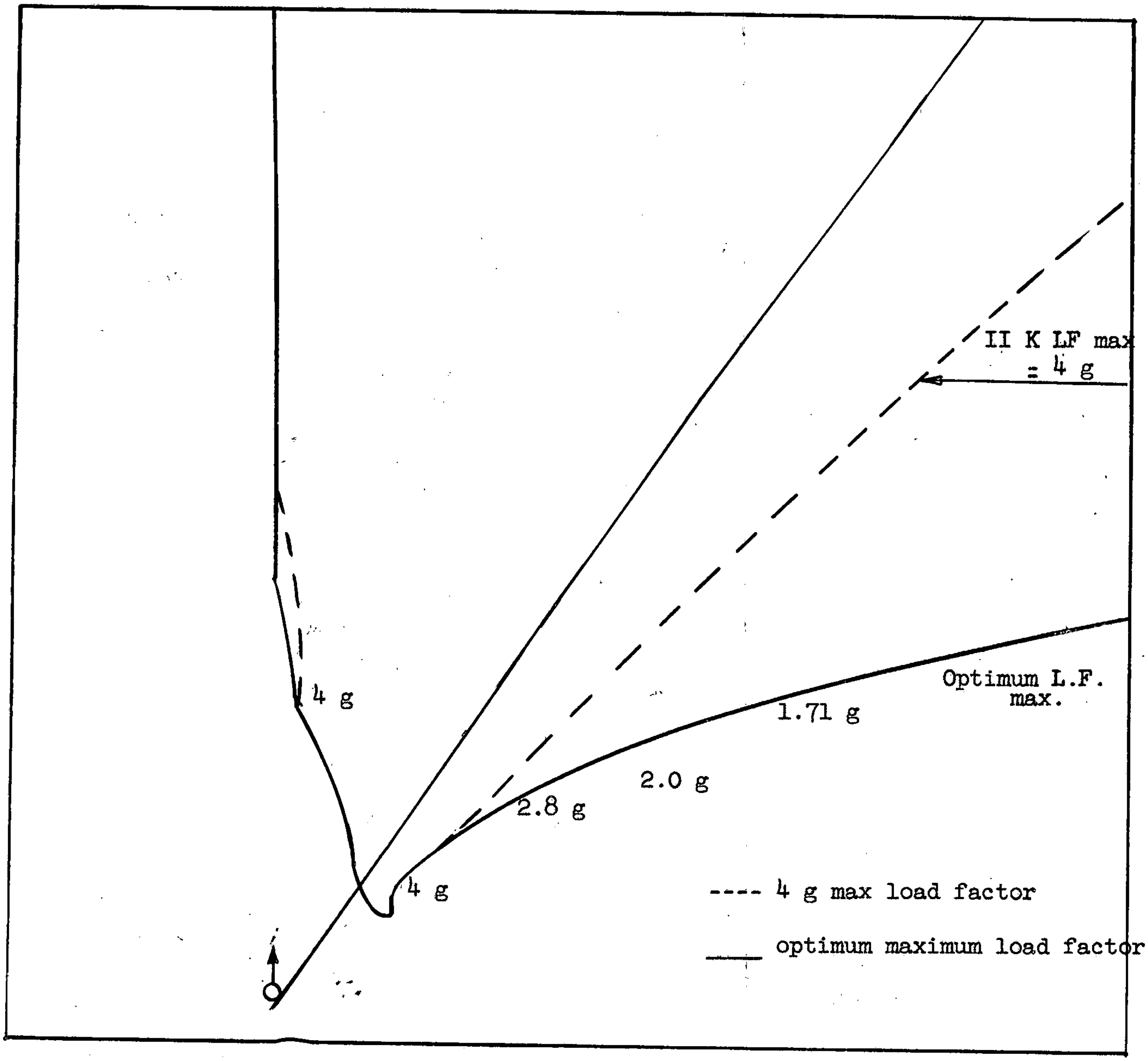

M_t = 2.0 h_t = 60 K

M_{fo} = 2.0 h_{fo} = 40 K

Γ_o = 110°

Scale 25,000 ft/cm

4.4.4.5 Maximum Load Factor and I.R. Look Angle Limits

If in a coaltitude attack interceptor maximum load factor is kept to 1.5 a high placement probability can be achieved against a non-maneuvering target.

4.4.5.0 Subsonic Interceptor - Problems XV and XVII

In order to test the effectiveness of the CF 105 against lower speed targets, some studies were carried out against a subsonic target (M0.95), at 50 K feet. For this study the CF 105 maximum speed was limited to M0.95.

Two cases of two situations were studied.

PROBLEM CONDITIONS

	XVII A	XV A	XVII B	XV B
h_{fo}	50 K	50 K	40 K	40 K
δ^*_c	0	15°	0	15°

$M_{fo} = M_t = 0.95$ $\Gamma_o = 135^\circ$ $h_t = 50$ K

$t_f = 8$ secs δ^*_c = allowable heading error at launch.

4.4.5.1 Results

The results of this study are optimistic because although the interceptor is unsuccessful against a non-maneuvering target, it is in a very vulnerable position from the point of view of target evasion.

This point is discussed below in Problem XIX, section 4.4.8.0.

4.4.6.0 Subsonic Target Studies - Problem XVI

The principal difference between this problem and Problem XV (above) is that the missiles cannot be launched successfully over a range of aspects near the nose of the target. In the forward hemisphere the target IR emission and hence the IR seeker maximum range falls off rapidly as the interceptor approaches the nose of the target. The maximum seeker range contour intersects the minimum time-to-go circle leaving a failure region for aspects near 180° (measured from the tail of the target). In the case of M2.0 target and fighter this was set tentatively at $\pm 30^\circ$ ie

Prob. XV A & XVII A

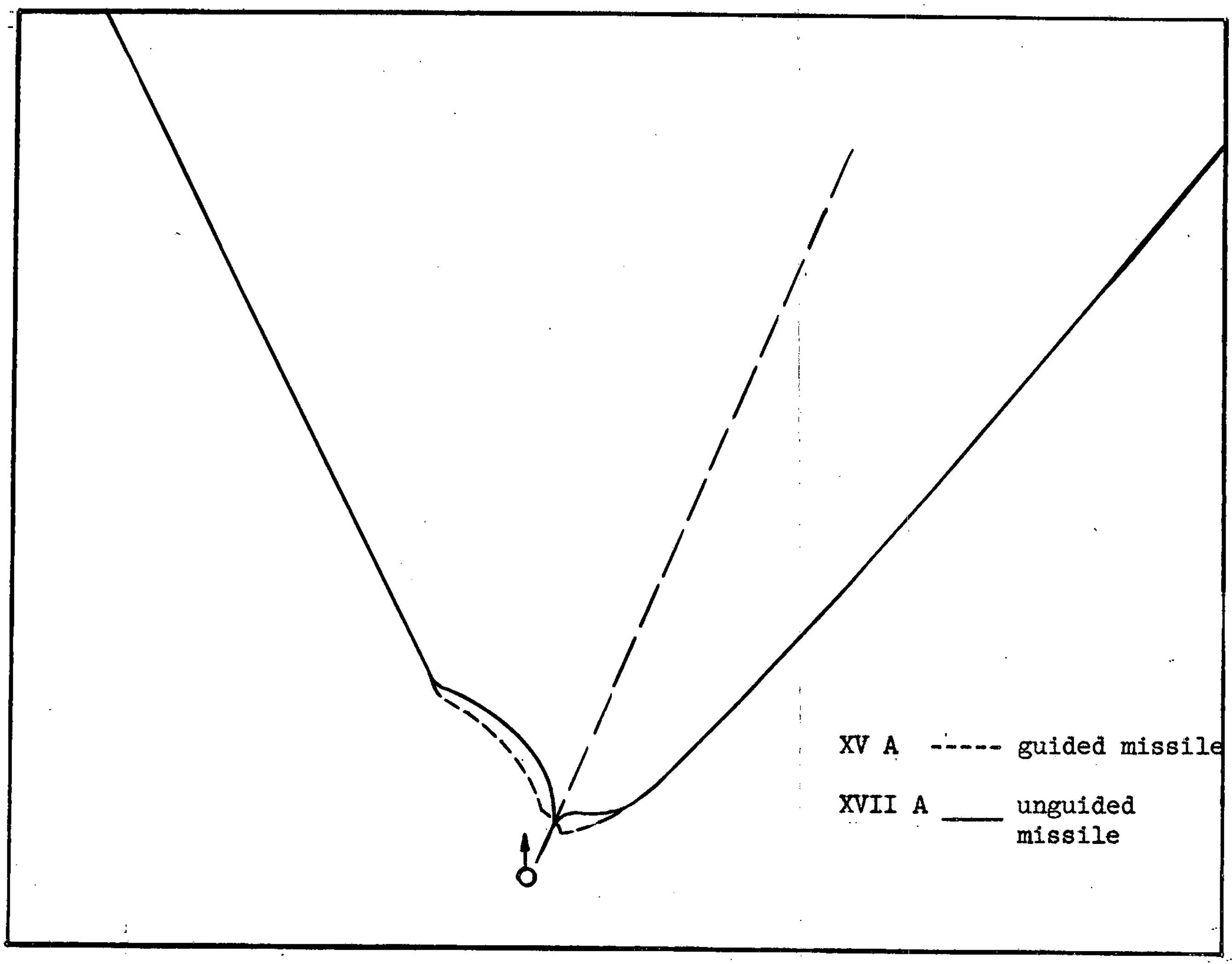

M_t = 0.95 h_t = 50 K

M_{fo} = 0.95 h_{fo} = 50 K

Γ_o = 135°

Scale 25,000 ft/cm

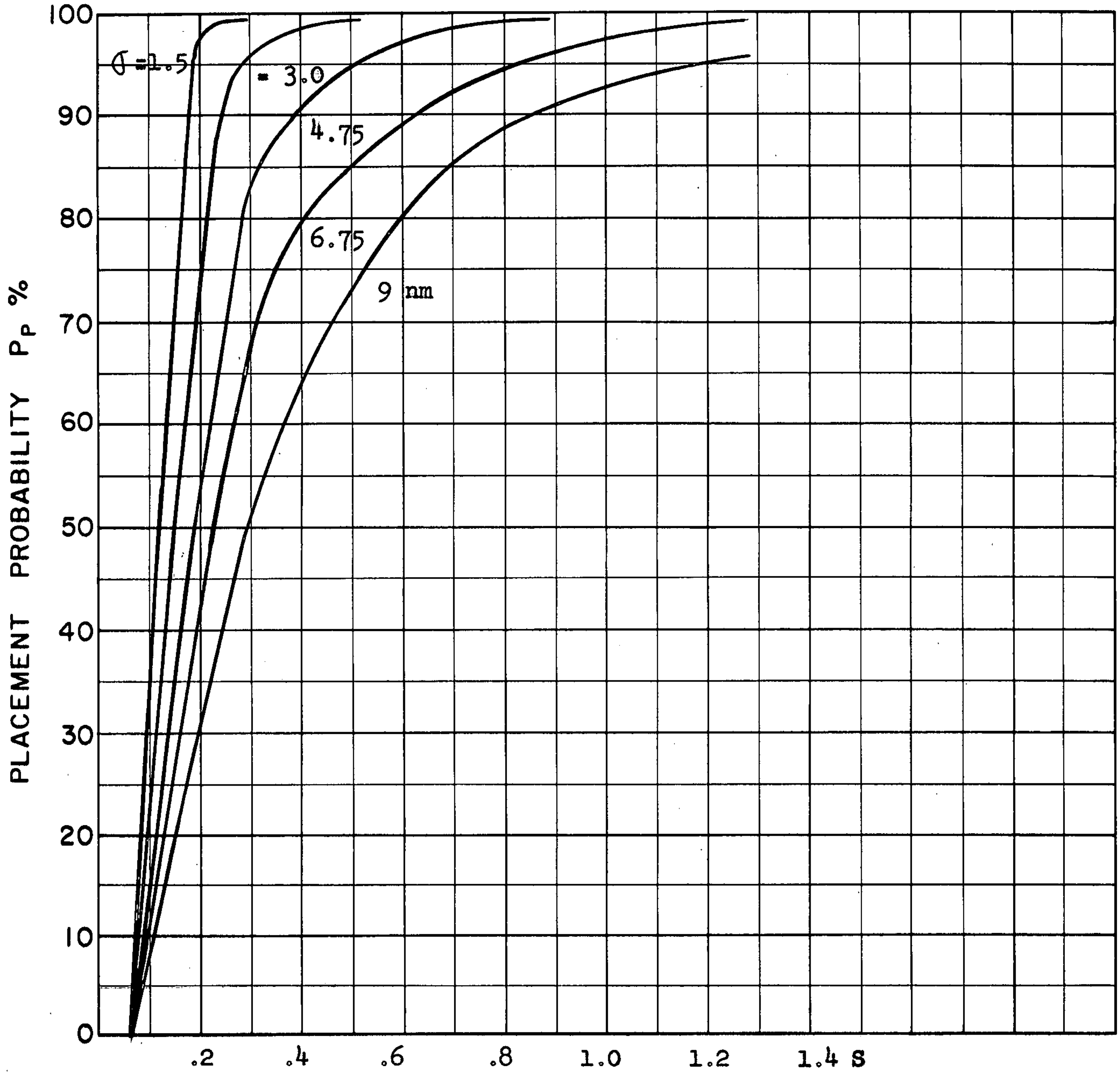

COURSE DIFFERENCE: 135°
TARGET EVASION: 0
TARGET MACH NO.: 0.95
INTERCEPTOR LATERAL G's: Avro 3.3
INTERCEPTOR MACH NO.: 0.95
σ OF G.C.I. ACCURACY: 5 Values
A.I. DETECTION RANGE AS FRACTION OF SPECIFICATION RANGE, S: Abscissa
A.I. DETECTION RANGE CONTOUR: Delta
ALTITUDE: 50 K

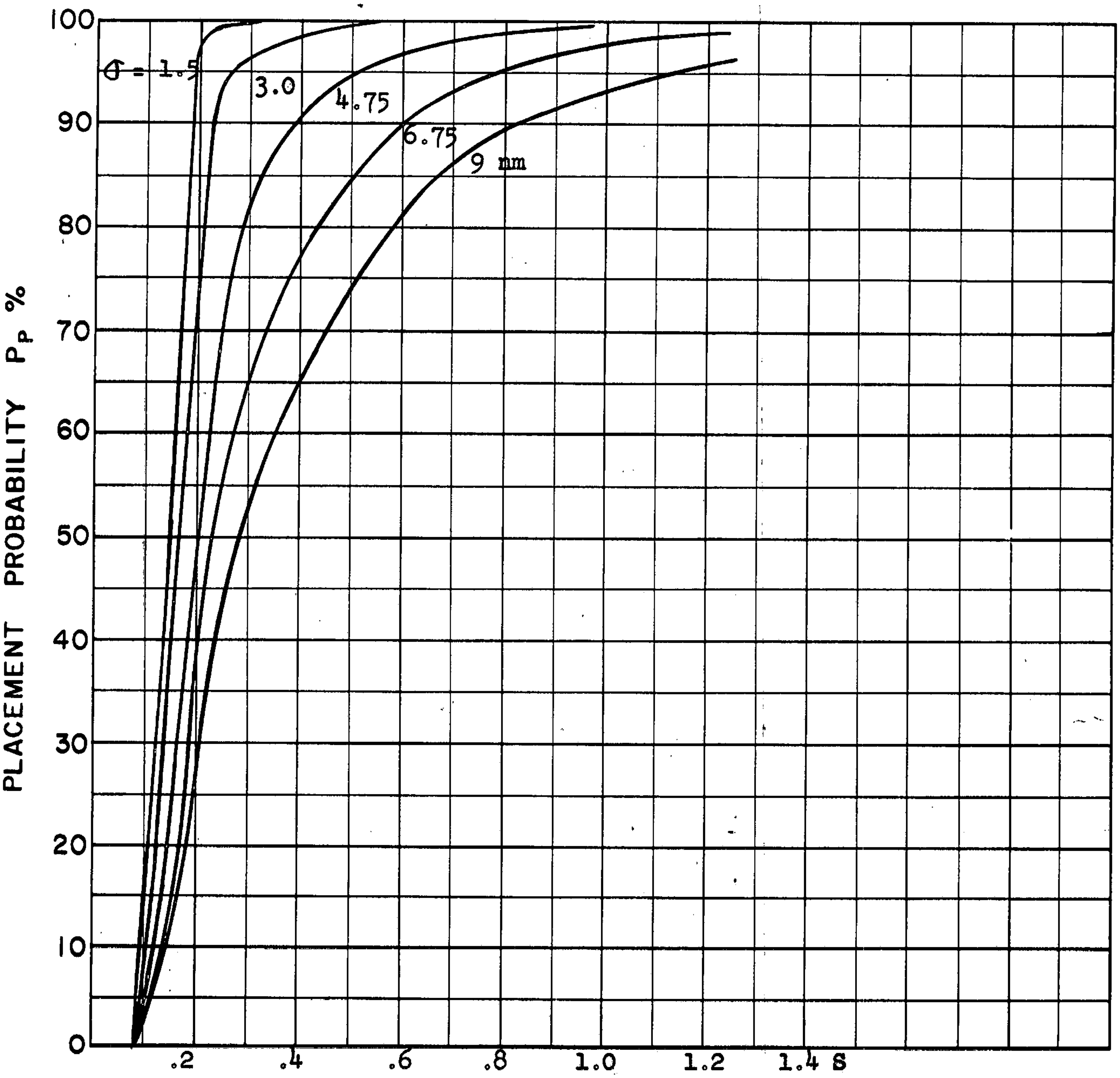

COURSE DIFFERENCE: 135°
TARGET EVASION: 0
TARGET MACH NO.: 0.95
INTERCEPTOR LATERAL G's: Avro 3.3
INTERCEPTOR MACH NO.: 0.95
σ OF G.C.I. ACCURACY: 5 Values
A.I. DETECTION RANGE AS FRACTION OF SPECIFICATION RANGE, S: Abscissa
A.I. DETECTION RANGE CONTOUR: Delta
ALTITUDE: 50 K

Prob. XV B & XVII B

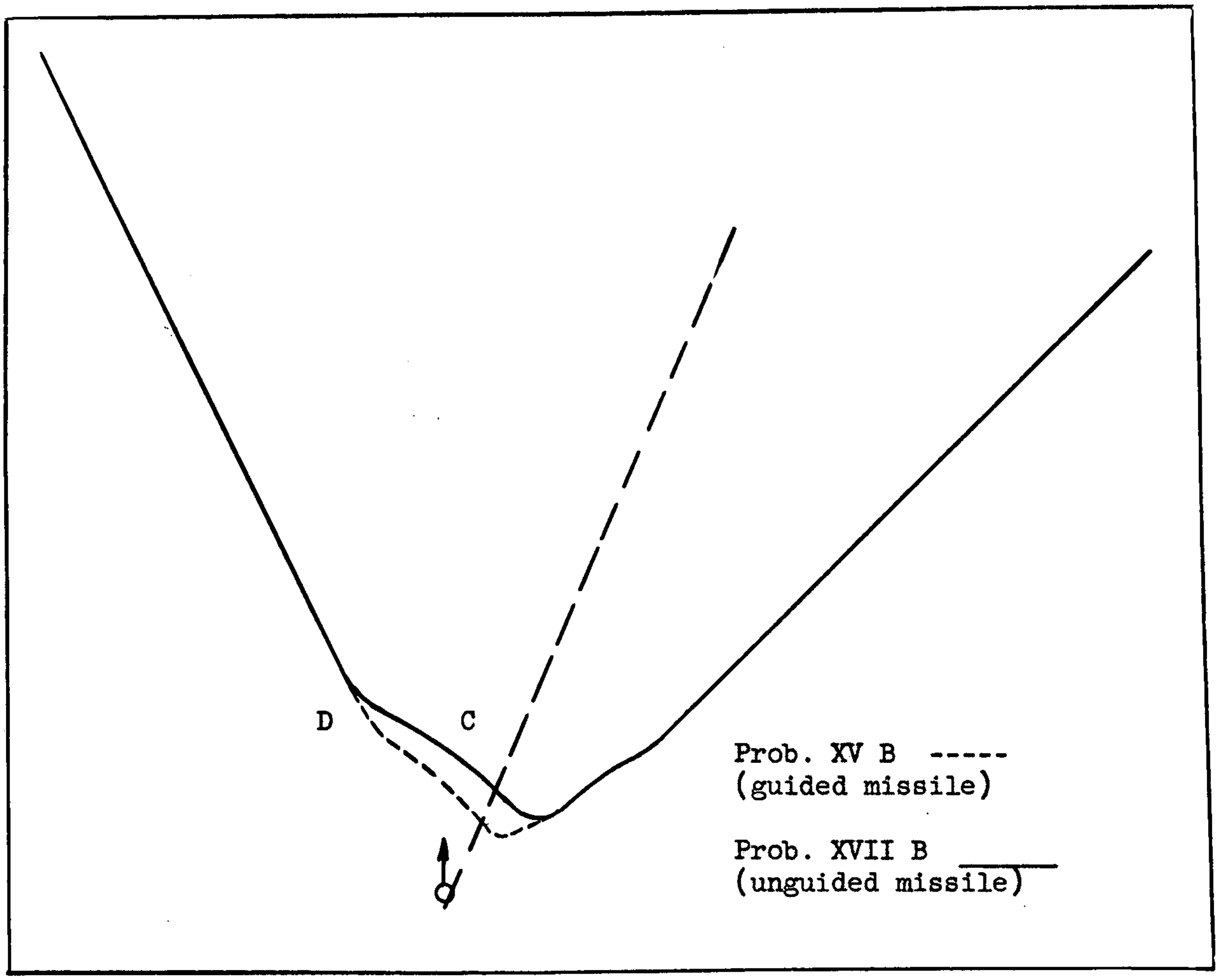

$M_t = 0.95 \quad h_t = 50$ K

$M_{fo} = 0.95 \quad h_{fo} = 40$ K

$\Gamma_o = 135^{\circ}$

Scale 25,000 ft/cm

Subsonic Interceptor & Target Prob. XV B

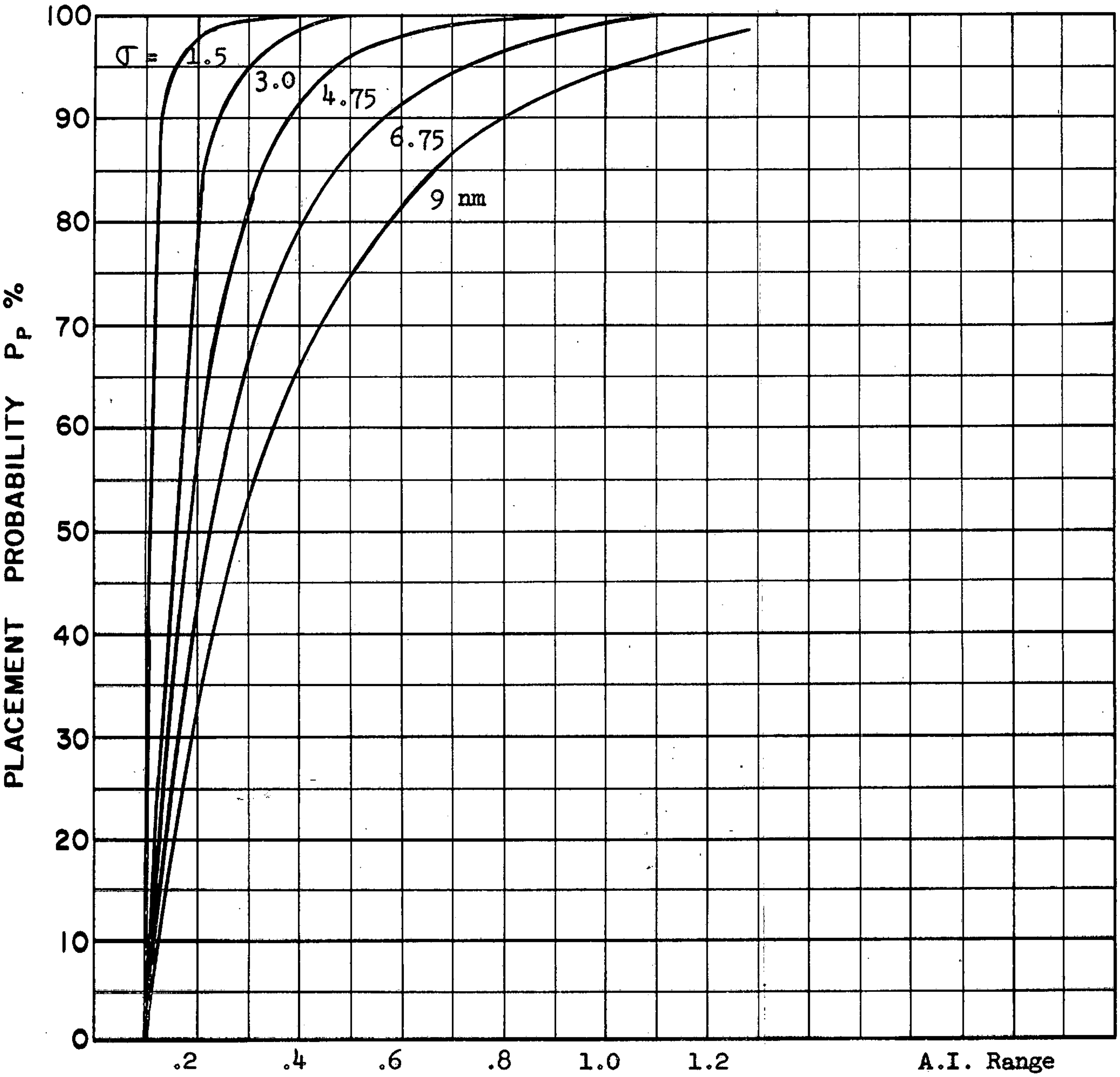

COURSE DIFFERENCE: 135°
TARGET EVASION: 0
TARGET MACH NO.: 0.95
INTERCEPTOR LATERAL G's: Avro 3.3
INTERCEPTOR MACH NO.: (Max. 0.95)
σ OF G.C.I. ACCURACY: 5 Values
A.I. DETECTION RANGE AS FRACTION OF SPECIFICATION RANGE, S: Abscissa
A.I. DETECTION RANGE CONTOUR: Delta
ALTITUDE: H_t = 50 K

H_{fo} = 40 K

Unguided Missile

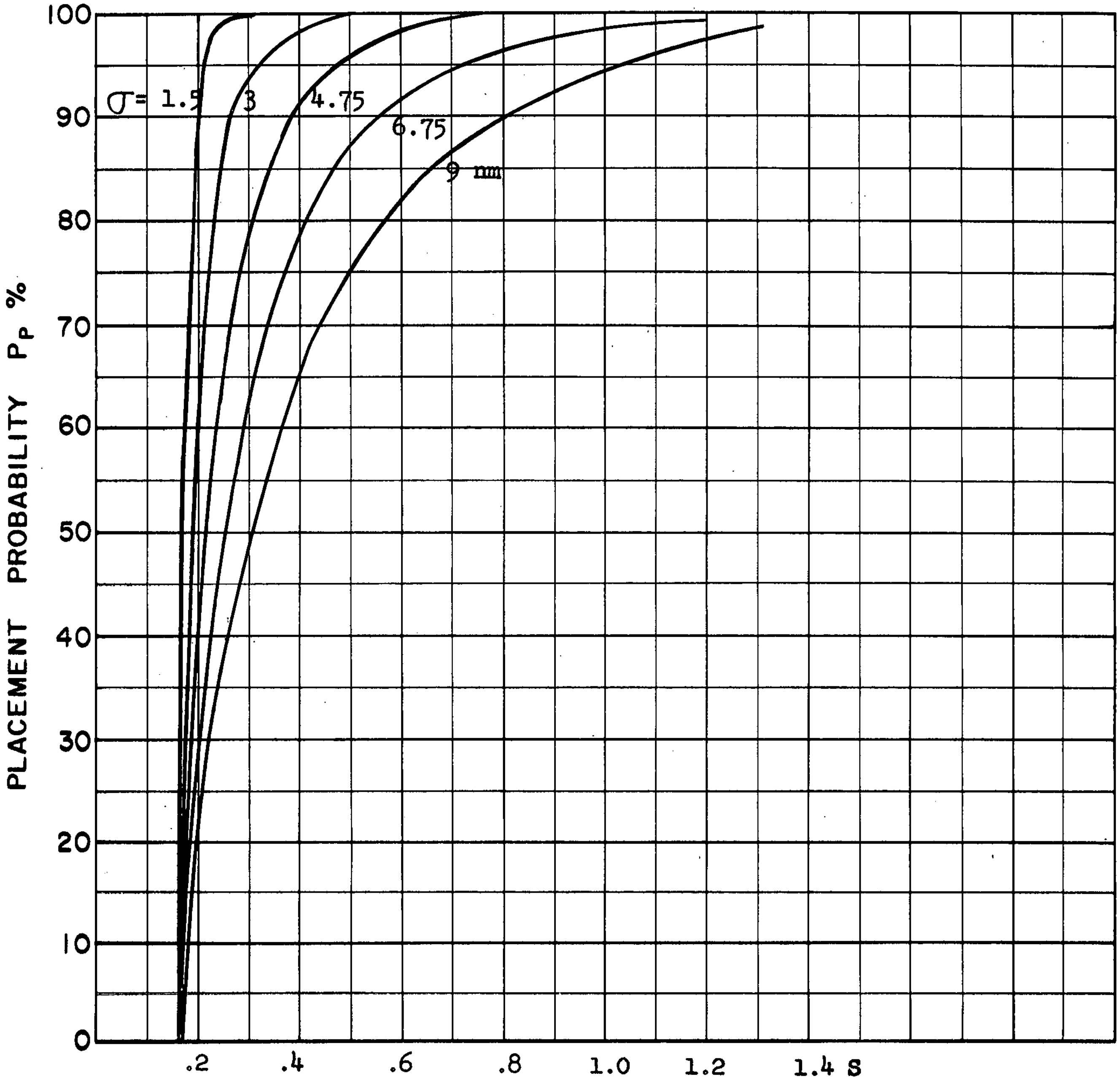

COURSE DIFFERENCE: 135°
TARGET EVASION: 0
TARGET MACH NO.: 0.95
INTERCEPTOR LATERAL G's: Avro 3.3
INTERCEPTOR MACH NO.: 0.95
σ OF G.C.I. ACCURACY: 5 Values
A.I. DETECTION RANGE AS FRACTION OF SPECIFICATION RANGE, S: Abscissa
A.I. DETECTION RANGE CONTOUR: Delta
ALTITUDE: H_t = 50 K
H_{fo} = 40 K

launch aspects of 150° to 210° are failures. For a M0.95 fighter and M0.85 fighter this corresponds to $\pm 20^\circ$. However, it was assumed that the emission from a M0.85 target would be less than M2.0 target and again a figure of $\pm 30^\circ$ was used.

4.4.6.1 Problem Conditions

Prob. XVI	A	B
Γ_o	135°	110°

$h_{fo} = h_t = 50$ K $\qquad M_{fo} = .95 \qquad M_t = .85$

$F = 7$ K $\qquad t_f = 8$ secs.

4.4.6.2 Conclusions

For course differences of 135° and more the probabilities are low owing to the predominance of final aspects $\pm 30^\circ$ off the nose of the target.

For course differences of 110° and less, high placement probabilities are encountered.

Here again the target has a good chance of escaping by maneuvering.

4.4.7.0 Problem XVIII - IR AI, Fixed Range Lead Pursuit Study (Called "Fixed R & T" in ref. 7)

This study was carried out in conjunction with a general study of Fixed Range lead pursuit navigation. The main study is reported separately in refs. 7 and 8. As in section 4.4.2.0 above cross-over was assumed. That is, at close range the AI radar is effective and fire control is handled in the usual way.

IR Missile

Prob. XVI A

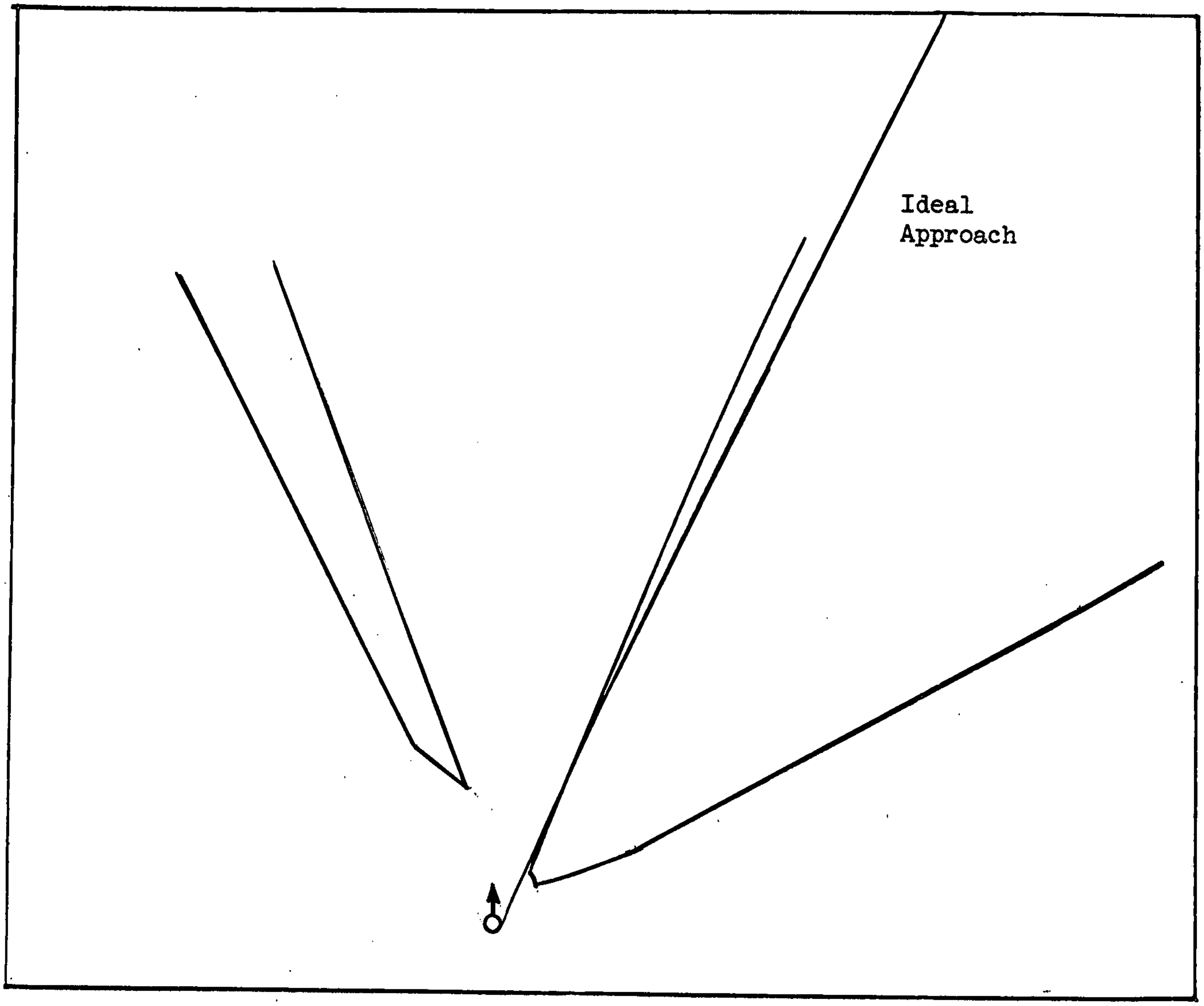

M_t = .85 h_t = 50 K

M_{fo} = .95 h_f = 50 K

Γ_o = 135°

Scale 25,000 ft/cm

IR Missile

Prob. XVI A

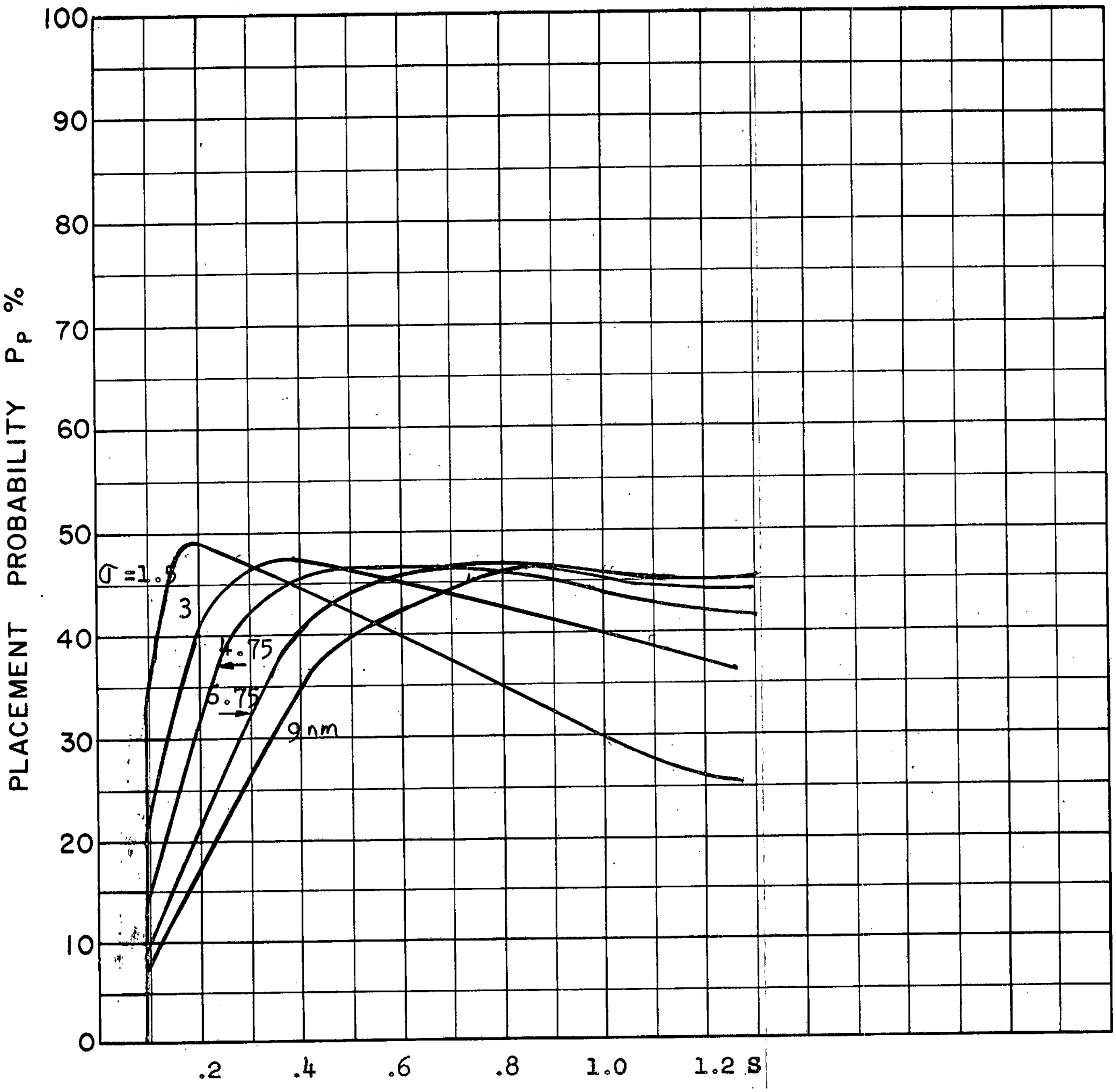

COURSE DIFFERENCE: 135°
TARGET EVASION: 0
TARGET MACH NO.: 0.85
INTERCEPTOR LATERAL G's: Avro 3.3
INTERCEPTOR MACH NO.: 0.95 max.
σ OF G.C.I. ACCURACY: 5 Values
A.I. DETECTION RANGE AS FRACTION OF SPECIFICATION RANGE, S: Abscissa
A.I. DETECTION RANGE CONTOUR: Delta
ALTITUDE: $H_f = H_t = 50$ K

IR Missile   Prob. XVI B

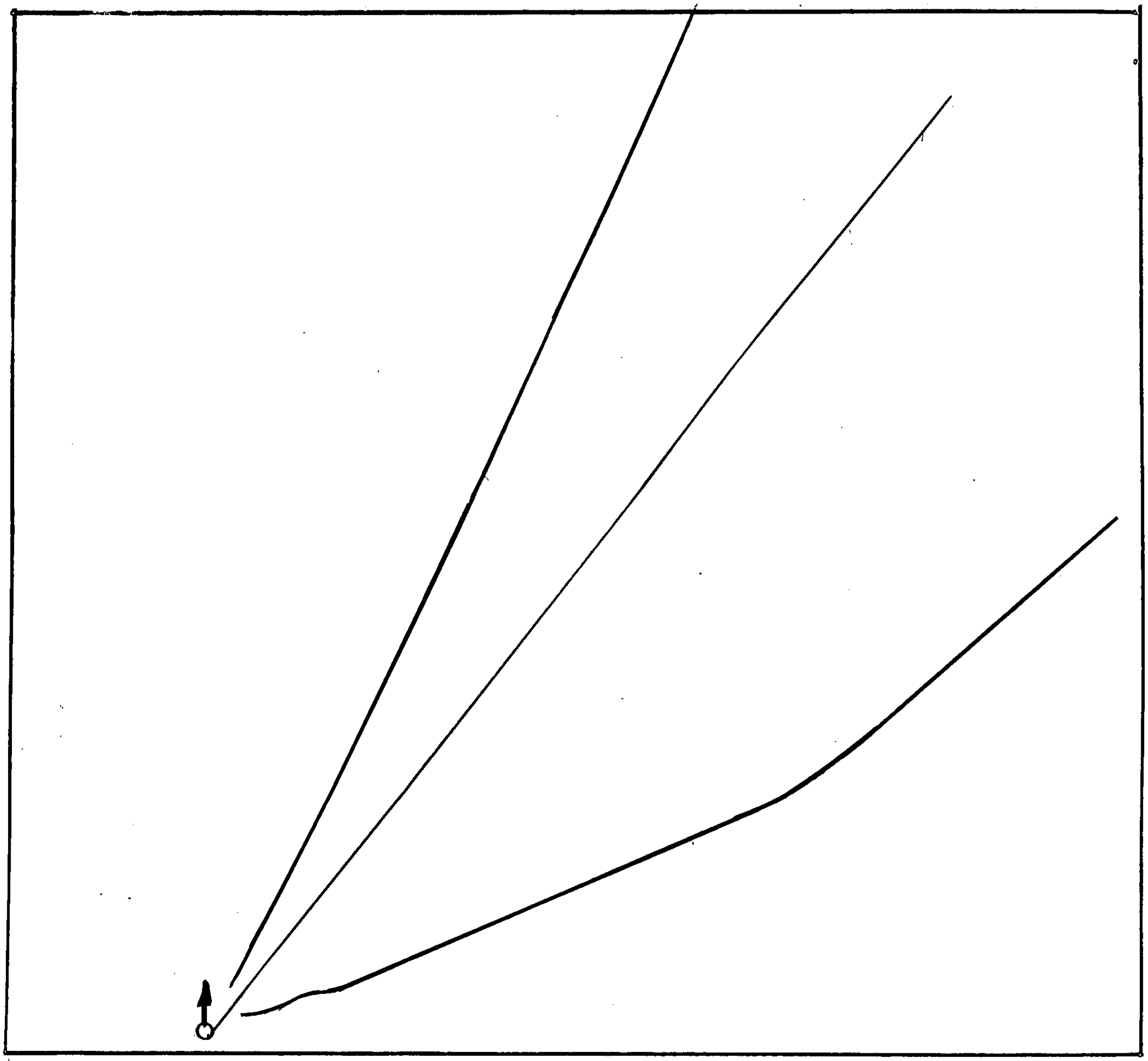

M_t = 0.85 h_t = 50 K   Scale 25,000 ft/cm

M_{fo} = 0.95 h_{fo} = 50 K

Γ_o = 110°

IR Missile

Prob. XVI B

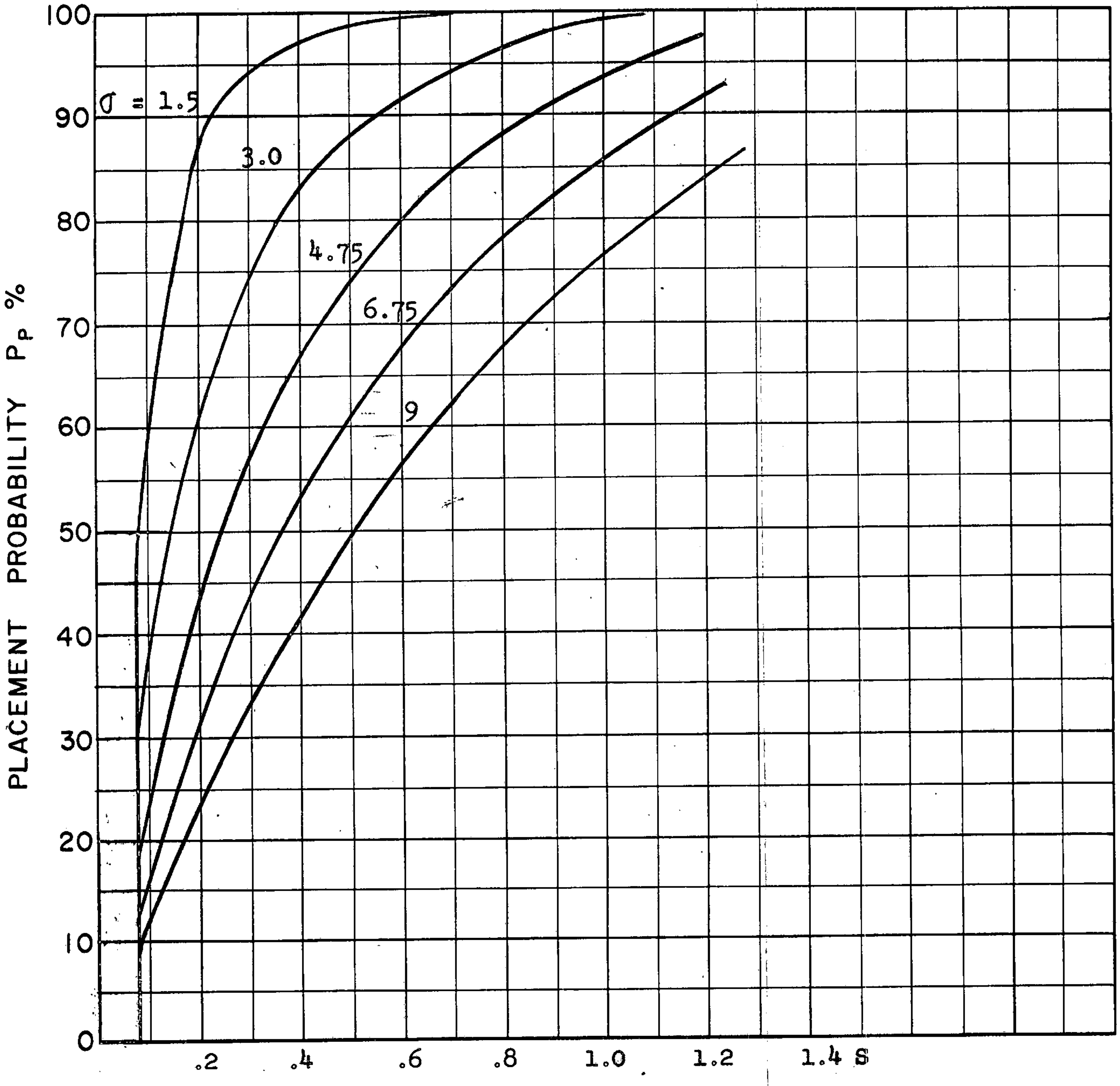

COURSE DIFFERENCE: 110°
TARGET EVASION: 0
TARGET MACH NO.: .85
INTERCEPTOR LATERAL G's: Avro 3.3
INTERCEPTOR MACH NO.: .95 max.
σ OF G.C.I. ACCURACY: 5 Values
A.I. DETECTION RANGE AS FRACTION OF SPECIFICATION RANGE, S: Abscissa
A.I. DETECTION RANGE CONTOUR: Delta
ALTITUDE: 50 K

Subsonic Target

Prob. XVIII A, B

IR AI Phase using Fixed Range Lead Pursuit Navigation

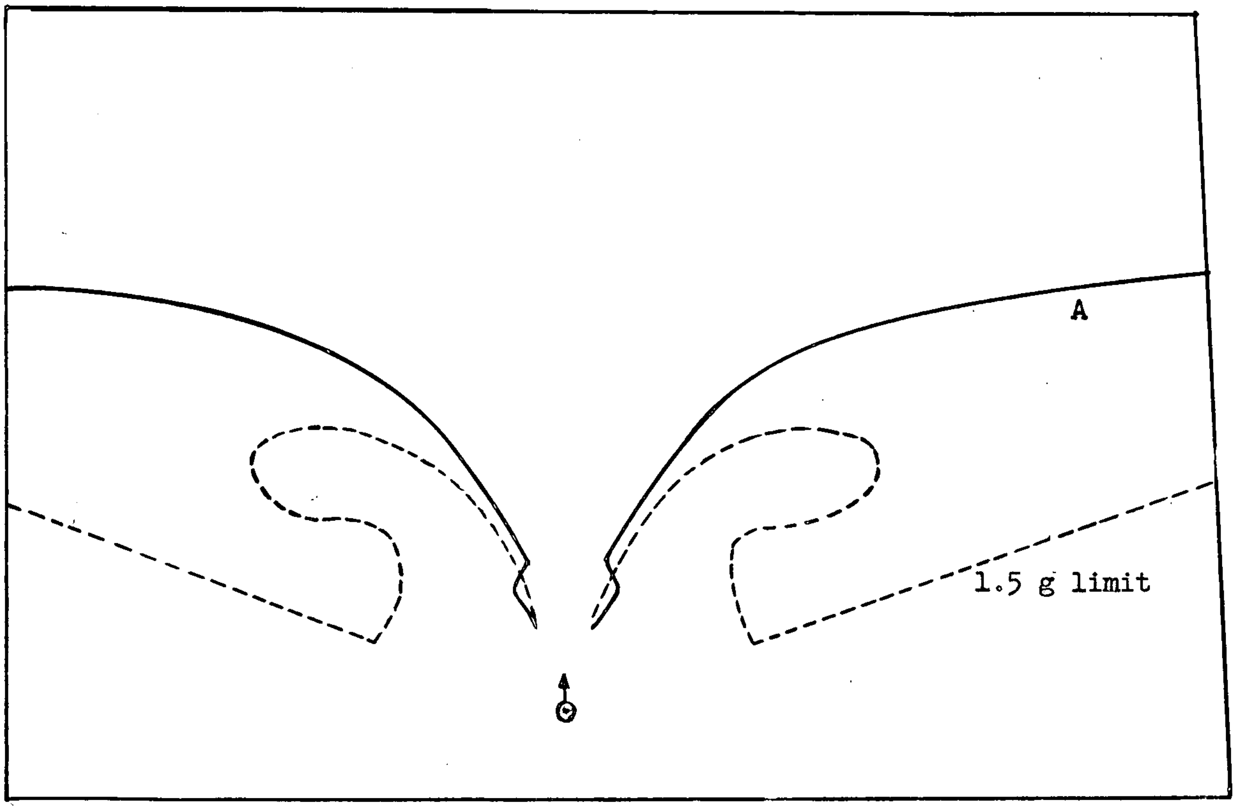

Γ_o = 180°

M_{fo} = 1.5

M_t = 0.85

h = 50 K

Scale 25 K/cm

IR AI Phase Subsonic Target Prob. XVIII A

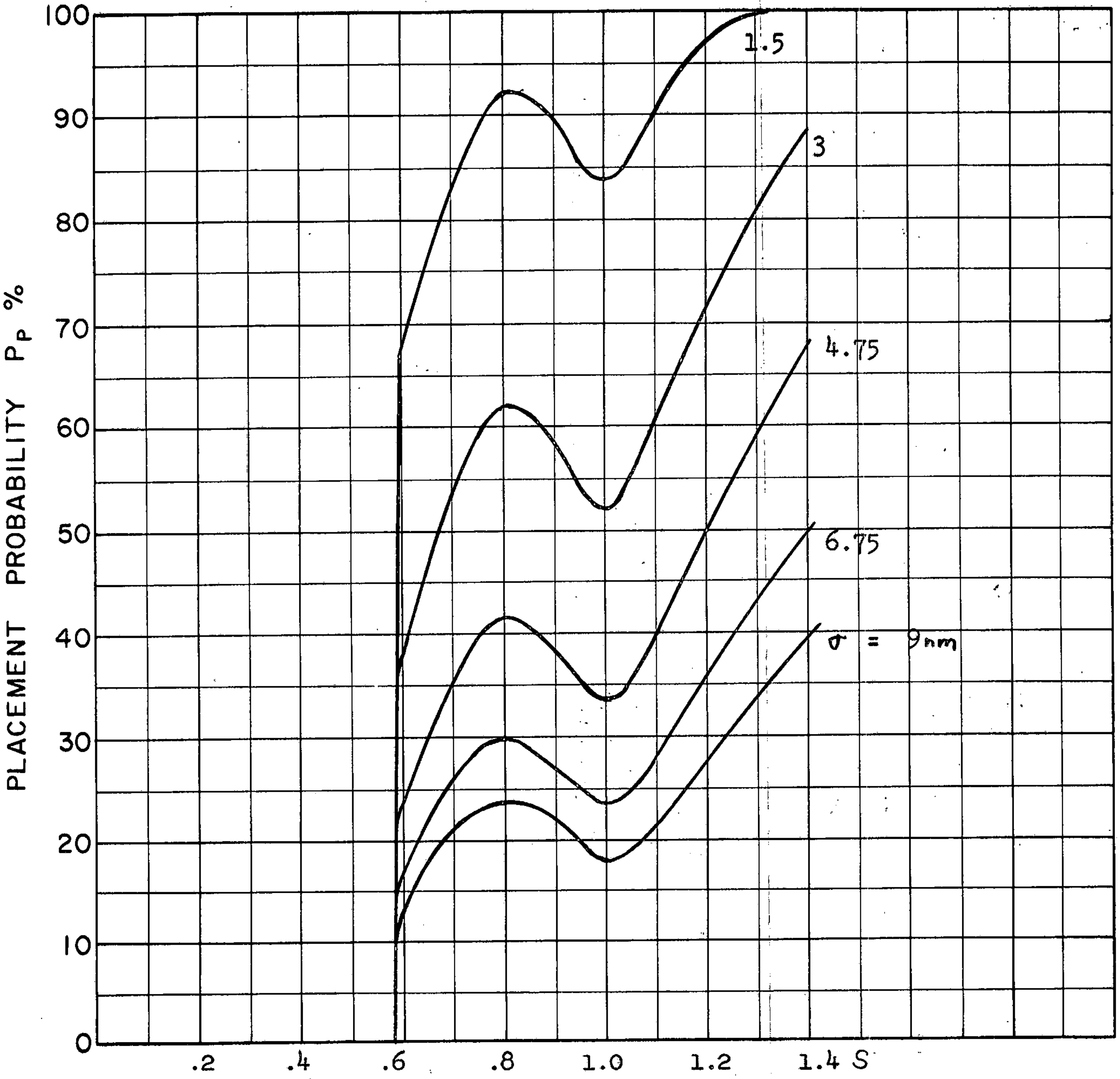

Fixed Range Lead Pursuit Navigation

COURSE DIFFERENCE: 180°
TARGET EVASION: 0
TARGET MACH NO.: 0.85
INTERCEPTOR LATERAL G's: Avro 3.3
INTERCEPTOR MACH NO.: 1.5
σ OF G.C.I. ACCURACY: 5 values
A.I. DETECTION RANGE AS FRACTION OF SPECIFICATION RANGE, S abscissa
A.I. DETECTION RANGE CONTOUR: I.R. B 52
ALTITUDE: 50 K

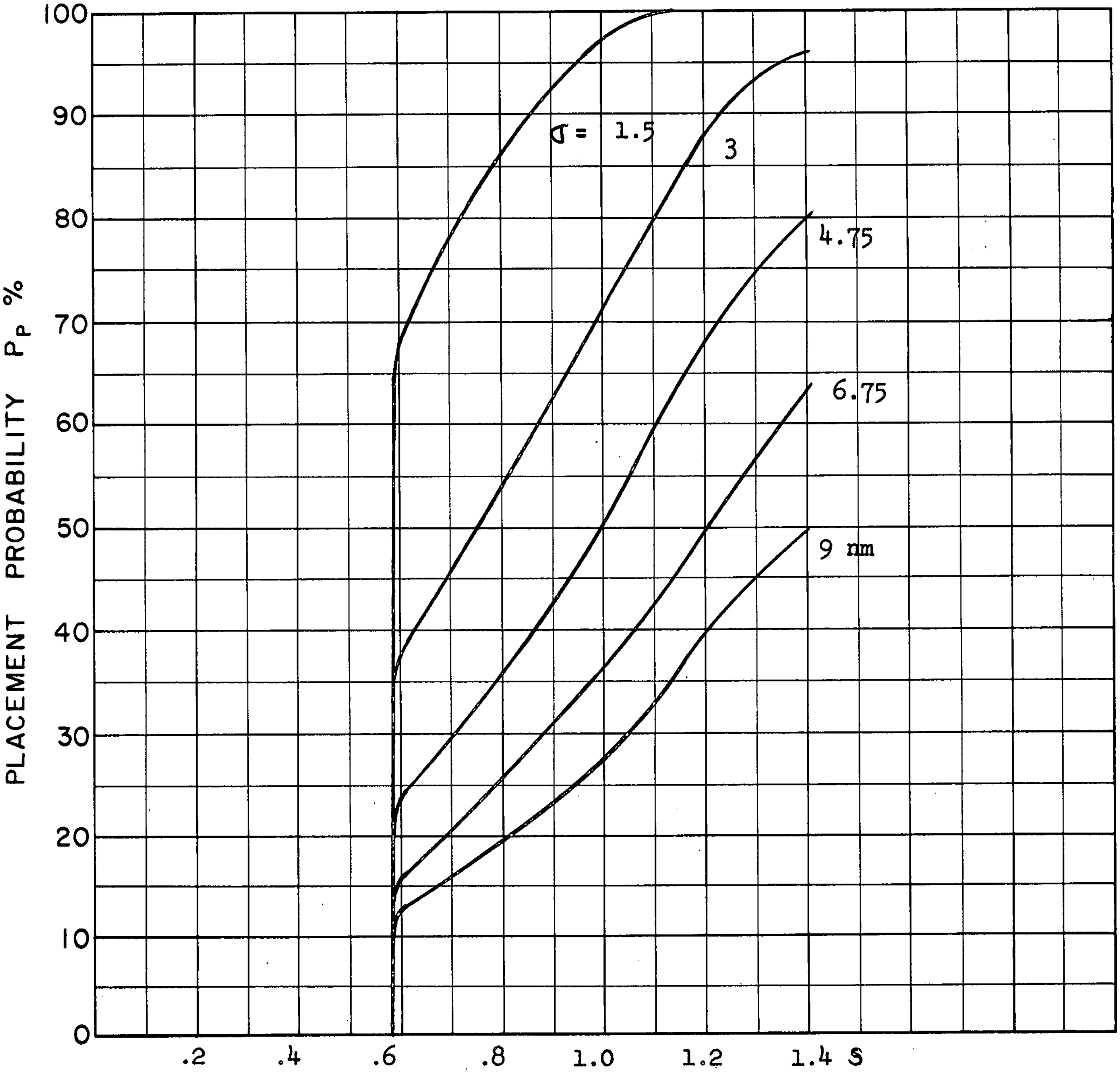

Fixed Range Lead Pursuit Navigation

COURSE DIFFERENCE: 180°
TARGET EVASION: 0
TARGET MACH NO.: 0.85
INTERCEPTOR LATERAL G's: Avro 3.3 with 1.5g max.
INTERCEPTOR MACH NO.: 1.5
σ OF G.C.I. ACCURACY: 5 Values
A.I. DETECTION RANGE AS FRACTION OF SPECIFICATION RANGE, S: Abscissa
A.I. DETECTION RANGE CONTOUR: IR B 52
ALTITUDE: 50 K

Subsonic Target   Prob XVIII C D

IR AI Phase using Fixed Range Lead Pursuit Navigation

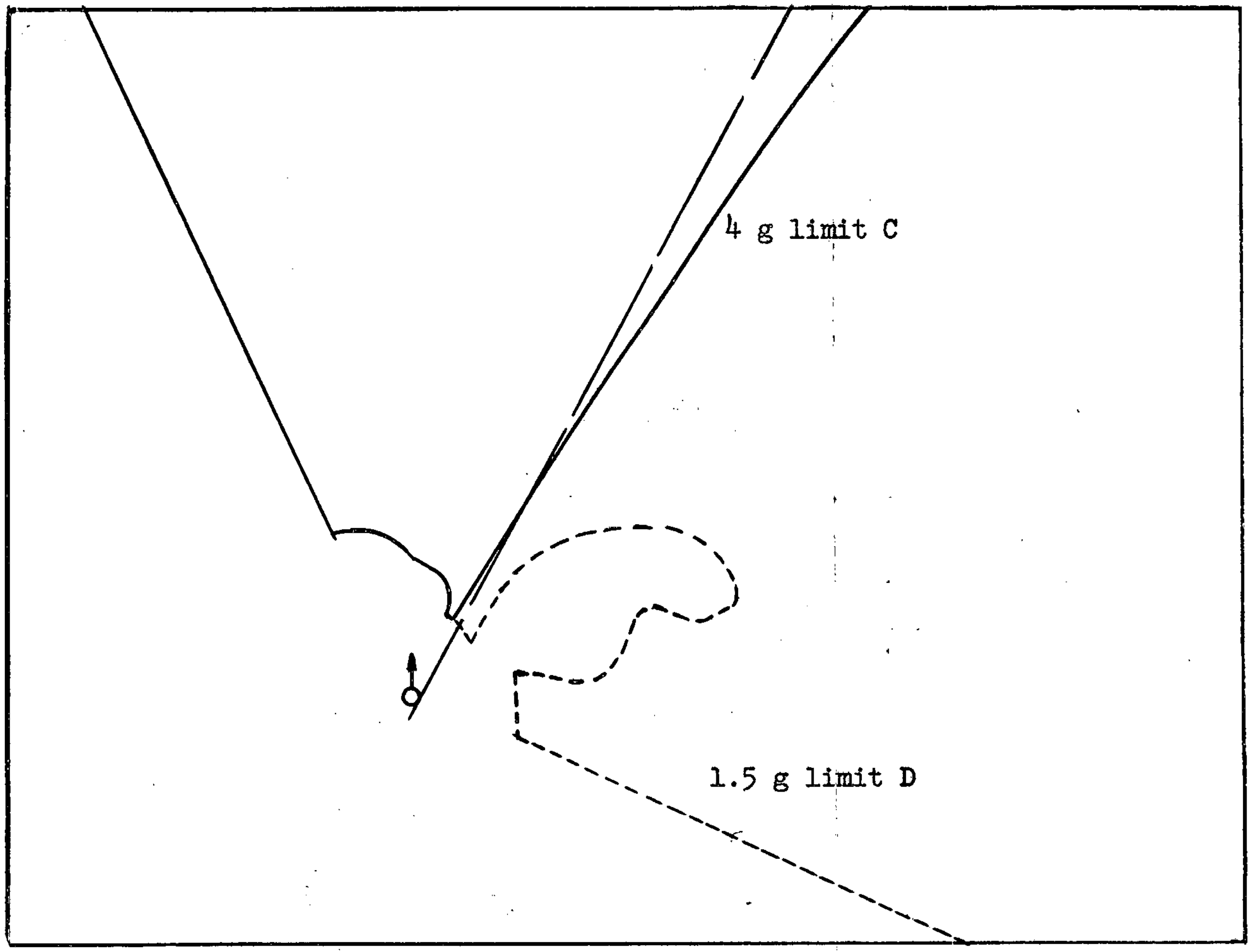

Γ_o = 135°   25 K ft/cm.

M_{fo} = 1.5

M_t = 0.85

h = 50 K

IR AI Phase Subsonic Target

Prob. XVIII C

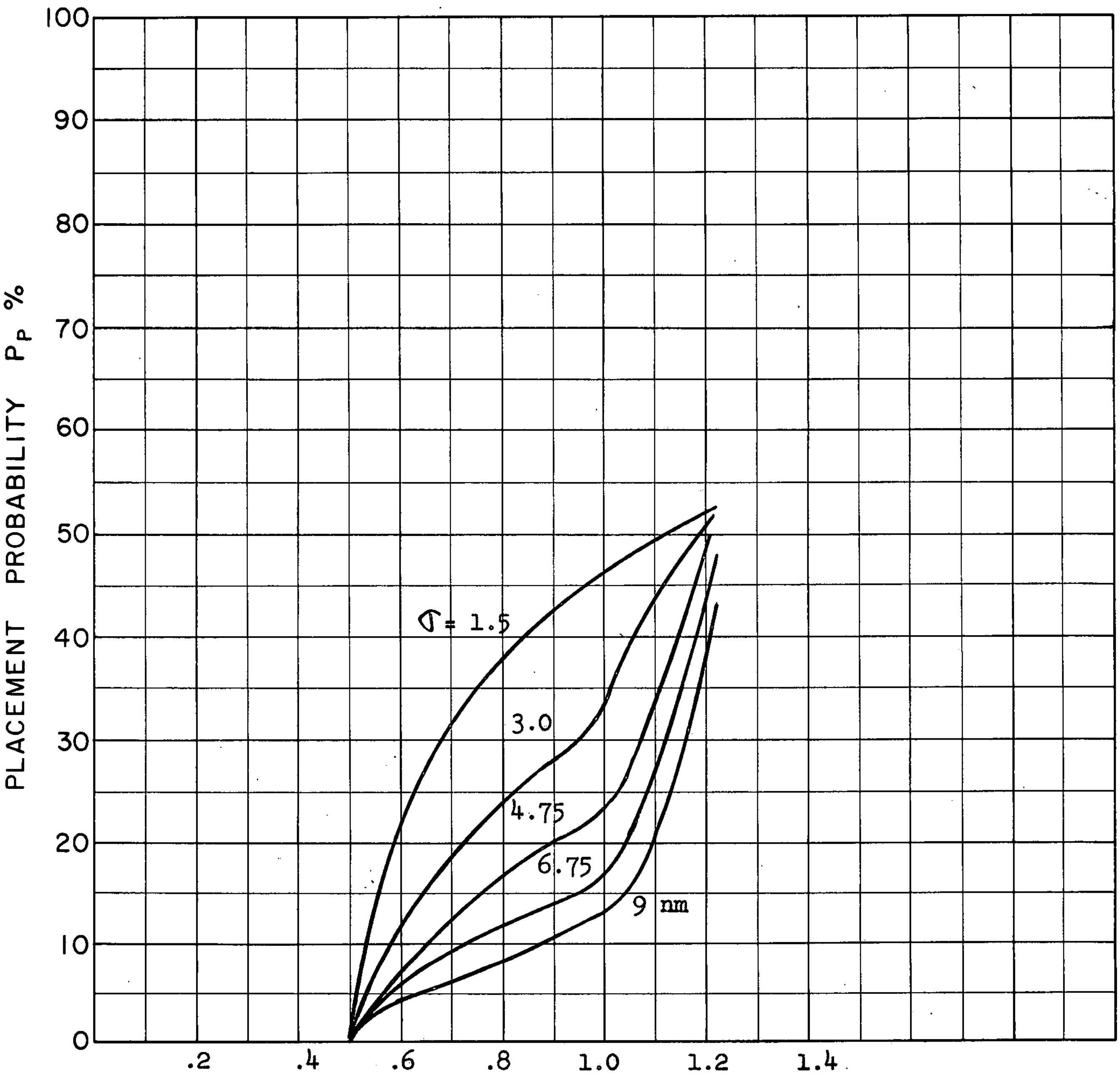

Fixed Range Lead Pursuit Navigation

COURSE DIFFERENCE: 135°
TARGET EVASION: 0
TARGET MACH NO.: 0.85
INTERCEPTOR LATERAL G's: Avro 3.3
INTERCEPTOR MACH NO.: 1.5
σ OF G.C.I. ACCURACY: 5 Values
A.I. DETECTION RANGE AS FRACTION OF SPECIFICATION RANGE, S: Abscissa
A.I. DETECTION RANGE CONTOUR: IR B 52
ALTITUDE: 50 K

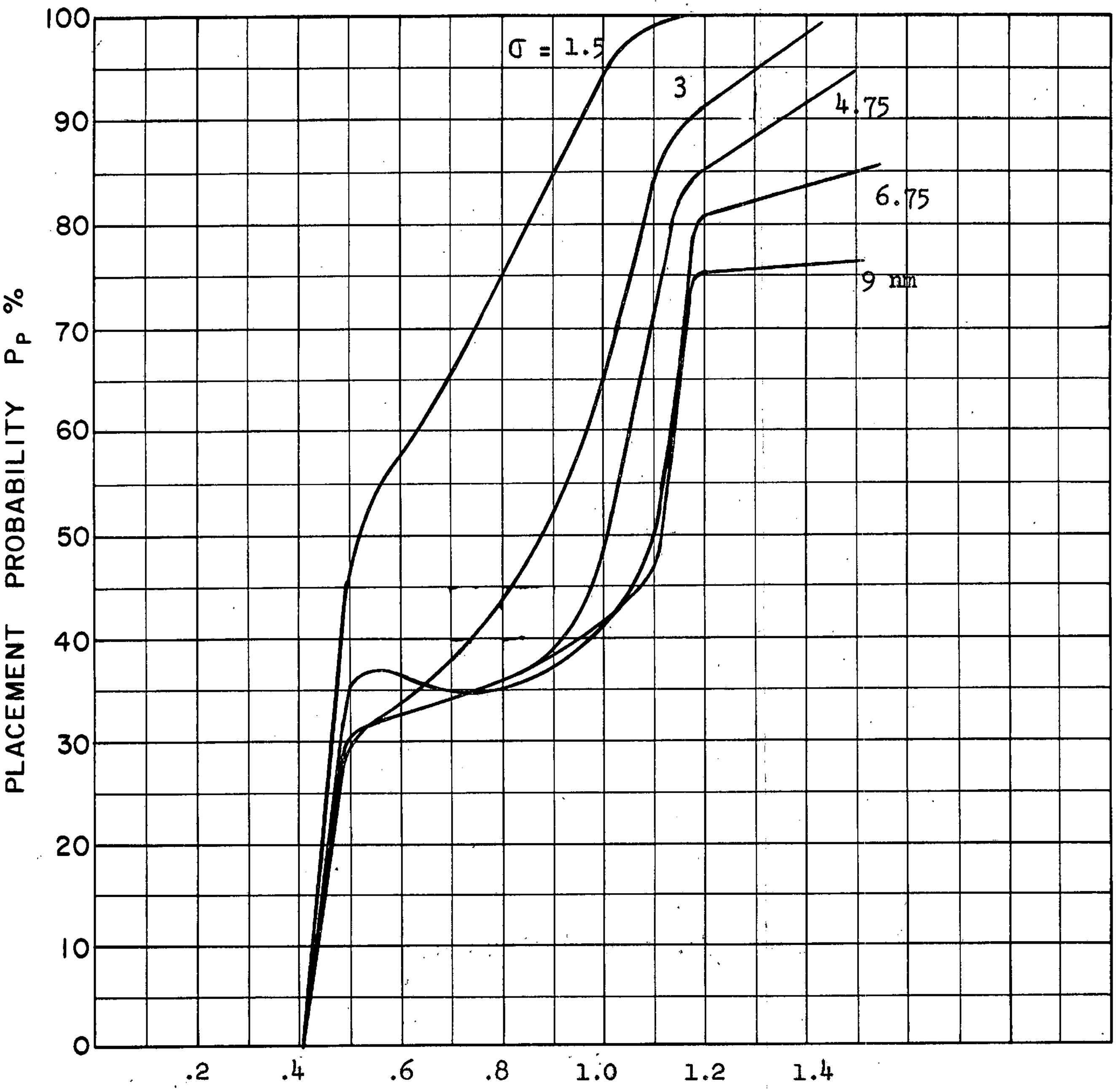

Fixed Range Lead Pursuit Navigation
COURSE DIFFERENCE: 135°
TARGET EVASION: 0
TARGET MACH NO.: 0.85
INTERCEPTOR LATERAL G's: Avro 3.3 with 1.5 g max
INTERCEPTOR MACH NO.: 1.5
σ OF G.C.I. ACCURACY: 5 Values
A.I. DETECTION RANGE AS FRACTION OF SPECIFICATION RANGE, S: Abscissa
A.I. DETECTION RANGE CONTOUR: I.R. B 52
ALTITUDE: 50 K

Subsonic Target

Prob. XVIII E, F

IR AI Phase using Fixed Range Lead Pursuit Navigation

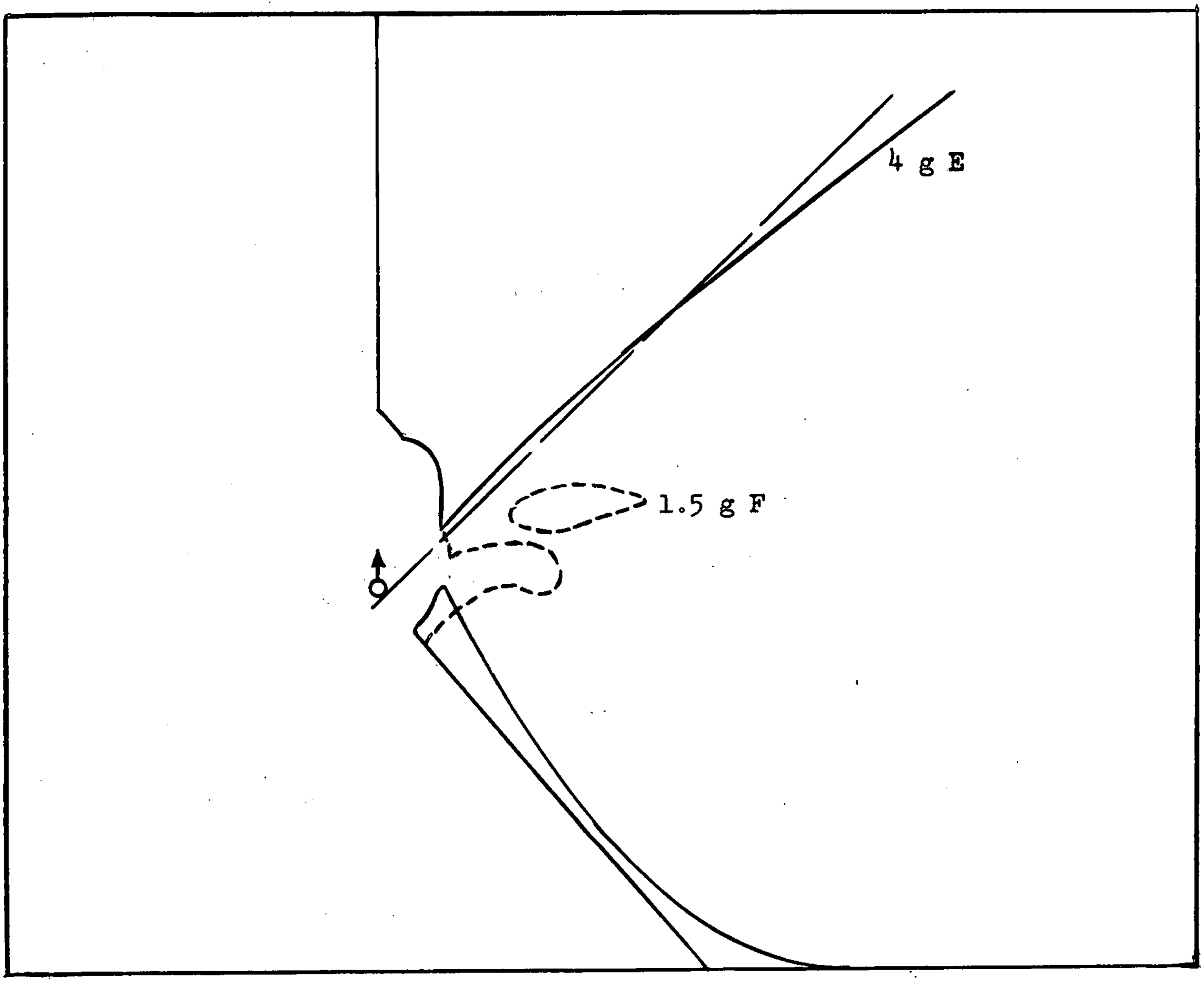

$\Gamma_o = 110^\circ$

Scale 25,000 ft/cm

$M_{fo} = 1.5$

$M_t = 0.85$

$h = 50$ K

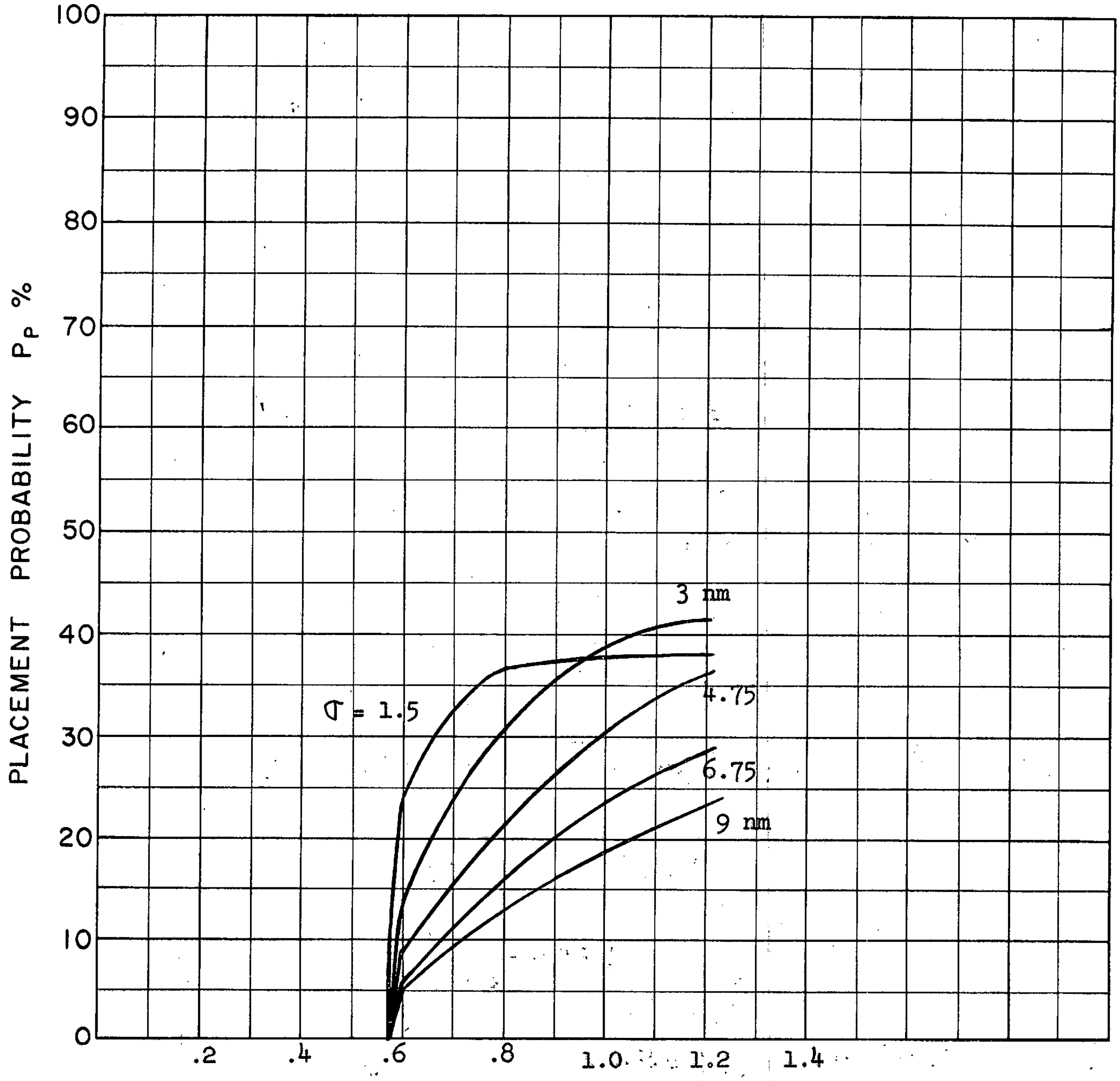

Fixed Range Lead Pursuit Navigation

COURSE DIFFERENCE: 110°
TARGET EVASION: 0
TARGET MACH NO.: 0.85
INTERCEPTOR LATERAL G's: Avro 3.3
INTERCEPTOR MACH NO.: 1.5
σ OF G.C.I. ACCURACY: 5 Values
A.I. DETECTION RANGE AS FRACTION OF SPECIFICATION RANGE, S: Abscissa
A.I. DETECTION RANGE CONTOUR: IR B 52
ALTITUDE: 50 K

IR AI Phase Subsonic Target

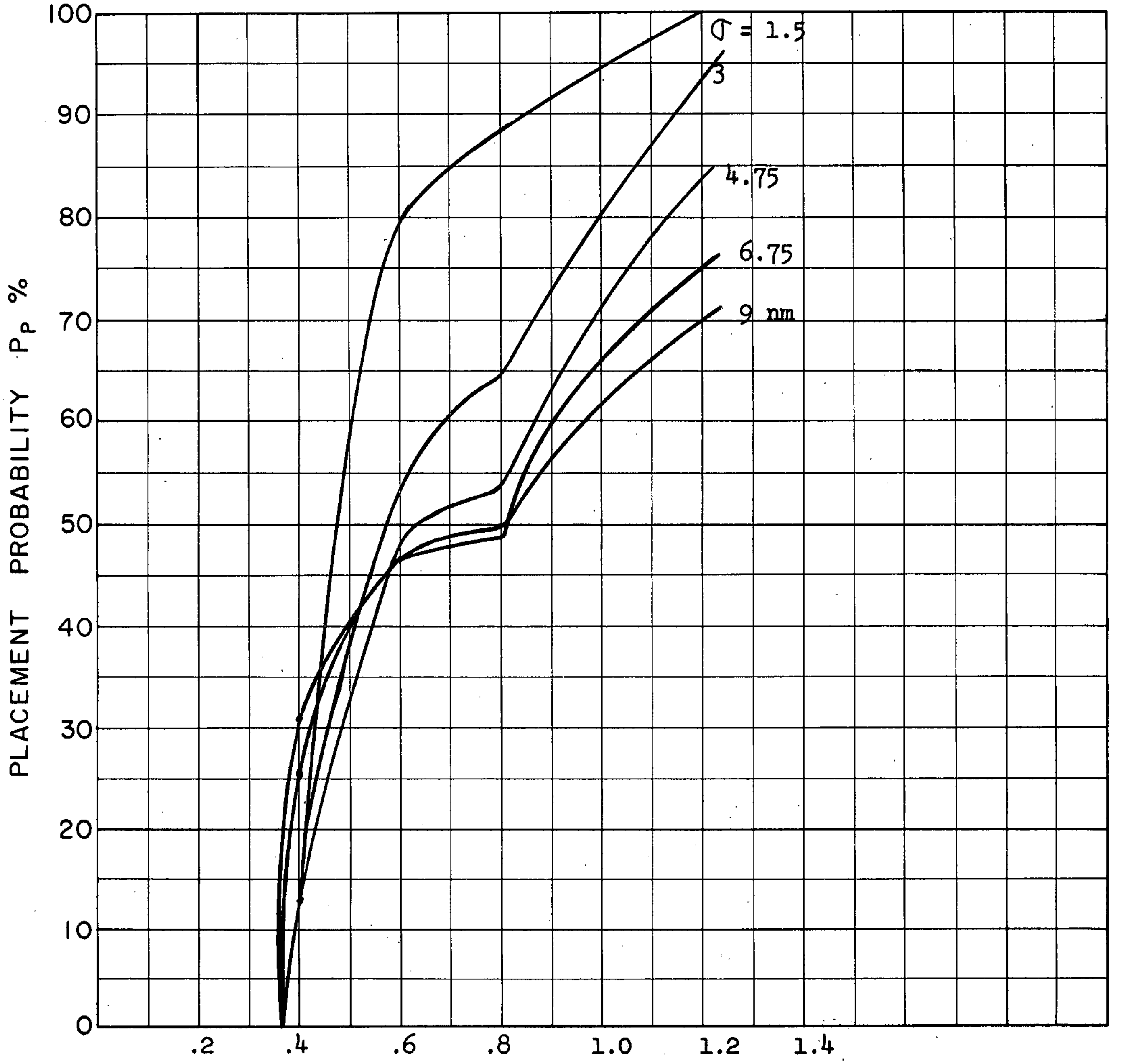

Fixed Range Lead Pursuit Navigation

COURSE DIFFERENCE: 110°
TARGET EVASION: 0
TARGET MACH NO.: 0.85
INTERCEPTOR LATERAL G's: Avro 3.3 with 1.5 g max
INTERCEPTOR MACH NO.: 1.5
σ OF G.C.I. ACCURACY: 5 Values
A.I. DETECTION RANGE AS FRACTION OF SPECIFICATION RANGE, S: Abscissa
A.I. DETECTION RANGE CONTOUR: IR B 52
ALTITUDE: 50 K

Subsonic Target

Prob. XVIII G H

IR AI Phase with Fixed Range Lead Pursuit Navigation

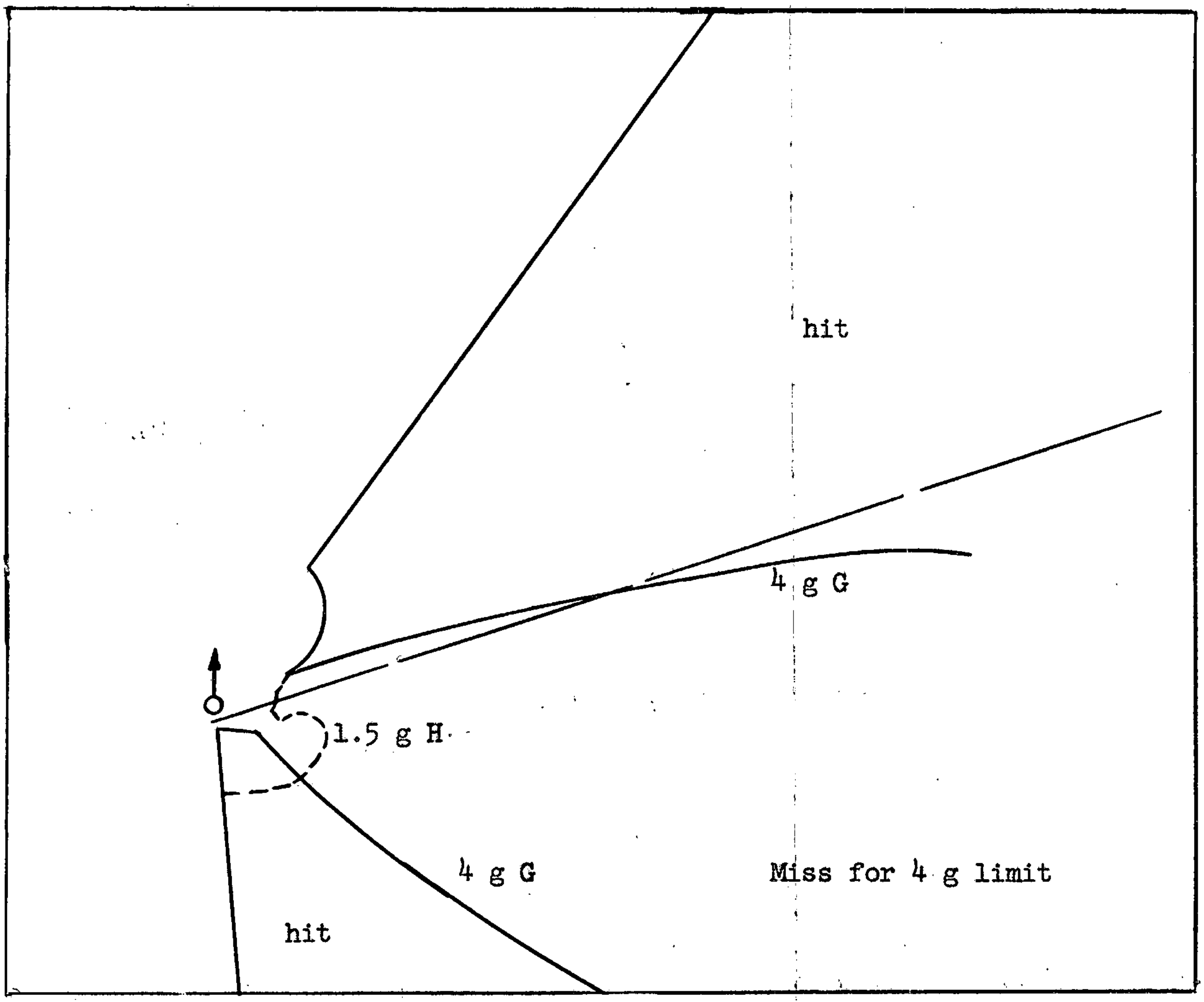

$\Gamma_o = 75^\circ$

$M_{fo} = 1.5$

$M_t = 0.85$

$h = 50$ K

Scale 25,000 ft/cm

Radar AI Phase Subsonic Target

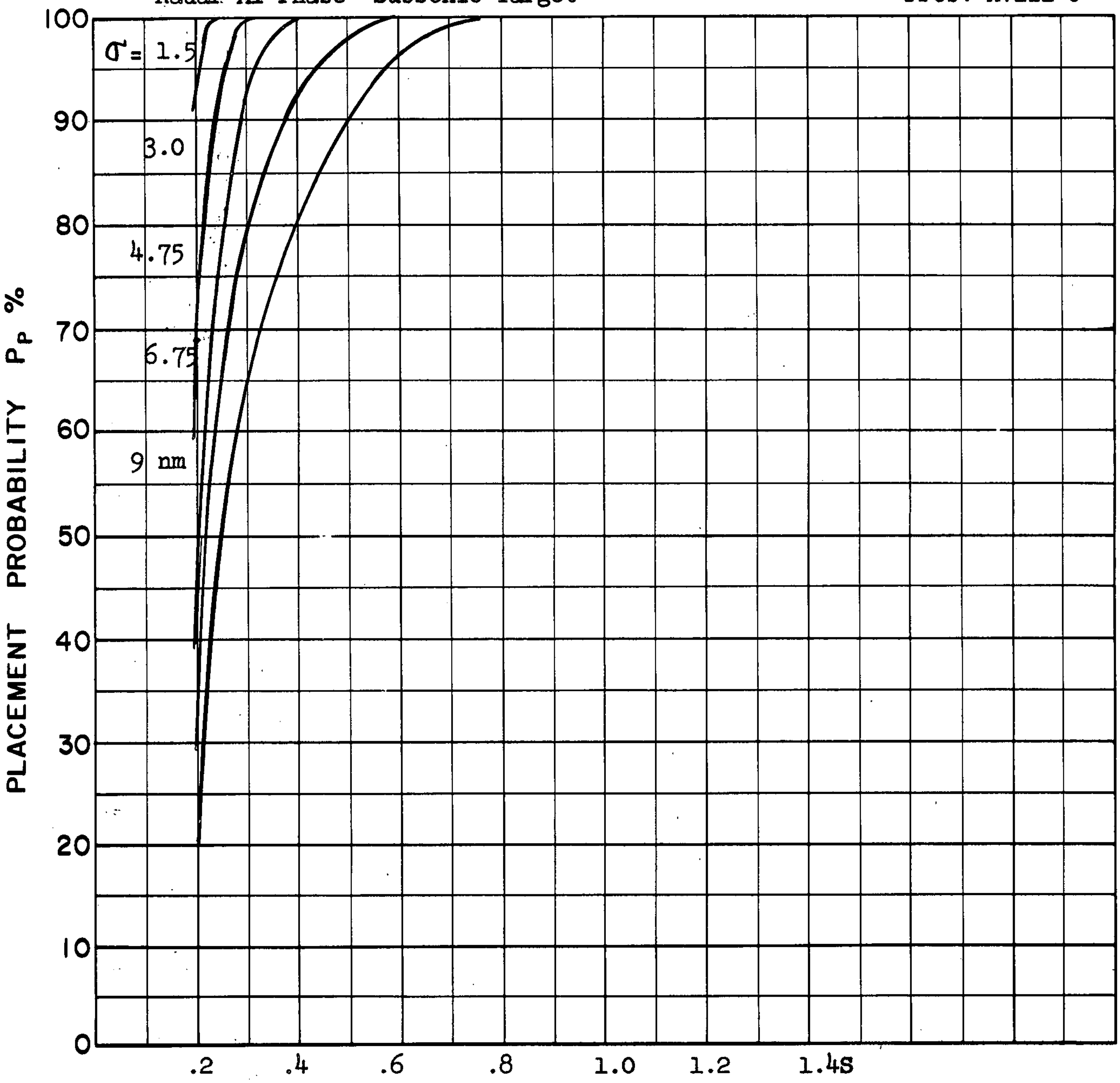

Lead Collision Navigation
COURSE DIFFERENCE: 180°
TARGET EVASION: 0
TARGET MACH NO.: 0.85
INTERCEPTOR LATERAL G's: Avro 3.3
INTERCEPTOR MACH NO.: 1.5 Initially
σ OF G.C.I. ACCURACY: 5 Values
A.I. DETECTION RANGE AS FRACTION OF SPECIFICATION RANGE, S: Abscissa
A.I. DETECTION RANGE CONTOUR: Delta
ALTITUDE: 50 K

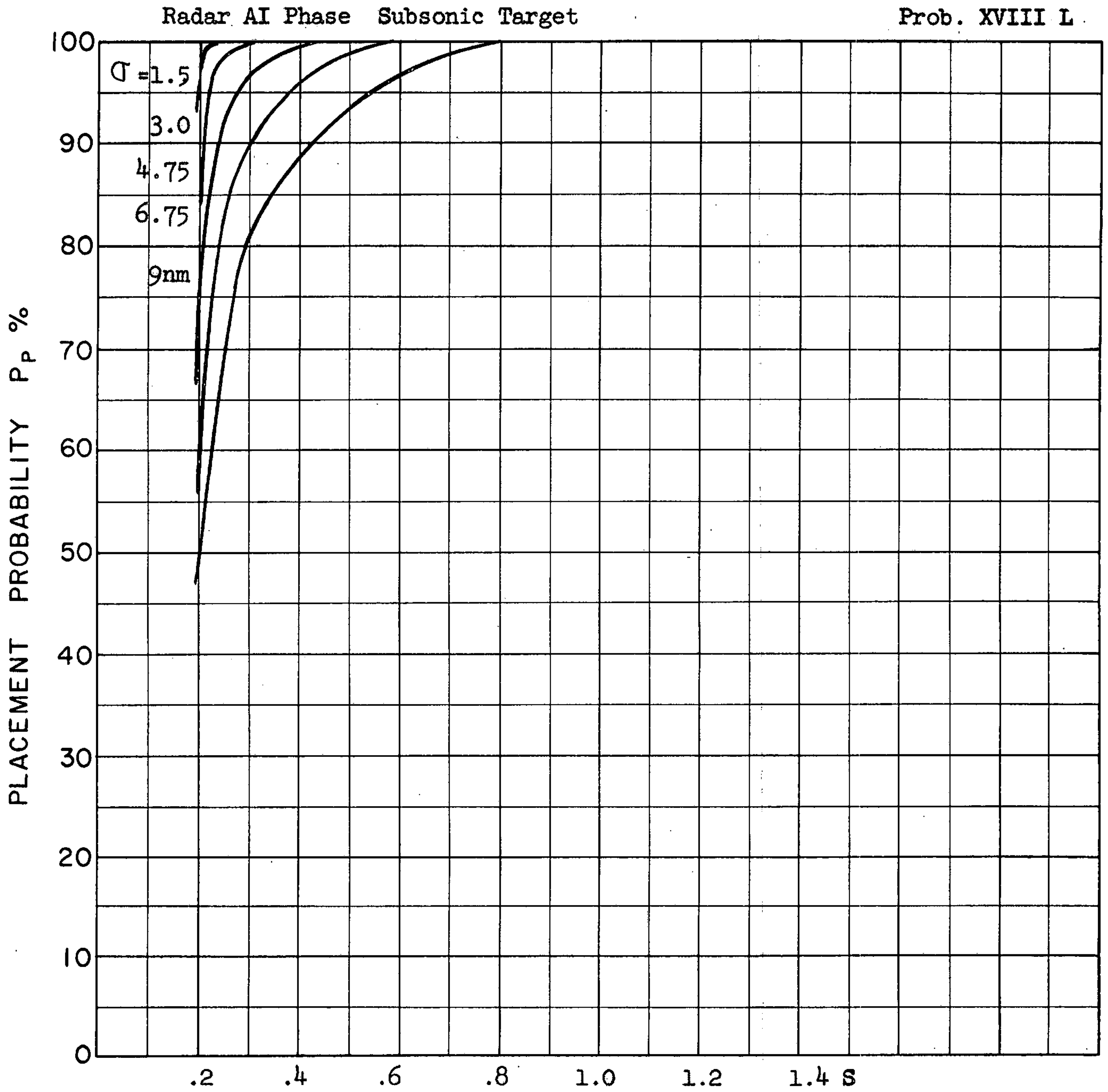

Lead Collision Navigation
COURSE DIFFERENCE: 135°
TARGET EVASION: 0
TARGET MACH NO.: .85
INTERCEPTOR LATERAL G's: Avro 3.3
INTERCEPTOR MACH NO.: 1.5 Initially
σ OF G.C.I. ACCURACY: 5 Values
A.I. DETECTION RANGE AS FRACTION OF SPECIFICATION RANGE, S: Abscissa
A.I. DETECTION RANGE CONTOUR: Delta
ALTITUDE: 50 K

Radar AI Subsonic Target

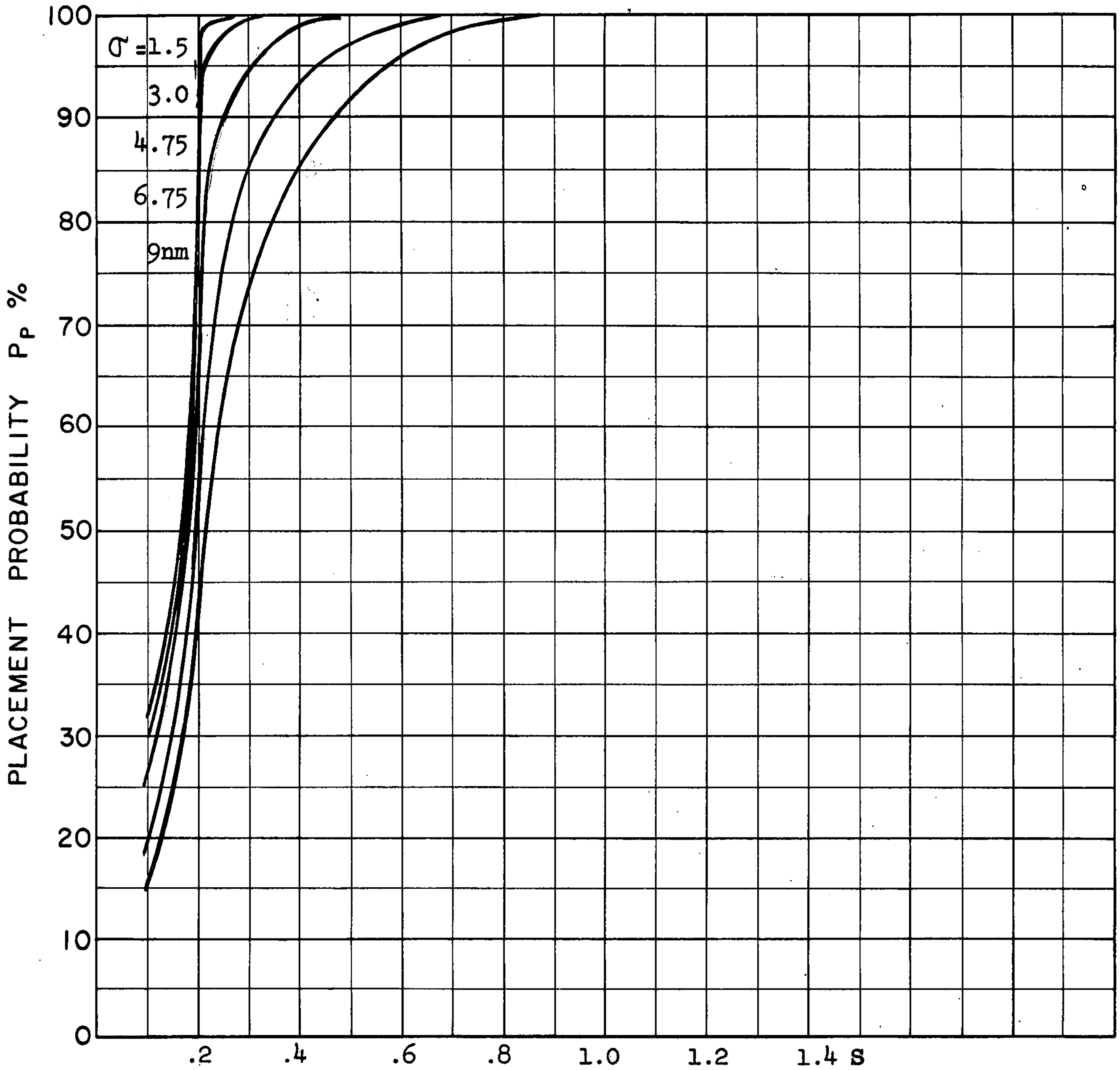

Lead Collision Navigation

COURSE DIFFERENCE: 110°
TARGET EVASION: 0
TARGET MACH NO.: 0.85
INTERCEPTOR LATERAL G's: Avro 3.3
INTERCEPTOR MACH NO.: 1.5 Initially
σ OF G.C.I. ACCURACY: 5 Values
A.I. DETECTION RANGE AS FRACTION OF SPECIFICATION RANGE, S: Abscissa
A.I. DETECTION RANGE CONTOUR: Delta
ALTITUDE: 50 K

Radar AI Phase Subsonic Target Prob. XVIII M

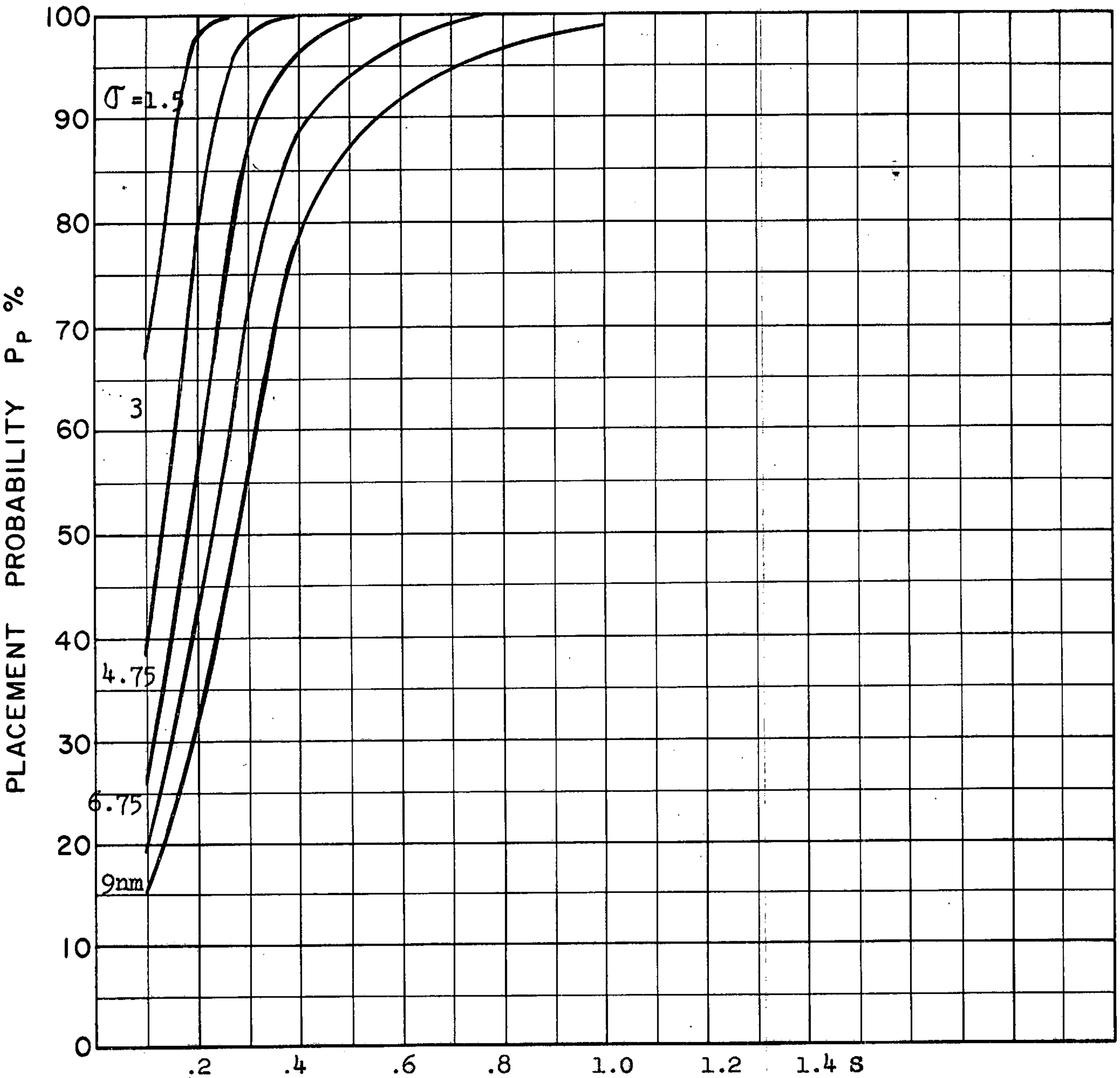

Lead Collision Navigation

COURSE DIFFERENCE: 75°
TARGET EVASION: 0
TARGET MACH NO.: 0.85
INTERCEPTOR LATERAL G's: Avro 3.3
INTERCEPTOR MACH NO.: 1.5 Initially
σ OF G.C.I. ACCURACY: 5 Values
A.I. DETECTION RANGE AS FRACTION OF SPECIFICATION RANGE, S: Abscissa
A.I. DETECTION RANGE CONTOUR: Delta
ALTITUDE: 50 K

4.4.7.1 Problem XVIII Conditions

Missile incremental velocity ΔV = M1.0
Missile flight time t_f = 9 seconds
Target speed = M0.85
Initial interceptor speed M1.5
Interceptor maximum load factor 4.0 and 1.5
Altitude 50,000 feet.

Initial course differences of 180°, 135°, 110° and 75° were tried.

4.4.7.2 Results

The fixed range lead pursuit navigation is very effective in this situation if the field of view is unrestricted. With IR look angles and course differences less than 180° the probability falls to 50% unless the maximum interceptor load factor is below 1.5 g. In this case the target may escape by turning with greater than 1.5 g. Another deteriorating factor is the low acquisition range expected in the forward hemisphere from a subsonic target.

4.4.8.0 Problem XIX - Subsonic Evading Target

In this study the target was assumed to fly at M0.85 with 2 g load factor evasion. The interceptions were carried out at 50,000 ft.

A sustained 2 g maneuver at M0.85 is beyond the capability of the CF 105. At M2.0 the power limit is just under 2 g; at M1.2, just under 1.5 g and at M0.85 the power limited load factor is 1.2.

Hence for initial fighter speeds near M0.85 the CF 105 is badly out classed by this target.

4.4.8.1 Problem Conditions

M_T 0.85, g_t = 2.0 h_t = h_f = 50 K

M_{fo} = 0.95, 1.5, 2.0

g_{fmax} = 4 g and 1.25 g

ΔV = M1.0 and t_f = 9 secs.

Γ_o = 180° and 110°

g_t is varied for the M_{fo} = 0.95 case.

Subsonic Evading Target — Prob. XIX A,B,C

Effect of Initial Fighter Speed

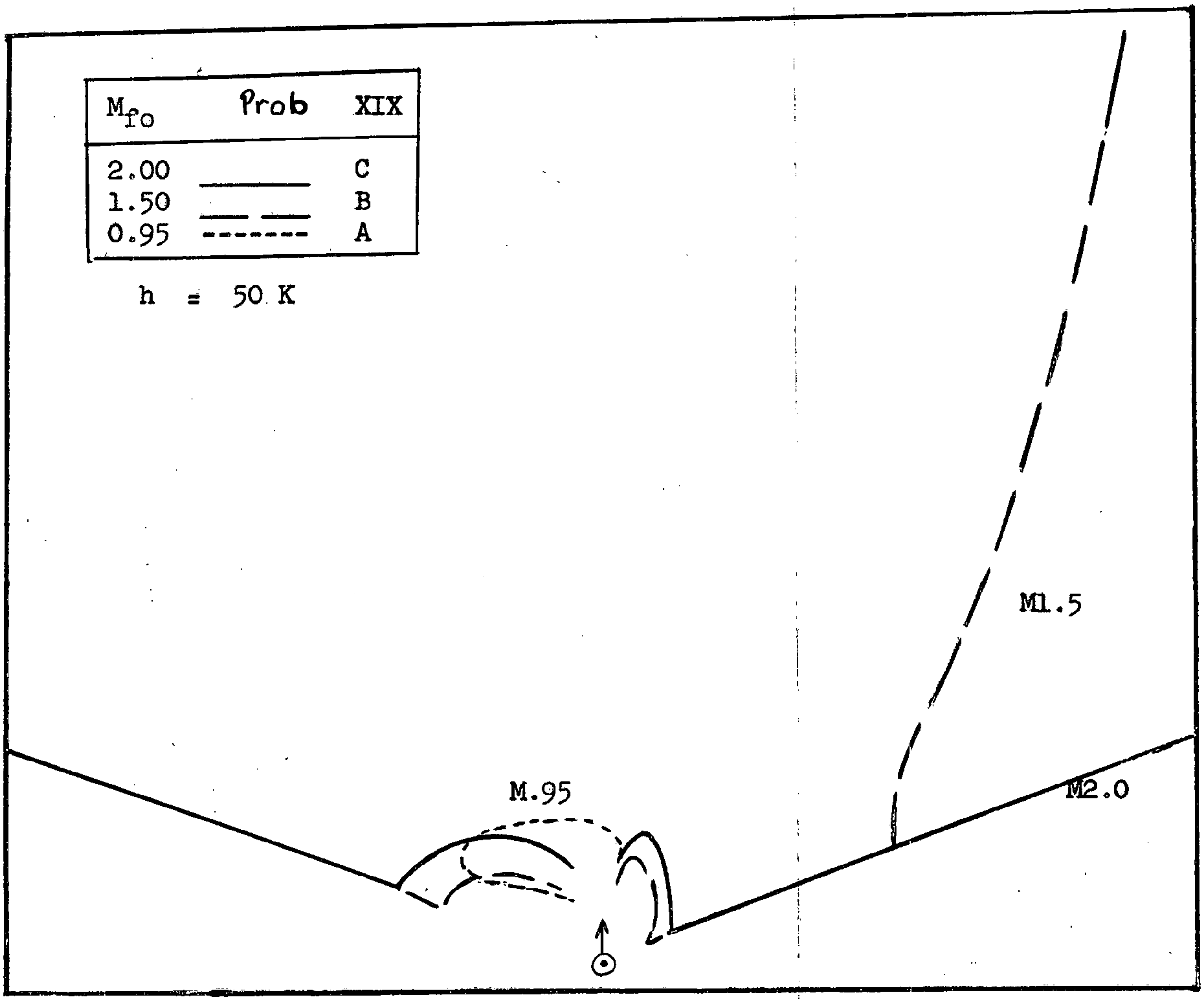

V_t = 0.85

G_t = 2.0 + ve

G_f Avro 3.3

Γ_o = 180°

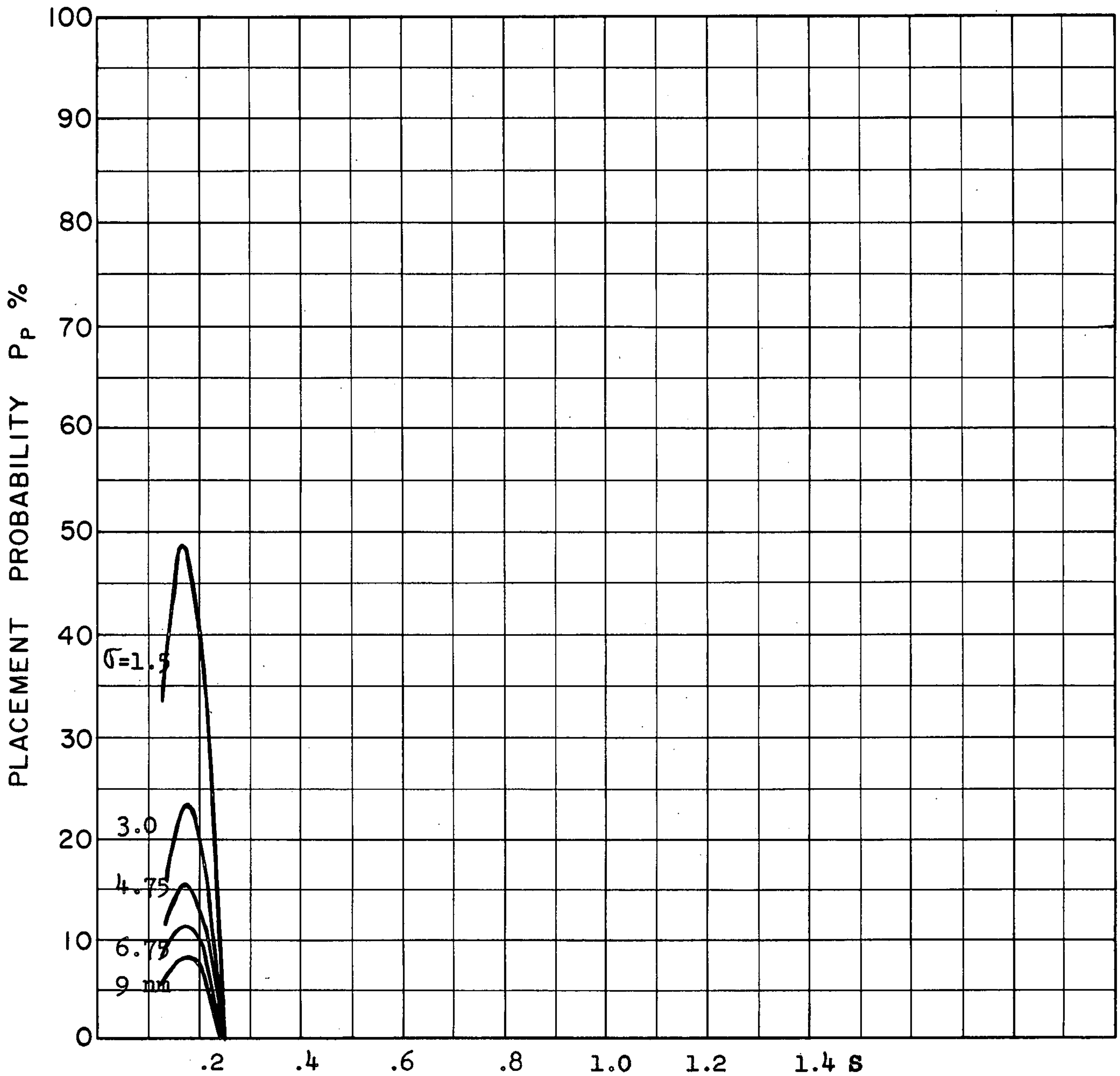

COURSE DIFFERENCE: 180°
TARGET EVASION: 2.0 g load factor
TARGET MACH NO.: 0.85
INTERCEPTOR LATERAL G's: Avro 3.3
INTERCEPTOR MACH NO.: 0.95 Initially
σ OF G.C.I. ACCURACY: 5 Values
A.I. DETECTION RANGE AS FRACTION OF SPECIFICATION RANGE, S: Abscissa
A.I. DETECTION RANGE CONTOUR: Delta
ALTITUDE: 50 K

Subsonic Evading Target Prob. XIX B

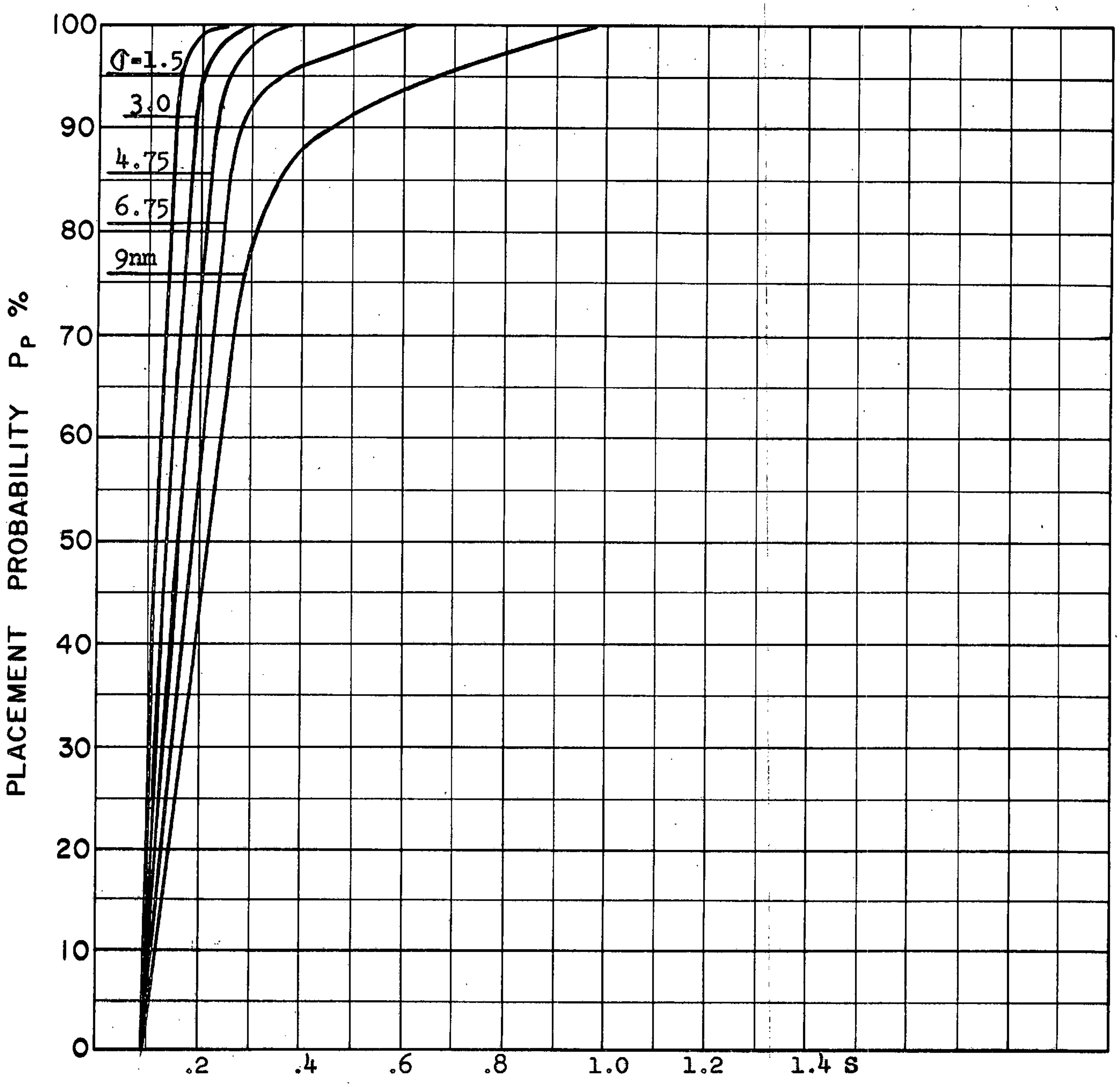

COURSE DIFFERENCE: 180°
TARGET EVASION: 2 g Load factor
TARGET MACH NO.: 0.85
INTERCEPTOR LATERAL G's: Avro 3.3
INTERCEPTOR MACH NO.: 1.5 Initially
σ OF G.C.I. ACCURACY: 5 Values
A.I. DETECTION RANGE AS FRACTION OF SPECIFICATION RANGE, S: Abscissa
A.I. DETECTION RANGE CONTOUR: Delta
ALTITUDE: 50 K

Prob. XIX C

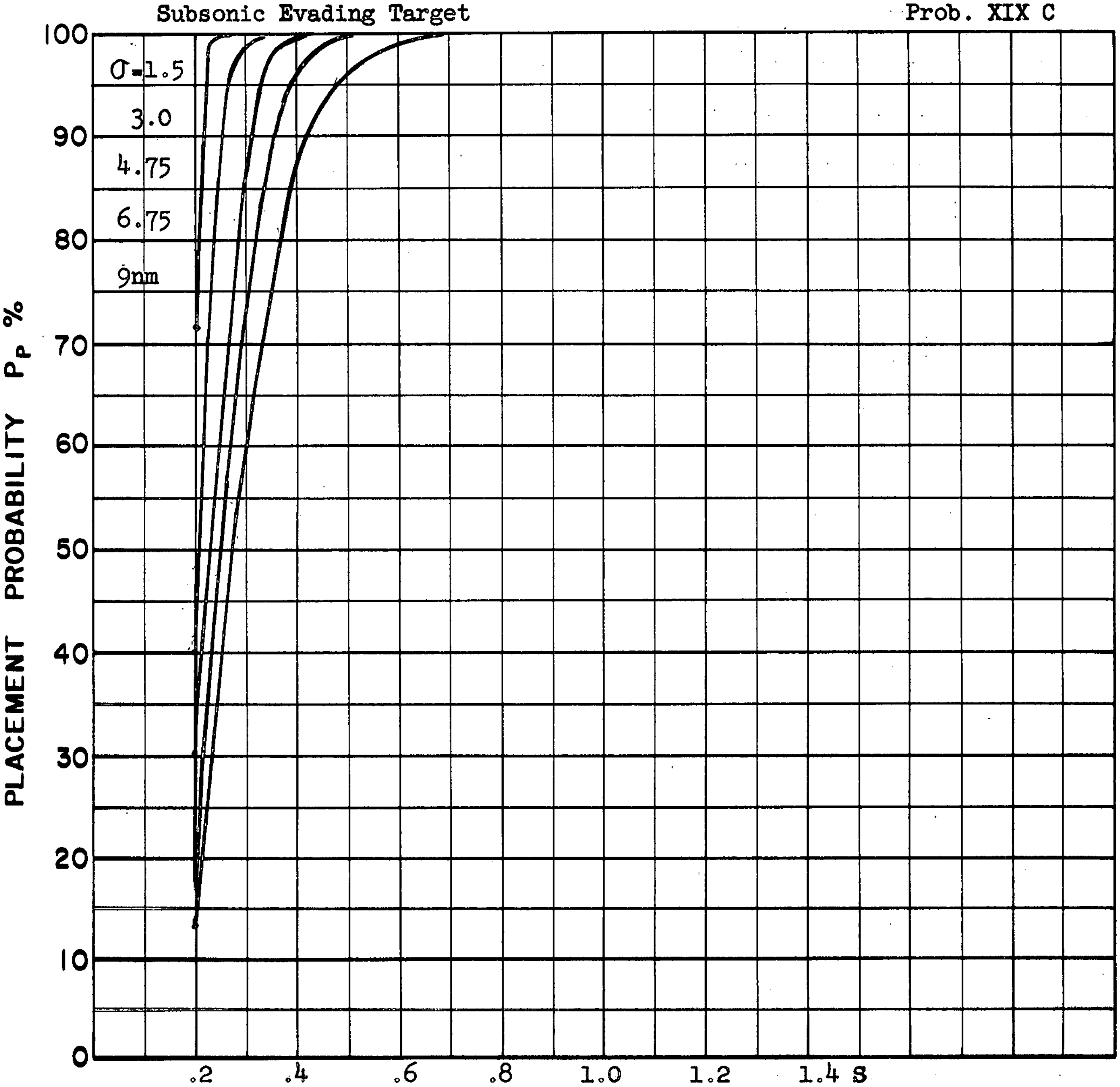

COURSE DIFFERENCE: 180°
TARGET EVASION: 2 g
TARGET MACH NO.: 0.85
INTERCEPTOR LATERAL G's: Avro 3.3
INTERCEPTOR MACH NO.: 2.0 Initially
σ OF G.C.I. ACCURACY: 5 Values
A.I. DETECTION RANGE AS FRACTION OF SPECIFICATION RANGE, S: Abscissa
A.I. DETECTION RANGE CONTOUR: Delta
ALTITUDE: 50 K feet

Subsonic Evading Target

Prob. XIX A, D

Effect of Fighter Load Factor

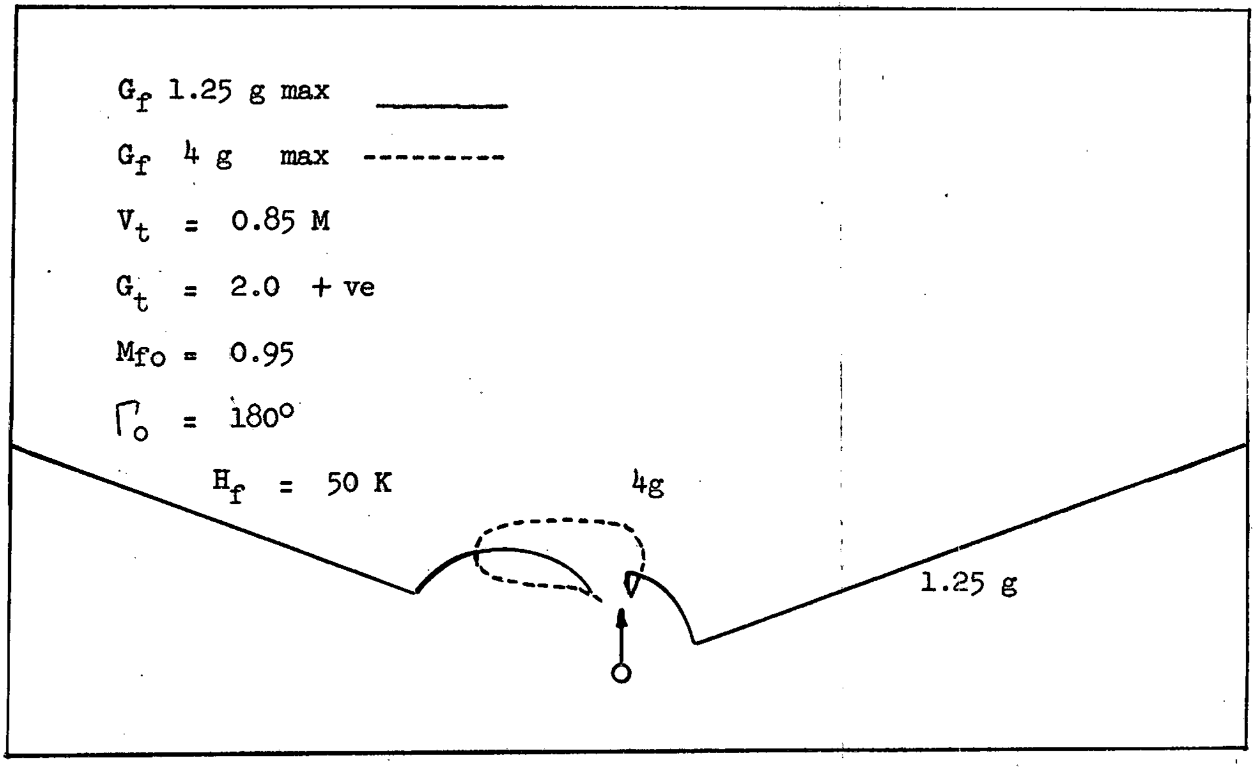

Subsonic Evading Target

Prob. XIX D

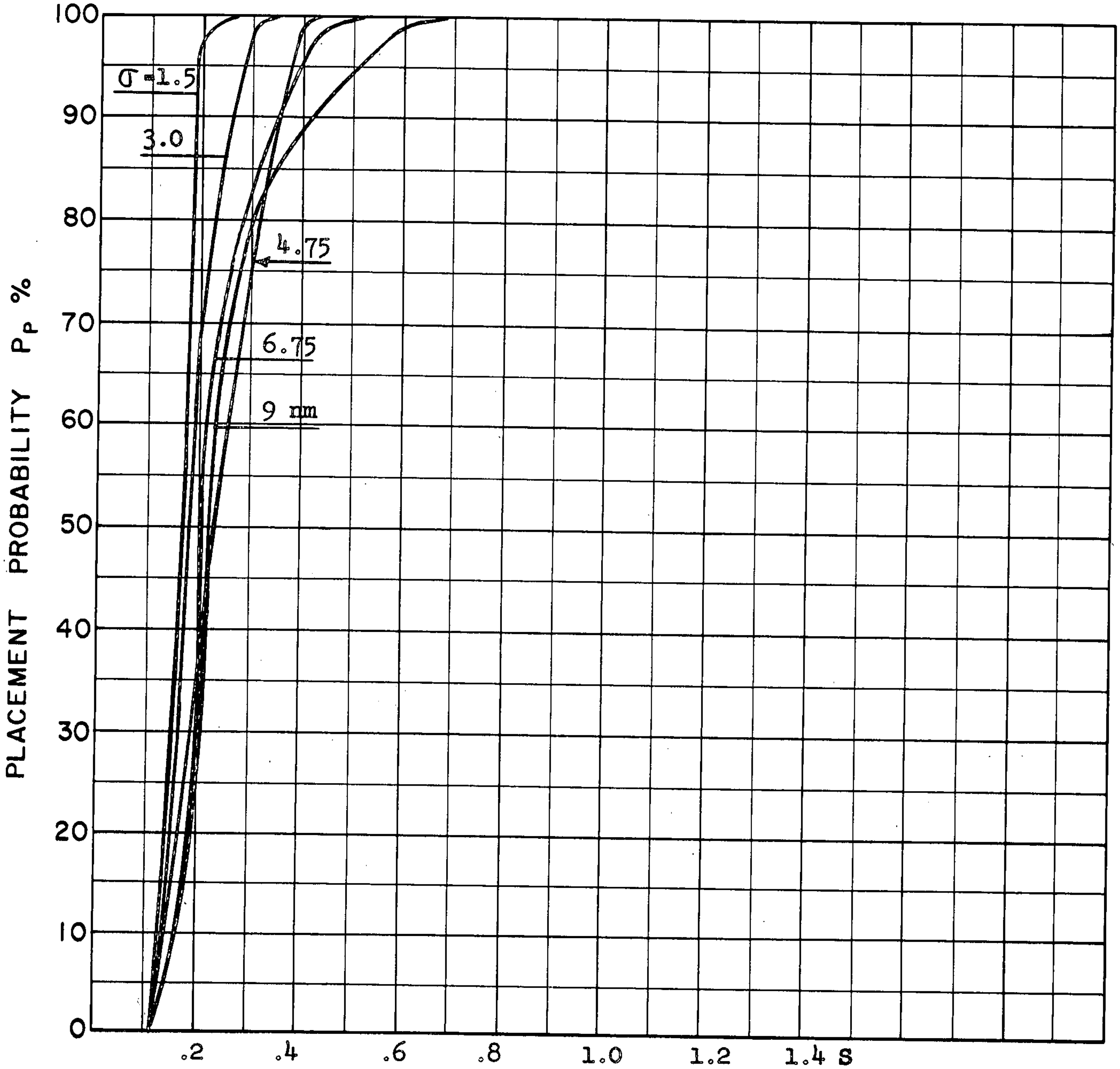

COURSE DIFFERENCE: 180°
TARGET EVASION: 2.0 g Load Factor
TARGET MACH NO.: 0.85
INTERCEPTOR LATERAL G's: Avro 3.3 1.25 g max.
INTERCEPTOR MACH NO.: 0.95 Initially
σ OF G.C.I. ACCURACY: 5 Values
A.I. DETECTION RANGE AS FRACTION OF SPECIFICATION RANGE, S: Abscissa
A.I. DETECTION RANGE CONTOUR: Delta
ALTITUDE: 50 K

Subsonic Evading Target

Prob. XIX A,E,F

Effect of Target Load Factor

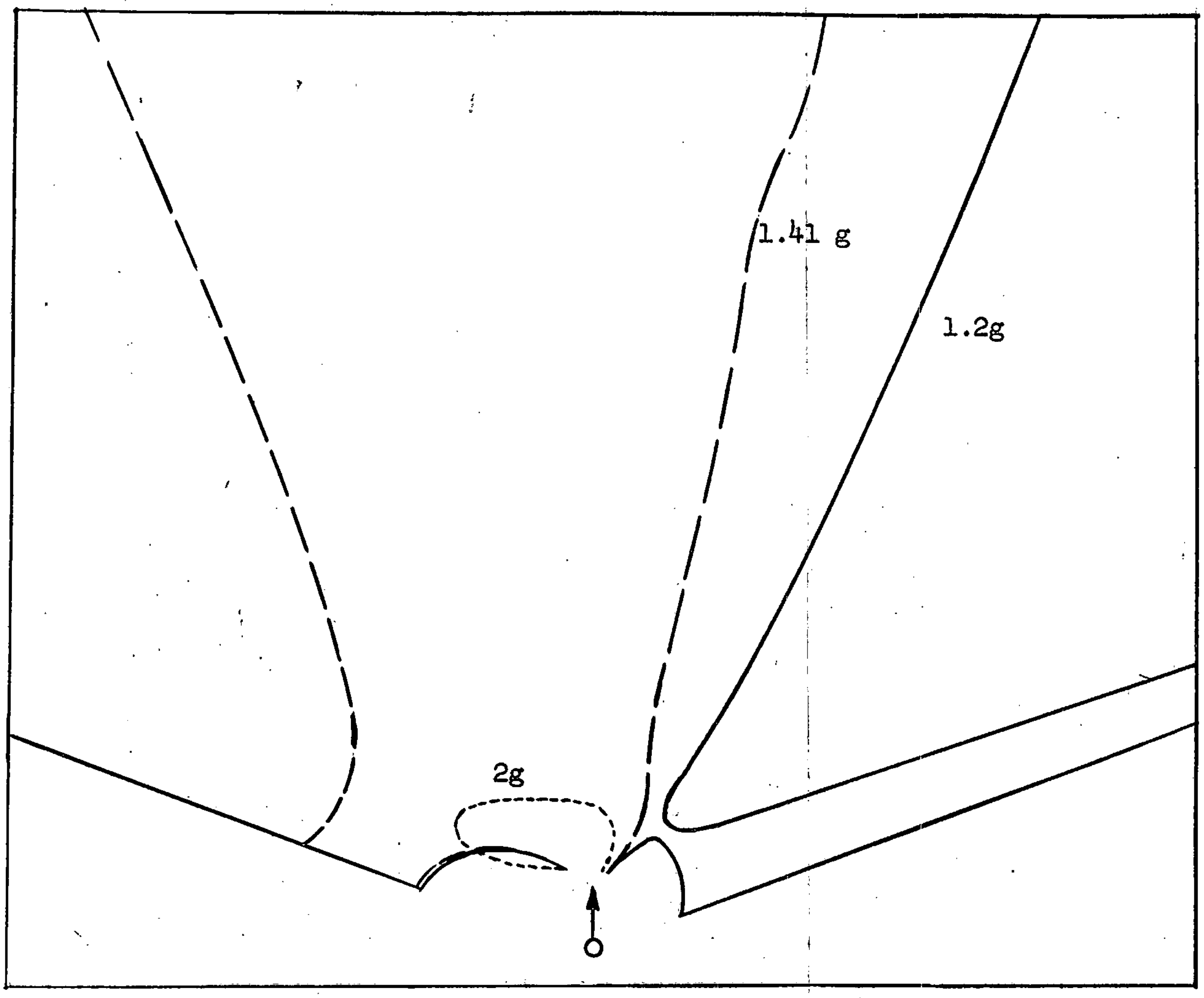

G_f	Avro 3.3
V_{fo} =	M0.95
V_t =	M0.85
Γ_o =	180°

$H_f = H_t = 50$ K

G_t = 1.20		———————	F
G_t = 1.41		— — —	E
G_t = 2.00		------------	A

all + ve.

Subsonic Evading Target

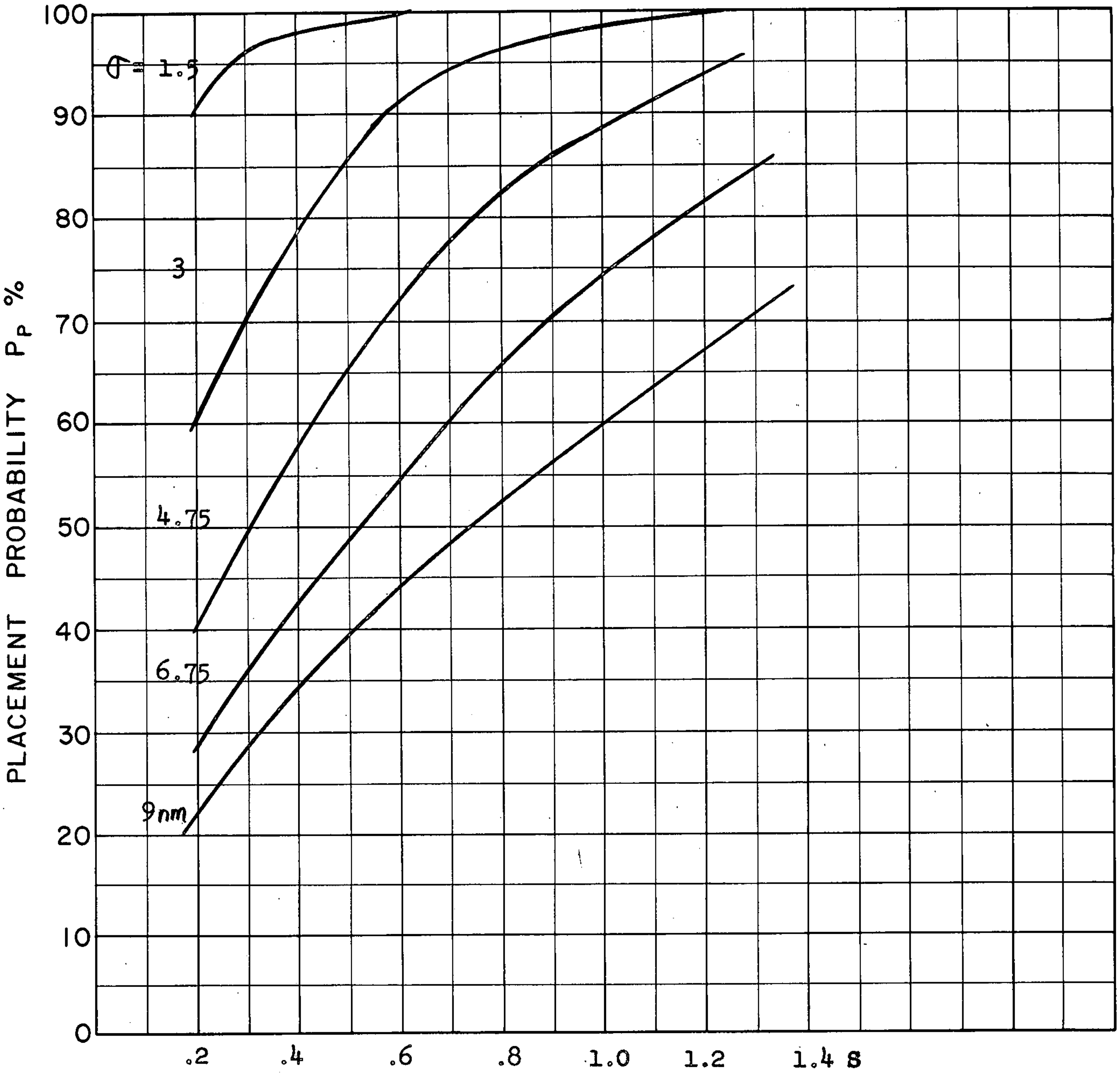

COURSE DIFFERENCE: 180°
TARGET EVASION: 1.41 g Load Factor
TARGET MACH NO.: 0.85
INTERCEPTOR LATERAL G's: Avro 3.3
INTERCEPTOR MACH NO.: 0.95 Initially
σ OF G.C.I. ACCURACY: 5 Values
A.I. DETECTION RANGE AS FRACTION OF SPECIFICATION RANGE, S: Abscissa
A.I. DETECTION RANGE CONTOUR: Delta
ALTITUDE: 50 K

Subsonic Evading Target | Prob. XIX F

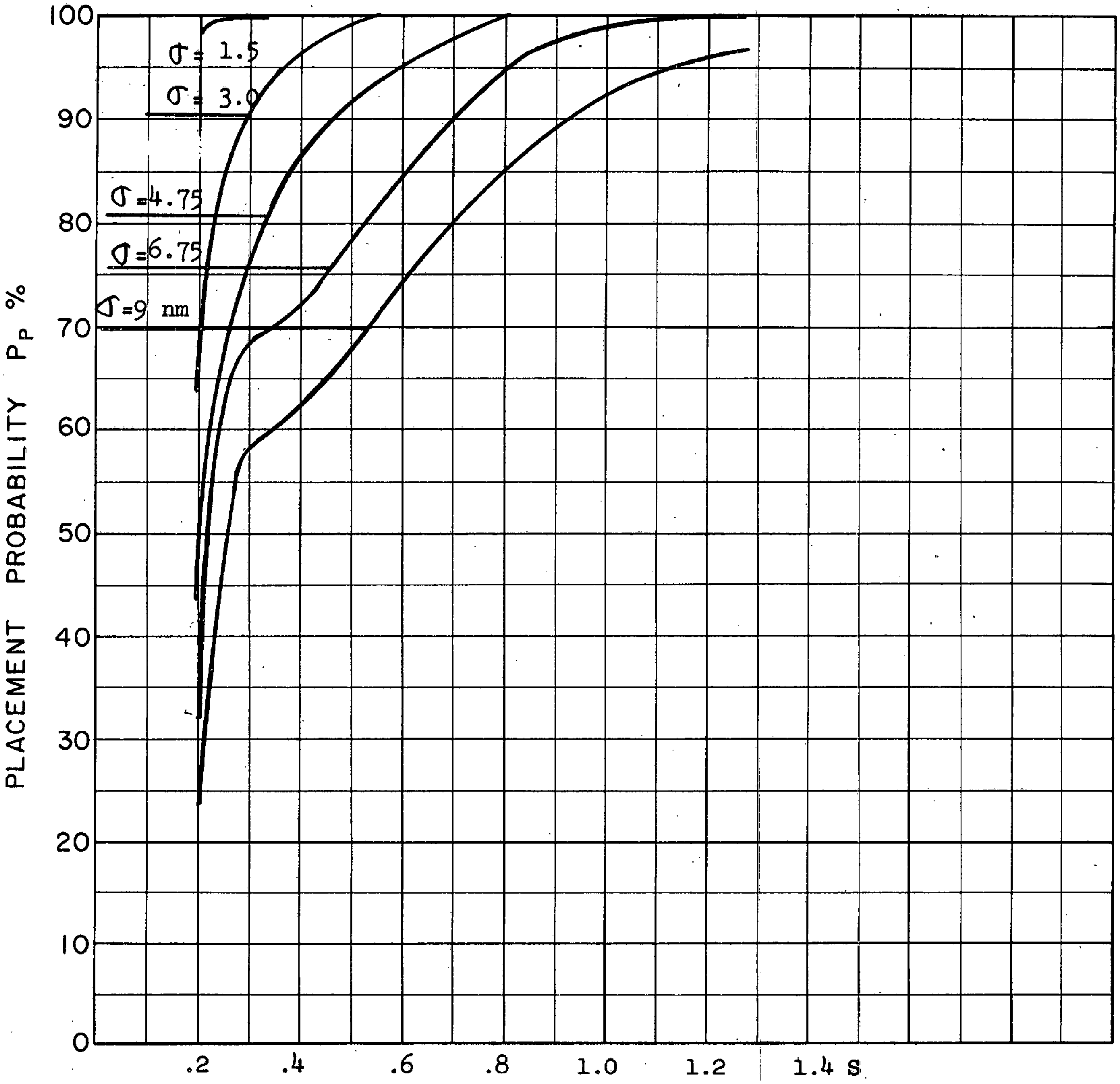

COURSE DIFFERENCE: 180°
TARGET EVASION: 1.2 g Load Factor
TARGET MACH NO.: 0.85
INTERCEPTOR LATERAL G's: Avro 3.3
INTERCEPTOR MACH NO.: 0.95 Initially
σ OF G.C.I. ACCURACY: 5 Values
A.I. DETECTION RANGE AS FRACTION OF SPECIFICATION RANGE, S: Abscissa
A.I. DETECTION RANGE CONTOUR: Delta
ALTITUDE: 50 K

Subsonic Evading Target

Prob. XIX G,H

Effect of Initial Fighter Speed

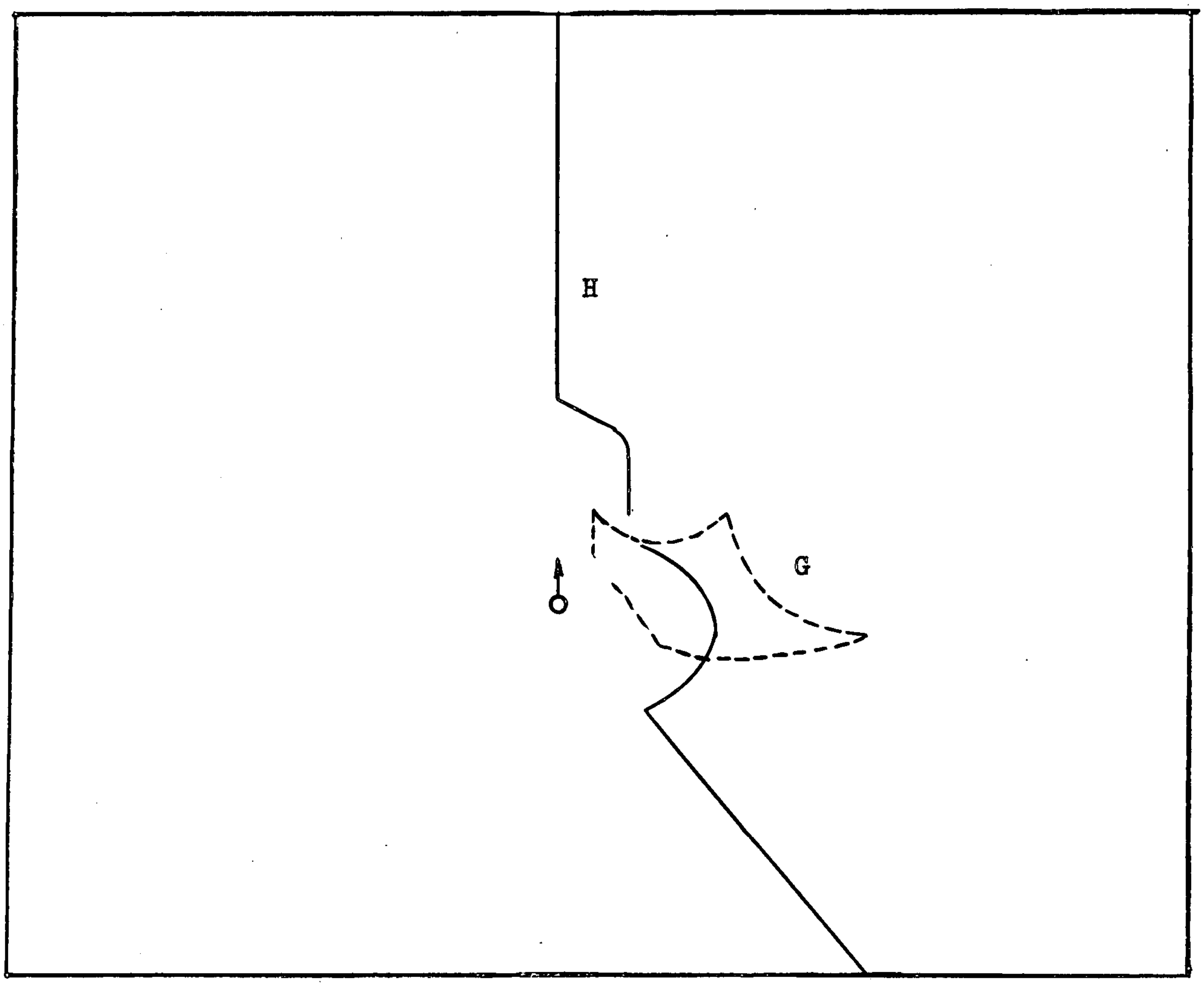

Γ_o = 110°

V_t = 0.85M

G_t = 2

G_f Avro 3.3

M_{fo} 2.00 ————————

M_{fo} 0.95 ------------

Area between placement zones for
ve & -ve evasion.

Prob. XIX G

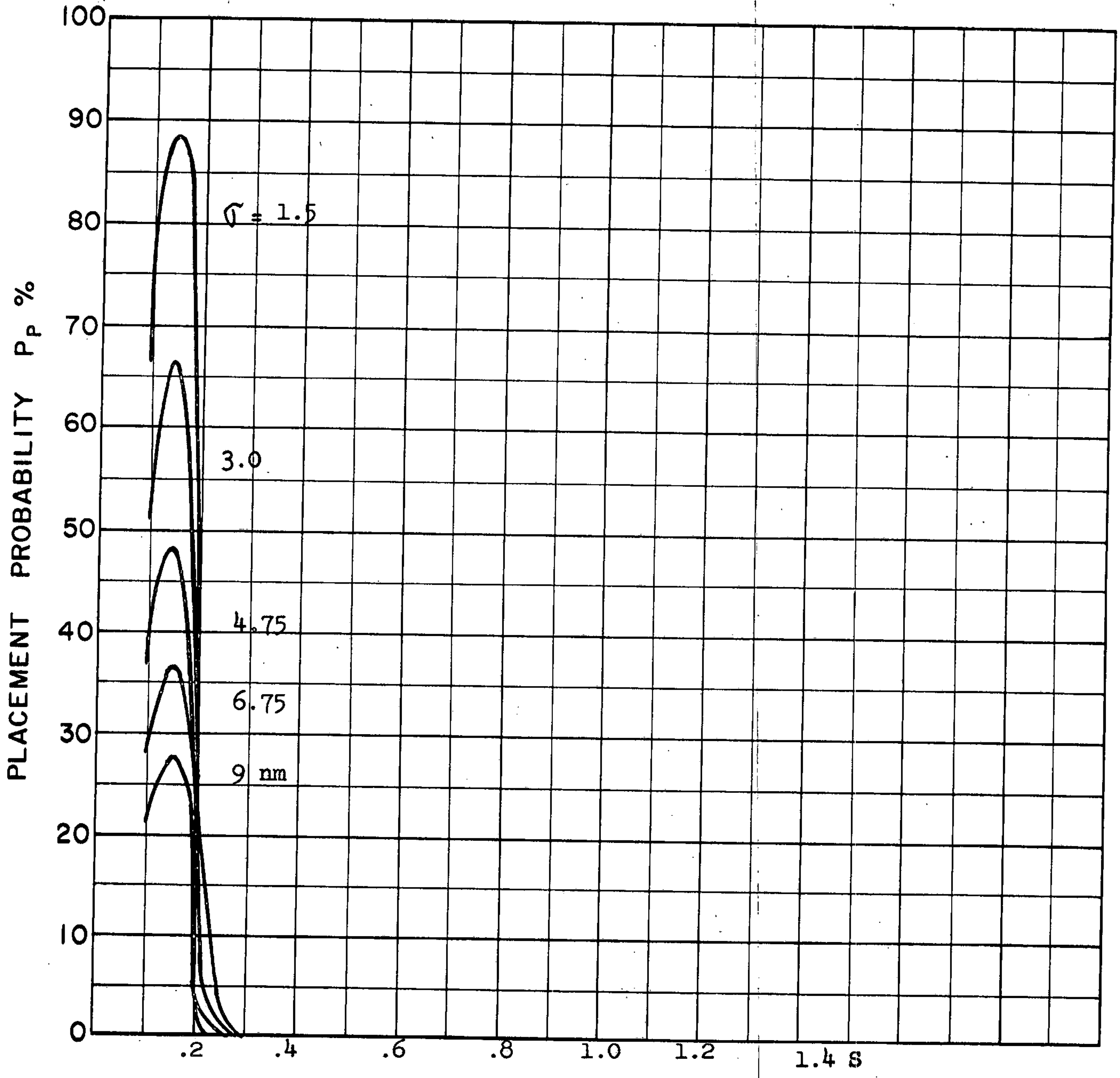

COURSE DIFFERENCE: 110°
TARGET EVASION: 2 g Load Factor
TARGET MACH NO.: 0.85
INTERCEPTOR LATERAL G's: Avro 3.3
INTERCEPTOR MACH NO.: 0.95 Initially
σ OF G.C.I. ACCURACY: 5 Values
A.I. DETECTION RANGE AS FRACTION OF SPECIFICATION RANGE, S: Abscissa
A.I. DETECTION RANGE CONTOUR: Delta
ALTITUDE: 50 K

Subsonic Evading Target Prob. XIX H

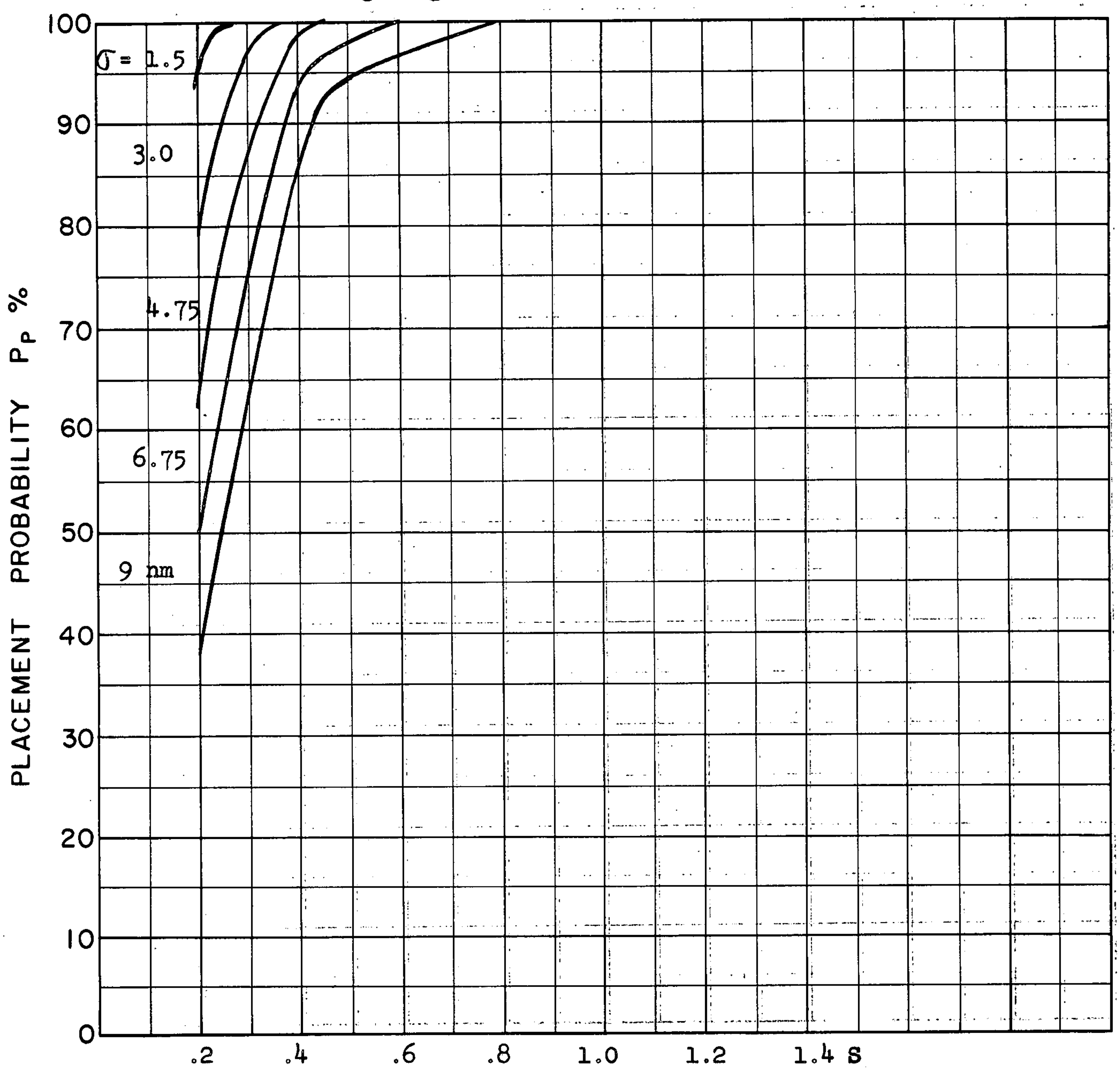

COURSE DIFFERENCE: 110°
TARGET EVASION: 2.0
TARGET MACH NO.: 0.85
INTERCEPTOR LATERAL G's: Avro 3.3
INTERCEPTOR MACH NO.: 2.0 Initially
σ OF G.C.I. ACCURACY: 5 Values
A.I. DETECTION RANGE AS FRACTION OF SPECIFICATION RANGE, S: Abscissa
A.I. DETECTION RANGE CONTOUR: Delta
ALTITUDE: 50 K

Subsonic Evading Target

Prob. XIX G,J

Effect of Fighter Load Factor

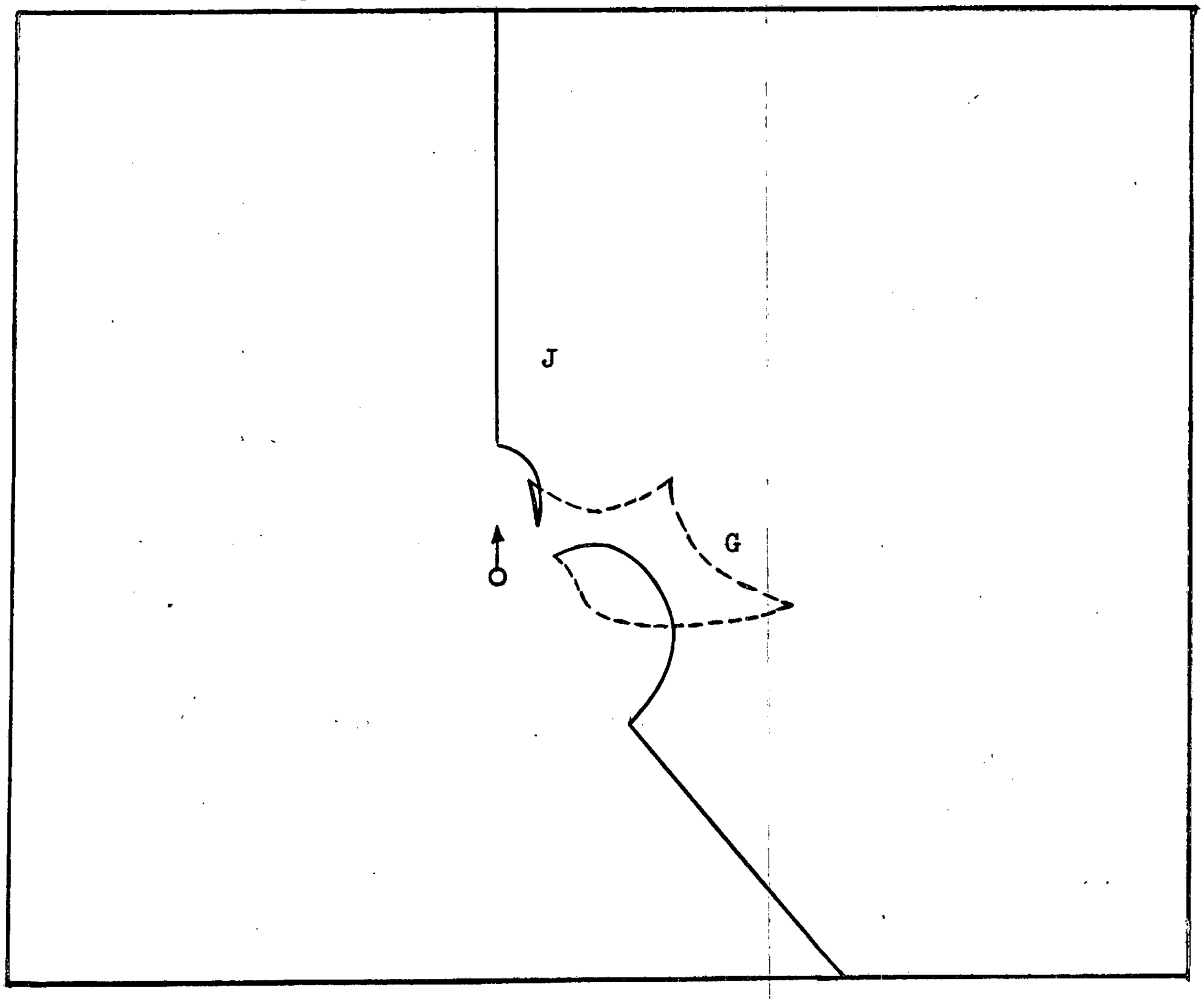

Γ_o = 110°

V_t = 0.85 M

G_t = 2.0

G_f Avro 3.3 ----------

G_f Avro 3.3 with 1.25 g max) ————

V_f = 0.95 M

Area between placement zones for -ve & ve evasion.

Subsonic Evading Target   Prob. XIX J

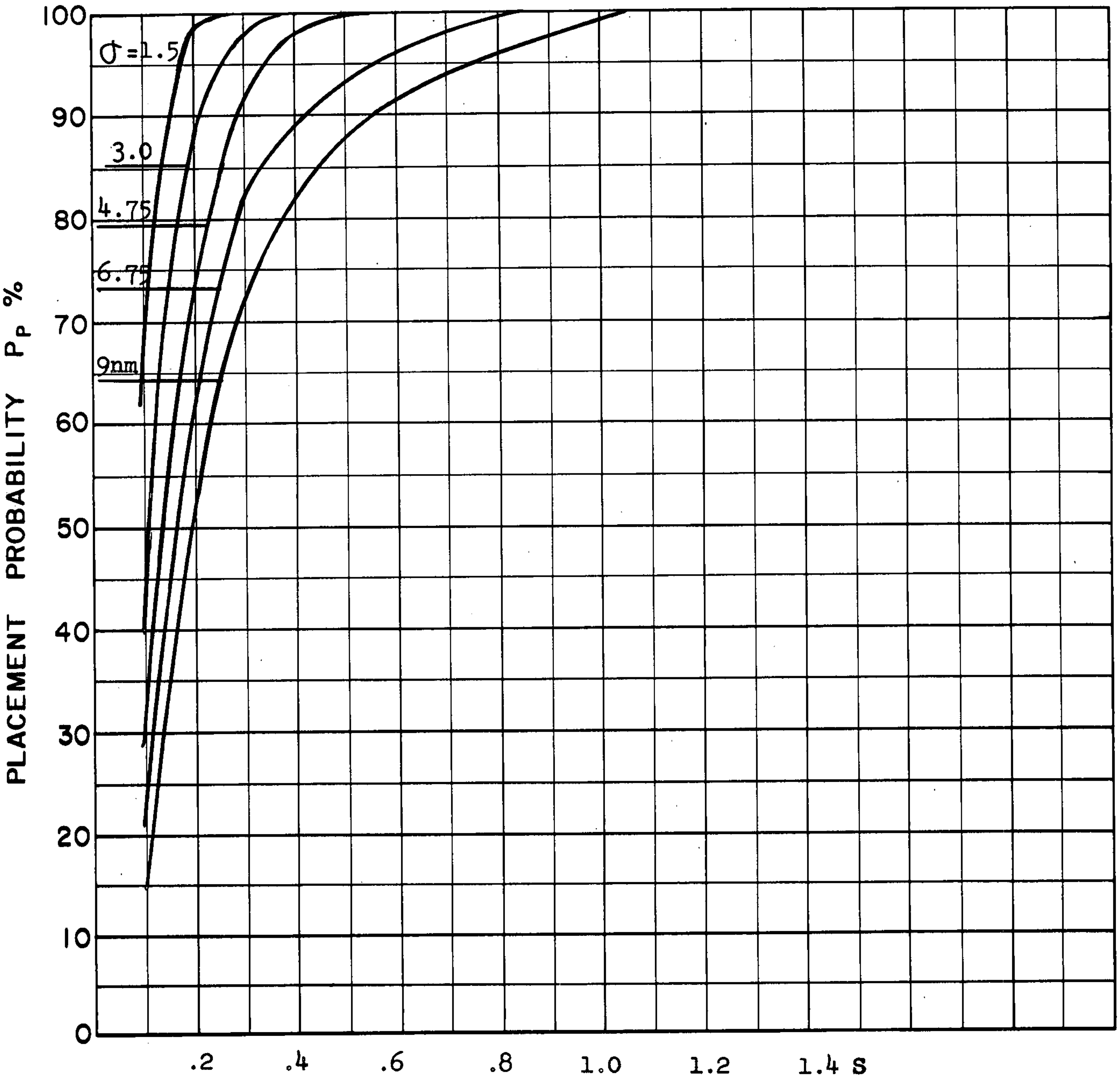

COURSE DIFFERENCE: 110°
TARGET EVASION: 2.0 g Load Factor
TARGET MACH NO.: 0.85
INTERCEPTOR LATERAL G's: Avro 3.3   1.25 g Limit
INTERCEPTOR MACH NO.: 0.95 Initially
σ OF G.C.I. ACCURACY: 5 Values
A.I. DETECTION RANGE AS FRACTION OF SPECIFICATION RANGE, S: Abscissa
A.I. DETECTION RANGE CONTOUR: Delta
ALTITUDE: 50 K

Prob.	M_{fo}	g_t	g_{fm}
XIX A	0.95	2.0	4 g
XIX B	1.5	2.0	4 g
XIX C	2.0	2.0	4 g
XIX D	0.95	2.0	1.25 g
XIX E	0.95	1.41	4 g
XIX F	0.95	1.20	4 g
XIX G	0.95	2.0	4 g
XIX H	2.0	2.0	4 g
XIX J	0.95	2.0	1.25 g

Conclusions

1. High Initial Fighter Speed (M2.0) Very High Probabilities. Zones are bounded by maneuver and initial look angle barriers.

2. Medium Initial Fighter Speed (M1.5) High Probabilities which are increased if the fighter is restricted to power limited turns.

3. Fighter Initially Subsonic (M0.95) Very low probabilities unless turns are restricted to 1.25 g in which case the probabilities become very high.

NOTE: Low turn rate maneuvers are only successful if the interceptor has a large speed advantage and can permit temporary escape of target. The above situation is perhaps unrealistic as a sustained 2 g maneuver at high altitude would probably result in target deceleration - hence perhaps the lower 'g' cases are more likely.

Type of Target Maneuver

1. Simple Turn (say 60° Off Course) Quite ineffective against all initial fighter speeds.

2. Sustained Turn Effective when initial fighter speed is low and fighter attempts to turn with maximum g's.

3. Dog-Leg More effective than a continuous turn but not successful if fighter initial speed is high or if g's are restricted to allow it to pick up speed.

This maneuver has a change of success due to delays in the fighter detecting the change in maneuver. Such delays are not instrumented on the REAC.

4.5 Diving Turning Studies

In many situations attacks from lower altitude are more successful than say coaltitude attacks. Hence to take advantage of improved aerodynamic capabilities at low altitude it may be profitable to dive in the early stages of the interception and climb later.

Coaltitude attacks at 60,000 feet were studied for possible advantages of diving in the initial stages.

4.5.1 Simple Diving Attacks

Instead of pulling 1 g vertically to maintain level flight, this was reduced in the initial stages and the vertical steering error resulting was disconnected until some predetermined time-to-go. From this instant the fighter proceeded on a normal coordinated 3D interception.

If the interceptor is correcting azimuth errors, reduction of vertical g's corresponds to an increased bank angle. This unfortunately caused look angle failures in previously successful areas and caused a net reduction in placement probability.

If azimuth errors are not corrected in the initial stages the advantages of early lock-on are lost. Another defect of this system is the tendency to lose velocity when pulling from a dive into a climb.

When the fighter is flying at M2.0 a dive is a poor maneuver as the speed is restricted to M2.0 maximum.

4.5.2 Improved Diving Attacks

The defects of the simple dive maneuver are overcome in a coordinated diving attack. This dive is used only to reduce deceleration of the fighter. A new term was included in the vertical steering demand. This term was zero when the fighter was accelerating and proportional to deceleration when it was decelerating.

This means that the fighter dives only when asked to turn sufficiently fast to lose speed. As it dives (i) the increasing vertical steering error tends to counteract the command to dive. (ii) the deceleration due to the drag is counteracted by a component of gravity.
As the azimuth error is corrected the demand to turn and the corresponding drag falls off, and the interceptor automatically pulls out of the dive.

This coordinated dive turn is quite successful when initiated at fairly long ranges. It causes an improvement in fall back, look angle and minimum velocity barriers.

At short and medium ranges it is not worth while as insufficient time is available to lose enough altitude to make an appreciable difference.

The problem was studied for course differences of 180°, 135°, 110°

$F = 7\ K, \quad t_f = 8\ secs. \quad h_{fo} = h_t = 60\ K$

$M_{fo} = M_t = 2.0$

These cases are normally quite successful and although the placement zones are increased the improvement is not significant in turns of placement probability except for a course difference of 110°. However, in some situations where the probability is low it may be possible to improve it by means of this maneuver. In particular where ceiling difficulties are encountered due to low velocity, it may be possible to recover in a diving turn maneuver.

5.0 REFERENCES

1. CARDE Technical Letter N-47-8 "First Quarterly Report on CF 105 Weapon System Assessment" Appendix 'G' (SECRET)

2. CARDE Technical Letter N-47-12 "Second Quarterly Report on CF 105 Weapon System Assessment" Appendix "D" (SECRET)

3. CARDE Technical Letter N-47-18 "Third Quarterly Report on CF 105 Weapon System Assessment" Appendix 'G' (SECRET)

4. CARDE Technical Letter 1012/57 "Fourth Progress Report on CF 105 Weapon System Assessment" Appendix 'A' (SECRET)

5. CARDE Technical Letter 1091/58 "Fifth Progress Report on CF 105 Weapon System Assessment" Appendix 'A' (SECRET)

6. First Interim Report on IR Subsystem on Astra I Advanced Electronic System - RCA/Astra I/AR-9 (SECRET)

7. CARDE Technical Letter 1091/58 "Fifth Progress Report on CF 105 Weapon System Assessement" Appendix 'B' (SECRET)
   NOTE: Fixed "R & T Navigation" described in reference 7 called in other work "Fixed Range Lead Pursuit".

8. Appendix 'B' of this (Sixth) ProgressReport (SECRET)

APPENDIX 'B'

MINIMUM INFORMATION STUDY

by G.P. Coverley and A.B. Bell

1.0 INTRODUCTION

This Appendix describes work which has been completed since the writing of Appendix 'B' in the Fifth Progress Report (CARDE Technical Letter No. 1091/58) which described the problems and methods of this minimum information study.

Results are now available for the five navigation courses considered. These courses are:

1) Fixed Range Lead Pursuit (Fixed R & T)

2) Fixed lead

3) Zero lead (Pure Pursuit)

4) Fixed line of sight rate

5) Zero line of sight rate (True collision)

Overall probabilities of success have been completed for fire control* by $R/\dot{R}$ measurement and by visual (or Infrared) range finding. The effectiveness of the courses and factors influencing the choice of course were studied.

2.0 CASES STUDIED

Success probabilities are given for each course, under varying conditions as stated in Table III. Table III provides a reference to the probability curves.

3.0 ANALYSIS OF RESULTS

3.1 The success probabilities are considered in three groups, each group referring to a mode of fire control as follows:

* With the possibility that the radar cross-over range is reached at a point outside the launch zone, fire control by "time-to-go" is considered (for the R & T course only).
Fire control in this Appendix means control of missile firing and does not have its more usual meaning.

(a) $R/\dot{R}$ determination

(b) Range (R) determination

(c) Time-to-go (in the event of AI radar lock-on).

3.2 The following tables describe the most effective courses based on a knowledge of the course difference and expected GCI accuracy. All groups refer to the same conditions of target and fighter speed and height. (M1.5; M1.5, at 50,000 ft).

Group I - Fire Control by $R/\dot{R}$

Γ_o	GCI ACCURACY		
	σ = 1.5 n m	σ = 4.75 n m	σ = 9 n m
180	L_a = 0	ω = 0	R & T
135	R & T ω = 0 L_a = 20°	R & T	R & T
110	R & T	R & T	R & T

Table Ia showing best course under given conditions.

Γ_o	GCI ACCURACY		
	σ = 1.5 n m	σ = 4.75 n m	σ = 9 n m
180	95 ± 2	77 ± 4	58 ± 4
135	75	78 ± 3	67 ± 7
110°	84 ± 5	68 ± 5	65 ± 3

Table Ib showing expected success probabilities (%) of the courses shown in Table Ia. The tolerances in probability in the above table are due to variations in target detection range from 0.6 to 1.28S.

Group II - Fire Control by Range Estimation

Γ_o	GCI ACCURACY		
	σ = 1.5 n m	σ = 4.75 n m	σ = 9 n m
180	$\omega = 0$ $L_a = 0$	$\omega = 0$ R & T	R & T
135	R & T	R & T	R & T
110	R & T	R & T	R & T

Table IIa - showing best course under given conditions.

Γ_o	GCI ACCURACY		
	σ = 1.5 n m	σ = 4.75 n m	σ = 9 n m
180	95	93	87
135	90	96	89
110	98	93	81

Table IIb - showing expected success probabilities (%) for the courses shown in Table IIa, target detection at S.

Group III - Fire Control by Time-to-go in the Event of Radar Cross-Over

Two cases, (Fixed R & T course) were studied. The success probability of a M1.5 fighter against a 0.85 M target is > 95% for AI ranges greater than 0.6S, even when the target manoeuvres with 1/2 g lateral acceleration. For a M1.5 fighter and target the probabilities decrease as the course difference changes from 180 - 110°. For σ = 1.5 n.m. the probability is > 95% at Γ = 180° and 135° for AI > 0.6S.

4.0 CONCLUSIONS

4.1 Group I - Fire Control by $R/\dot{R}$ Measurement.

An important aspect of this group, (but not investigated in detail in this study), is the effect of choice of $R/\dot{R}$ for fire control. As explained in the 5th Progress Report the choice of $R/\dot{R}$ was made from $R/\dot{R}$ contour and residual launch zone, derived from a constant speed study. The chosen $R/\dot{R}$ contour was the contour best fitting the residual launch zone (i.e. dividing the zone equally).

In two courses particularly, $L_a = 0$, $L_a = 20^\circ$ the residual launch zone is small and it was easy to select an $R/\dot{R}$ contour to pass through the zone. In other words an optimum $R/\dot{R}$ value is easily achieved. The effect of this shows in the overall success probabilities in Tables Ia, b, where Fixed Lead shows an advantage (or equality) in two cases. On the other hand the R & T course seems consistently good except for $\Gamma = 180^\circ$ and "good to fair" GCI accuracy. There seems to be no reason why the R & T course should be inferior in these cases. However, the explanation in this study is the difficulty of choosing an optimum $R/\dot{R}$ value which would give superior results over the whole residual launch zone. This is the reverse situation to the Fixed Lead courses; with the R & T course there is a large residual launch zone and the $R/\dot{R}$ curves do not fit this zone well. Hence, a compromise is necessary and in this case the head-on attack probabilities have suffered. However, the R & T course is the most satisfactory in this group.

4.2 Group II - Fire Control by Range Estimation

In this group the selection of a satisfactory range is straightforward. The results are given at AI detection range equal to S only and with a 20% standard deviation in the range estimation error curve. The R & T course with its large residual zone is easily the most satisfactory although other courses show good results in their residual zones.

4.3 Group III - Fire Control by "Time-to-go"

Under ECM conditions it is still probable that there exists a radar cross-over range at a useful distance from the target, assuming that this range exists outside the launch zone, the radar of the interceptor is able to compute 'time-to-go' in the R & T mode. This time is used as the fire control parameter, whilst the interceptor continues to fly on its R & T course. In one of the two cases considered the speed advantage of the fighter yields very high probabilities. For the equal speed case the probabilities are only high with good GCI placement and with $\Gamma = 180^\circ$ and 135°. It is suggested that more work be done, changing various parameters such as 'firing time', error sensitivity and look angle limits.

5.0 SELECTION OF NAVIGATION MODE UNDER E.C.M. USING R/R FIRING

5.1 Introduction

The navigational modes giving the highest probabilities for different Γ 's, and σ 's were given in sections 3 and 4. Depending on conditions, one or another of these courses seems preferable over the rest. Hence probability of a successful interception can be enhanced if the fighter is able to choose the "best" navigational mode for its particular situation. Some simple criterion for doing this would be useful. It should be stated here, however, that the fixed R and T course seems to be suited for the widest range of initial conditions, and if a single course has to be chosen, then this course holds good promise. Still, it may be desirable to choose and it is this problem that will now be discussed.

5.2 A Priori Condition

As an initial approach to the question of selecting the "best" course, the decision might be made at the very beginning of an interception based on the G.C.I. approach to be used. For example, suppose G.C.I. sets out to vector the interceptor in on a lead collision course with $\Gamma = 120^\circ$ where the fighter aspect at large ranges ideally would be about 150°. Then, a priori, the interceptor could be instructed to use $L_a = 20^\circ$ in the event of E.C.M. since in general $L_a = 20^\circ$ yields the best results for $\Gamma = 120^\circ$. For $\Gamma = 180^\circ$, $L_a = 0^\circ$ might be chosen, and so on.

This method is simple, but it does not take into account G.C.I. placement errors. Thus, with poor G.C.I. accuracy, the interceptor with $\Gamma = 120^\circ$ might be approaching the target at large ranges with an aspect angle around 180° instead of the intended 150° and to use $L_a = 20^\circ$ in case of E.C.M. would give poor success probabilities.

5.3 Aspect Criterion

With aspect information, obtained, say, just before jamming or from G.C.I., it turns out that a useful criterion can be set down to overcome this difficulty. This is so because the effectiveness of each navigational mode can be defined fairly well in terms of aspect so as to be independent of range and course difference. (course differences from 180 to 110° were considered in this study). In so doing, some of the usefulness of the modes is lost. For instance, at some aspect, a particular mode may give good results at some ranges but not at others, or for some course differences but not others, and according to the above criterion, this aspect would not be a useful one for that mode. Fortunately, these effects are small, and the use of an aspect criterion seems quite reasonable.

A list of useful aspects for each course is given below. It should be considered only as a guide.

No	Course	Useful Aspects	Comments
1	Fixed R & T	138 - 162	Probabilities fall off slowly outside this interval
2	L_a = 20	142 - 155	Fairly abrupt fall-off
3	L_a = 0	172 - 180	Abrupt fall-off.
4	ω = .005 rad/sec	160 - 180	Moderate fall-off
5	ω = 0	165 - 180	Moderate fall-off

5.4 Conclusions

From the above list, possible combinations of courses to achieve good results for some continuous range of aspects become apparent. The best combination would be 1 and 4, although 1 and 5, 2 and 4, 2 and 5, and even 1 and 3 might be suitable. It should be noted that for $L_a = 20^{\circ}$ and $\omega =$ .005 r/sec., modes with both positive and negative signs must be used.

It might be possible to choose parameters to optimize a particular combination. For instance, the values of L_a and ω could be mutually chosen to get better coverage and the choice of the $R/\dot{R}$ value for each mode in the combination could be selected so as to optimize results.

In conclusion, by using an aspect criterion to select the "best" navigational mode to be used in case of E.C.M., it should be possible to obtain good interception probability in the interval $138^{\circ} \leq A \leq 180^{\circ}$. With manipulation of parameters, it might be possible to increase this interval.

CASE	COURSE	TARGET Speed/Ht	Kft	Evasion	INTERCEPTOR Initial Speed	Max	Min	Kft	Γ°	FIRE CONTROL	RADAR CROSS-OVER
1	R & T	M1.5	50	None	M1.5	M2.0	M1.0	50	180	$R/\dot{R}$ = 12Sec.	No
2	"	"	"	"	"	"	"	"	135	"	"
3	"	"	"	"	"	"	"	"	110	"	"
4	"	"	"	1/2 g	"	"	"	"	180	"	"
5	"	"	"	1/2 g	"	"	"	"	135	"	"
6*	"	"	"	1/2 g	"	"	"	"	110	"	"
7	"	"	"	None	"	"	"	"	180	R = 25 Kft	"
8	"	"	"	"	"	"	"	"	135	"	"
9	"	"	"	"	"	"	"	"	110	"	"
10	"	"	"	"	"	"	"	"	180	T = 7.7 Sec.	Yes
11	"	"	"	"	"	"	"	"	135	"	"
12	"	"	"	"	"	"	"	"	110	"	"
13	"	"	"	1/2 g	"	"	"	"	180	"	"
14	"	M0.85	50	None	M0.95	M0.95	M0.76	50	180	$R/\dot{R}$ = 17 Sec.	No
15	"	"	"	"	"	"	"	"	135	"	"
16	"	"	"	"	"	"	"	"	110	"	"
17	"	"	"	"	M1.5	M2.0	M1.0	50	180	T = 9 Sec.	Yes
18	"	"	"	"	"	"	"	"	135	T = 9	"
19	"	"	"	"	"	"	"	"	110	T = 9	"
20	"	"	"	1/2 g	"	"	"	"	180	T = 9	"
21	L_a = 20°	M1.5	50	None	"	"	"	"	180	$R/\dot{R}$ = 12 Sec.	No
22	"	"	"	"	"	"	"	"	135	"	"
23	"	"	"	"	"	"	"	"	110	"	"
24	"	"	"	"	"	"	"	"	180	R = 28 kft.	"
25	"	"	"	"	"	"	"	"	135	"	"
26	"	"	"	"	"	"	"	"	110	"	"
27	L_a = 0	"	"	"	"	"	"	"	180	$R/\dot{R}$ = 10 Sec.	"
28	"	"	"	"	"	"	"	"	135	"	"
29	"	"	"	"	"	"	"	"	180	R = 30 kft	"
30	ω = .005	"	"	"	"	"	"	"	180	$R/\dot{R}$ = 12 Sec.	"
31	"	"	"	"	"	"	"	"	135	"	"
32	"	"	"	"	"	"	"	"	110	"	"
33	ω = 0	M1.5	50	None	M1.5	M2.0	M1.0	50	180	$R/\dot{R}$ = 11 Sec.	No
34	"	"	"	"	"	"	"	"	135	"	"
35	"	"	"	"	"	"	"	"	110	"	"

<u>TABLE III</u> - * Page 6 not drawn, zero prob. all over.

CASE I

Fixed Range Lead Pursuit

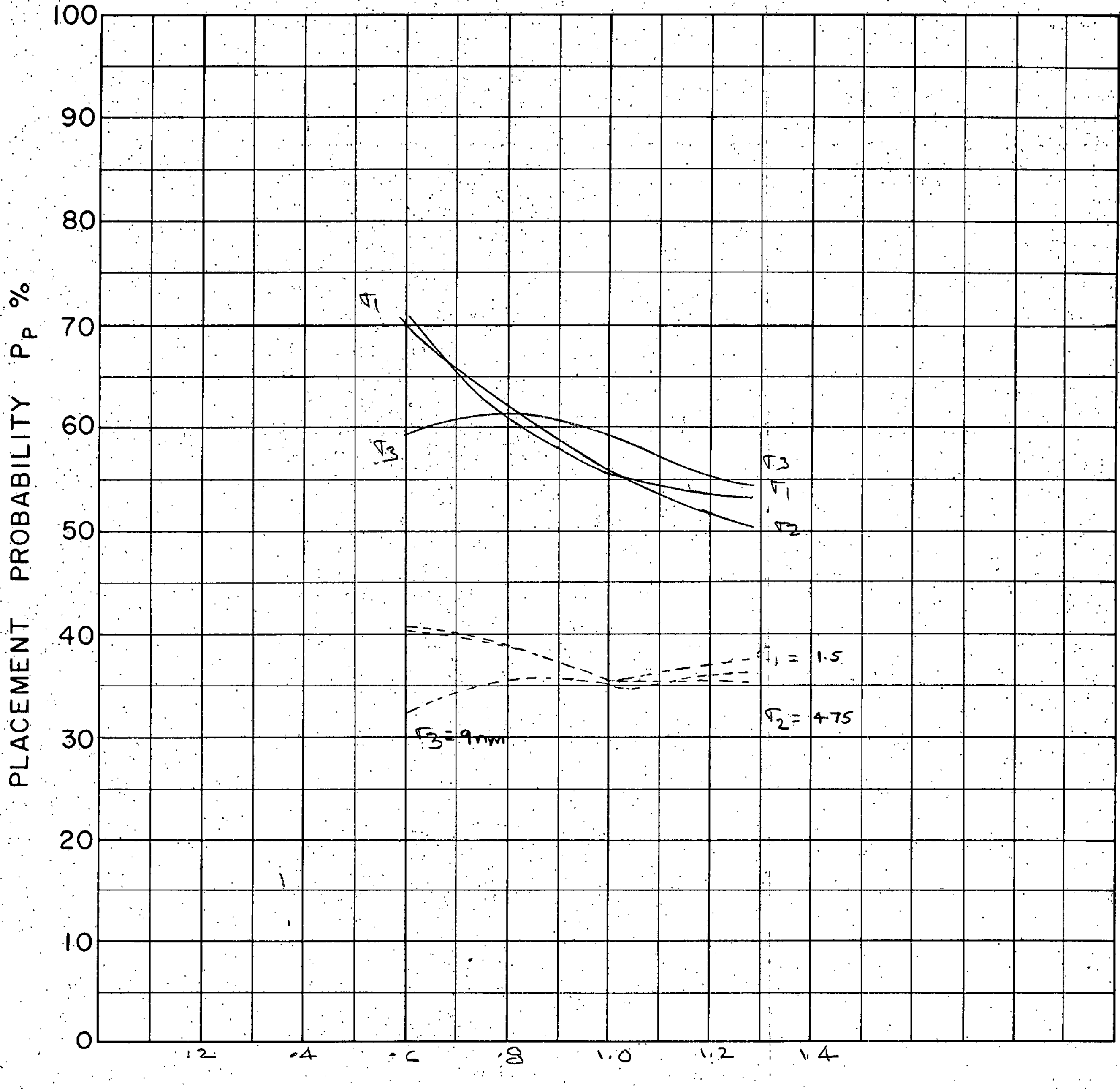

COURSE DIFFERENCE: 180
TARGET EVASION: None
TARGET MACH NO.: 1.5
INTERCEPTOR LATERAL G's: Avro 3.3
INTERCEPTOR MACH NO.: 1.5
σ OF G.C.I. ACCURACY: 3 values
A.I. DETECTION RANGE AS FRACTION OF SPECIFICATION RANGE, S: Abscissa
A.I. DETECTION RANGE CONTOUR: Delta
ALTITUDE: 50,000 ft.

o———————o 20% STANDARD DEVIATION IN R/Ṙ = 12

o— — — — —o 60% " " " " "

Fixed Range Lead Pursuit

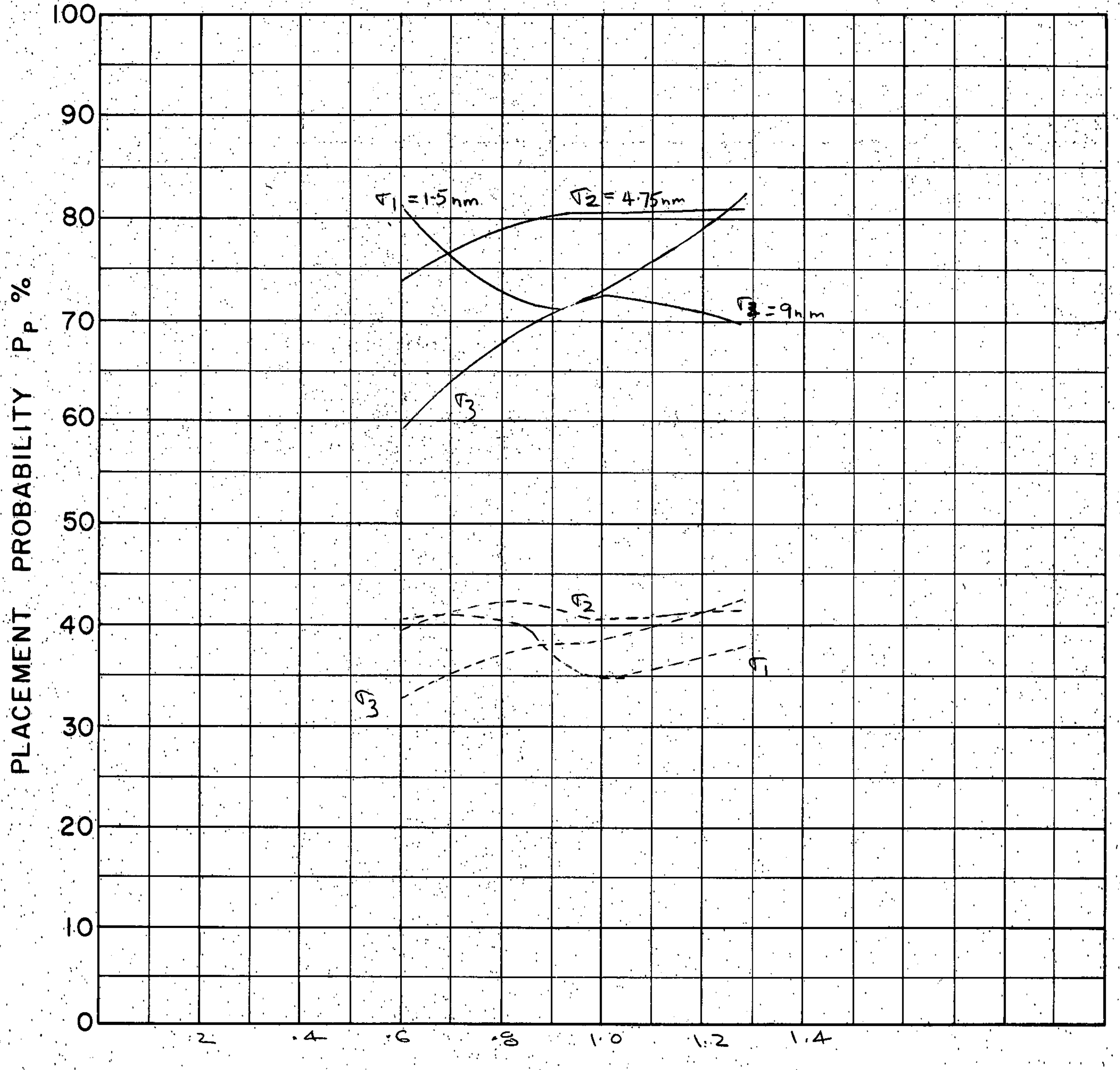

COURSE DIFFERENCE: 135
TARGET EVASION: None
TARGET MACH NO.: 1.5
INTERCEPTOR LATERAL G's: Avro 3.3
INTERCEPTOR MACH NO.: 1.5
σ OF G.C.I. ACCURACY: 3 Values
A.I. DETECTION RANGE AS FRACTION OF SPECIFICATION RANGE, S: Abscissa
A.I. DETECTION RANGE CONTOUR: Delta
ALTITUDE: 50,000 ft.

o———————o 20 % STANDARD DEVIATION IN R/R = 12

o- - - - - - -o 60 % " " " " "

CASE 3

Fixed Range Lead Pursuit

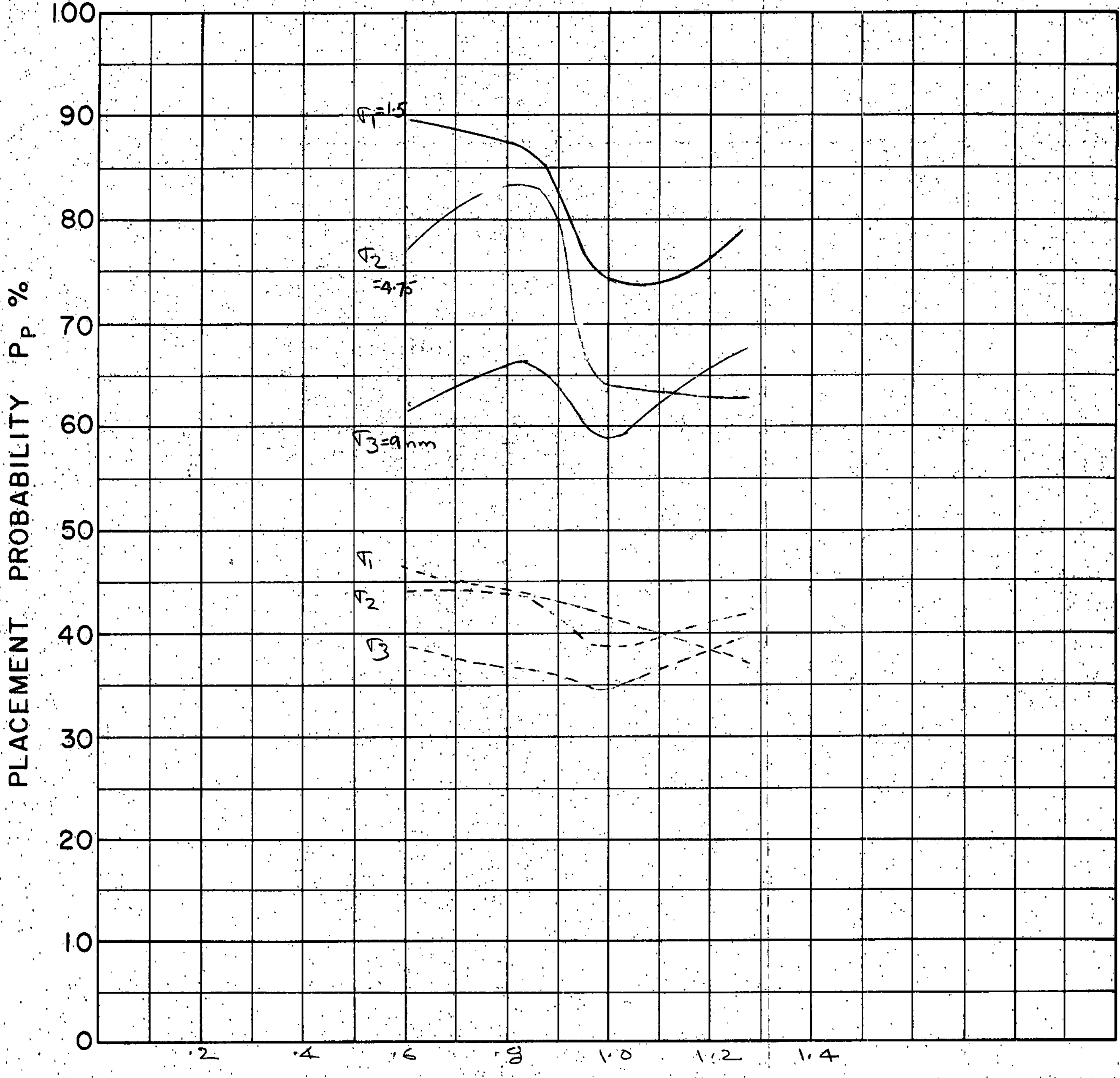

COURSE DIFFERENCE: 110
TARGET EVASION: None
TARGET MACH NO.: 1.5
INTERCEPTOR LATERAL G's: Avro 3.3
INTERCEPTOR MACH NO.: 1.5
σ OF G.C.I. ACCURACY: 3 Values
A.I. DETECTION RANGE AS FRACTION OF SPECIFICATION RANGE, S: Abscissa
A.I. DETECTION RANGE CONTOUR: Delta
ALTITUDE: 50,000 ft.

o————o 20% STANDARD DEVIATION IN R/R = 12

o- - - - -o 60% " " " " "

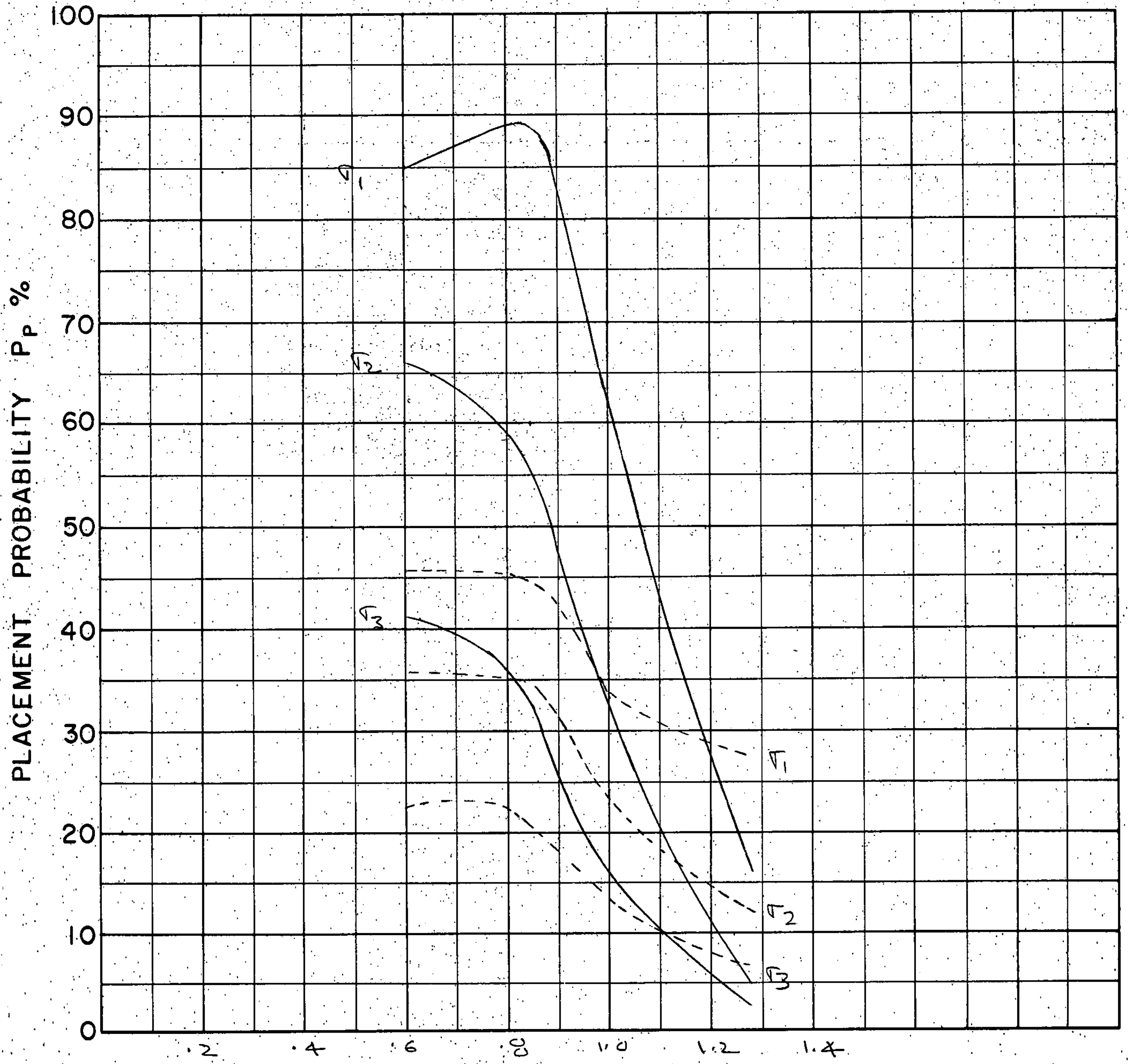

COURSE DIFFERENCE: 180
TARGET EVASION: 1/2 g
TARGET MACH NO.: 1.5
INTERCEPTOR LATERAL G's: Avro 3.3
INTERCEPTOR MACH NO.: 1.5
σ OF G.C.I. ACCURACY: 3 Values
A.I. DETECTION RANGE AS FRACTION OF SPECIFICATION RANGE, S: Abscissa
A.I. DETECTION RANGE CONTOUR: Delta
ALTITUDE: 50,000 ft.

o————o 20% STANDARD DEVIATION IN $R/\dot{R}$ = 12

o- - - - - -o 60% " " " " "

CASE 5

Fixed Range Lead Pursuit

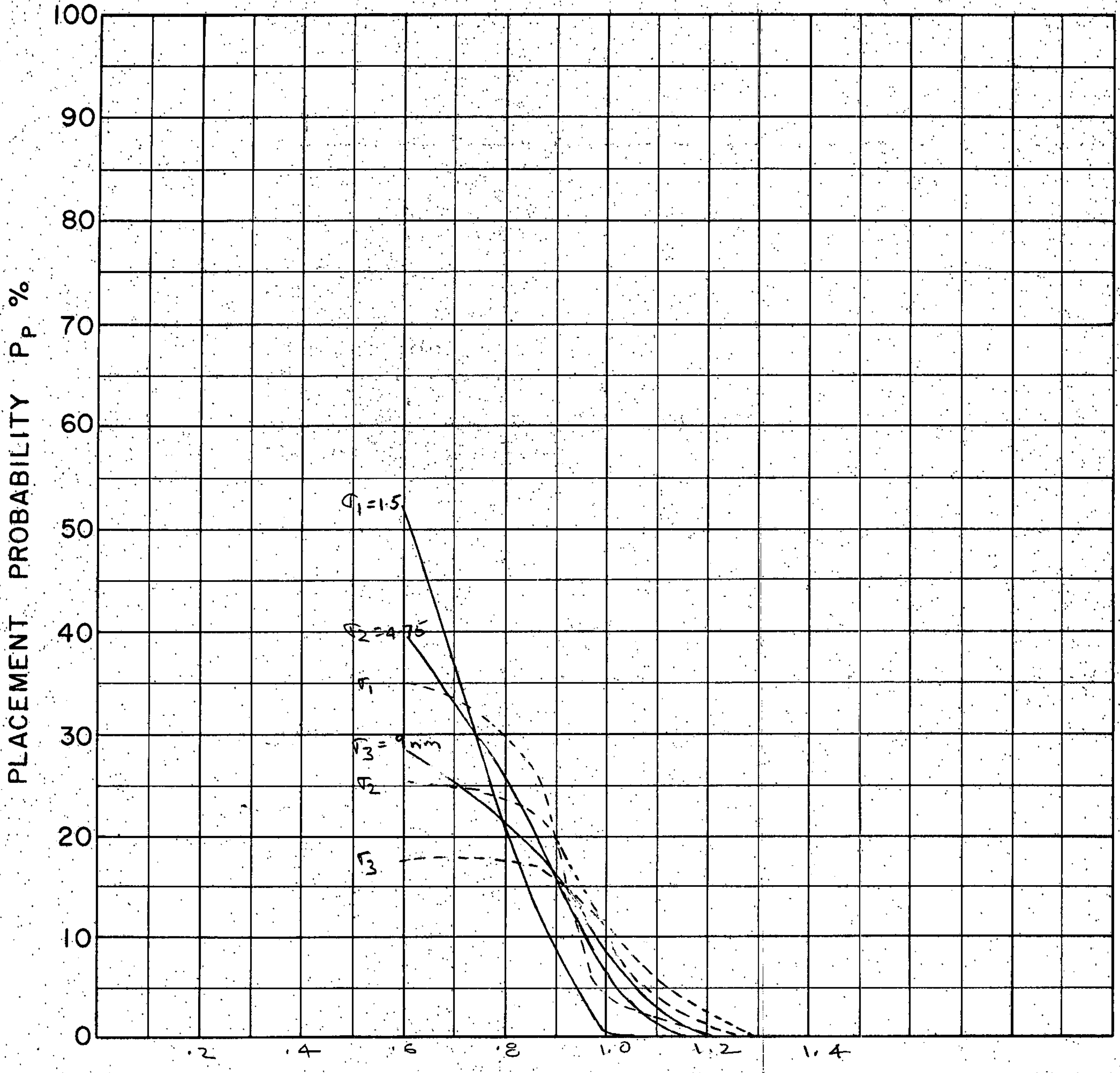

COURSE DIFFERENCE: 135
TARGET EVASION: 1/2 g
TARGET MACH NO.: 1.5
INTERCEPTOR LATERAL G's: Avro 3.3
INTERCEPTOR MACH NO.: 1.5
σ OF G.C.I. ACCURACY: 3 Values
A.I. DETECTION RANGE AS FRACTION OF SPECIFICATION RANGE, S: Abscissa
A.I. DETECTION RANGE CONTOUR: Delta
ALTITUDE: 50,000 ft.

o———————o 20% STANDARD DEVIATION IN R/R = 12

o- - - - - -o 60% " " " " "

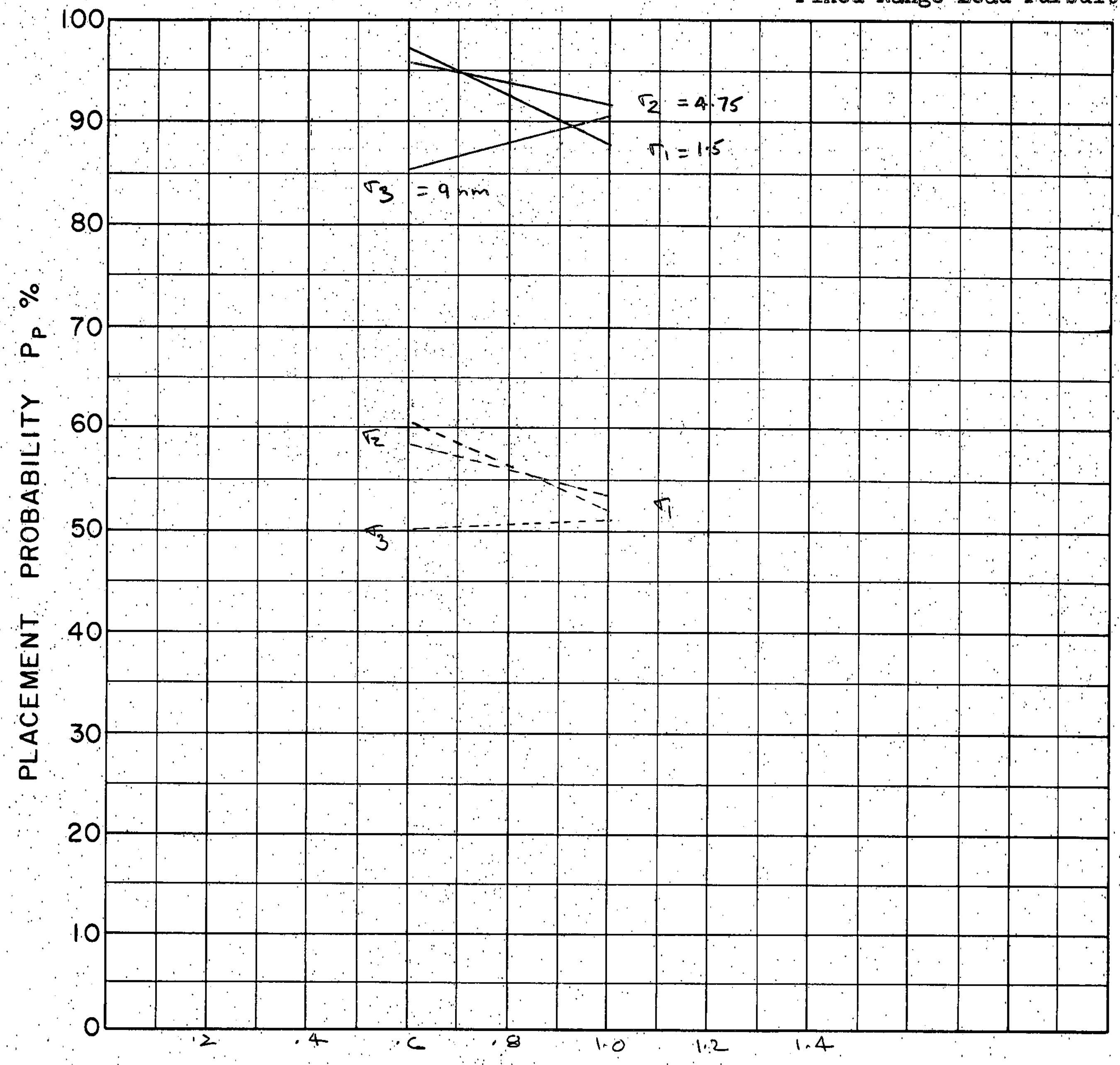

COURSE DIFFERENCE: 180
TARGET EVASION: None
TARGET MACH NO.: 1.5
INTERCEPTOR LATERAL G's: Avro 3.3
INTERCEPTOR MACH NO.: 1.5
σ OF G.C.I. ACCURACY: 3 Values
A.I. DETECTION RANGE AS FRACTION OF SPECIFICATION RANGE, S: Abscissa
A.I. DETECTION RANGE CONTOUR: Delta
ALTITUDE: 50,000 ft.

o———————o 20% STANDARD DEVIATION IN R = 25 Kft

o– – – – – –o 60% " " " " "

CASE 8

Fixed Range Lead Pursuit

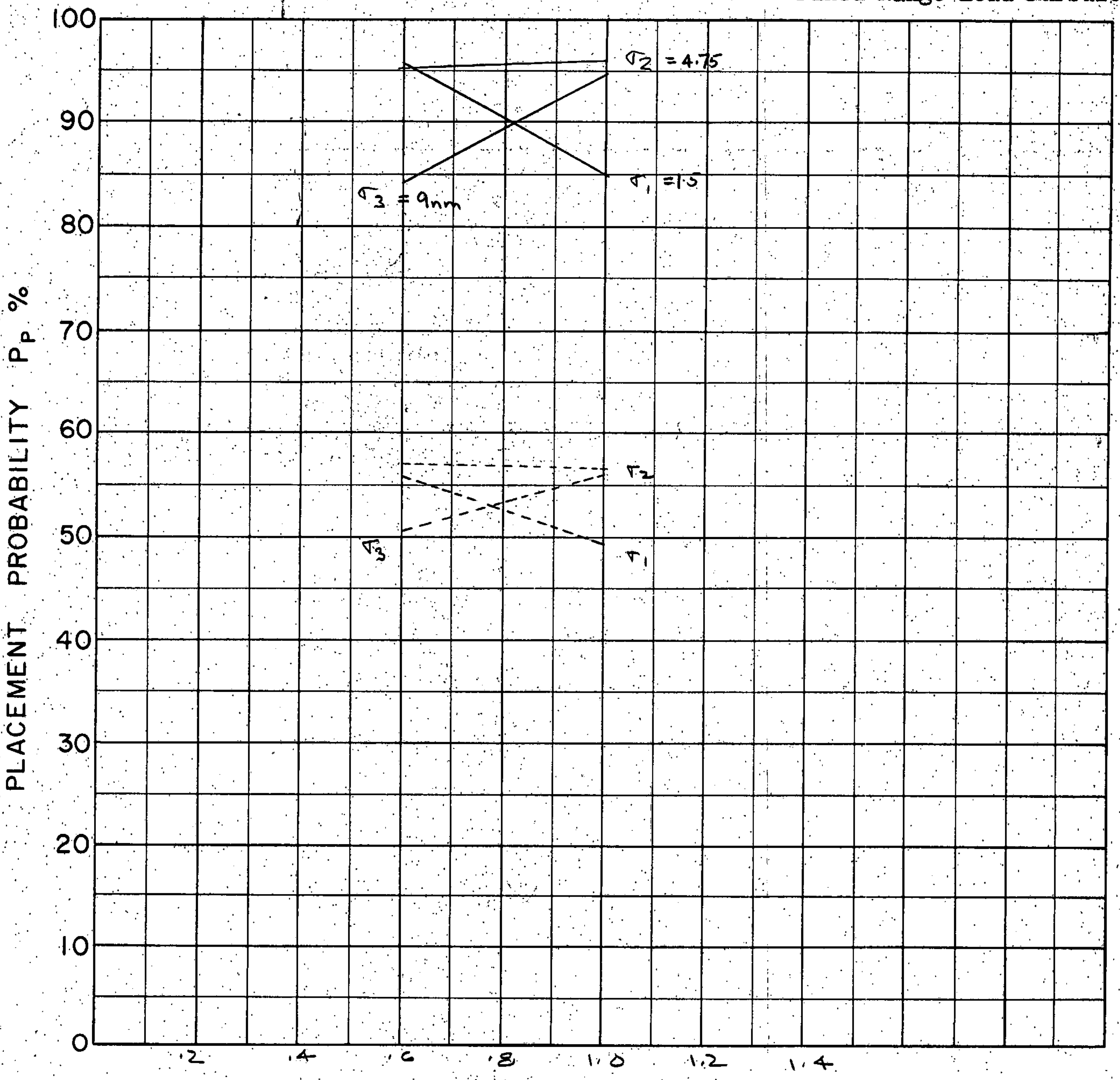

COURSE DIFFERENCE: 135
TARGET EVASION: None
TARGET MACH NO.: 1.5
INTERCEPTOR LATERAL G's: Avro 3.3
INTERCEPTOR MACH NO.: 1.5
σ OF G.C.I. ACCURACY: 3 Values
A.I. DETECTION RANGE AS FRACTION OF SPECIFICATION RANGE, S: Abscissa
A.I. DETECTION RANGE CONTOUR: Delta
ALTITUDE: 50,000 ft.

o————o 20% STANDARD DEVIATION IN R = 25Kft

o- - - - - -o 60% " " " " "

Fixed Range Lead Pursuit

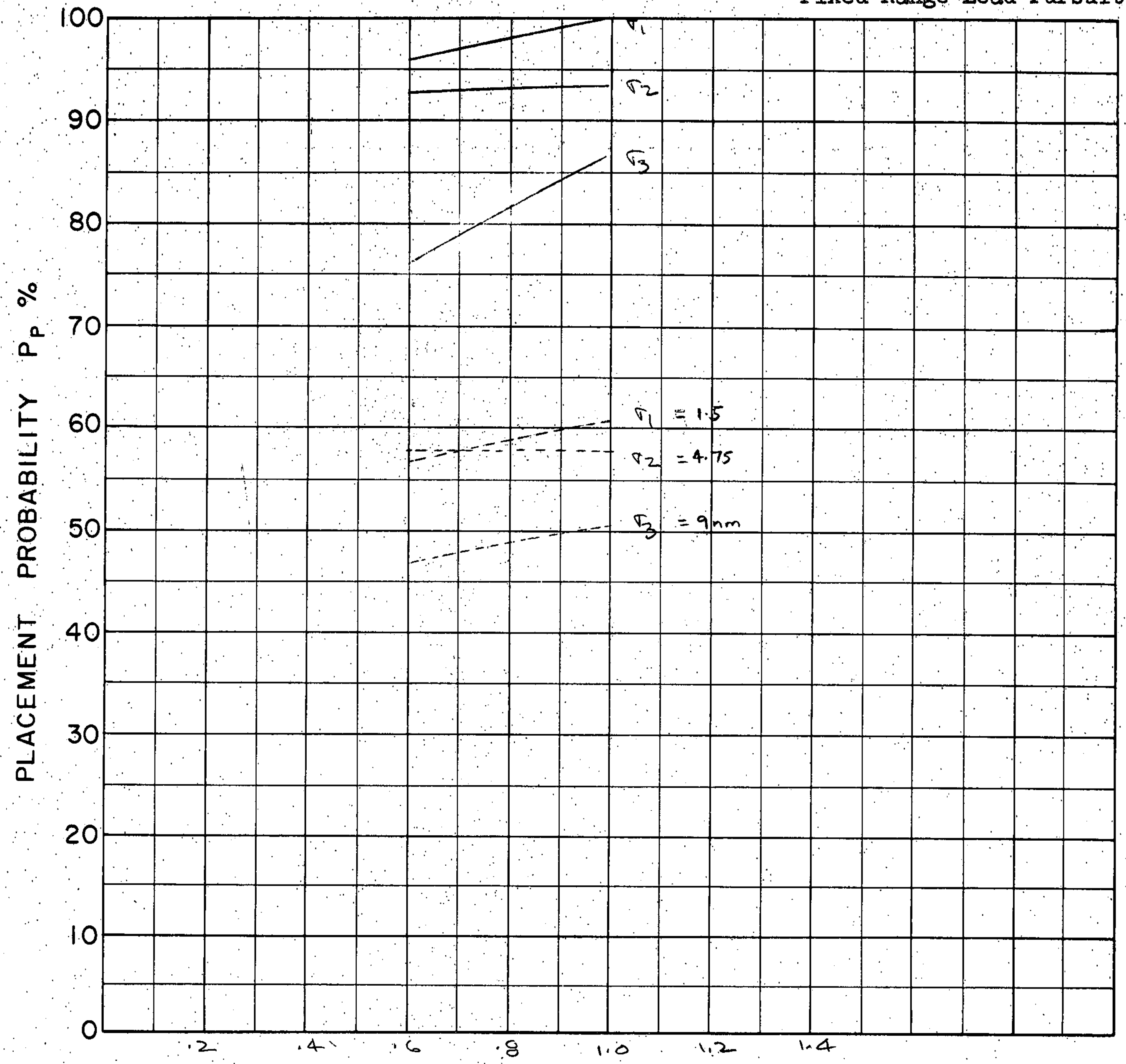

COURSE DIFFERENCE: 110
TARGET EVASION: None
TARGET MACH NO.: 1.5
INTERCEPTOR LATERAL G's: Avro 3.3
INTERCEPTOR MACH NO.: 1.5
σ OF G.C.I. ACCURACY: 3 Values
A.I. DETECTION RANGE AS FRACTION OF SPECIFICATION RANGE, S: Abscissa
A.I. DETECTION RANGE CONTOUR: Delta
ALTITUDE: 50,000 ft.

o———o 20% STANDARD DEVIATION IN R = 25 Kft

o— — — —o 60% " " " " " "

CASE 10

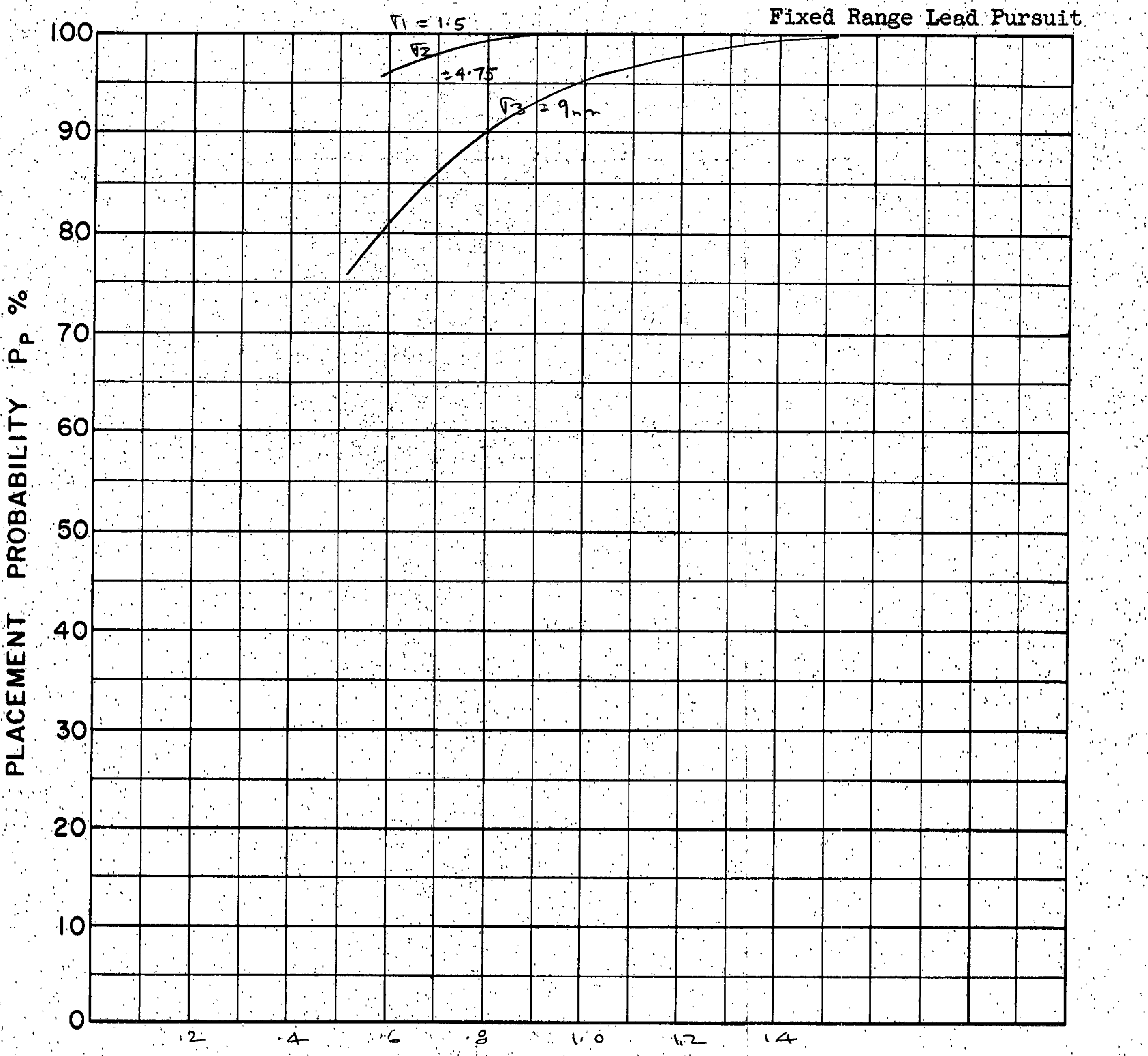

COURSE DIFFERENCE: 180
TARGET EVASION: None
TARGET MACH NO.: 1.5
INTERCEPTOR LATERAL G's: Avro 3.3
INTERCEPTOR MACH NO.: 1.5
σ OF G.C.I. ACCURACY: 3 Values
A.I. DETECTION RANGE AS FRACTION OF SPECIFICATION RANGE, S: Abscissa
A.I. DETECTION RANGE CONTOUR: Delta
ALTITUDE: 50,000 ft.

Fixed Range Lead Pursuit

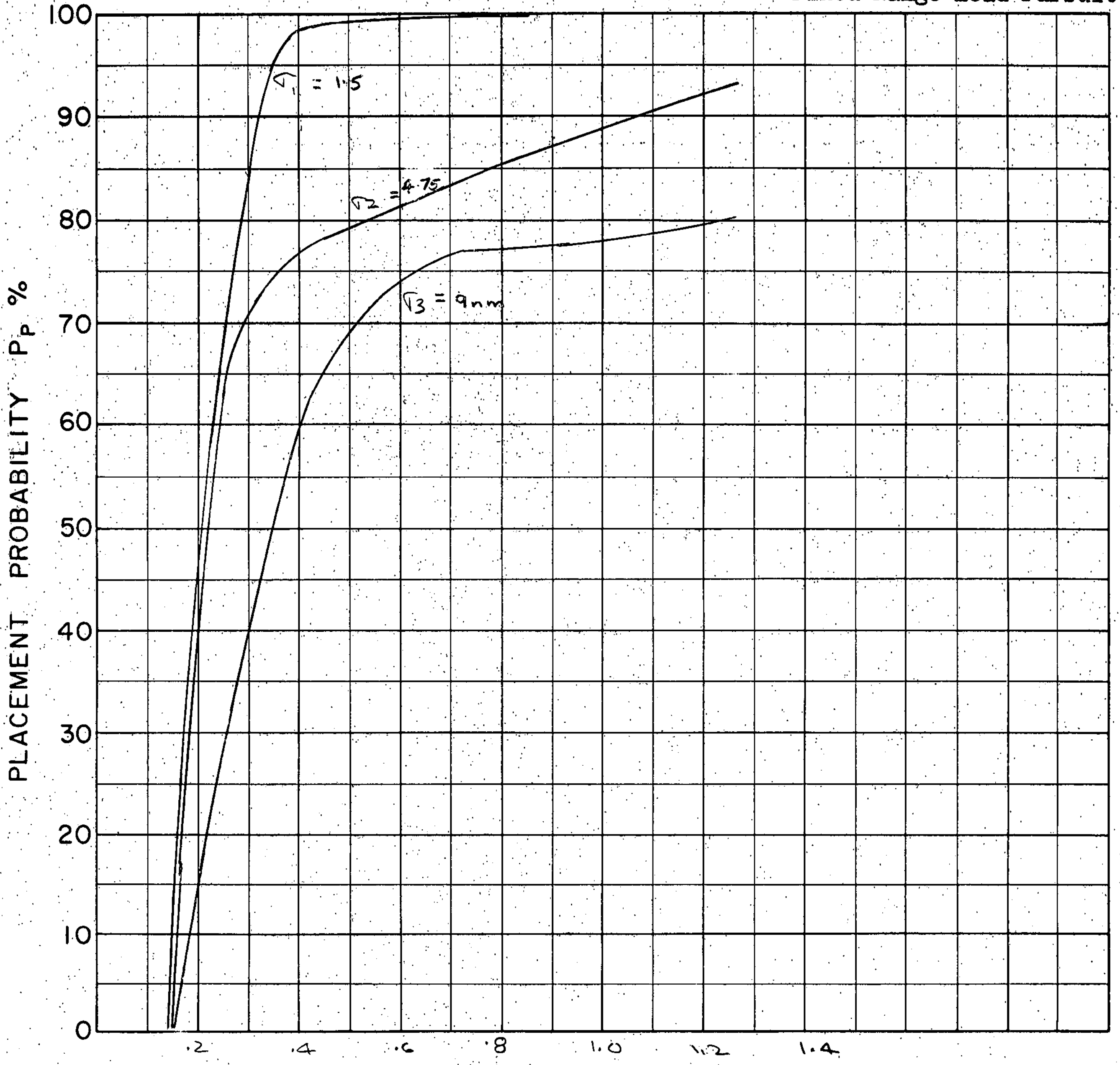

COURSE DIFFERENCE: 135
TARGET EVASION: None
TARGET MACH NO.: 1.5
INTERCEPTOR LATERAL G's: Avro 3.3
INTERCEPTOR MACH NO.: 1.5
σ OF G.C.I. ACCURACY: 3 Values
A.I. DETECTION RANGE AS FRACTION OF SPECIFICATION RANGE, S: Abscissa
A.I. DETECTION RANGE CONTOUR: Delta
ALTITUDE: 50,000 ft.

CASE 12

Fixed Range Lead Pursuit

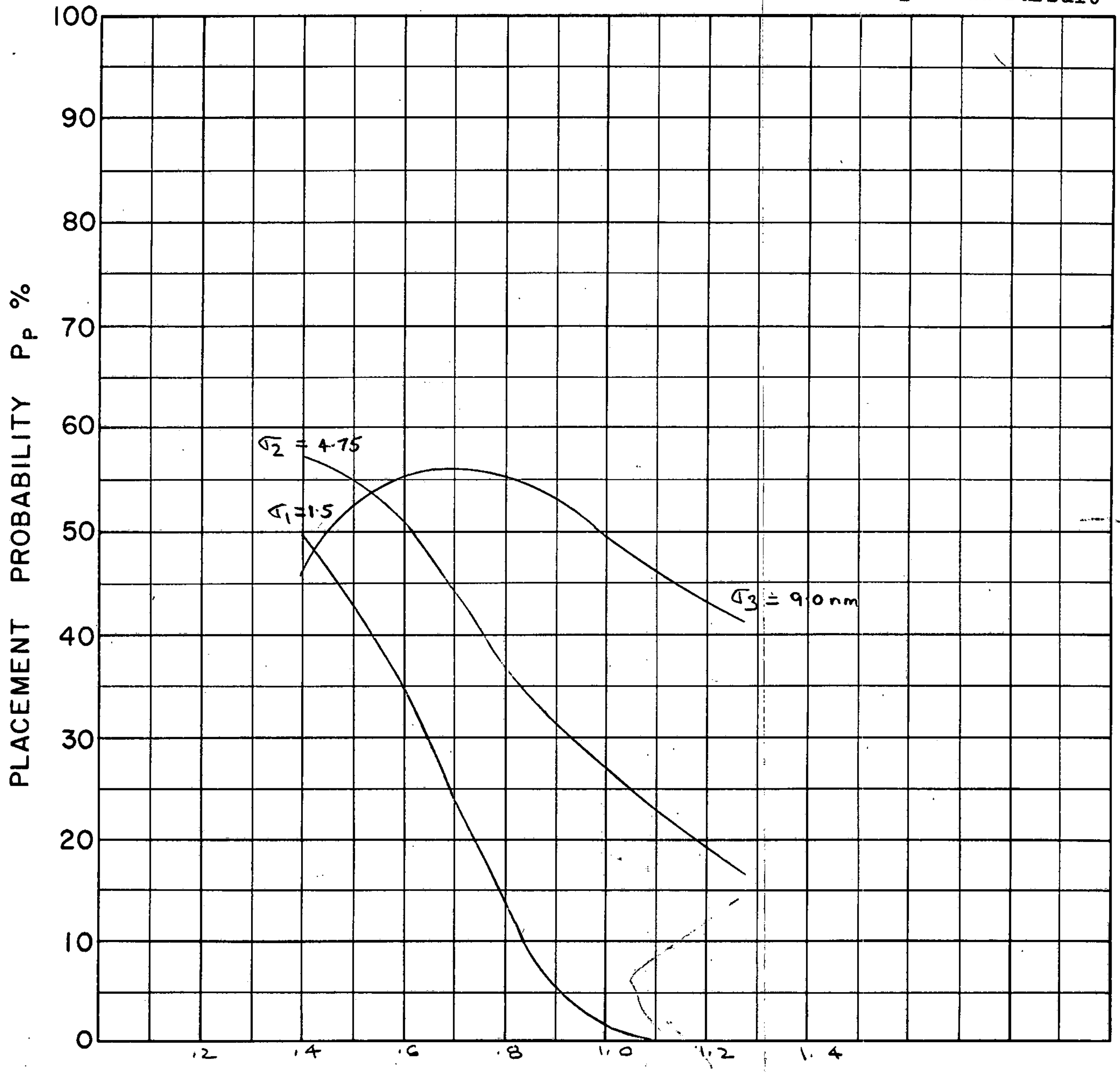

COURSE DIFFERENCE: 110
TARGET EVASION: None
TARGET MACH NO.: 1.5
INTERCEPTOR LATERAL G's: Avro 3.3
INTERCEPTOR MACH NO.: 1.5
σ OF G.C.I. ACCURACY: 3 Values
A.I. DETECTION RANGE AS FRACTION OF SPECIFICATION RANGE, S: Abscissa
A.I. DETECTION RANGE CONTOUR: Delta
ALTITUDE: 50,000 ft.

CASE 13

Fixed Range Lead Pursuit

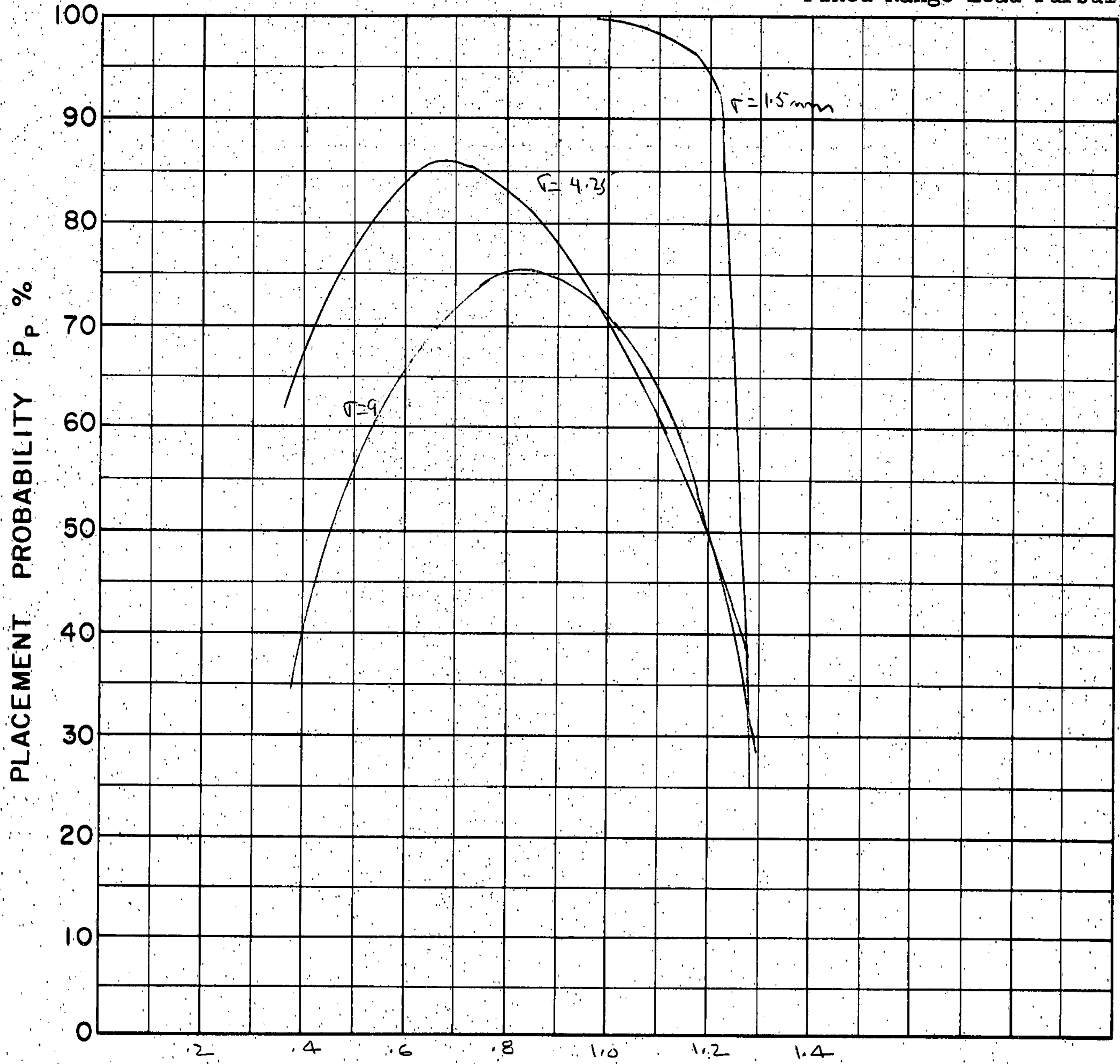

COURSE DIFFERENCE: 180
TARGET EVASION: 1/2 g
TARGET MACH NO.: 1.5
INTERCEPTOR LATERAL G's: Avro 3.3
INTERCEPTOR MACH NO.: 1.5
σ OF G.C.I. ACCURACY: 3 Values
A.I. DETECTION RANGE AS FRACTION OF SPECIFICATION RANGE, S: Abscissa
A.I. DETECTION RANGE CONTOUR: Delta
ALTITUDE: 50,000 ft.

CASE 14

Fixed Range Lead Pursuit

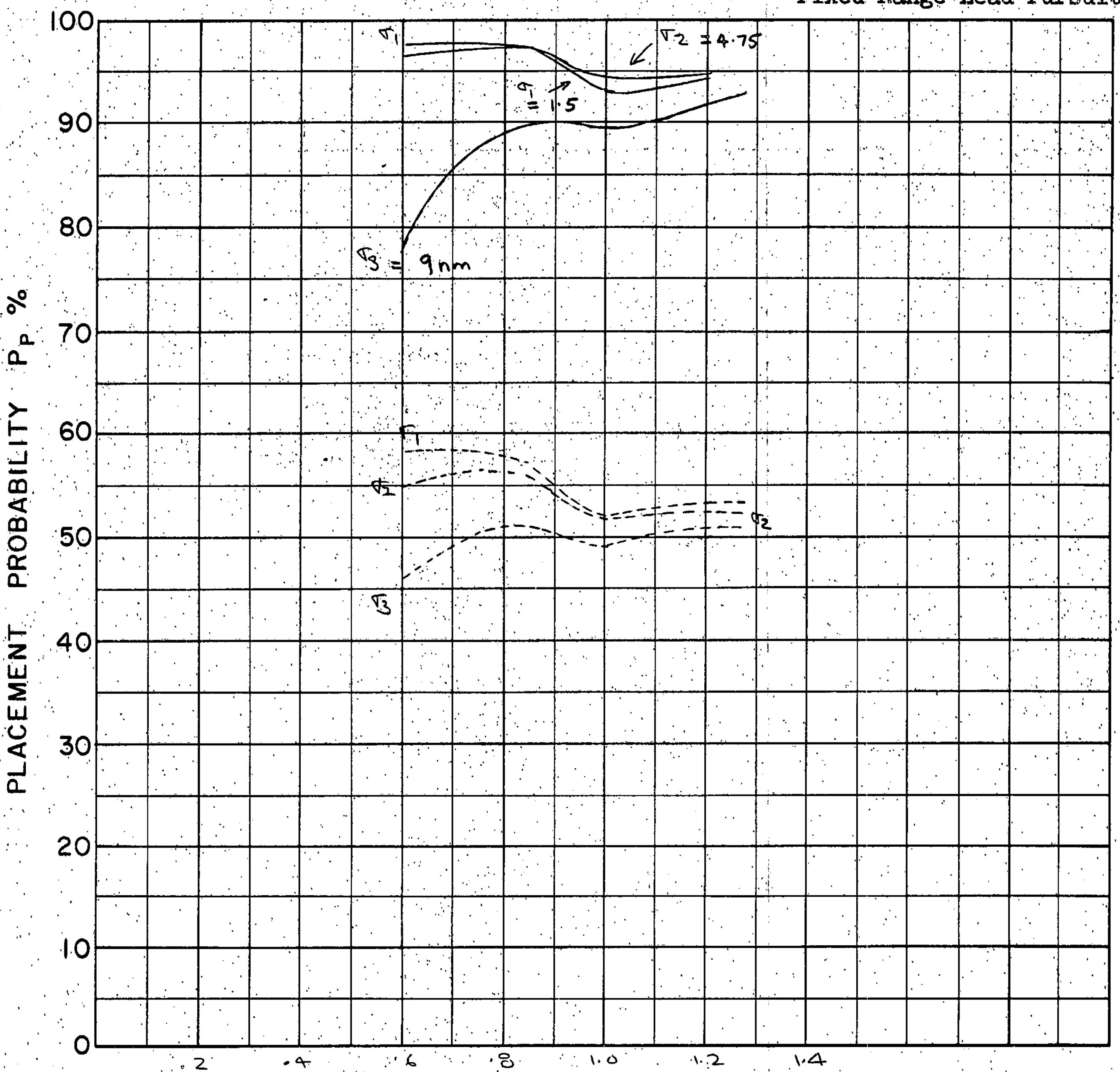

COURSE DIFFERENCE: 180
TARGET EVASION: None
TARGET MACH NO.: 0.85
INTERCEPTOR LATERAL G's: Avro 3.3
INTERCEPTOR MACH NO.: 0.95
σ OF G.C.I. ACCURACY: 3 Values
A.I. DETECTION RANGE AS FRACTION OF SPECIFICATION RANGE, S: Abscissa
A.I. DETECTION RANGE CONTOUR: Delta
ALTITUDE: 50,000 ft.

o———————o 20% STANDARD DEVIATION IN R/R = 17

o— — — — —o 60% " " " " ".

Fixed Range Lead Pursuit

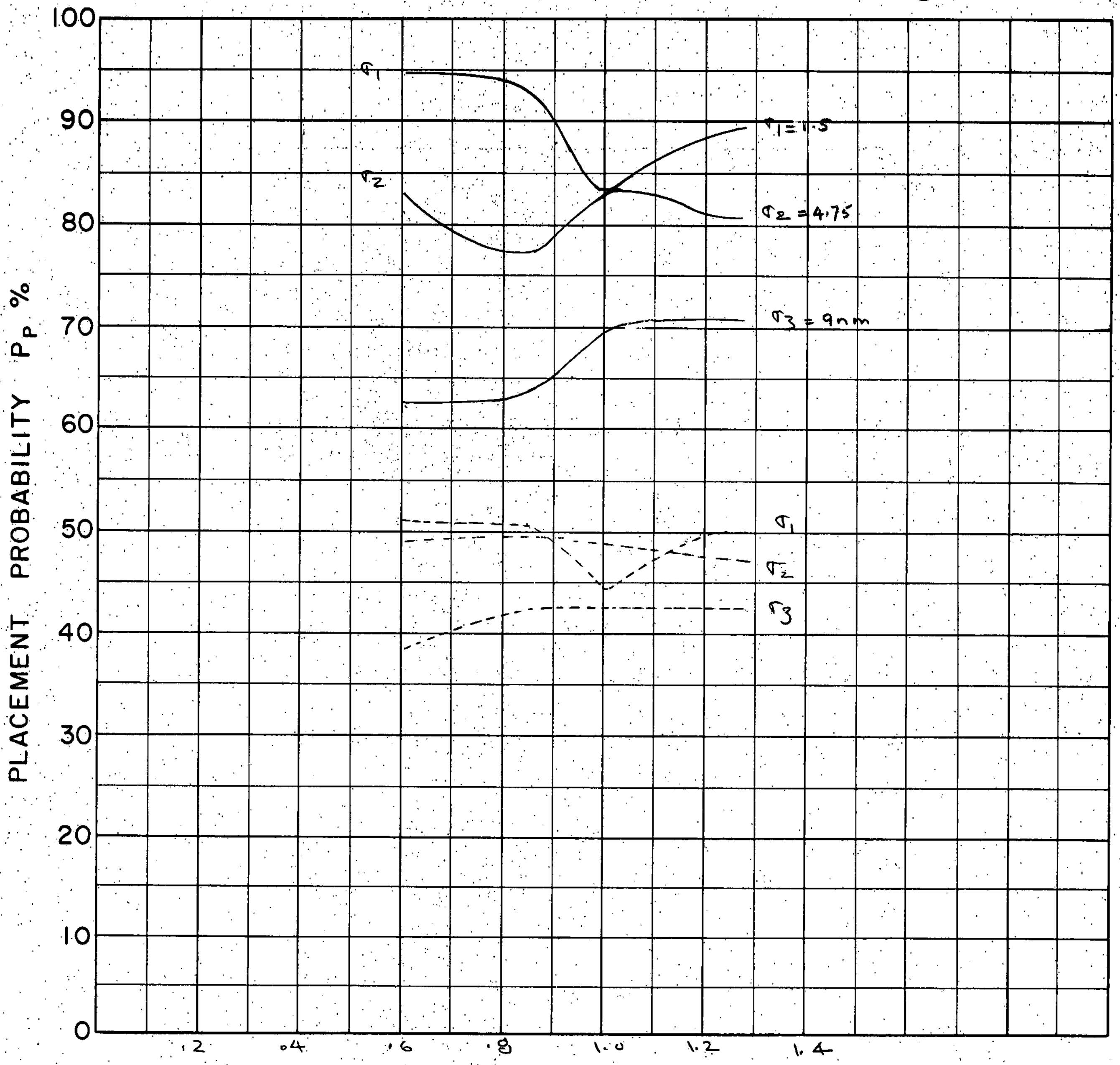

COURSE DIFFERENCE: 135
TARGET EVASION: None
TARGET MACH NO.: 0.85
INTERCEPTOR LATERAL G's: Avro 3.3
INTERCEPTOR MACH NO.: 0.95
σ OF G.C.I. ACCURACY: 3 Values
A.I. DETECTION RANGE AS FRACTION OF SPECIFICATION RANGE, S: Abscissa
A.I. DETECTION RANGE CONTOUR: Delta
ALTITUDE: 50,000 ft.

o———————o 20% STANDARD DEVIATION IN R/R = 17

o- - - - - - -o 60% " " " " "

CASE 16

Fixed Range Lead Pursuit

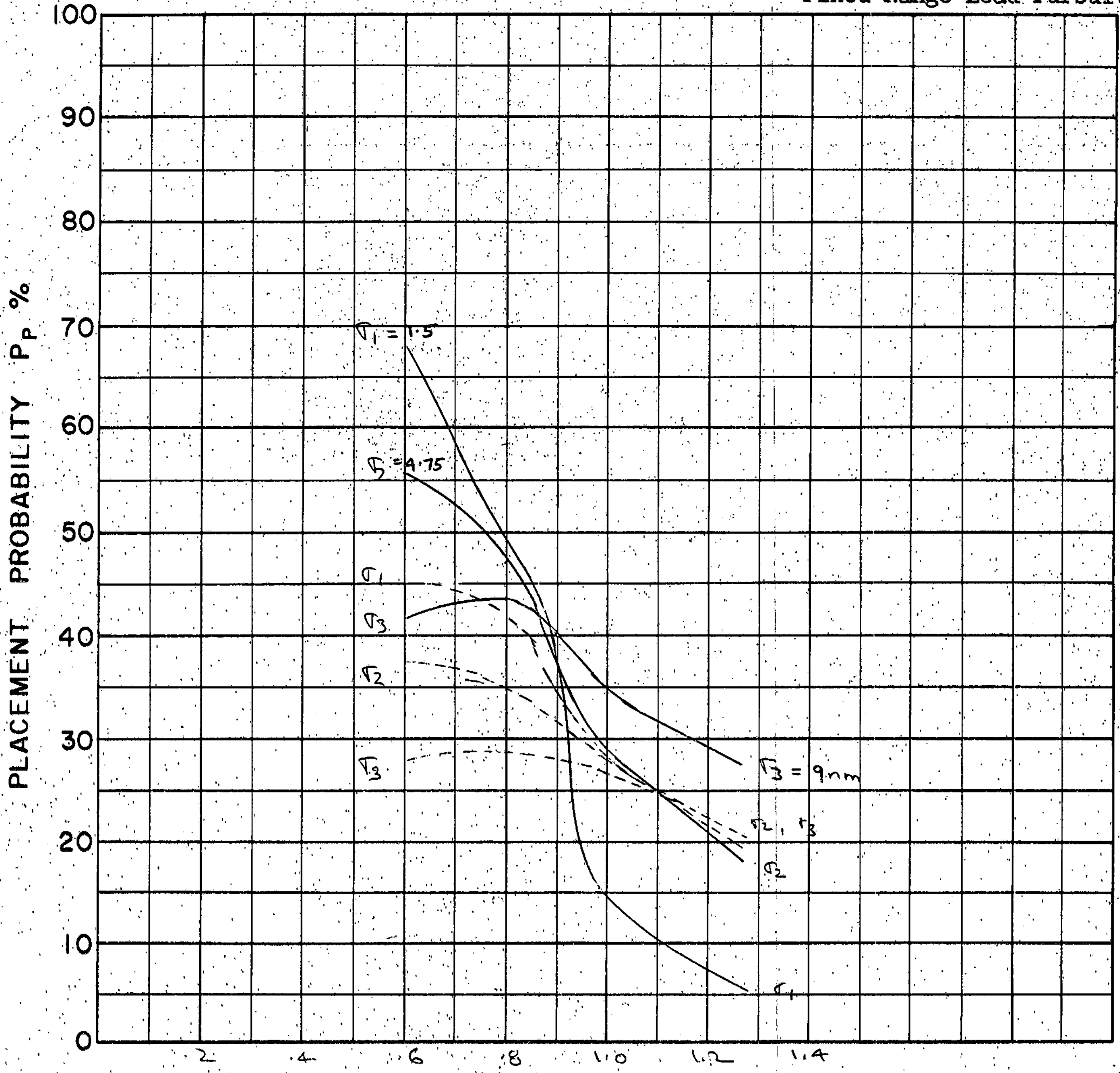

COURSE DIFFERENCE: 110
TARGET EVASION: None
TARGET MACH NO.: 0.85
INTERCEPTOR LATERAL G's: Avro 3.3
INTERCEPTOR MACH NO.: 0.95
σ OF G.C.I. ACCURACY: 3 Values
A.I. DETECTION RANGE AS FRACTION OF SPECIFICATION RANGE, S: Abscissa
A.I. DETECTION RANGE CONTOUR: Delta
ALTITUDE: 50,000 ft.

o———————o 20 % STANDARD DEVIATION IN $R/\dot{R}$ = 17

o- - - - - - -o 60 % " " " " "

CASE 17

Fixed Range Lead Pursuit

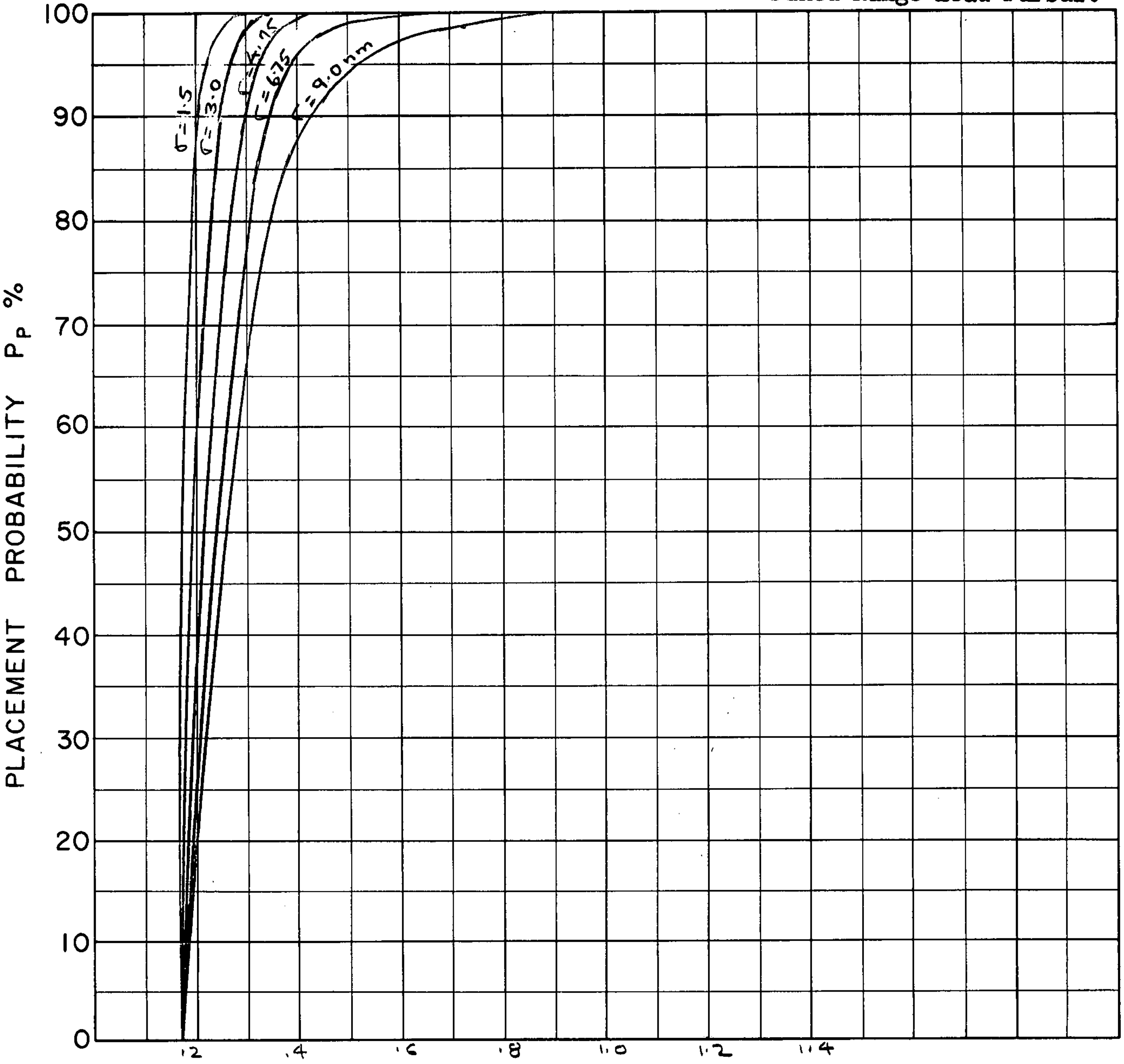

COURSE DIFFERENCE: 180
TARGET EVASION: None
TARGET MACH NO.: 0.85
INTERCEPTOR LATERAL G's: Avro 3.3
INTERCEPTOR MACH NO.: 1.5
σ OF G.C.I. ACCURACY: 5 Values
A.I. DETECTION RANGE AS FRACTION OF SPECIFICATION RANGE, S: Abscissa
A.I. DETECTION RANGE CONTOUR: Delta
ALTITUDE: 50,000 Ft.

CASE 18

Fixed Range Lead Pursuit

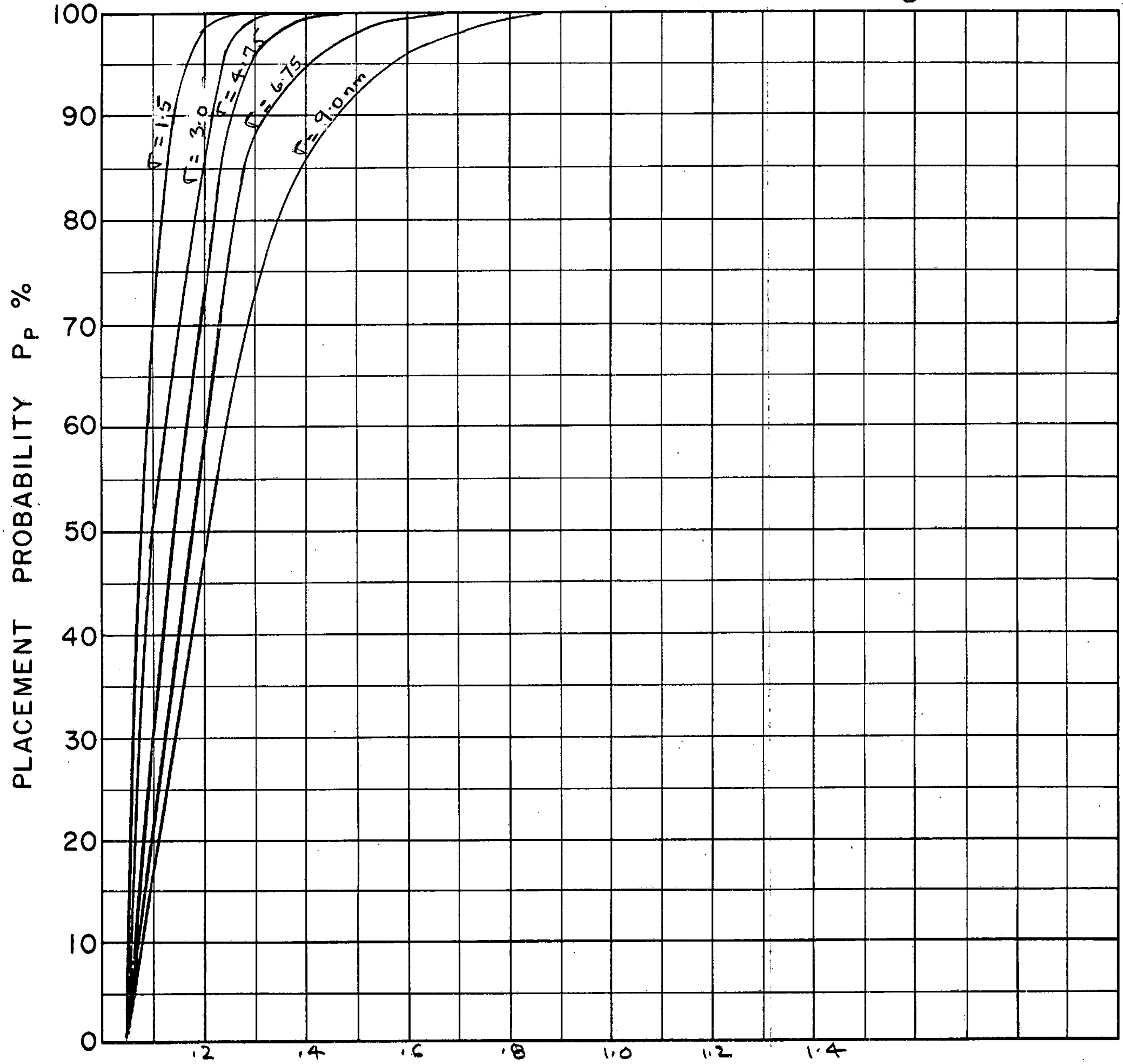

COURSE DIFFERENCE: 135
TARGET EVASION: None
TARGET MACH NO.: 0.85
INTERCEPTOR LATERAL G's: Avro 3.3
INTERCEPTOR MACH NO.: 1.5
σ OF G.C.I. ACCURACY: 5 Values
A.I. DETECTION RANGE AS FRACTION OF SPECIFICATION RANGE, S: Abscissa
A.I. DETECTION RANGE CONTOUR: Delta
ALTITUDE: 50,000 ft.

CASE 19

Fixed Range Lead Pursuit

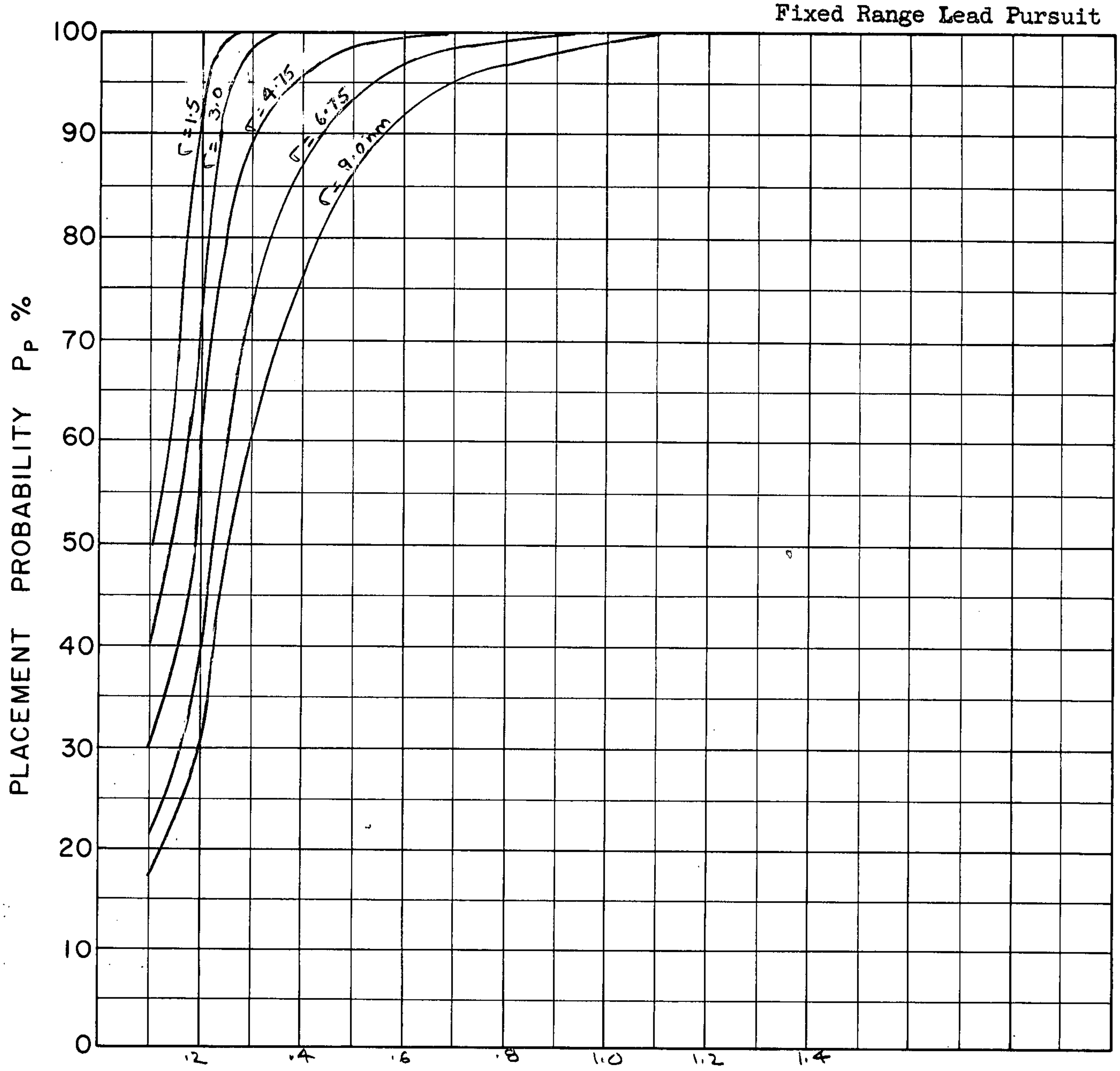

COURSE DIFFERENCE: 110
TARGET EVASION: None
TARGET MACH NO.: 0.85
INTERCEPTOR LATERAL G's: Avro 3.3
INTERCEPTOR MACH NO.: 1.5
σ OF G.C.I. ACCURACY: 5 Values
A.I. DETECTION RANGE AS FRACTION OF SPECIFICATION RANGE, S: Abscissa
A.I. DETECTION RANGE CONTOUR: Delta
ALTITUDE: 50,000 ft.

CASE 20

Fixed Range Lead Pursuit

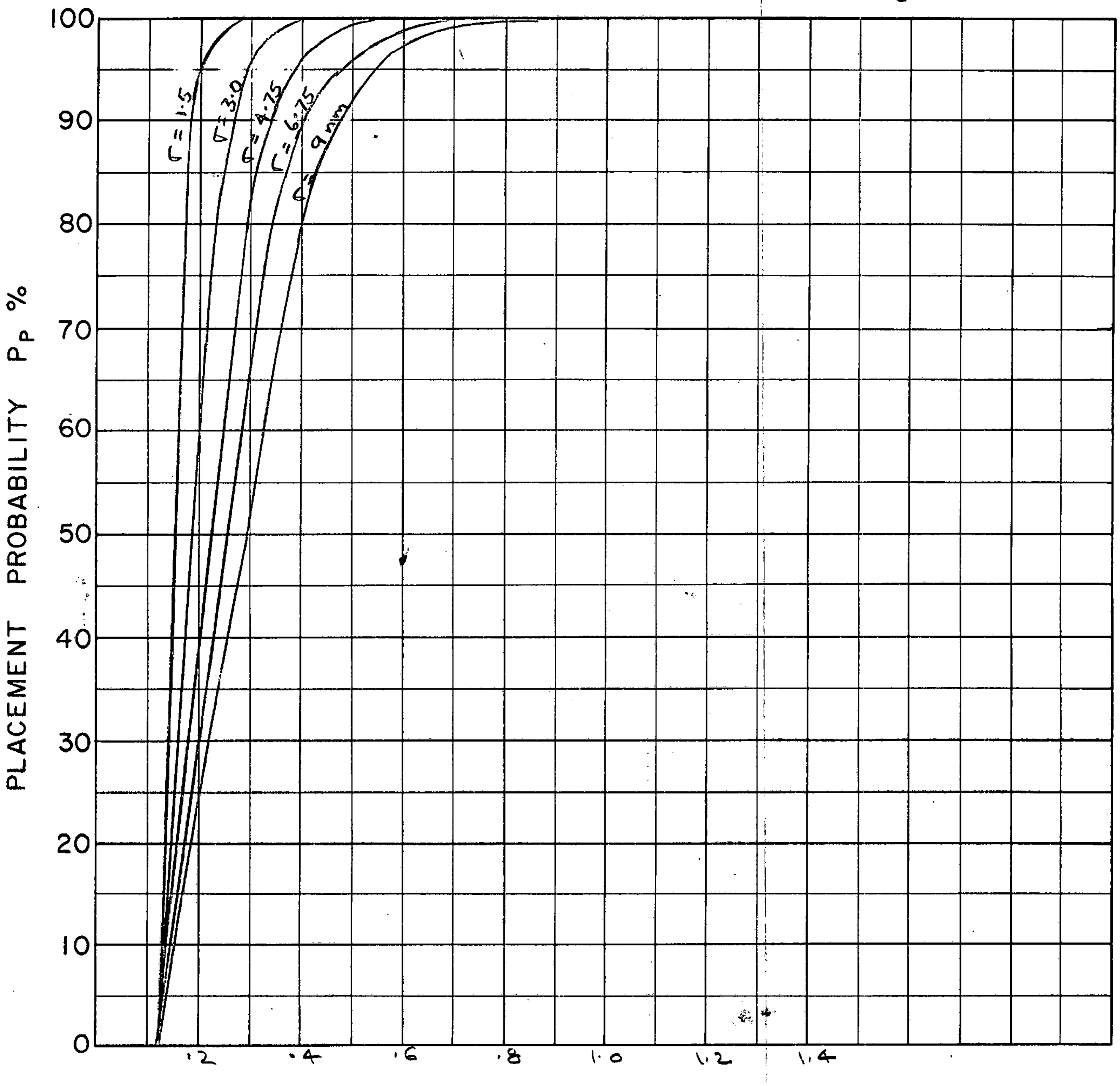

COURSE DIFFERENCE: 180
TARGET EVASION: 1/2 g
TARGET MACH NO.: 0.85
INTERCEPTOR LATERAL G's: Avro 3.3
INTERCEPTOR MACH NO.: 1.5
σ OF G.C.I. ACCURACY: 5 Values
A.I. DETECTION RANGE AS FRACTION OF SPECIFICATION RANGE, S: Abscissa
A.I. DETECTION RANGE CONTOUR: Delta
ALTITUDE: 50,000 ft.

Fixed Lead L_a = 20°

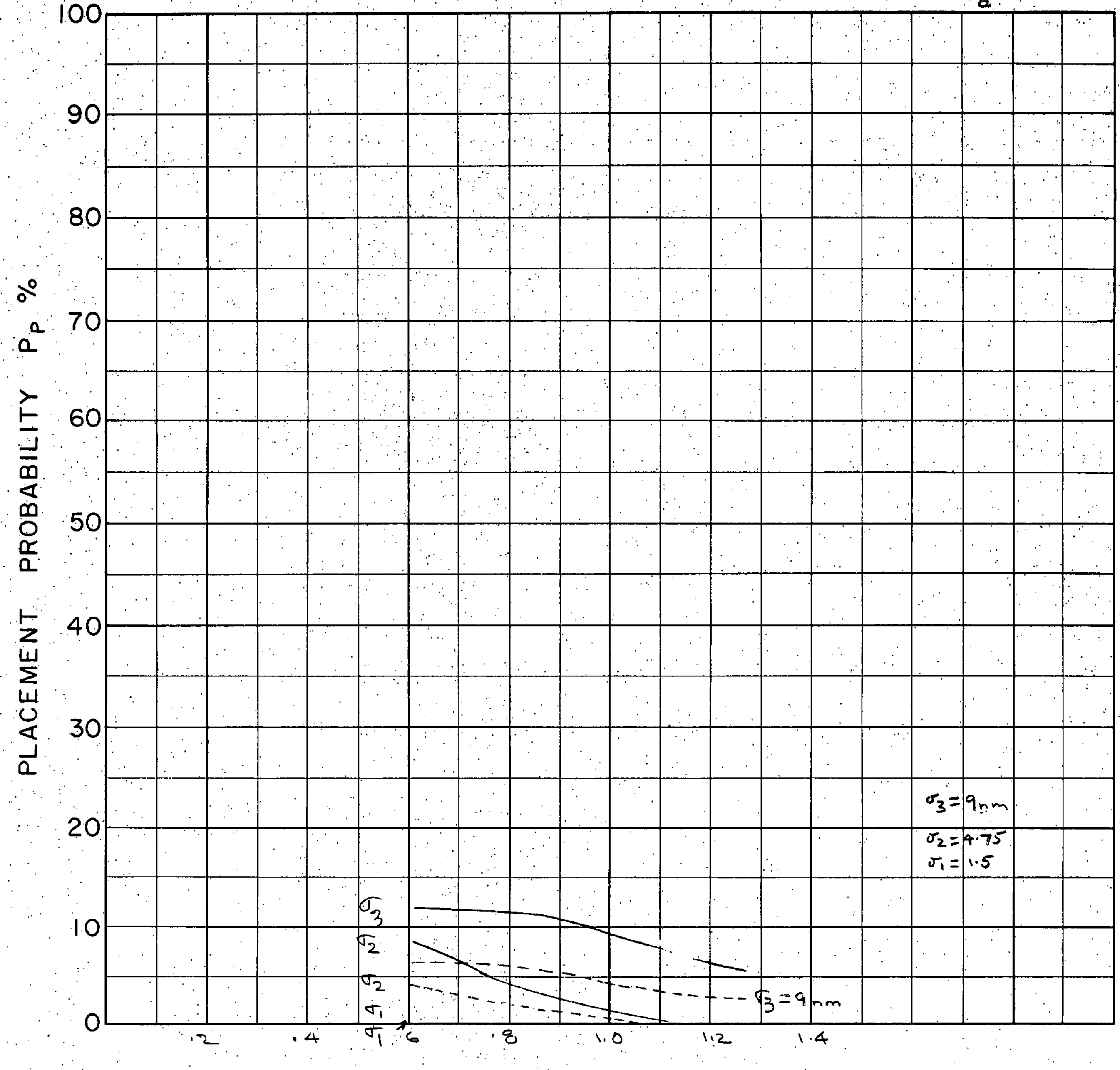

COURSE DIFFERENCE: 180
TARGET EVASION: None
TARGET MACH NO.: 1.5
INTERCEPTOR LATERAL G's: Avro 3.3
INTERCEPTOR MACH NO.: 1.5
σ OF G.C.I. ACCURACY: 3 Values
A.I. DETECTION RANGE AS FRACTION OF SPECIFICATION RANGE, S: Abscissa
A.I. DETECTION RANGE CONTOUR: Delta
ALTITUDE: 50,000 ft.

———— 20% STANDARD DEVIATION IN $\dot{R}/R$ = 12

– – – – 60% " " " " "

CASE 22

Fixed Lead L_a = 20°

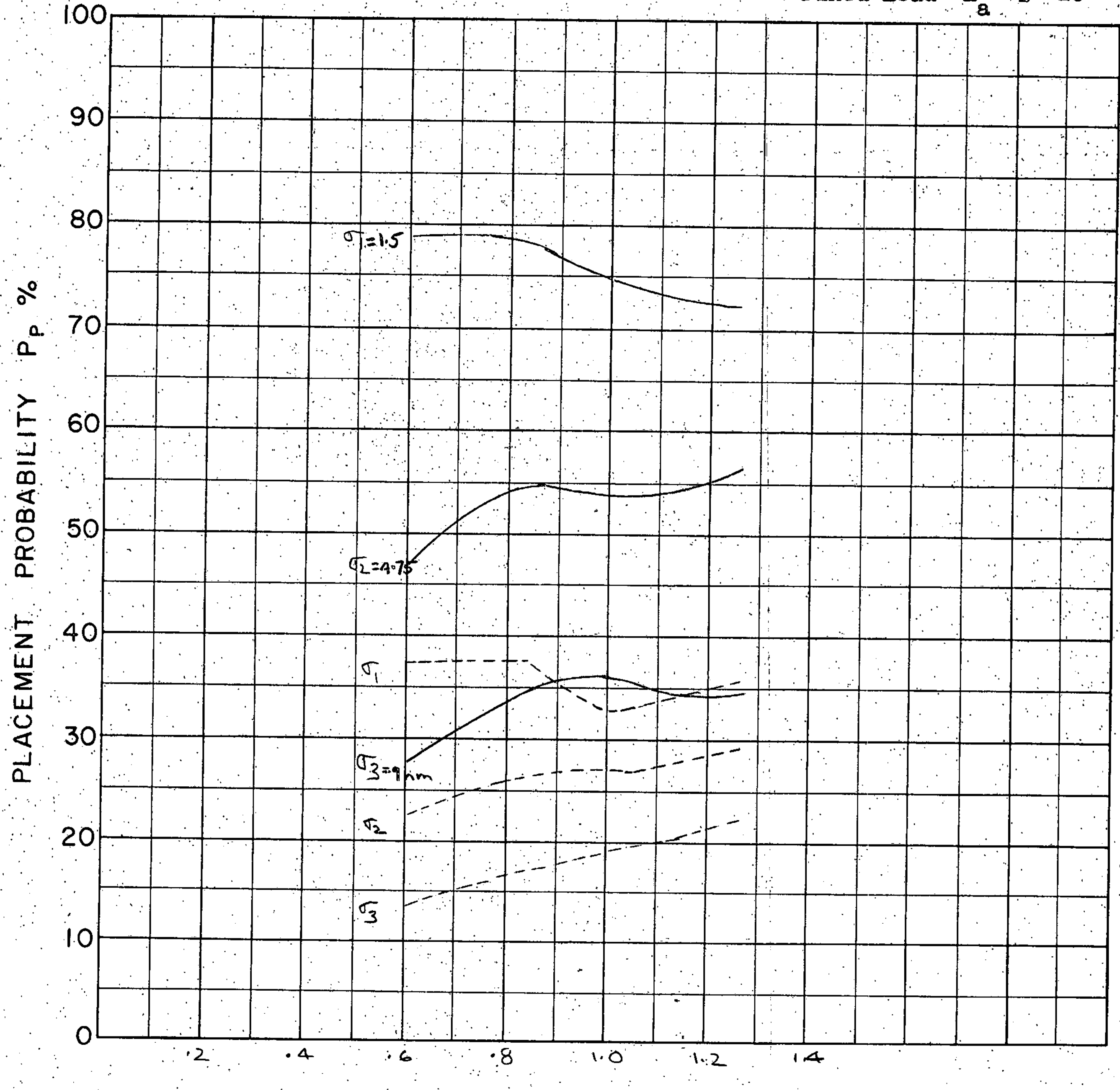

COURSE DIFFERENCE: 135
TARGET EVASION: None
TARGET MACH NO.: 1.5
INTERCEPTOR LATERAL G's: Avro 3.3
INTERCEPTOR MACH NO.: 1.5
σ OF G.C.I. ACCURACY: 3 Values
A.I. DETECTION RANGE AS FRACTION OF SPECIFICATION RANGE, S: Abscissa
A.I. DETECTION RANGE CONTOUR: Delta
ALTITUDE: 50,000 ft.

———— 20% STANDARD DEVIATION IN $\dot{R}/R$ = 12

- - - - - 60% " " " "

CASE 23

Fixed Lead L_a = 20°

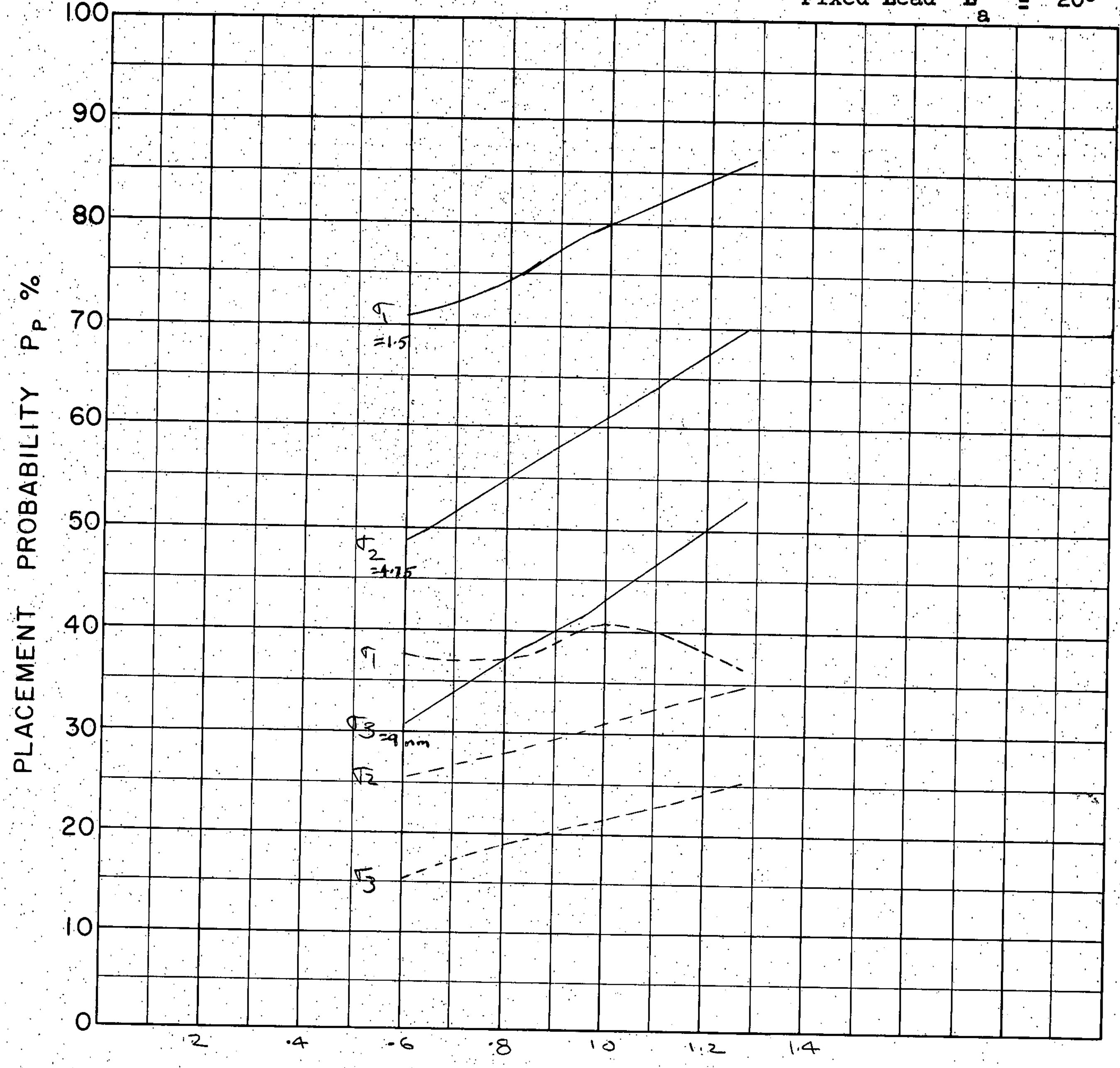

COURSE DIFFERENCE: 110
TARGET EVASION: None
TARGET MACH NO.: 1.5
INTERCEPTOR LATERAL G's: Avro 3.3
INTERCEPTOR MACH NO.: 1.5
σ OF G.C.I. ACCURACY: 3 Values
A.I. DETECTION RANGE AS FRACTION OF SPECIFICATION RANGE, S: Abscissa
A.I. DETECTION RANGE CONTOUR: Delta
ALTITUDE: 50,000 ft.

———— 20% STANDARD DEVIATION IN R/R = 12

– – – – – 60% " " " " "

CASE 24

Fixed Lead L_a = 20°

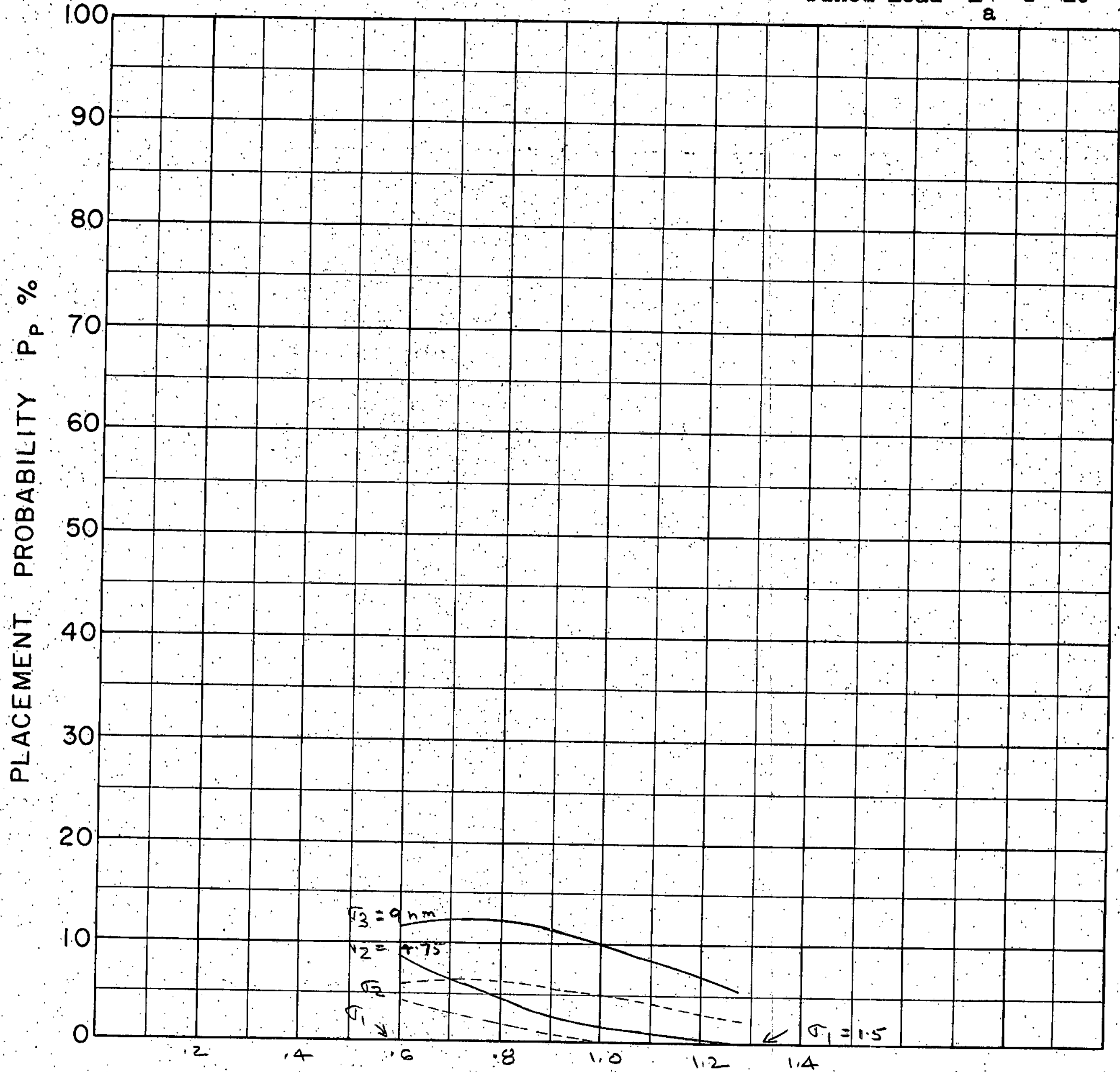

COURSE DIFFERENCE: 180
TARGET EVASION: None
TARGET MACH NO.: 1.5
INTERCEPTOR LATERAL G's: Avro 3.3
INTERCEPTOR MACH NO.: 1.5
σ OF G.C.I. ACCURACY: 3 Values
A.I. DETECTION RANGE AS FRACTION OF SPECIFICATION RANGE, S: Abscissa
A.I. DETECTION RANGE CONTOUR: Delta
ALTITUDE: 50,000 ft.

———— 20% STANDARD DEVIATION IN R = 28 kft
- - - - - 60% " " " " "

CASE 25

Fixed Lead L_a = 20°

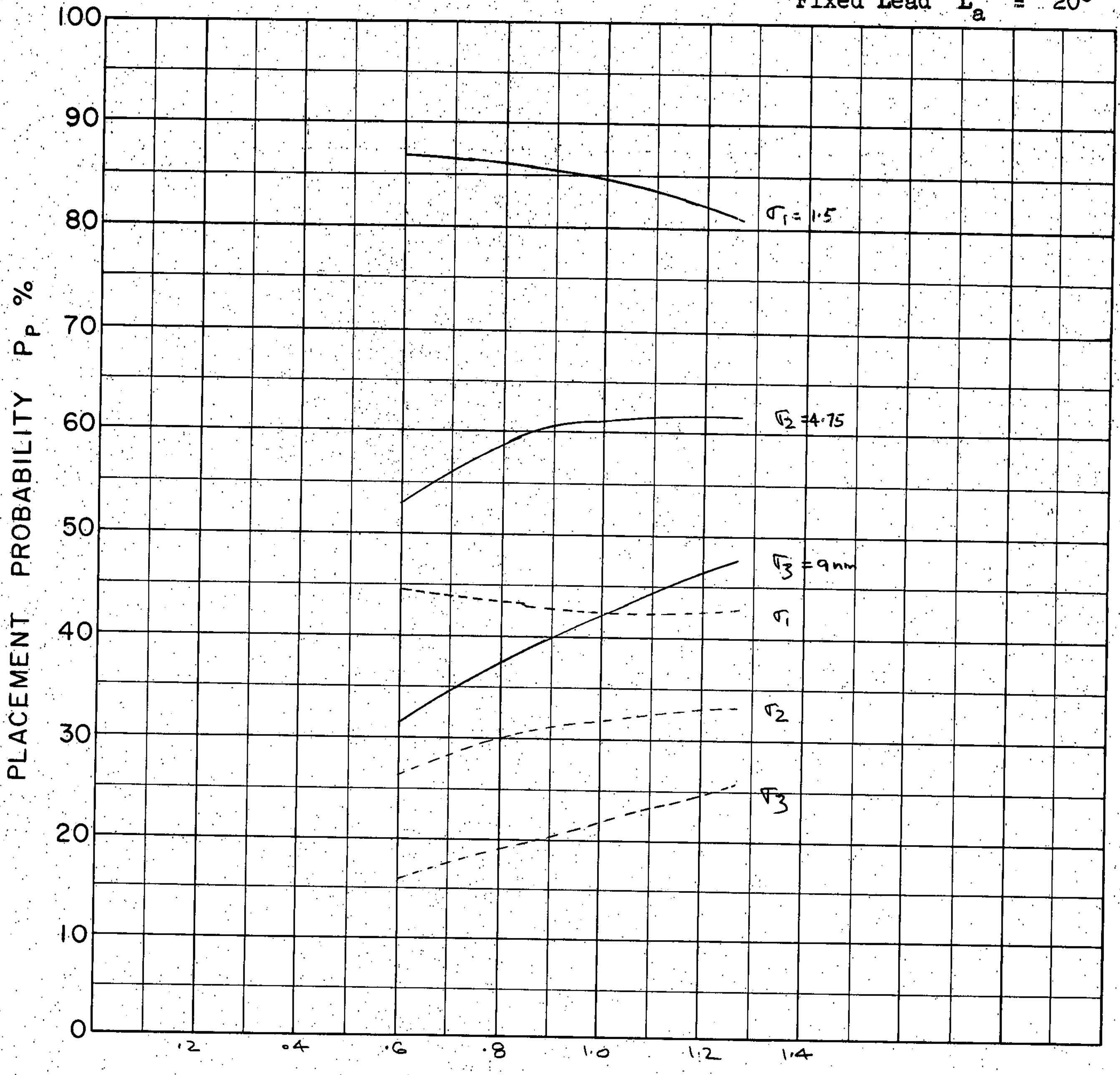

COURSE DIFFERENCE: 135
TARGET EVASION: None
TARGET MACH NO.: 1.5
INTERCEPTOR LATERAL G's: Avro 3.3
INTERCEPTOR MACH NO.: 1.5
σ OF G.C.I. ACCURACY: 3 Values
A.I. DETECTION RANGE AS FRACTION OF SPECIFICATION RANGE, S: Abscissa
A.I. DETECTION RANGE CONTOUR: Delta
ALTITUDE: 50,000 ft.

o———————o 20% STANDARD DEVIATION IN R = 28 Kft
o— — — — —o 60% " " " " "

CASE 26

Fixed Lead L_a = 20°

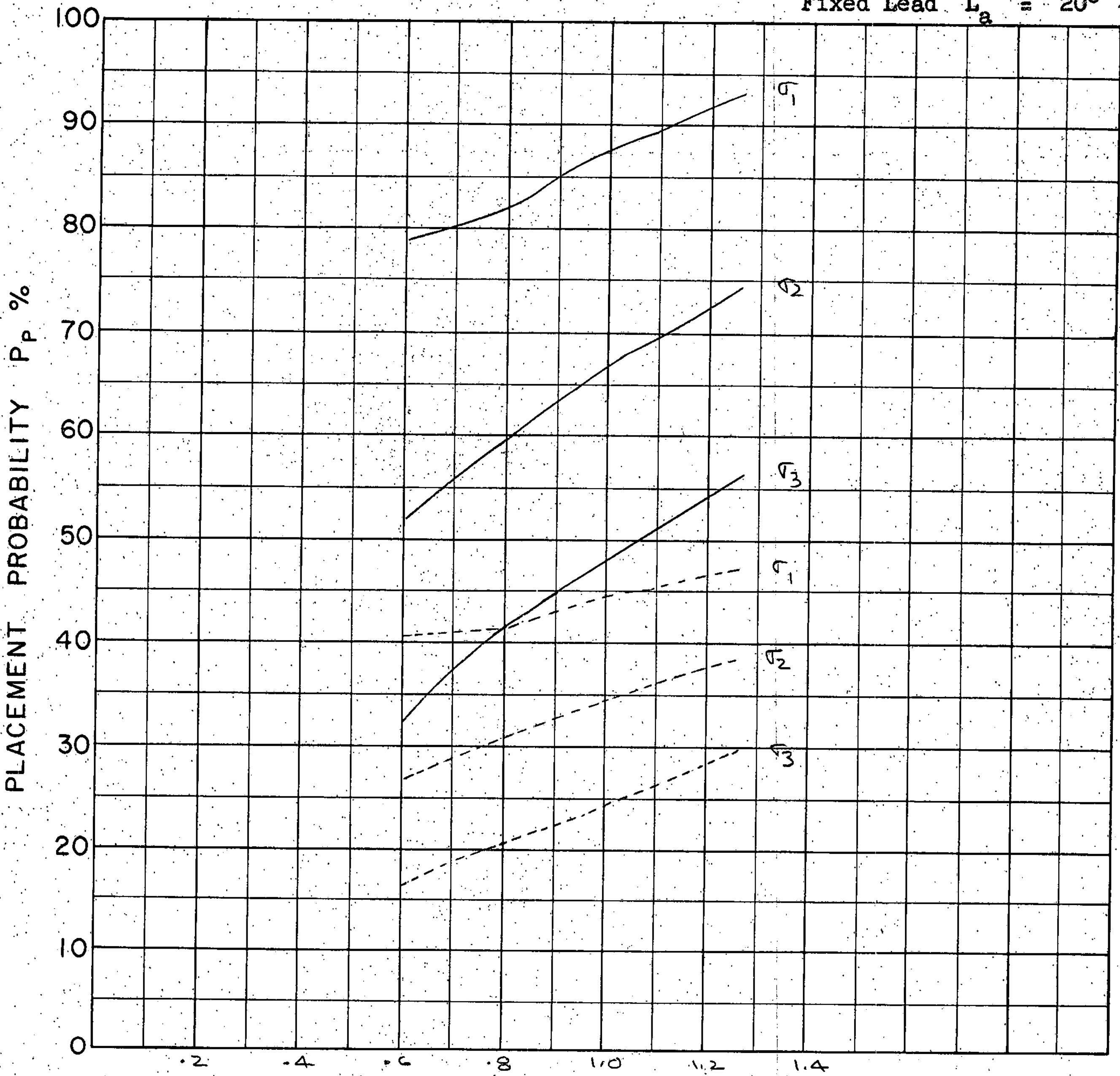

COURSE DIFFERENCE: 110
TARGET EVASION: None
TARGET MACH NO.: 1.5
INTERCEPTOR LATERAL G's: Avro 3.3
INTERCEPTOR MACH NO.: 1.5
σ OF G.C.I. ACCURACY: 3 Values
A.I. DETECTION RANGE AS FRACTION OF SPECIFICATION RANGE, S: Abscissa
A.I. DETECTION RANGE CONTOUR: Delta
ALTITUDE: 50,000 ft.

———— 20 % STANDARD DEVIATION IN R = 28 Kft.
- - - - - - 60 % " " " " "

Zero Lead Angle

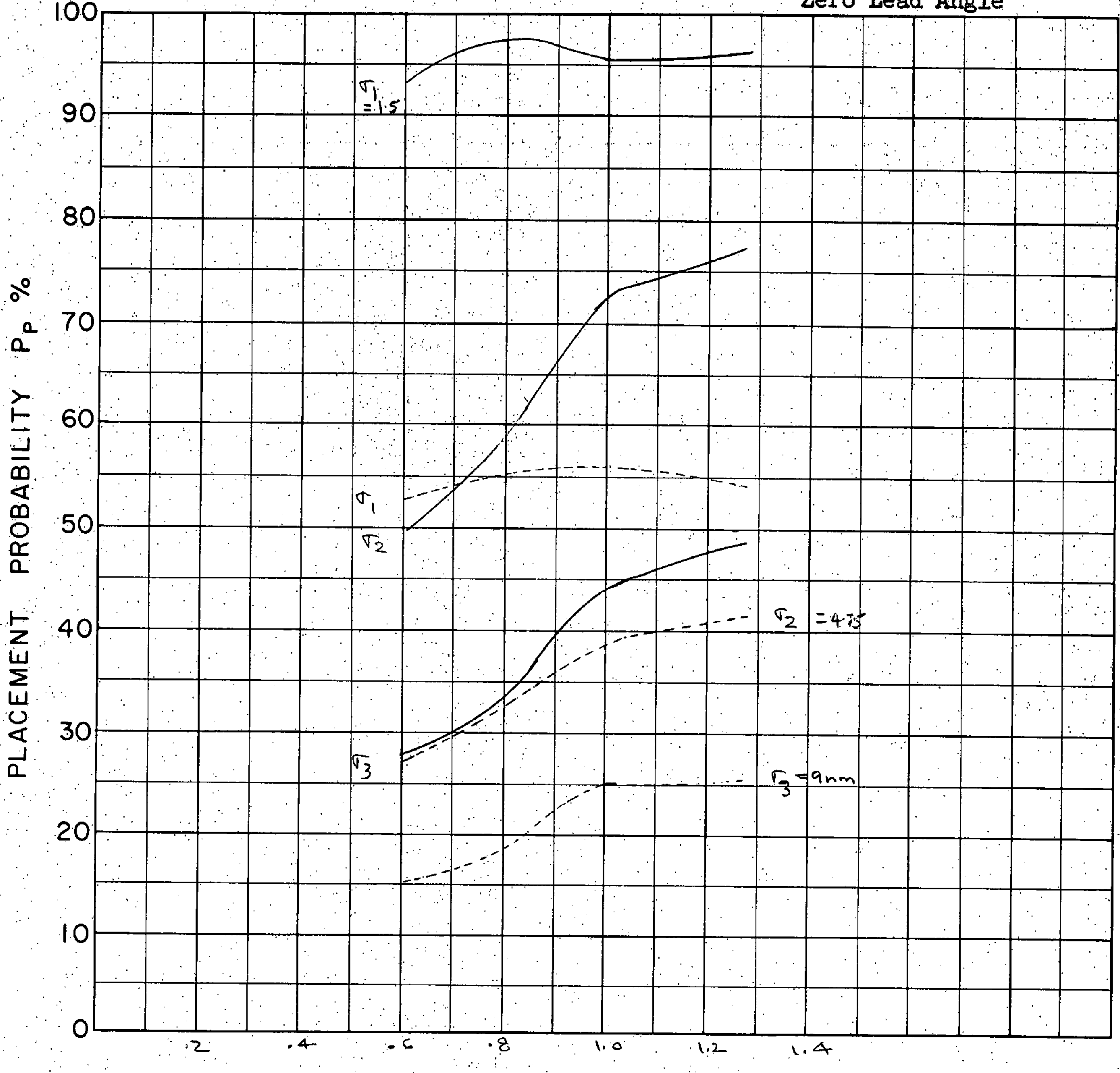

COURSE DIFFERENCE: 180
TARGET EVASION: None
TARGET MACH NO.: 1.5
INTERCEPTOR LATERAL G's: Avro 3.3
INTERCEPTOR MACH NO.: 1.5
σ OF G.C.I. ACCURACY: 3 Values
A.I. DETECTION RANGE AS FRACTION OF SPECIFICATION RANGE, S: Abscissa
A.I. DETECTION RANGE CONTOUR: Delta
ALTITUDE: 50,000 ft.

———— 20 % STANDARD DEVIATION IN $R/\dot{R}$ = 10 s

— — — — 60 % " " " " "

CASE 28

Zero Lead Angle

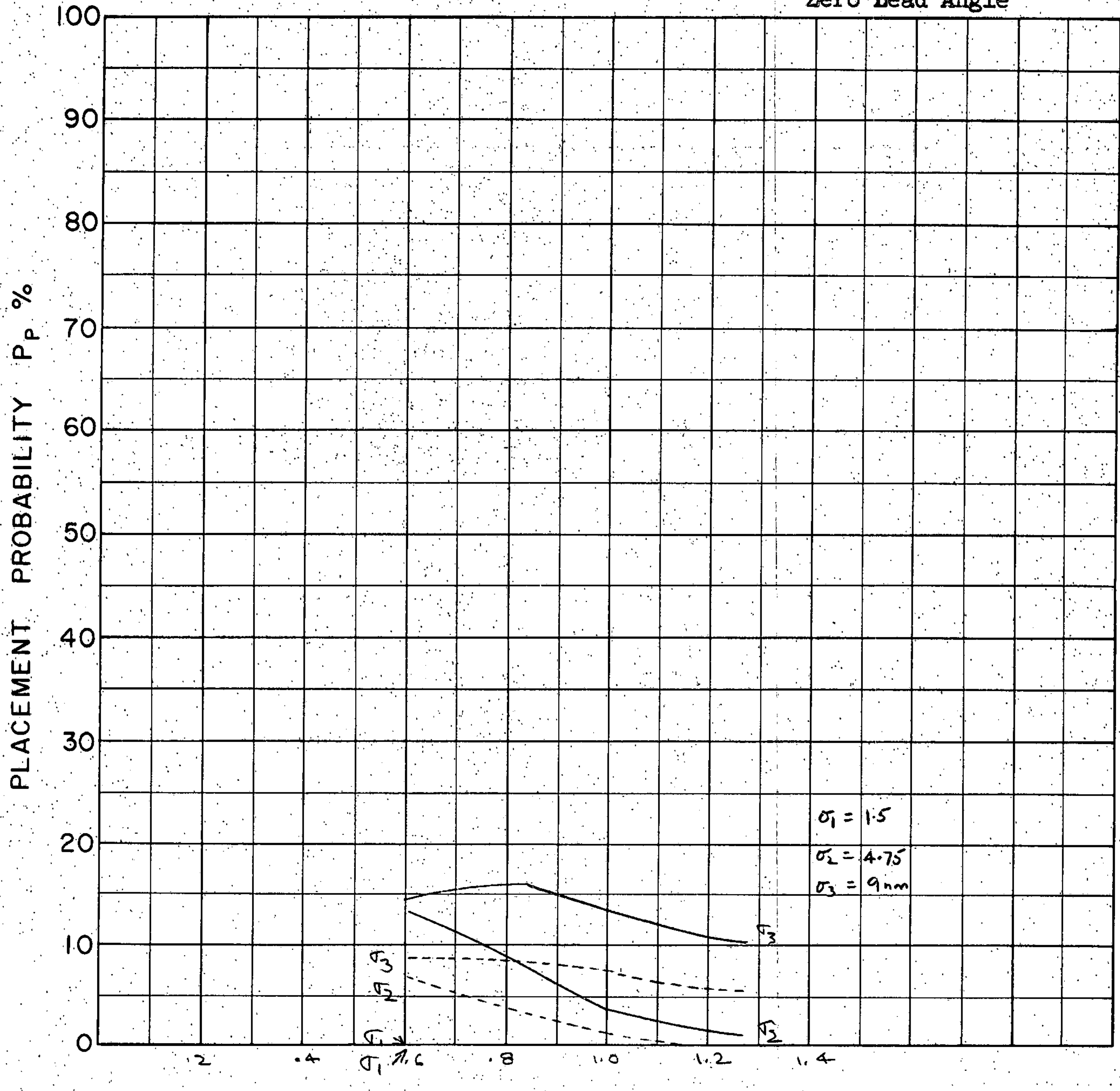

COURSE DIFFERENCE: 135
TARGET EVASION: None
TARGET MACH NO.: 1.5
INTERCEPTOR LATERAL G's: Avro 3.3
INTERCEPTOR MACH NO.: 1.5
σ OF G.C.I. ACCURACY: 3 Values
A.I. DETECTION RANGE AS FRACTION OF SPECIFICATION RANGE, S: Abscissa
A.I. DETECTION RANGE CONTOUR: Delta
ALTITUDE: 50,000 ft.

——————— 20 % STANDARD DEVIATION IN $\dot{R}/R$ = 10

— — — — — 60 % " " " " " .

Zero Lead Angle

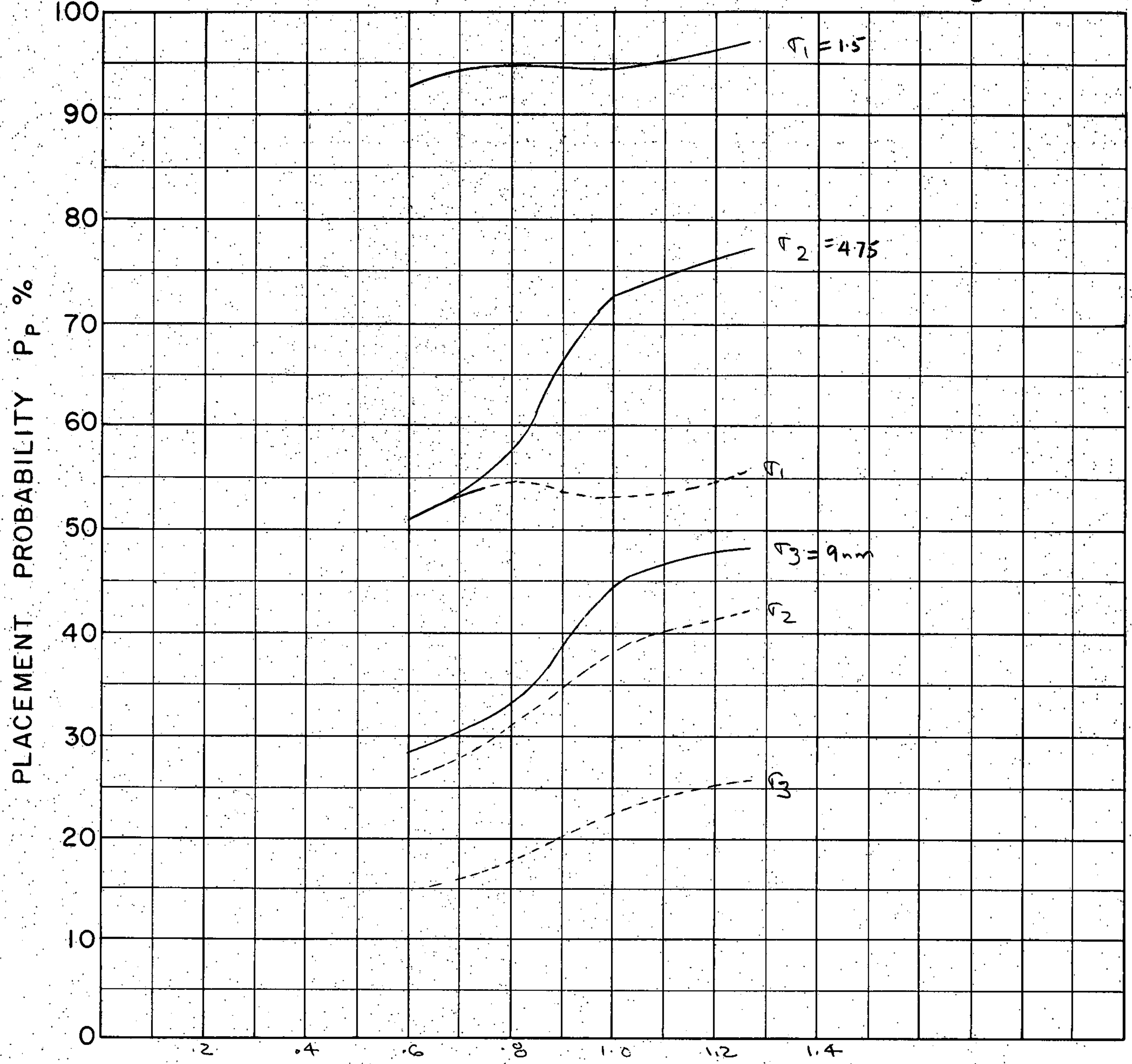

COURSE DIFFERENCE: 180
TARGET EVASION: None
TARGET MACH NO.: 1.5
INTERCEPTOR LATERAL G's: Avro 3.3
INTERCEPTOR MACH NO.: 1.5
σ OF G.C.I. ACCURACY: 3 Values
A.I. DETECTION RANGE AS FRACTION OF SPECIFICATION RANGE, S: Abscissa
A.I. DETECTION RANGE CONTOUR: Delta
ALTITUDE: 50,000 ft.

———— 20 % STANDARD DEVIATION IN R = 30 Kft

– – – – 60 % " " " " "

CASE 30

Fixed Lime Sight Rate

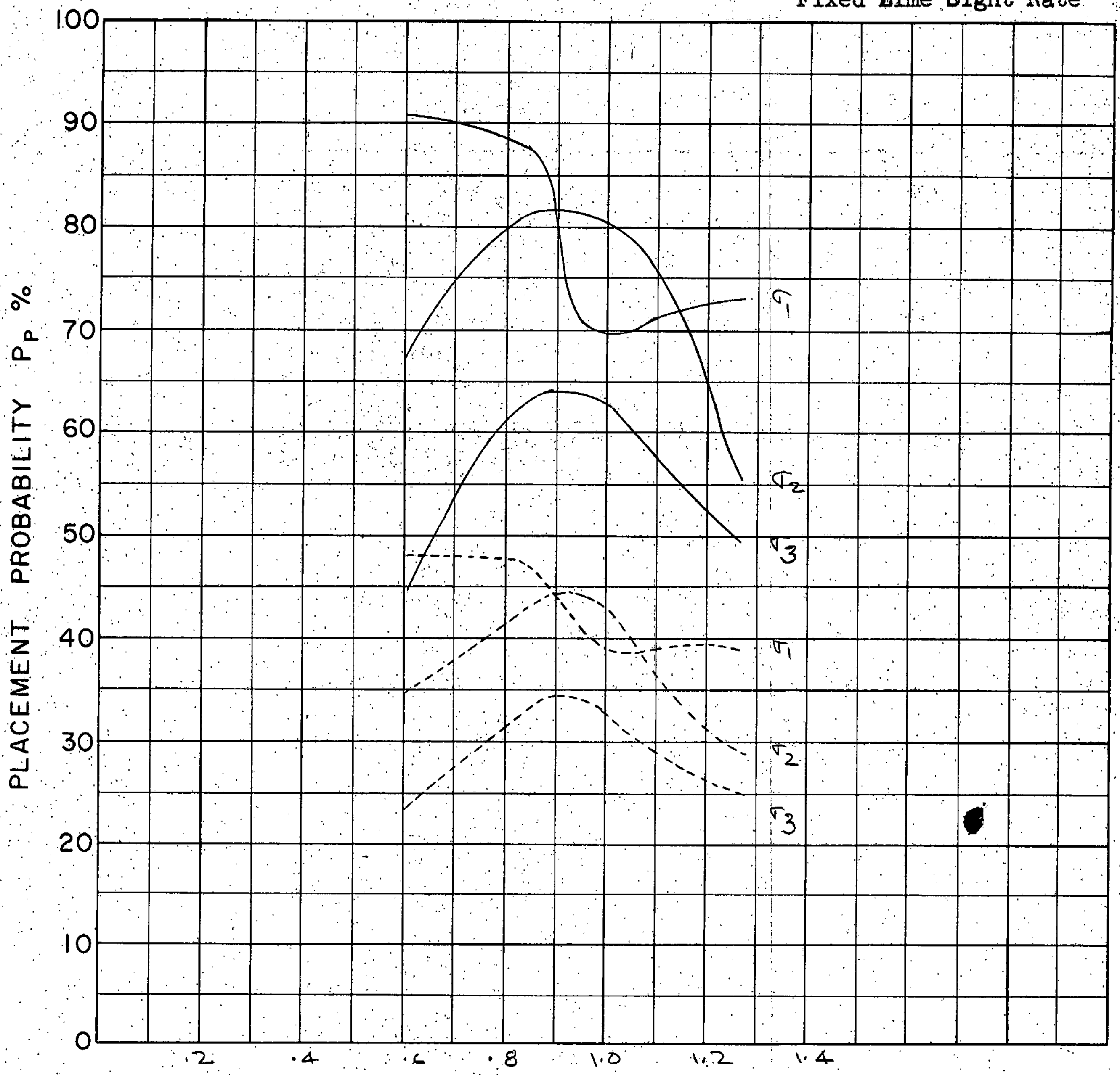

COURSE DIFFERENCE: 180
TARGET EVASION: None
TARGET MACH NO.: 1.5
INTERCEPTOR LATERAL G's: Avro 3.3
INTERCEPTOR MACH NO.: 1.5
σ OF G.C.I. ACCURACY: 3 Values
A.I. DETECTION RANGE AS FRACTION OF SPECIFICATION RANGE, S: Abscissa
A.I. DETECTION RANGE CONTOUR: Delta
ALTITUDE: 50,000 ft.

CASE 31

Fixed Lime of Sight Rate

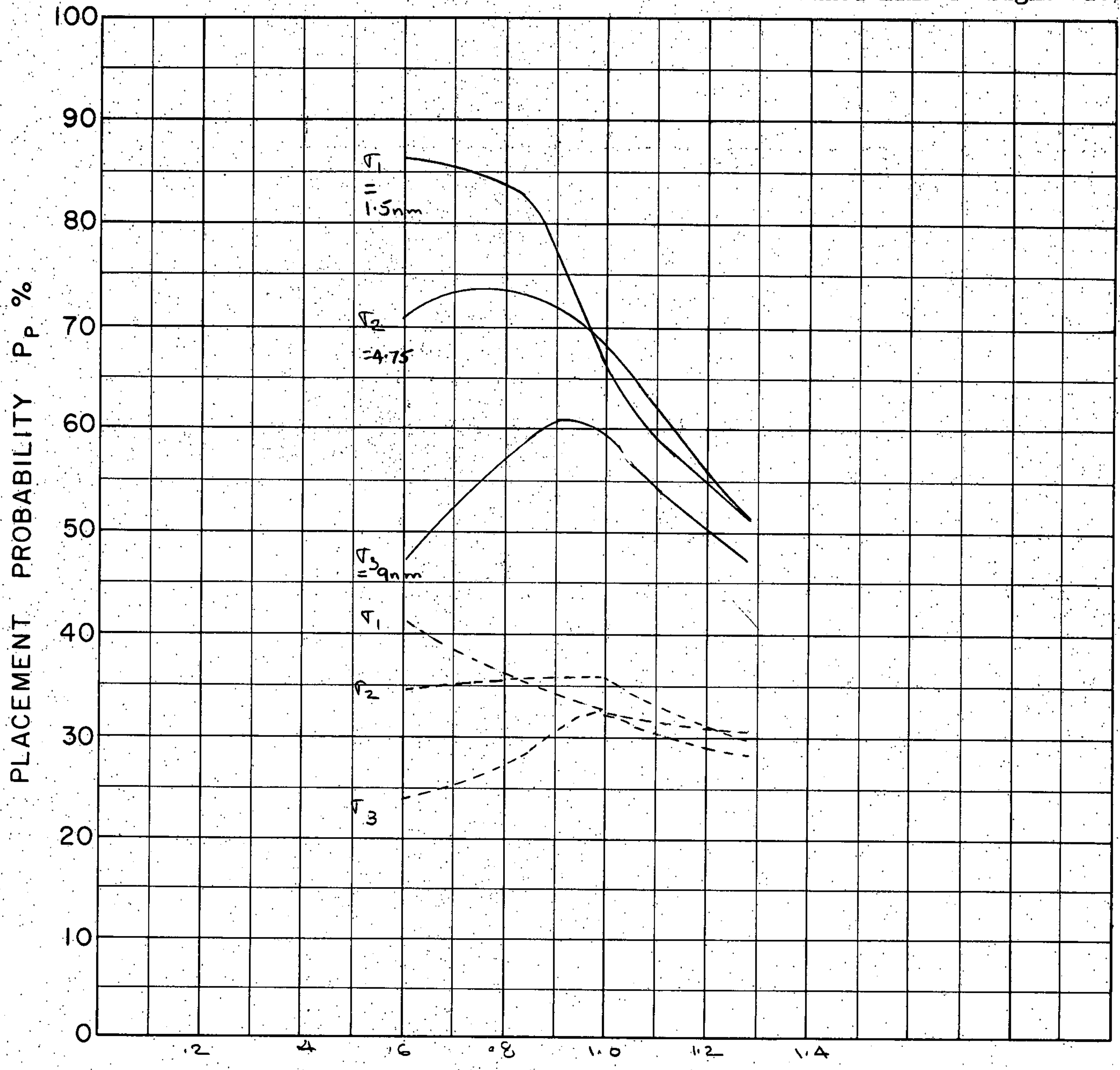

COURSE DIFFERENCE: 135
TARGET EVASION: None
TARGET MACH NO.: 1.5
INTERCEPTOR LATERAL G's: Avro 3.3
INTERCEPTOR MACH NO.: 1.5
σ OF G.C.I. ACCURACY: 3 Values
A.I. DETECTION RANGE AS FRACTION OF SPECIFICATION RANGE, S: Abscissa
A.I. DETECTION RANGE CONTOUR: Delta
ALTITUDE: 50,000 ft.

———— 20% STANDARD DEVIATION IN R/R = 12
– – – – – 60% " " " " "

CASE 32

Fixed Lime of Sight Rate

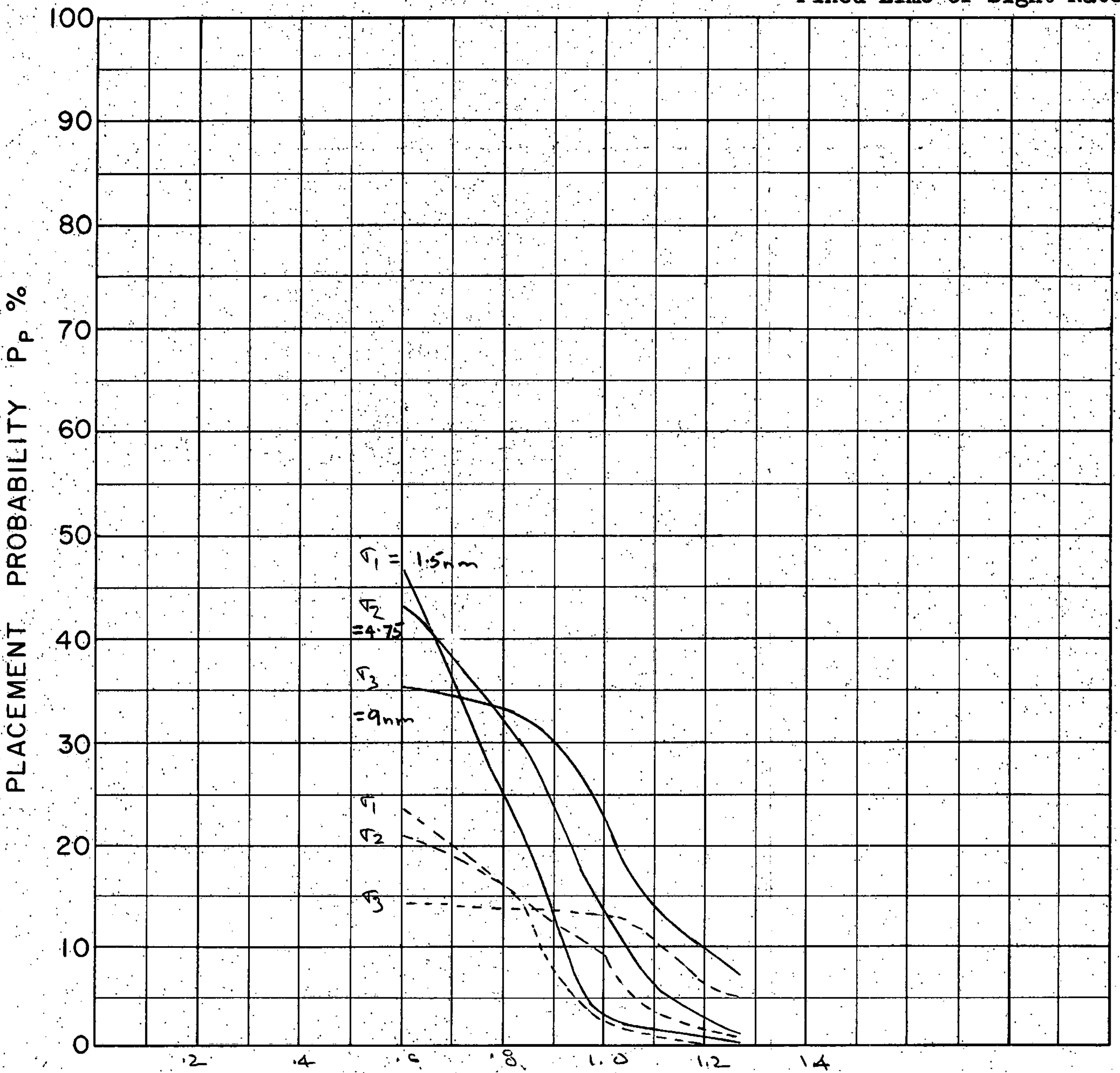

COURSE DIFFERENCE: 110
TARGET EVASION: None
TARGET MACH NO.: 1.5
INTERCEPTOR LATERAL G's: Avro 3.3
INTERCEPTOR MACH NO.: 1.5
σ OF G.C.I. ACCURACY: 3 Values
A.I. DETECTION RANGE AS FRACTION OF SPECIFICATION RANGE, S: Abscissa
A.I. DETECTION RANGE CONTOUR: Delta
ALTITUDE: 50,000 ft.

——— 20% STANDARD DEVIATION IN R/R = 12 s

- - - - 60 % " " " " "

True Collision

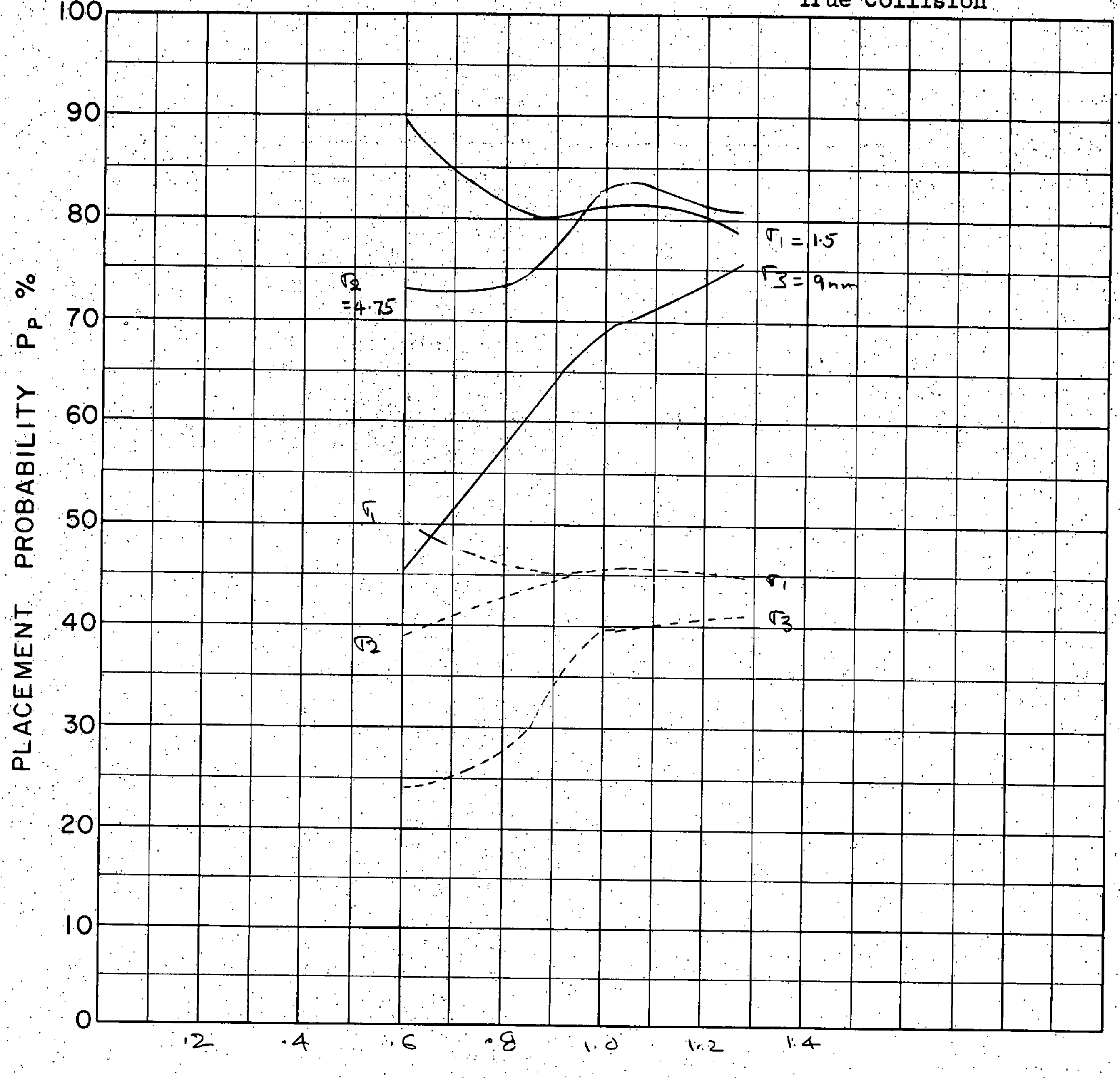

COURSE DIFFERENCE: 180
TARGET EVASION: None
TARGET MACH NO.: 1.5
INTERCEPTOR LATERAL G's: Avro 3.3
INTERCEPTOR MACH NO.: 1.5
σ OF G.C.I. ACCURACY: 3 Values
A.I. DETECTION RANGE AS FRACTION OF SPECIFICATION RANGE, S: Abscissa
A.I. DETECTION RANGE CONTOUR: Delta
ALTITUDE: 50,000 ft.

———— 20 % STANDARD DEVIATION IN R/R = ·11 S

– – – – 60 % " " " " ".

CASE 34

True Collision

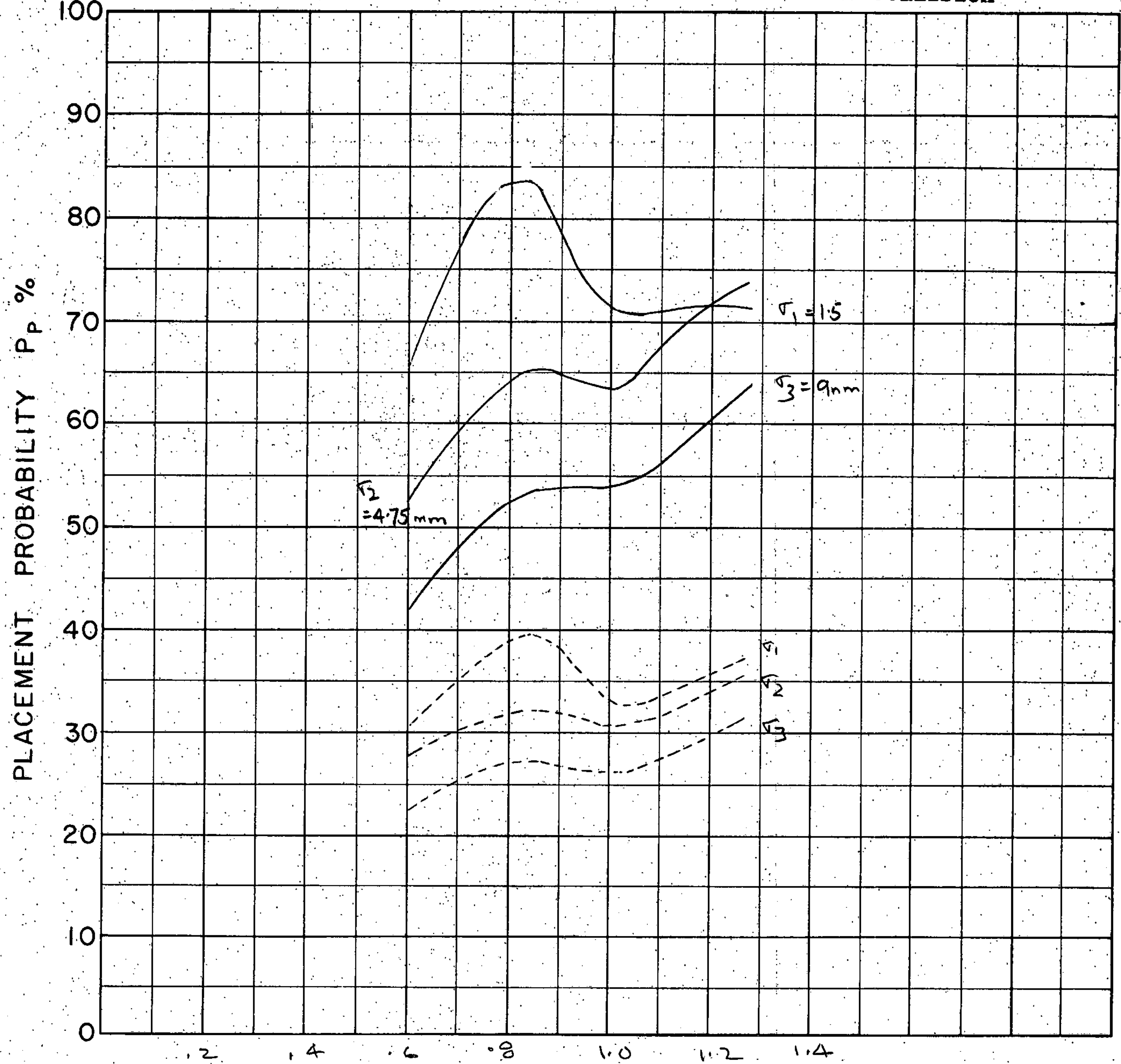

COURSE DIFFERENCE: 135
TARGET EVASION: None
TARGET MACH NO.: 1.5
INTERCEPTOR LATERAL G's: Avro 3.3
INTERCEPTOR MACH NO.: 1.5
σ OF G.C.I. ACCURACY: 3 Values
A.I. DETECTION RANGE AS FRACTION OF SPECIFICATION RANGE, S: Abscissa
A.I. DETECTION RANGE CONTOUR: Delta
ALTITUDE: 50,000 ft.

———— 20% STANDARD DEVIATION IN R/R = 11 s

- - - - - 60% " " " " "

True Collision

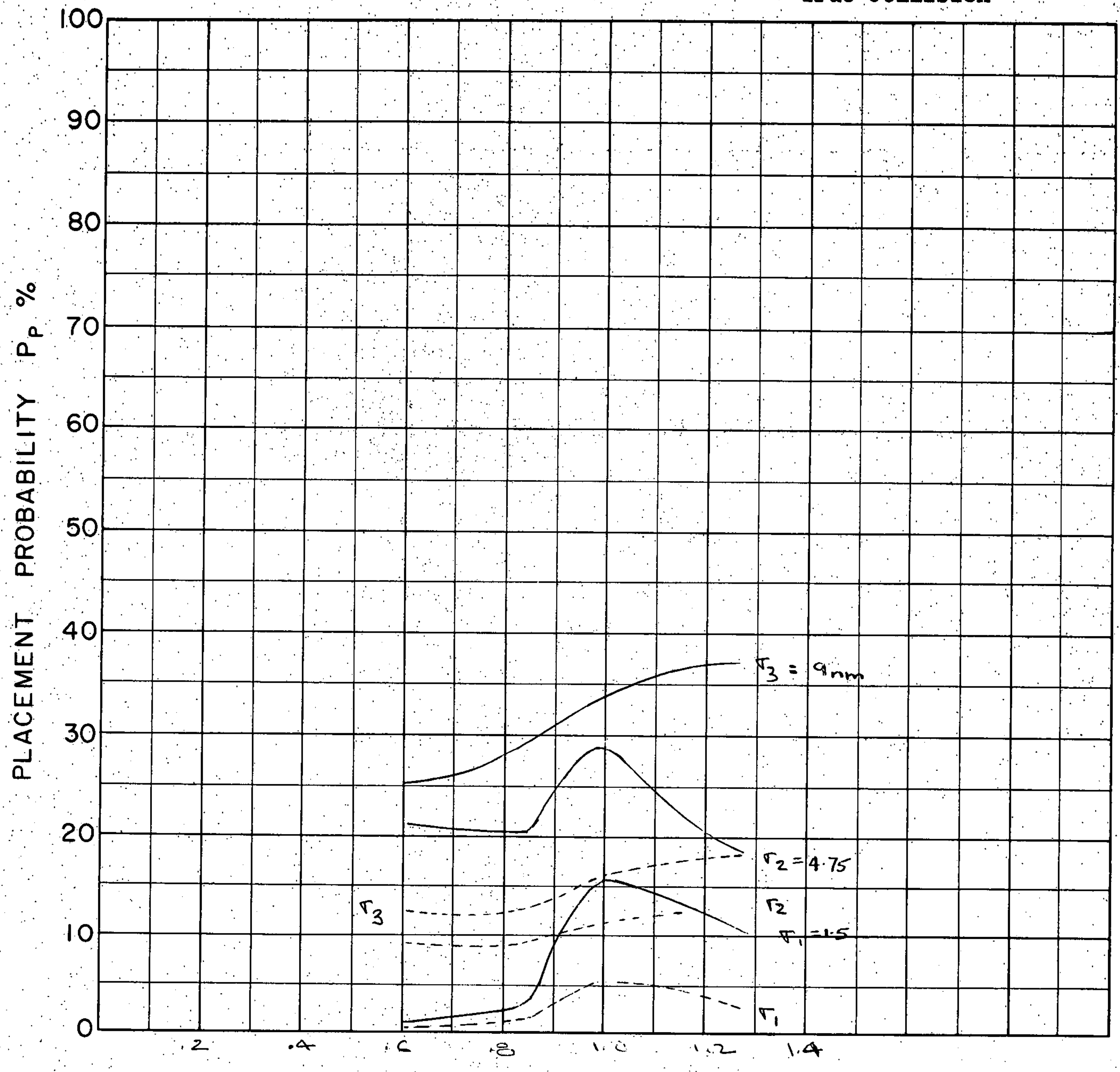

COURSE DIFFERENCE: 110
TARGET EVASION: None
TARGET MACH NO.: 1.5
INTERCEPTOR LATERAL G's: Avro 3.3
INTERCEPTOR MACH NO.: 1.5
σ OF G.C.I. ACCURACY: 3 Values
A.I. DETECTION RANGE AS FRACTION OF SPECIFICATION RANGE, S: Abscissa
A.I. DETECTION RANGE CONTOUR: Delta
ALTITUDE: 50,000 ft.

——— 20% STANDARD DEVIATION IN R/Ṙ = 11

- - - - - 60% " " " " " .

APPENDIX 'C'

LAUNCH ZONES FOR A SPARROW II TYPE MISSILE

by A.B. Bell, G.P. Coverley and D.R. Tait.

1. INTRODUCTION

This Appendix will attempt to bring reporting on all phases of the missile launch zones up to date. Since the last report on launch zones (ref. 1) launch zone data has been used in the REAC simulation of three dimensional interceptions and in the Minimum Information Study. A study has been made of the launch zone mechanization method proposed by RCA and this has been fully reported in the Fifth Progress Report (ref. 9). No comprehensive set of launch zones was available for any of this work: the information which was available is discussed below in Section 2.

For the three dimensional simulation work the lack of detailed launch zone data was of little consequence. A simplified launch zone representation was used, it having been shown that variations in launch zone data do not have large effects on placement probability so long as the fire-control and missile launch zones are compatible. This is discussed at greater length in Section 3.

In the minimum information study the actual missile launch zone was needed to obtain the probability of firing anywhere in the launch zone. A method for obtaining a launch zone for a particular case from the limited data is described in Section 4.

2. AVAILABLE LAUNCH ZONE DATA

The two available sets of launch zones obtained by Douglas (refs. 10 and 11) were spot-checked and seem to be mutually consistent. It is presumed that these are correct and may be used as a basis for extrapolation to give other launch zones and as a check on other launch zone data. A method for extrapolation is given in section 4: this method was used to spot check the following case from some Canadair launch zone results (ref. 13):

Altitude: 50,000 ft.
Launch Speed: Mach no. 1.5
Target Speed: Mach no. 1.2
Target Manoeuvre: 1.2 g's
Attack Aspect: 90°.

Good agreement was obtained.

On checking launch zones derived earlier at CARDE (refs. 2 and 3) generally poor agreement was found. Reliance should not be placed on these results in the light of the Douglas data.

Most recent information from Douglas (ref. 8) requires that the minimum launch ranges be increased by up to 2000 ft. and heading allowances at other ranges be decreased by up to 2^{o} because of the effects of noise in the missile System. Adjustment of the maximum range may also be necessary because of changes in the time estimated for oil consumption. At 50,000 ft. this might be 22 seconds instead of 26 seconds.

3. SIMPLIFIED LAUNCH ZONE FOR SPARROW II USED IN THE REAC SIMULATION OF 3 D CF 105 INTERCEPTIONS

The simulation covers the AI controlled phase from lock-on to the time when the missile is launched. Permissible launch conditions are required to distinguish between successful and unsuccessful interceptions.

The launch zone, as described by Douglas and other sources, is a wide region limited by maximum missile flight time, maximum seeker range, minimum range and minimum flight time. The mechanisation of the launch zone in the fighter is highly critical and must be carefully matched to the performance of the missiles and the accuracy of range measuring equipment and the time-to-go computer.

In the assessment of placement probabilities, however, as long as the missile and the heading error computer are consistent the configuration of the launch zone is relatively unimportant. Permissible heading error is a function of range and aspect, but since the navigation computer is usually demanding maximum rate turns to produce zero heading error a change of a few degrees has a small effect on the location of manoeuvre barriers and no effect on the location of other barriers.

The missile time of flight which is selected has an effect on the rate at which the fighter must turn at close ranges because it is more economical to let the missile manoeuvre than for the fighter to manoeuvre. This has only a slight effect on look angle and fall-back barriers. If the simplified contour corresponds to the mean real launch zone the placement results will be quite accurate.

If coaltitude attacks are considered, a constant flight time is taken as the condition for launch and the missile incremental velocity ΔV is known, then

$$F = \Delta V . t_f$$

where t_f is the time of flight and F the relative flight distance. When the launching aircraft is on course the locus t_f = constant is a circle about the collision point between missile and target. This circle is used as an approximation to the launch zone and corresponding values of F and t_f are instrumented in the fire control computer. In the REAC work a flight time of 8 secs. was chosen to match the real launch zone.

The launch and hence the interception is classified as success or failure according as the heading error at launch is or is not within a prescribed limit.

Allowable heading error is assumed to be proportional to air pressure plus a constant to allow for increased manoeuvrerability at lower altitudes.

Allowable error $\delta^*_c = 15^\circ$ at 50,000 ft.

$\delta^*_c = 8^\circ$ at 60,000 ft.

Errors in the vertical plane present a greater problem. It was assumed that the allowable heading error in space was independent of attitude, so that vertical heading errors have the same effect as horizontal errors.

Time-to-go was calculated on the basis of the horizontal velocity only and some trigonometrical approximations were made in solving for the heading errors. However as the same equipment was used in the navigation computer and in the heading error computer no inconsistency is introduced.

The effects of these approximations are discussed in more detail in a technical letter on the REAC simulation (ref. 5). It was shown that the effects on placement probability are small.

It appears that the greatest advantages of a guided missile over an unguided one are not in the improved placement probabilities which it produces but rather in making the weapon system simpler and more reliable. If the missile were not guided the tolerances in the navigation of the aircraft, the performance of the missile and the instrumentation of the fire control would be much smaller. The navigation computer would have to consider target acceleration, not merely velocity and position, and could not handle changes in acceleration near or subsequent to launch. The exact missile trajectory relative to the fighter would have to be taken into account while in the guided case, this is not so.

4.0 EXTENSION OF LAUNCH ZONE DATA

Much data has been published on launch zones for the Sparrow II missile but occasionally there is a need for launch zone data with different conditions than those available. In most of these cases it is possible to interpolate or extrapolate existing data to provide the information required. This note explains a method of extending launch zone data.

4.1 Theory and Assumptions

A parameter common to all launch zones, constant for a given altitude and missile time of flight, will be derived. This parameter is then used to extend launch zone data.

Consider the position vector diagram of Fig. C1

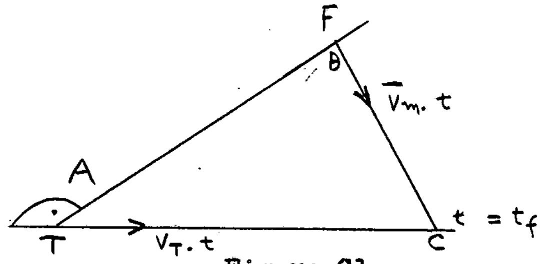

Figure C1

A = aspect angle

θ = missile ideal lead angle

$\overline{V_m}$ = average missile speed

F & T show the positions of the interceptor and target, respectively, at the instant of missile launch. The missile is assumed to travel in a straight line, when launched with ideal lead angle θ, to reach the collision point C in a flight time of t_f seconds.

Now, given a missile lateral acceleration capability (Γ_m), let us calculate the allowable change in heading so that the missile will reach the collision point at C. The limits of lead angle will be shown as $(\theta + \frac{\Delta H}{2})$, $(\theta - \Delta H/2)$, so that $\frac{\Delta H}{2}$ is the allowable heading error.

We shall derive this angle (see Figure C2).

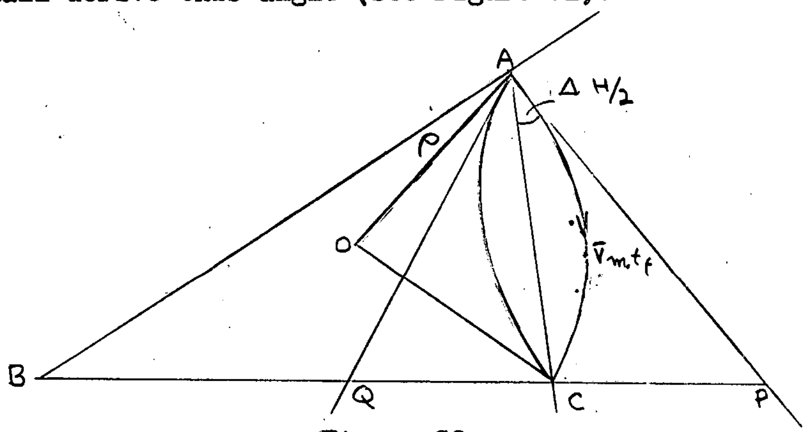

Figure C2

$$AC = V_m t_f$$

$$\hat{PAC} = \hat{CAQ} = \Delta H/2$$

$$\hat{BAC} = \theta$$

Let the lead angle be $\theta + \Delta H/2$. The missile is then assumed to fly a circular path, arc AC in the direction of the arrow. The radius of curvature is ρ with centre O since AP is a tangent to the arc.

Then to a first approx., if ΔH is small, AC $\doteq$ arc AC

Then $AC = \rho \Delta H$. (1)

Now $\Gamma_m = \dfrac{\overline{V}_m^2}{\rho}$

and $AC = V_m t_f$.

(1) becomes

$$V_m t_f = \frac{\overline{V}_m^2}{\Gamma_m} \Delta H$$

or $t_f \Gamma_m = V_m \Delta H$

For a given time of flight, t_f, and lateral acceleration Γ_m, the LHS is a constant and is designated D.

$$\overline{V_m} \Delta H = \text{const} = D. \quad (1a)$$

Γ_m is sensitive to height and hence D is a constant for given time of flight and height. D is the parameter used to link launch zones together.

4.2 <u>Calculation of V_m, t_f and D</u>

The available launch zone data is presented in the form shown in Fig. C3.

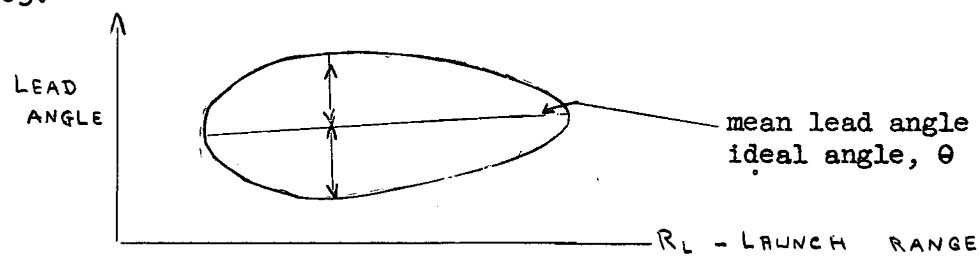

Given Aspect angle, A
Fighter speed, V_f
Target speed, V_t
Altitude

<u>Figure C3</u>

The average missile speed, corresponding to a launch range R_L can be found from the following equation.

$$\overline{V_m} = \frac{V_T \sin A}{\sin \theta} \qquad \theta = \text{ideal lead angle} \qquad (2)$$

Hence $\overline{V_m}$ at a given R_L is known.

$\frac{d R_L}{dt}$ is calculated from the equation

$$\frac{-d R_L}{dt} = \overline{V_m} \cos \theta - V_T \cos A \qquad (3)$$

.. assuming constant bearing flight for the ideally directed missile,

$$t_f = \frac{R_L}{\frac{-d R_L}{dt.}} \qquad (4)$$

A table is built up in the following way from left to right, from the known launch zone. Equations 1a to 4 are used.

sin A	R_L	θ^o	sin θ	cos θ	ΔH^o	$\overline{V_m}$	V_m cos θ	V_T cos A	$-\dot{R}_L$	D	t_f
.707	15 Kft	20	.342	.940	0	2.48	2.33	-.848	3.18	0	4.87
.707	20	17.5	.300	.954	20	2.83	2.70	-.848	3.55	50.66	5.8
.707	25	17.5	.300	.954	25	2.83	2.70	-.848	3.55	70.7	7.25

Typical case: $A = 135^o$, $V_L = 1.8M$

$V_T = 1.2M$, $H = 50$ K ft.

4.3 Determination of $\overline{V_m}$, and D for the Required Case

We can make plots of $\overline{V_m}$ against t_f for the known cases and by assuming linear interpolation (extrapolation), obtain $\overline{V_m}$ vs t_f for the required case (Fig. C4). To make the determination of D for the unknown case more certain (compensating for assumptions made in the theory of Section 4.1) it is advisable to plot D vs t_f for the known cases and by linear interpolation obtain a D curve for the required case (Fig. C5).

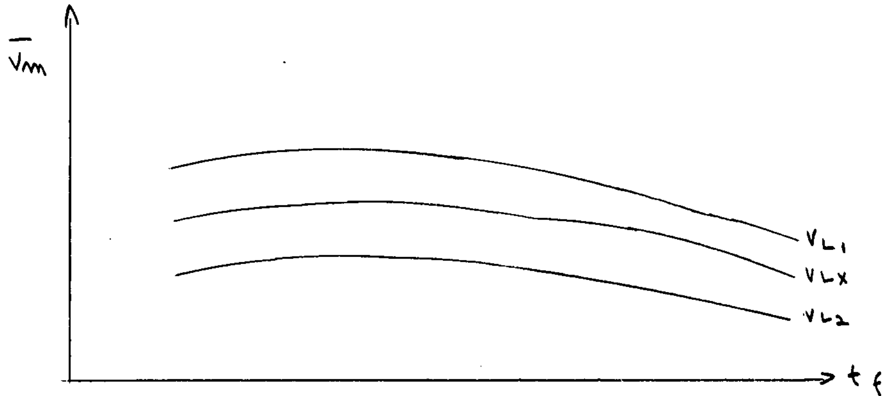

$\overline{V}_m$ vs t_f with V launch as parameter.

V_{Lx} = req'd case

Figure C4

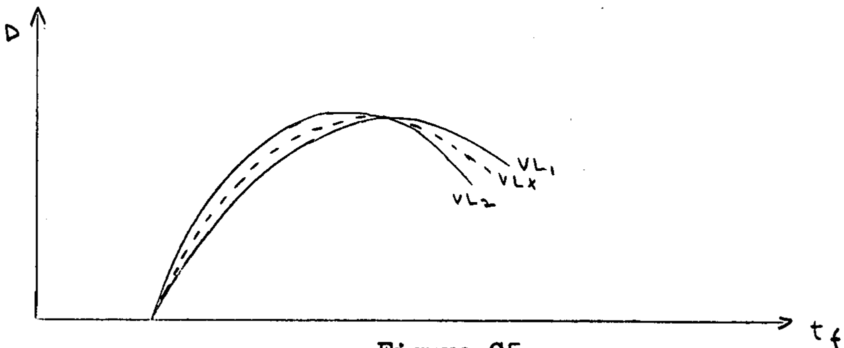

Figure C5

4.4 Derivation of New Launch Zone

Using curves of Figs. C4 and C5 we can build up a table from left to right, thus:-

given	t_f	$\overline{V}_m$	D	A	sin θ	θ	$-R_L$	R_L	ΔH
V_{Lx}		from curves		given	use		use	use	use
V_T		(figs. C4 & C5)			eq. 2		eq. 3	eq. 4	eq. 1a

Hence using R_L, θ, ΔH a new zone can be drawn.

4.5 Special Case Where A = 0° or 180°

Unfortunately in these cases of tail and head-on approaches the ideal lead angle is zero and the equation (2) for $\overline{V}_m$ becomes indeterminate. A new method, which is somewhat laborious, is now described step by step.

(1) Obtaining Parameter D from Known Data

It is necessary to construct curves of average missile velocity $\overline{V}_m$ against time of flight t_f. This may be obtained by a REAC solution and manipulation of an equation

$$\dot{V}_m = \frac{\text{Thrust - drag}}{\text{mass}} \qquad \text{(ref. 2, page 31)}$$

A series of curves with different initial launch speeds is necessary. Taking the known data it is required to find the t_f, $\overline{V}_m$ (and hence D) corresponding to a given launch range R_L.

The equation:-

$$\overline{V}_m t_f \pm V_T t_f = R_L \qquad (5) \qquad \begin{matrix} + \text{ sign, } A = 180^\circ \\ - \text{ sign, } A = 0^\circ \end{matrix}$$

has to be solved graphically to yield $\overline{V}_m$ and t_f. Hence D may be found from eq. 1(a) and a curve of D vs t_f constructed.

(2) Constructing New Launch Zone

Time of flight is selected from the D vs t_f curve. From t_f and reference to V_m vs t_f curves yields Δ H and R_L by using equs 1(a), 3 and 4.

4.6 CONCLUSION

Experience has shown that the parameter D is practically a constant under the stated conditions. The method has been used to evaluate data for a M1.5 fighter and target at 50 K ft. from other data at this altitude.

5.0 REFERENCES

1. CARDE Tech. Memo 159/57, "Launch Zones in the CF 105 Assessment Study" (SECRET)

2. CARDE Tech. Letter N-47-2, "Launch Zones for a Hypothetical Constant-Bearing Missile". (SECRET).

3. CARDE Tech. Letter N-47-4, "Sparrow II Launch Zones", (SECRET)

4. CARDE Tech. Letter N-47-16, "Report on a Visit to U.S. Establishments" Section IX B. (SECRET).

5. CARDE Tech. Letter 1084/57 "CF 105 Aircraft Interceptor Placement Problem", (SECRET).

6. CARDE Tech. Letter 1091/58, "Fifth Progress Report on CF 105 Weapon System Assessment" Appendix 'A' (SECRET).

7. CARDE Tech. Letter 1091/58, "Fifth Progress Report on CF 105 Weapon System Assessment" Appendix 'B' (SECRET).

8. CARDE Tech Letter 1091/58, "Fifth Progress Report on CF 105 Weapon System Assessment", Appendix 'D' (SECRET).

9. CARDE Tech. Letter 1091/58, "Fifth Progress Report on CF 105 Weapon System Assessment", Appendix 'J', (SECRET).

10. Douglas-Bendix Report SM 19564 "Sparrow II Quarterly Progress Report" (SECRET).

11. Douglas Letter A2-260-SP-AN-92, "Comments Regarding the CF 105/ Sparrow II Weapon System", to Chief of the Air Staff, Ottawa. (CONFIDENTIAL).

12. RCA Report AR-3, "Quarterly Progress Report 4" Section IA-2 (SECRET)

13. Canadair Letter, Feb. 17, 1958, "Minimum Launch Ranges for Sparrow Type Missiles", to Mr. D. Bogdanoff. (CONFIDENTIAL).

APPENDIX 'D'

CF-105 SNAP-UP ATTACKS

by A.B. Bell

1.0 GENERAL BACKGROUND (ref. 1)

It is anticipated that enemy bombers will often possess an altitude advantage over interceptors at A.I. lock-on. If the altitude difference is large enough, it may be desirable for the interceptor to use a snap-up attack. This consists of two phases. In phase I, the interceptor maintains its altitude at lock-on and steers to wipe out horizontal heading errors, or a major part thereof, making optimum use of its manoeuvrability at this lower altitude. Then, in phase II, the interceptor proceeds to wipe out the large vertical heading error by pulling up. At the same time, the remaining horizontal heading errors may be corrected with a coordinated turn, or the interceptor may execute a "wings level" constant g pull-up.

In this report, the usefulness and execution of snap-up attacks will be discussed and R.C.A.'s method of velocity slowdown compensation will be outlined.

2.0 SNAP-UP APPLICATION

With a difference in elevation between interceptor and bomber, the interceptor has the choice of using snap-up or climbing. In the latter case, the interceptor corrects horizontal and elevation heading errors simultaneously right from lock-on. Both types of attack were studied at CARDE (ref. 2). From this work, the following brief rule may be made: snap-up is preferable when the following conditions are met:

(a) The elevation difference is quite large, say 30 K feet. (Sometimes 20 K feet is enough).

(b) The initial course difference, Γ_o, is not small. Γ_o should be greater than about 110°.

(c) σ is not small. σ should be greater than 1.5 n.m. For $\sigma \doteq 1.5$, climbing is probably better because it gives more consistent results.

The above applies for radar-controlled missile armament of the conventional Sparrow II type. A short study was also made for an I.R. missile (ref. 3) and the results indicated that snap-up was the only effective type of attack in frontal aspects. This is due to the low I.R. emission around the nose of a bomber which makes climbing and certainly co-altitude attacks less attractive. It should be noted that this result is very dependent on missile parameters and these were known only approximately.

3.0 EXECUTION OF SNAP-UP ATTACK

Whether or not snap-up is necessary, is determined from the differential altitude (Δh) at lock-on (ref. 4). The equation mechanized assumes small aircraft roll and antenna elevation angles:

$$\Delta h = R(\sin\epsilon \cos E + \sin E)$$

where E is aircraft elevation angle

ϵ is antenna elevation angle.

If snap-up is to be used, the interceptor is flown to eliminate only horizontal errors until the time of pull up. It was originally proposed to compute the snap-up angle and snap-up time from conditions at lock-on, but this has been changed. R.C.A. is now proposing to preset a time-to-go, T_s, at which time the pull-up phase is to be initiated. During this phase, any remaining horizontal heading error is to be corrected using a co-ordinated turn.

4.0 SNAP-UP TIME

The choice of the optimum T_s is a function of the target and fighter altitudes. In the CARDE 3-D study, the following values were used:

h_T	h_I	T_s
60,000 ft.	40,000 ft.	20 secs.
60,000 ft.	50,000 ft.	16 secs.
70,000 ft.	40,000 ft.	30 secs.

R.C.A. has suggested using one large value, namely 30 seconds, for all cases. This simplifies the instrumentation, but does not give an optimum condition for all cases.

5.0 VELOCITY SLOWDOWN COMPENSATION

During a snap-up attack, velocity slowdown can be expected. If the slowdown rate is sufficiently large, this means that the interceptor will fly a curved course with an appreciable roll angle and hence miss-distance.

A solution to this difficulty consists of anticipating the required change in heading due to the velocity slowdown. To do this, R.C.A. has proposed using a modified F distance, namely:

$$F' = F - g/2\,(T^2 - t_f^2)\,K$$

where F' is the modified F distance

g = acceleration due to gravity

T = time-to-go

t_f = time of flight of the weapon

K = a constant chosen on the basis of the average elevation angle of the interceptor. Apparently no attempt has yet been made to optimize the value of K. It is about equal to the average elevation angle. A typical value might be 0.4 radians.

To obtain this expression, it is assumed that

$$\dot{V}_I \approx -gE_{ave}$$

where $\dot{V}_I$ is the velocity slowdown rate during the pull-up phase and

E_{ave} is the average interceptor angle.

$\dot{V}_I$ actually depends upon the angle of climb and the thrust and drag of the interceptor.

In this method of compensation, R.C.A. has proposed using a modified F distance only on the co-ordinated turn during the pull-up phase of the attack. It might be profitable to use a modified F distance during the first phase as well. This could be given by

$$F'' = F - \frac{g}{2}.\,(T_s^{\,2} - t_f^{\,2})\;K.$$

where F" is the modified F distance during the first phase of the attack. This F" distance would remain fixed until snap-up, not varying with time as does F'.

Also, during the first phase of the attack, it might be profitable to take account of the velocity slowdown due to pulling g's when the fighter is manoeuvring to correct horizontal heading errors. This could be used to give a quick indication correction.

6.0 REFERENCES

1. R.C.A. Astra I Report QPR-1, "Quarterly Progress Report 1. "P. 13 (SECRET).

2. CARDE Tech. Letter 1091/58, "Fifth Progress Report on CF-105 Weapon System Assessment", Appendix 'A' (SECRET).

3. CARDE Tech. Letter, "Sixth Progress Report on CF-105 Weapon System Assessment", Appendix 'A' of this report. (SECRET)

4. R.C.A. Astra I Report QPR-1 "Quarterly Progress Report 1" P. 146 (SECRET).

5. R.C.A. Astra I Report QPR-3, "Quarterly Progress Report 3", P. 1-33 (SECRET).

APPENDIX 'E'

THE FEASIBILITY OF CHANGING ASPECT DURING AN ATTACK

by P.L. Roney

1.0 INTRODUCTION

The main part of this study is as defined by the above heading. The study was initiated by the possibility of the missile end-course study producing results which indicate higher probabilities at certain launch aspects. There are some indications of slightly higher probabilities of successful launch at the nose and tail regions than in the beam region. However, since there are other advantages, or disadvantages, in attacking from certain aspects a brief list was first compiled before continuing with the main portion of the study. This list follows:-

(1) Results of REAC 3-D Studies on Placement Probabilities

It appears that in many cases acceptable placement zones are greatly dependent on aspect. More specifically, head-on attacks are preferable and to a lesser extent tail attacks. Lower placement probabilities occur at the beam.

(2) Chaff

In order to determine whether or not there is any connection between aspect angle and the requirements necessary to minimise the effect of chaff used by the target the following report was referred to: - E L Report 5086-1 July 57 re "Susceptibility of the Astra I to ECM" (appearing in CARDE/TL/N-47-18 p. 435 et/ff.) From this report it is apparent that in order to reduce the effectiveness of chaff the beam region of attack is to be avoided for the following reasons.

(i) The effect of delay in chaff echo development with gravity launching gives certain regions where chaff is ineffective in the tail and nose areas of the target.

(ii) The Doppler Shift principle for tracking a target in the presence of chaff is recommended in this report. (see pp. 435 paragraph 4.1.4 and pp. 441 paragraph 4.7 for the case of forward fired chaff). If this were adopted, in preference to tracking radars operating on signal amplitude, then this would necessarily restrict useful target aspects to the nose and tail regions in order to maintain the line of sight components of target velocity high.

(3) Chaff Area Effect (When the Target is in the form of a Group of Bombers of formation).

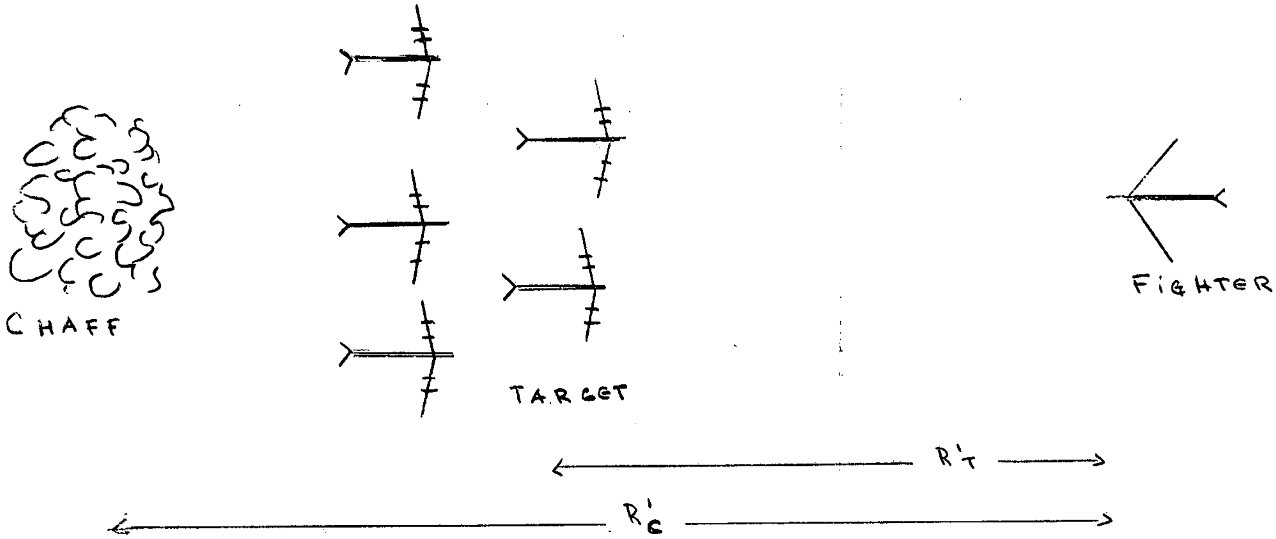

Figure E1

In the illustration above the fighter is approaching the target head-on, and the target is distributing chaff behind it. Here the difference in range rates between the chaff and target, relative to fighter, is used to enable the fighter to distinguish between the two. Obviously the greatest difference in range rates occurs at either head on or tail aspects and is equal to V_t.

At the beam aspect

$$\dot{R}_c = V_f \cos \theta \qquad \dot{R}_t = V_f \cos \theta \pm V_t \cos A$$

$$\therefore \text{ Difference in range rates} = \dot{R}_c \sim \dot{R}_t = V_t \cos A$$

which is smaller than V_t in general. Thus from this point of view also, head or tail attacks are preferable.

(4) V.T. Fuzes and Chaff

The V.T. Fuze in the missile could respond to chaff, acting on the Doppler frequency of the chaff but being dependent on the latter's area. This would be most likely to occur in the tail region (gravity fed chaff) but could also occur in the nose region with forward fired chaff. This last case is probably much less likely as it would depend on the time of events; in general the target should have flown through the chaff, which would then be behind it, by the time the missile had approached the target from head-on. From this point of view a beam attack is preferable.

(5) ECM

(a) At crossover: - the beam aspect is preferable because of the larger echoing areas at this aspect.

(b) R_{min}: - the tail aspect is to be preferred because R_{min} is smallest in this region. Small cross-over range utilised which is proportional to square of the area.

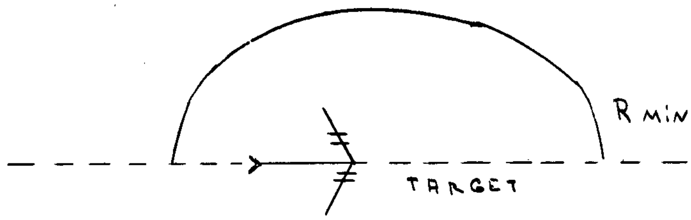

Figure E2

(6) P_k of Missile

It is thought that a plot of aspect P_k will give a minimum value at beam aspect and maxima at tail and nose, thus the beam is to be avoided.

(7) Bomber Defence

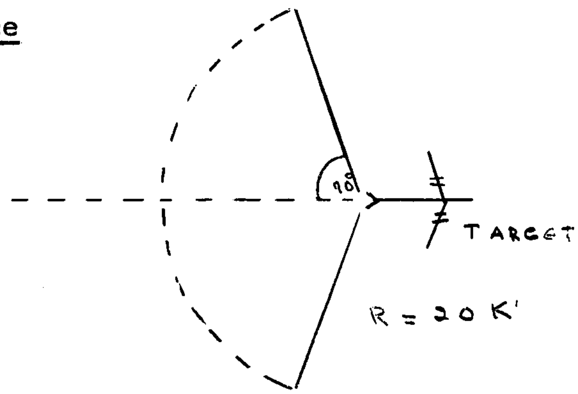

Figure E3

With the target defence armament centred in the tail region and giving a 70^{o} cone of fire and an effective radius of 20 K ft obviously the tail region attack must be avoided if possible.

(8) Target Penetration

The farther the target penetrates into home territory the more desirable it is to attack from a head-on aspect.

(9) I.R. Auxiliaries

Tail attacks are preferable because of the larger signal strength in this region.

(10) Anti-Jamming

More time is obtained in order to make anti-jamming decisions if a tail attack is used.

The above list gives some idea of the different reasons for avoiding or requiring attack from a particular region of aspect. The reasons are very varied and may depend on the attack situation. Decisions as to which factors would carry the most weight and which would decide the preferred region of aspect for attack in any given situation are beyond the scope of this report.

NOTE: Apart from (6), which concerns the missile itself, the aspects concerned are not launch aspects but general attack aspects existing from say lock-on to the firing point. Is it necessary to change the aspect as soon as possible after lock-on is achieved or is it merely necessary to ensure that the fighter fires at a certain launch aspect? This question will be dealt with in the next section.

2.0 GENERAL OUTLINE OF PROBLEM

Having established the desirability, in some attack situations, of changing the fighter aspect from an initial one to a different one, or of manoeuvring the fighter from one region of aspect into a more desirable region the rest of the task concerns the possibility of achieving this end. To do this comprehensively every single parameter should be taken into account, e.g. the aerodynamic characteristics of the CF-105, target evasion etc. This would necessarily involve a large scale investigation involving more than one person for it to be carried out adequately. Such an investigation being impracticable at this stage the study was limited to making the simplest assumptions in order to retain the required scale.

The assumptions were as follows. Coaltitude attack against a non-evasive target, fighter's turns were power limited, and the fighter flew at constant speed. No other aerodynamic factors regarding the fighter were taken into account. Two cases only were considered (a) Fighter speed advantage in the rear half of the target area (b) Fighter speed disadvantage in the front half of the target area. The change of aspect was assumed to be one from beam to tail or nose region.

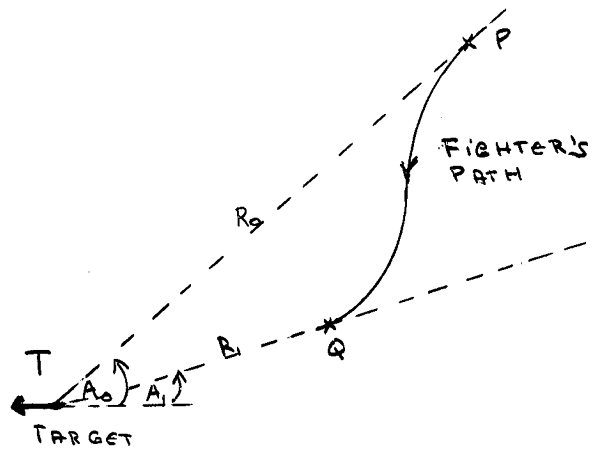

Figure E4

Referring to Figure E4 above (in target coordinates) the required manoeuvre is that the fighter initially at P, be steered to Q. At P the fighter has aspect A_0, range R_0, and lead angle Θ_0. At Q the values are A_1, R_1 and Θ_1.

Given an ideal situation, i.e. one in which GCI can communicate to the fighter that the latter is in a forbidden region of aspect before A.I. lock-on occurs, this point P would be at lock-on; say 40 miles from the target. The question now arises whether it is desirable to alter the fighter's aspect well before it reaches the launch zone or whether it is required to change from one region of aspect to a new aspect which is to be the launch aspect. The line TQ in figure 4 may be made either a particular aspect in which it is desired to place the fighter or it may represent a limiting aspect line separating a forbidden region and a desired region. Whichever viewpoint is employed, it does not affect the basic principle. Most of the reasons listed for changing aspect are related to conditions which are effective between lock-on and the launch zone and hence it seems desirable that the new aspect should be attained as soon as possible. The manoeuvre must in any case be completed outside the launch zone otherwise any additional manoeuvring the fighter has to perform would then be seriously restricted by the low value of the time to go. On the other hand there is the difficulty of performing the change of aspect manoeuvre in the limited time between lock-on and firing. The greatest restriction would probably be the aerodynamics of the fighter.

Although in some cases the desired aspect may be reached only just outside the launch zone it must be remembered that from lock-on onwards i.e. start of manoeuvre, the aspect situation is improving continuously. In addition the new aspect A_1 which the fighter is to acquire need not be boundary aspect between the forbidden and required regions of aspect but could of course be made to lie well within the latter region. A large safety margin could be attained under these conditions.

3.0 STEERING EQUATION FOR CHANGE OF ASPECT - A SINGLE, SIMPLE STEERING EQUATION

It was at first thought that the manoeuvre could be performed using one simple steering equation and the test was to determine such an equation, test it on the REAC and determine its limitations. Such an equation limited by the scope of the study, would not necessarily be an ideal or practical one but would serve to illustrate the feasibility of achieving a practical system.

The primary object was, given the fighter's position at P with a range R_0, aspect A_0, and lead angle θ_0, to alter its position to Q where it had a range R_1, aspect A_1, and lead angle θ_1. It was found that with the amount of information allowed the fighter by its radar, it was impossible to alter, by the use of a single steering equation only, the range, aspect and lead angle from one given set to another given set. One of the variables, aspect for instance as it is the primary variable, can be changed to another required value fairly easily. Even two variables, aspect and range, might be changed simultaneously but this is of little value since the third variable, lead angle, would then alter in an uncontrollable manner. Hence the manoeuvre could not be satisfactorily performed by the use of a single steering equation and the solution had to be found in a different form.

4.0 TWO PART STEERING EQUATION

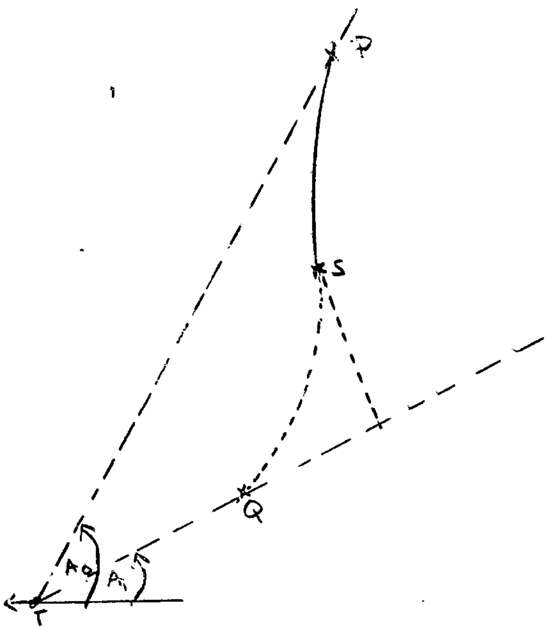

Figure E5(a)

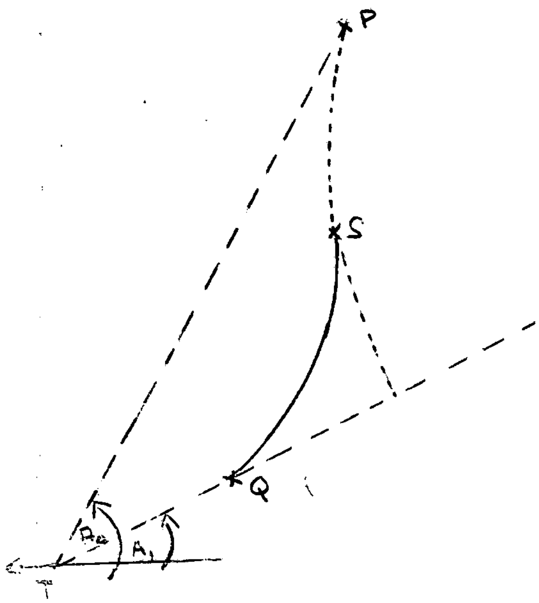

Figure E5(b)

As has been shown the chief difficulty encountered in manoeuvring from one aspect to another is the simultaneous control of range and lead angle. The latter is of course equally as important as aspect and range because of losing the target if the lead angle should exceed the limit set on it.

The end product of the manoeuvre requires three things: the desired aspect A_1, a specified range R_1 which leaves the fighter outside the launch zone and a lead angle consistent with the attack situation. A little leeway could be allowed on the accuracy of Θ_1, because provided the fighter at Q is outside the launch zone there would still be time to correct it. With these things in mind the following system was proposed. The manoeuvre would be divided into two parts. In the first part the fighter performs a turn dictated solely by a given aspect rate $\mathring{A}$. In Figure 5(a) the fighter thus moves from P to position S. For the second part the fighter follows the lead collision equations so that by the time it reaches Q it is in actual fact flying a lead collision course. Thus all three conditions are satisfied simultaneously because position Q is at the correct aspect A_1 and range R_1 and since the fighter is now on a lead collision course, the lead angle is also suitable.

The difficulty now lies in determining the values of $\mathring{A}$ and also for how long the fighter flies on the $\mathring{A}$ turn before switching over to a lead collision course. This was investigated on the REAC.

Two different cases were considered. The first case was for fighter speed disadvantage with changes of aspect from beam towards nose. The second case was with fighter speed advantage and changing aspect from beam towards tail. It was intended simply to obtain some idea of the variations of $\mathring{A}$ and the elapsed time, T_e, during the $\mathring{A}$ turn with A_o, A_1, and R_1 and then to study how these functions could be incorporated in the fighter's instrumentation.

5.0 EXAMINATION OF THE RESULTS

The first case above of fighter speed advantage in the front target region did not have to be taken very far before it became obvious that the fighter did not have enough time to complete the required manoeuvre due to the high closing rate. In order to make the manoeuvre possible the latter would have to commence at a range R_o very much greater than the present lock-on range of 40 miles. The possibility arose of overcoming the look-angle barrier but was beyond the scope of this study.

In the second case, of change of aspect from beam to tail region the results were quite good. The manoeuvres were restricted to ones of shortest time. Hence, this in turn imposed the limit that the tail aspect could not be achieved from an initial aspect near the beam region.

The trajectories obtained are reproduced (target coordinates) in Figure 6 onwards.

For a more detailed report on method and results see Memorandum: Roney - Wilson, CARDES 9736-21, dated 28 Jan. 1958.

6.0 CONCLUSIONS

(i) Two Part Steering Equation

The system appeared to work quite well for the second case considered. It was found that the fighter could not achieve large changes of aspect from near to beam region to the tail of the target. This does not mean that this is impossible, because it was intended that the fighter change aspect in as short a time as possible. The difficulty could be overcome by being less restrictive on the fighters trajectory during the manoeuvre, especially with a large fighter speed advantage.

In the case of fighter speed disadvantage in the region in front of the target change of aspect was found to be impossible due to the time allowed the fighter in which to perform the manoeuvre. This situation might be improved by making better use of GCI information, but the method itself would probably be still greatly restricted so as to make it relatively useless except for small changes of aspect.

(ii) General Conclusions on Change of Aspect Manoeuvre

(a) The REAC studies made in connection with this work assumed a complete knowledge of position and velocity relative to the target. It is unlikely that the interceptor will obtain this complete knowledge in adequate time to change aspect appreciables.

(b) In order to increase the chances of completing the manoeuvre it is essential that the GCI brings the fighter as close to the desired aspect as possible at lock-on. This will be limited by GCI's knowledge of attack situation; this means essentially the type of target because this will give knowledge of speed difference, and desired region of aspect. The proportion of success of attack contributed by a change of aspect manoeuvre will depend a great deal on the speed with which this manoeuvre can be carried out. Thus, if the type of manoeuvre can only be decided on after lock-on a lot of precious manoeuvre time might be lost.

It will, in general, be easier for G.C.I. to vector the interceptor to the desired aspect than for conversion to take place after lock-on.

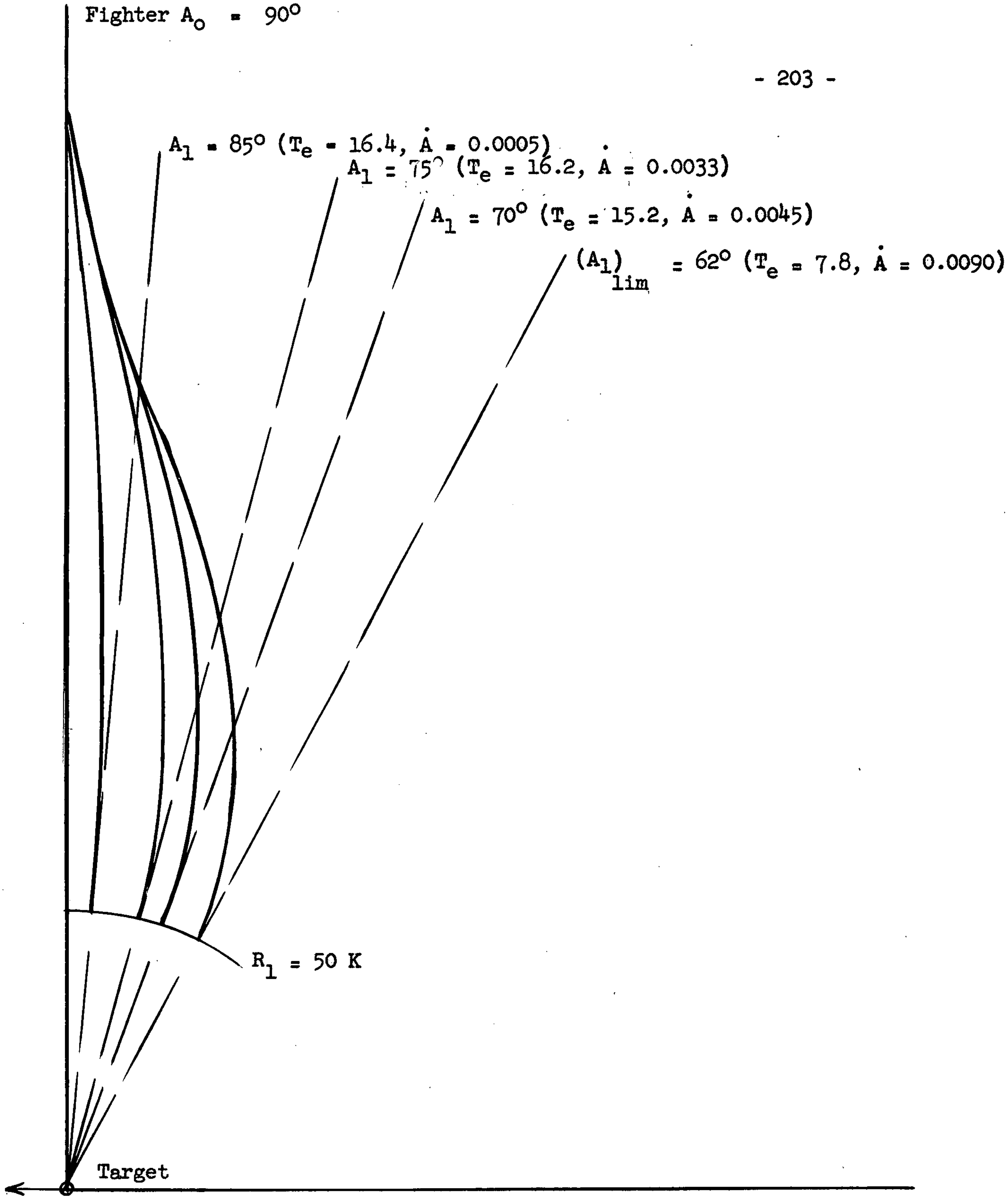
Fighter A_o = 90^o
A_1 = 85^o (T_e = 16.4, $\dot{A}$ = 0.0005)
A_1 = 75^o (T_e = 16.2, $\dot{A}$ = 0.0033)
A_1 = 70^o (T_e = 15.2, $\dot{A}$ = 0.0045)
$(A_1)_{lim}$ = 62^o (T_e = 7.8, $\dot{A}$ = 0.0090)
R_1 = 50 K
Target

Figure E-6

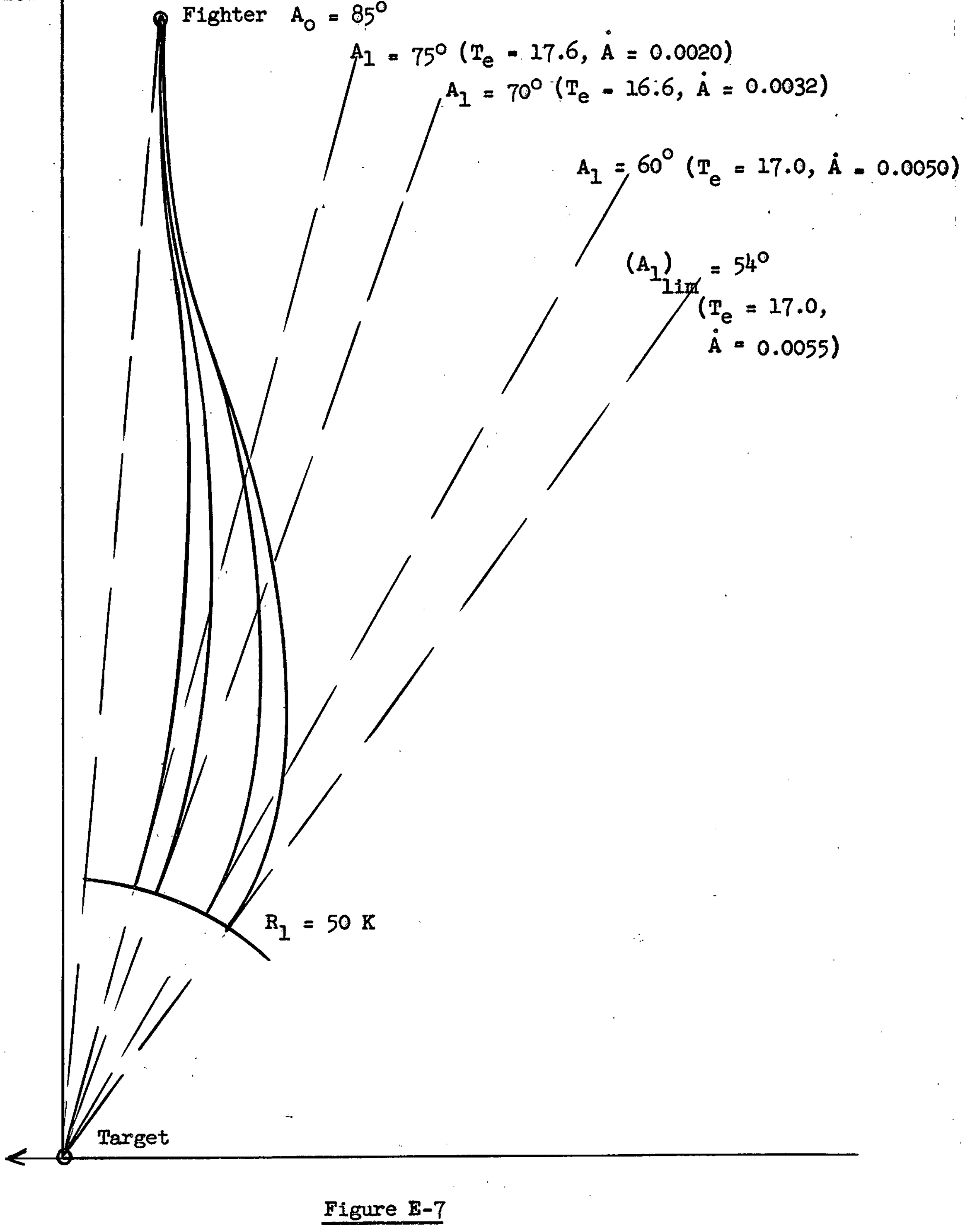
Fighter A o = 85°
A 1 = 75° (T e = 17.6, Ȧ = 0.0020)
A 1 = 70° (T e = 16.6, Ȧ = 0.0032)
A 1 = 60° (T e = 17.0, Ȧ = 0.0050)
(A 1) lim = 54° (T e = 17.0, Ȧ = 0.0055)
R 1 = 50 K
Target

Figure E-7

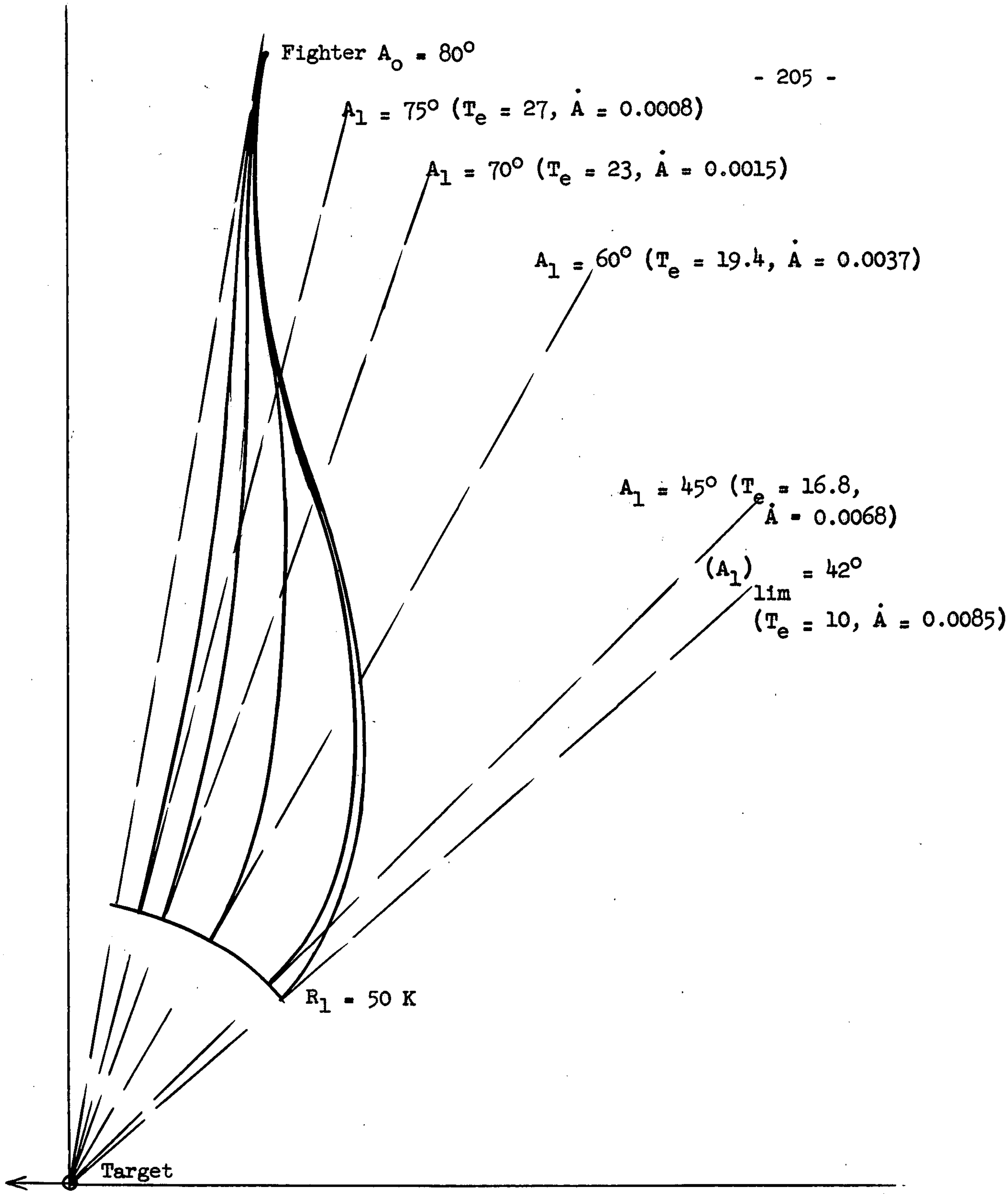
Fighter $A_o = 80^\circ$
$A_1 = 75^\circ$ ($T_e = 27$, $\dot{A} = 0.0008$)
$A_1 = 70^\circ$ ($T_e = 23$, $\dot{A} = 0.0015$)
$A_1 = 60^\circ$ ($T_e = 19.4$, $\dot{A} = 0.0037$)
$A_1 = 45^\circ$ ($T_e = 16.8$, $\dot{A} = 0.0068$)
$(A_1)_{lim} = 42^\circ$
($T_e = 10$, $\dot{A} = 0.0085$)
$R_1 = 50$ K
Target

Figure E-8

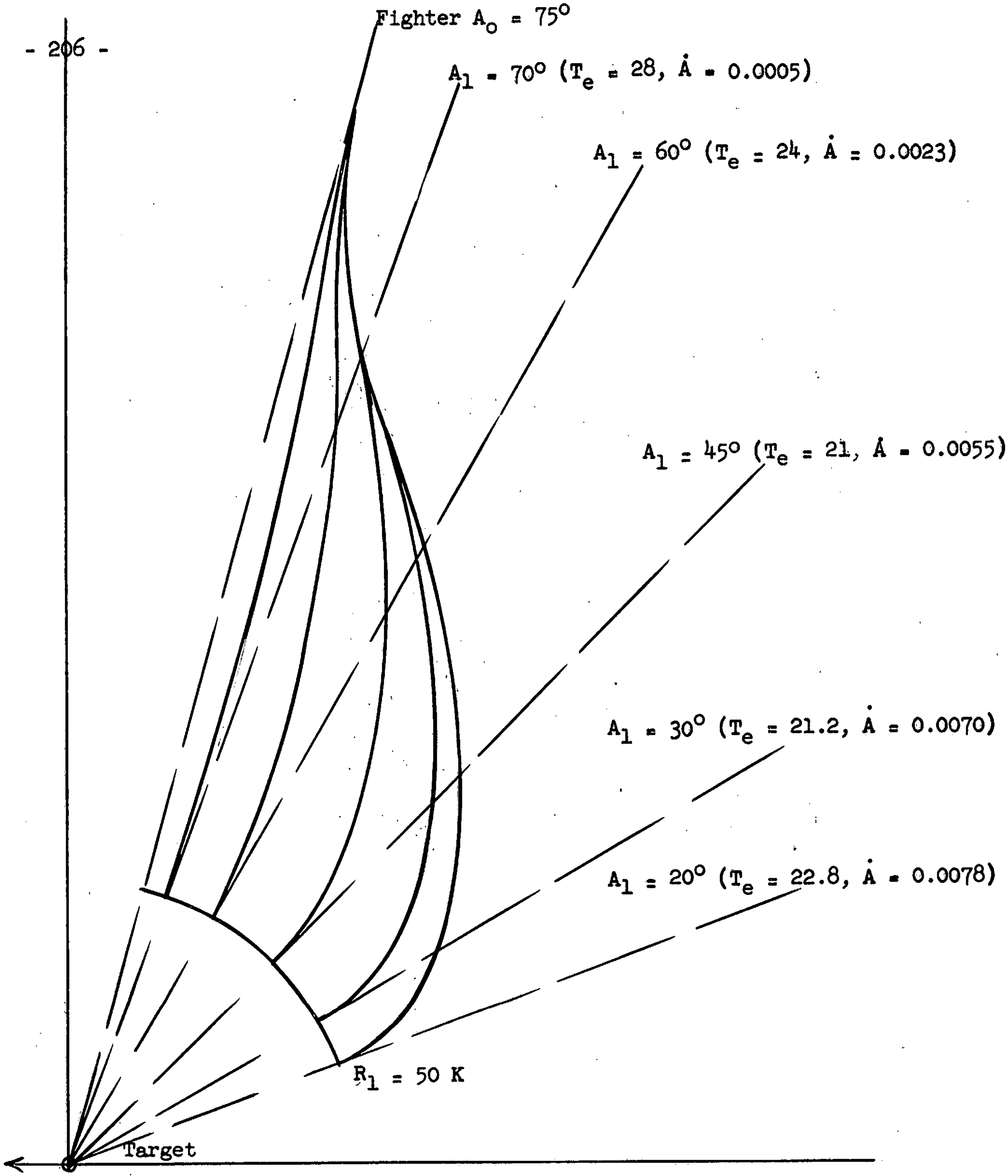
Fighter $A_o = 75°$
$A_1 = 70°$ ($T_e = 28$, $\dot{A} = 0.0005$)
$A_1 = 60°$ ($T_e = 24$, $\dot{A} = 0.0023$)
$A_1 = 45°$ ($T_e = 21$, $\dot{A} = 0.0055$)
$A_1 = 30°$ ($T_e = 21.2$, $\dot{A} = 0.0070$)
$A_1 = 20°$ ($T_e = 22.8$, $\dot{A} = 0.0078$)
$R_1 = 50$ K
Target

Figure E-9

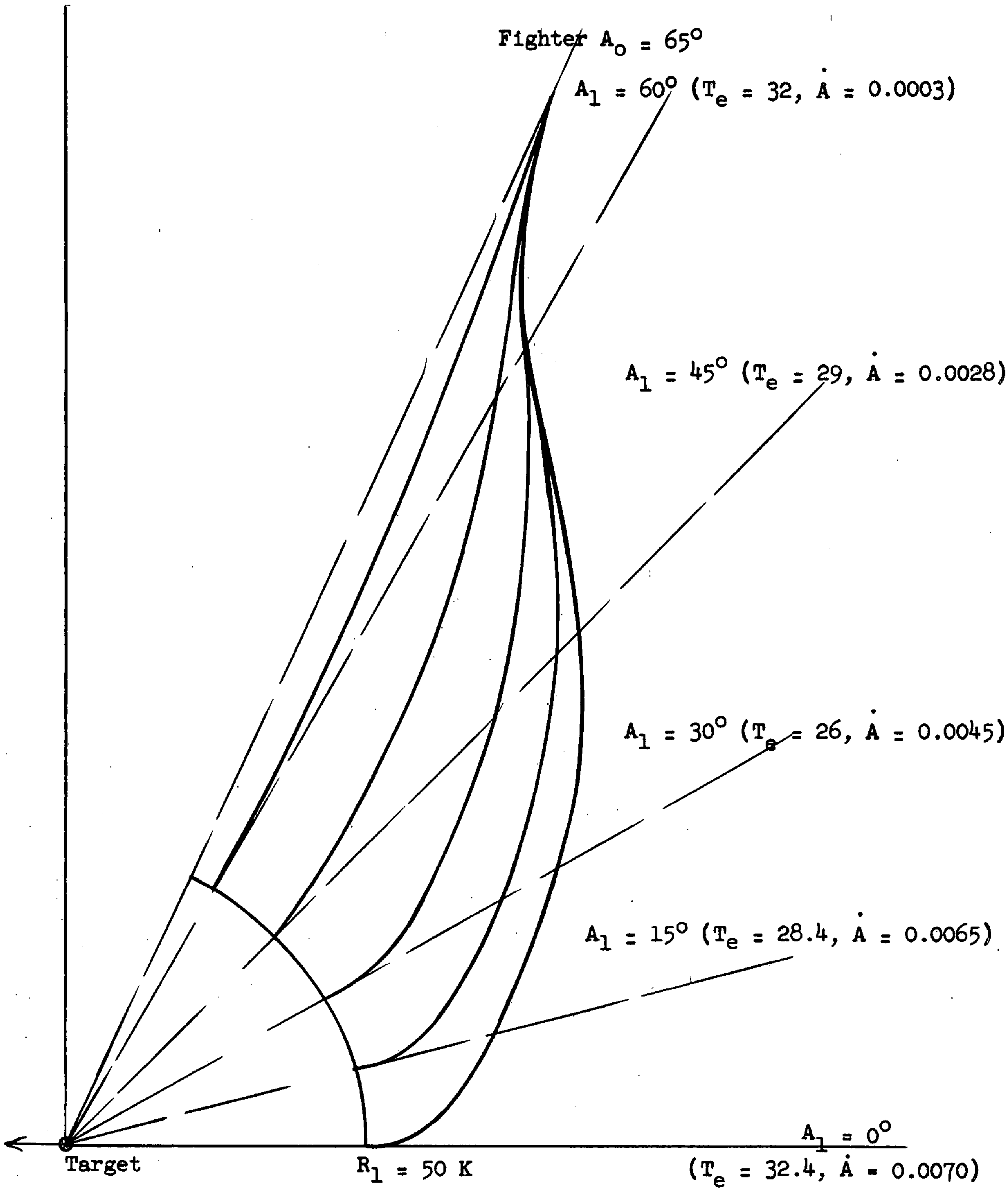

Fighter $A_o = 65^\circ$
$A_1 = 60^\circ$ ($T_e = 32$, $\dot{A} = 0.0003$)
$A_1 = 45^\circ$ ($T_e = 29$, $\dot{A} = 0.0028$)
$A_1 = 30^\circ$ ($T_e = 26$, $\dot{A} = 0.0045$)
$A_1 = 15^\circ$ ($T_e = 28.4$, $\dot{A} = 0.0065$)
$A_1 = 0^\circ$
($T_e = 32.4$, $\dot{A} = 0.0070$)
Target
$R_1 = 50$ K

Figure E-10

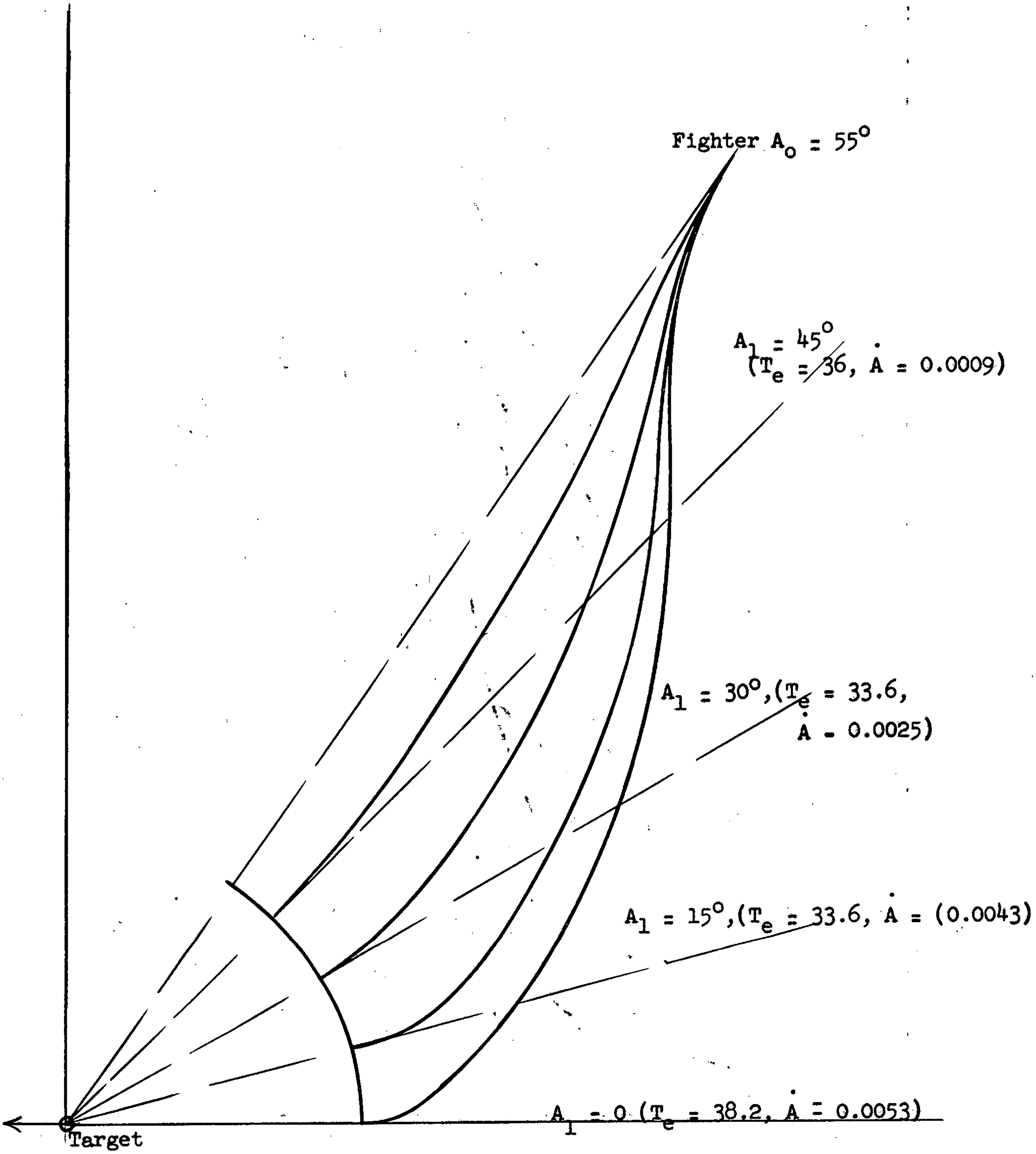
Fighter $A_o = 55^o$
$A_1 = 45^o$
$(T_e = 36, \dot{A} = 0.0009)$
$A_1 = 30^o, (T_e = 33.6,$
$\dot{A} = 0.0025)$
$A_1 = 15^o, (T_e = 33.6, \dot{A} = (0.0043)$
$A_1 = 0 (T_e = 38.2, \dot{A} = 0.0053)$
Target

Figure E-11

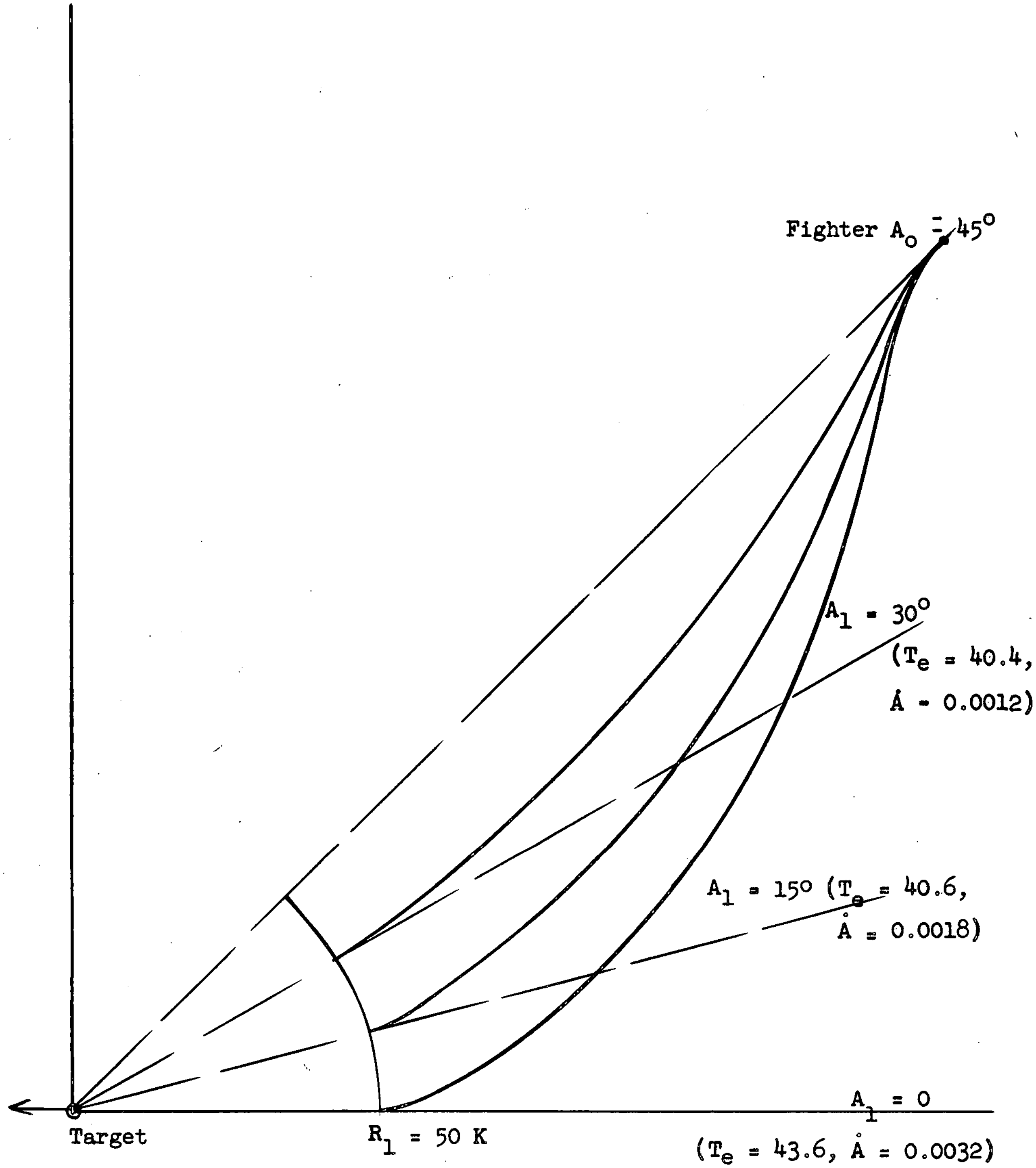
Fighter A_o = 45°
A_1 = 30°
(T_e = 40.4,
$\mathring{A}$ = 0.0012)
A_1 = 15° (T_e = 40.6,
$\mathring{A}$ = 0.0018)
A_1 = 0
(T_e = 43.6, $\mathring{A}$ = 0.0032)
Target
R_1 = 50 K

Figure E-12

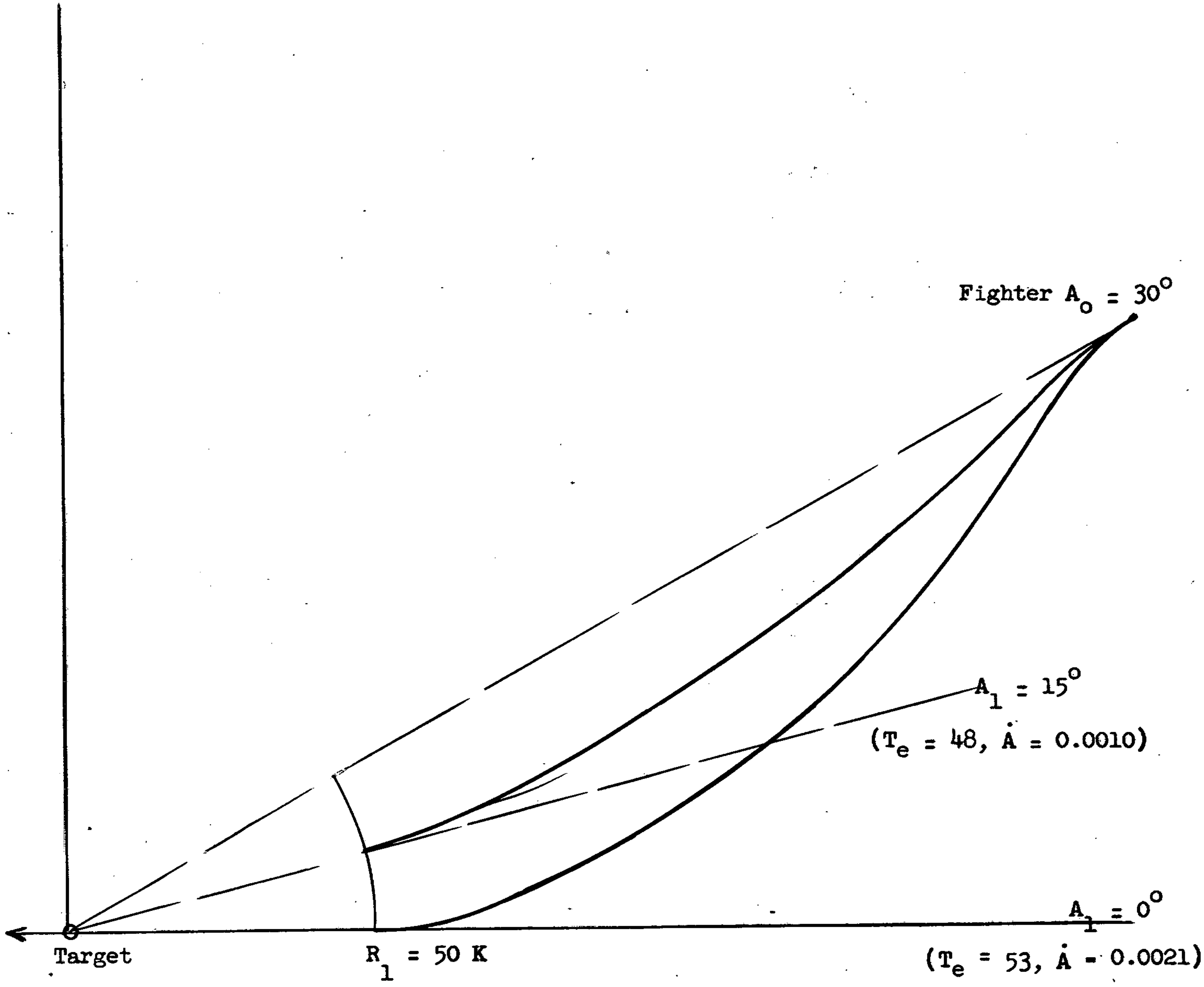

Figure E-13

APPENDIX 'F'

ATTACKS BY COORDINATED INTERCEPTORS

by G.A. Morley

1.0 INTRODUCTION

Single interceptor attacks sometimes render low probabilities of success against high speed targets because of the possibility of evasion by the target. If more than one interceptor is employed the probability of success is frequently increased and if sufficient interceptors are used the probability of success tends to unity. Sometimes the target may evade a succession of single interceptors by turning away from each one. Thus the use of coordinated interceptors has been suggested.

This is a report of a study of the probability of success of attacks by coordinated interceptors upon a target. Some general conclusions as to the relative position of two interceptors for maximum placement probability have been determined.

2.0 NON-EVADING TARGET

2.1 General

Considering a single interceptor attempting interception, one may find from the placement chart the placement probability of success in converting an approach into a successful attack if the AI acquisition range and ground control accuracy are known.

It is assumed that the ground control placement is characterized by a random distribution of displacements of the interceptor's track, relative to the target, from some ideal approach line. This distribution of displacements is assumed to follow the Gaussian function

$$\frac{1}{\sqrt{2\pi}\,\sigma}\,\varepsilon^{-\frac{x^2}{2\sigma^2}}$$

where, x = distance of approach from ideal approach line

σ = standard deviation

The Gaussian function and therefore the ground control accuracy may be defined by σ alone.

The AI acquisition range has been defined (ref. 1) as that range at which the AI radar after detection of the target may be "locked-on" so as to provide steering instructions.

The probability of a successful attack P is assumed to be the product of P_p the placement probability and P_k the probability that a successful attack is achieved after successful placement, i.e.

$$P = P_p P_k$$

The factor P_k will be dependent upon such things as probability of lock-on, probability of successfully firing missile, probability of missile functioning, etc.

2.2 Placement Probability - 1 Interceptor

To calculate the placement probability of a single interceptor attack, the 50% contour of probable AI acquisition is drawn on the placement chart as in Figure 1.

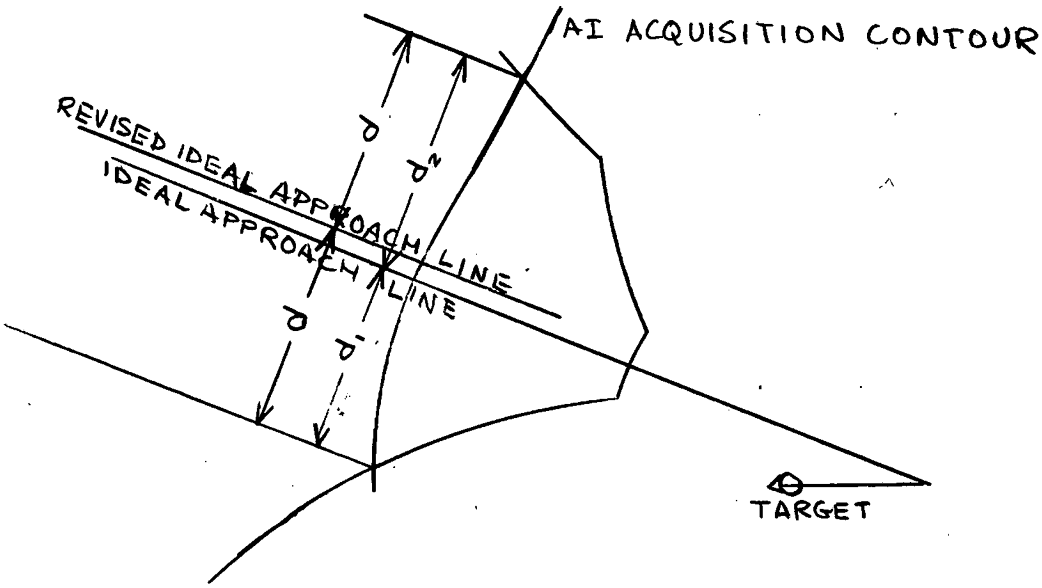

Figure 1

The lengths d_1 and d_2, the distances of the ideal approach line from the intersections of the AI acquisition contour and the edges of the placement zone, are then measured. If $\Phi(d)$ is defined by where d is in units of σ , the placement probability may be written as

$$\Phi(d_1) + \Phi(d_2)$$

If the sum $d_1 + d_2$ is constant, the value of placement probability is maximum if $d_1 = d_2$. This leads to the defining of a revised ideal approach line which is a line parallel to the original ideal approach line but displaced from it to make $d_1 = d_2$ at the anticipated AI acquisition range. The revised ideal approach line is in general different for different AI acquisition ranges. The placement probability P_{pl} for an interceptor approaching a target via the ideal approach line is

$$P_{pl} = 2\,\Phi(d).$$

2.3 Placement Probability - 2 Interceptors

The following development assumes that one interceptor is directed to the target some distance from the ideal approach line. It also assumes that a second interceptor can position itself at a fixed distance from the directed interceptor.

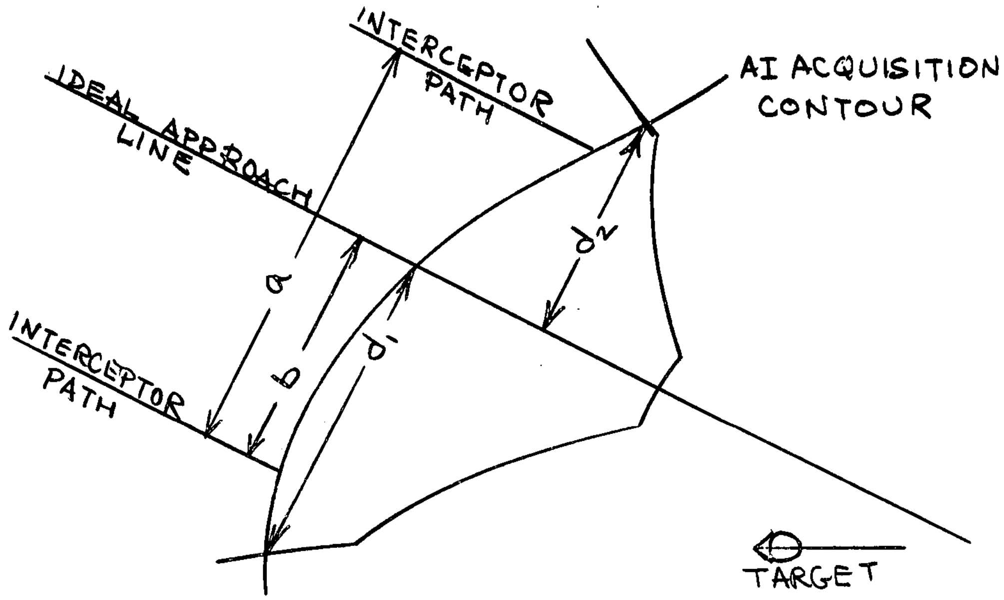

Figure 2

In such a case (see Figure 2) the placement probability is given by

$$\Phi(b + d_2) + \Phi(a - b + d_1) - \Phi(b - d_1) - \Phi(b - a - d_2),$$

$$\text{if} \quad a > d_1 + d_2$$

or

$$\phi(b + d_2) + \phi(a - b + d_1),$$

$$\text{if} \quad a < d_1 + d_2$$

where

b = distance of directed interceptor from ideal approach line

a = distance apart of interceptor paths

d_1, d_2 = distances from intersections of AI acquisition contour and edges of placement zone to ideal approach line.

For a given value of $d_1 + d_2$ this probability is a maximum if the ideal apporach line is revised such that $d = d_1 = d_2$ and if $b = \frac{a}{2}$. If, this is the case the placement probability is

$$2\,\phi\left(\frac{a}{2} + d\right) - 2\,\phi\left(\frac{a}{2} - d\right), \qquad \text{if } \frac{a}{2} > d$$

$$2\,\phi\left(\frac{a}{2} + d\right), \qquad \text{if } \frac{a}{2} \leq d$$

If $\frac{a}{2} = d$ the placement probab lity may be further maximized such that

$$P_{p2} = 2\,\phi(2d) = 2\,\phi(a)$$

Thus it may be said that to attain the maximum placement probability of two coordinated interceptors attacking a target, they must be arranged in target space so that their course headings be similar and there distance apart be such that each passes through an intersection of the AI acquisition contour and the boundaries of the placement zone.

If the interceptors are directed on paths not passing through the intersections of the AI acquisition contour and the edges of the placement zone $(\frac{a}{2} \neq d)$, but nevertheless equidistant from the revised ideal approach line $(b = \frac{a}{2})$ the placement probability may be considerably less than P_{p2} if $\frac{a}{2} > d$ (see Figure 3)

2.4 More than 2 Interceptors

It follows immediately that if three interceptors are sent against a non-evading target then to obtain maximum placement probability they must be arranged such that at the anticipated AI contour in target space one is midway between the intersections of the AI contour and the border of the placement zone and the other two are perpendicularly distant 2d from this interceptor's approach line one on each side. In such a case, the placement probability is given by

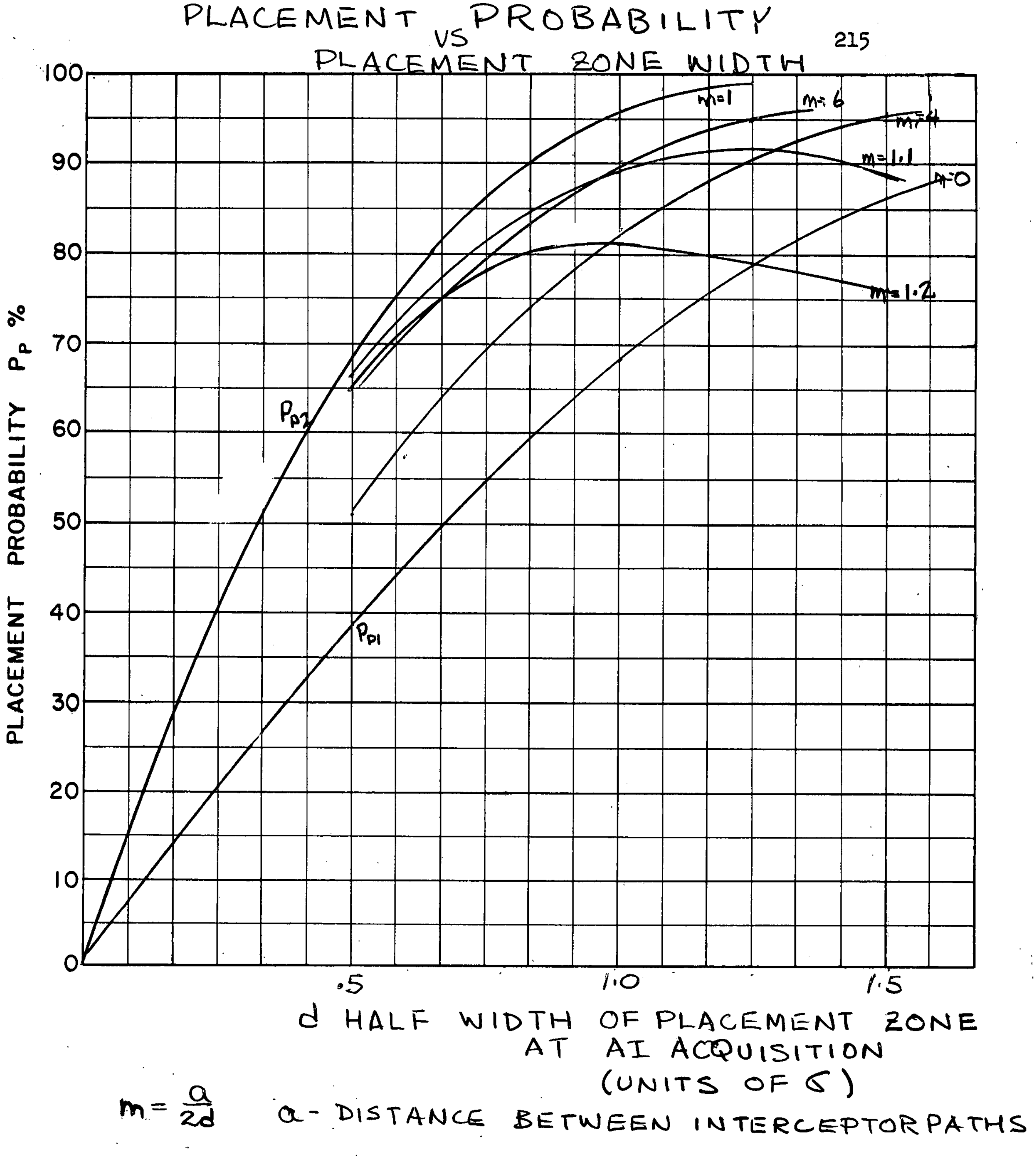
PLACEMENT vs PROBABILITY
PLACEMENT ZONE WIDTH
PLACEMENT PROBABILITY P_P %
100
90
80
70
60
50
40
30
20
10
0
.5
1.0
1.5
P_{p2}
P_{p1}
m=1
m=.6
m=.4
m=1.1
m=1.2
m=0
d HALF WIDTH OF PLACEMENT ZONE
AT AI ACQUISITION
(UNITS OF σ)
$m = \frac{a}{2d}$ a - DISTANCE BETWEEN INTERCEPTOR PATHS

Figure 3

$$P_{p3} = 2 \phi (3d)$$

Further, if n interceptors are sent against one target, their maximum placement probability is

$$P_{pn} = 2 \phi (nd)$$

For n sufficiently large $P_{pn} \rightarrow 1$

2.5 Probability of Success

From para. 2.1 it is seen that if P_1 is the total probability of success of a single interceptor against a single target it may be written that

$$P_1 = P_{p1} P_k.$$

For a two-interceptor independent attack the probability of success P_2 may be written as

$$P_2 = 1 - (1 - P_1)^2 = 1 - (1 - P_{p1} P_k)^2$$

For a two-interceptor correlated attack one may write the probability of success P_2' as

$$P_2' = P_{p2} P_k$$

since only one interceptor is assumed to complete the attack.

In order that the two-interceptor coordinated attack have a higher probability of success than the two-interceptor independent attack

$$P_2' > P_2$$

or

$$P_k > \frac{2 P_{p1} - P_{p2}}{P_{p1}^2} = P_{kmin}$$

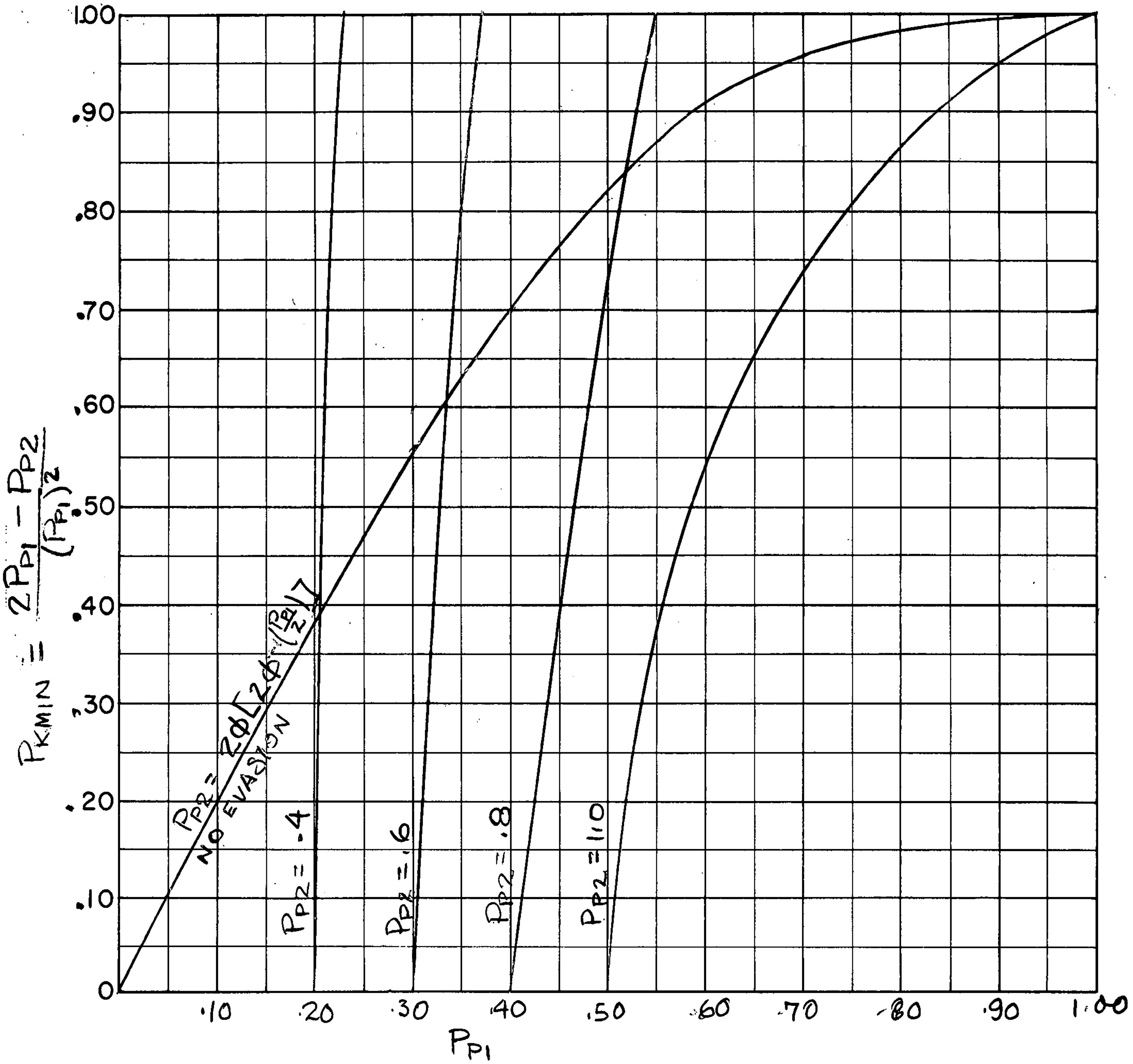
1.00
.90
.80
.70
.60
.50
.40
.30
.20
.10
0
.10
.20
.30
.40
.50
.60
.70
.80
.90
1.00
P_{P1}
$P_{KMIN} = \frac{2P_{P1} - P_{P2}}{(P_{P1})^2}$
NO EVASION
$P_{P2} = .4$
$P_{P2} = .6$
$P_{P2} = .8$
$P_{P2} = 1.0$

Figure 4

Figure 4 is a graph of P_{kmin} as function of P_{p1} (P_{p2} may be written as a function of P_{p1} for the non evading situation). It is noted that if $P_{p1} > .5$ P_k must be larger than .82 in order for $P_2' > P_2$.

3.0 2 INTERCEPTOR ATTACK ON EVADING TARGET

General

The effect of target evasion upon the placement probability of a single interceptor attack is discussed in (ref. 1, pp 63-69). A typical placement chart is shown in Figure 5.

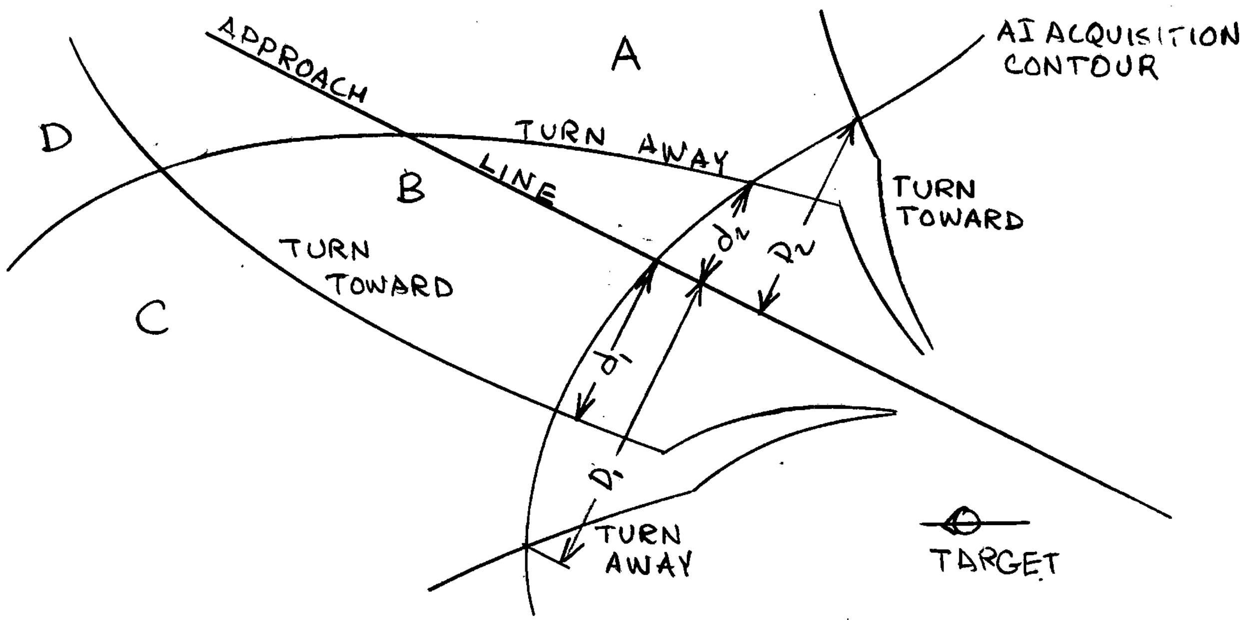

Figure 5

It is noted that AI acquisition occurs in regions A or B, a successful placement is achieved if the target turns toward the interceptor. If AI acquisition occurs in regions B or C, a successful placement is achieved if the target turns away from the interceptor. If AI acquisition occurs in D, the target can achieve successful evasion by turning in either direction. Assuming that the target acquires knowledge of the position of the interceptor at the instant of lock-on, it follows that it will evade in the direction most likely to succeed. Thus, it is assumed that for a successful attack of a single interceptor it must lie in region B in order to achieve successful placement i.e. successful placement whether the target turns left or right.

The same criterion may be applied to the case of two interceptors. If this be done, a successful placement is achieved if

(1) either interceptor crosses the AI acquisition contour in region B

(2) one interceptor crosses the AI acquisition contour in region A and the other in C.

Details of the calculation of the placement probability can be found in reference 2.

4.0 MEASUREMENTS

Some measurements from placement charts have been made. The placement charts used are shown in ref. 4. In all cases the revised ideal approach line with no target evasion was used and the distance apart of the aircraft was equal to the width of the placement zone for no evasion at the anticipated AI acquisition contour. The following conditions were used in the preparation of the placement charts.

Interceptor - CF 105

$M_t = 2.0$	$\Delta h = 0$
$M_f = 2.0$	$r_t = 0$ no evasion
$h_t = 60$ K ft.	$V_t\, r_t = 0.75$ g with evasion

Other conditions are available from the above-mentioned memorandum.

The first table of probabilities was made using the AI acquisition contour for S. In the cases of 2 independent interceptors the kill probability has been assumed to be unity ie $P_k = 1 - (1 - P_{pl})^2$. Figure 6 is a graph drawn of the placement probabilities for no evasion under different modes of attack. Figures 7 and 8 are graphs of the placement probabilities of success whether the target turns toward or away from the interceptor. Some of these data have been smoothed.

TABLE I

	AI - S															
	$\Gamma_o = 75^\circ$				$\Gamma_o = 110^\circ$				$\Gamma_o = 135^\circ$				$\Gamma_o = 180^\circ$			
σ = 3 n m	NE	A	T	A-T	NE	A	T	A-T	NE	A	T	A-T	NE	A	T	A-T
1	.95	.94	0	0	1.00	.94	.01	0	1.00	.94	.71	.65	1.00	.96	.96	.92
2 independent	1.00	1.00	0	0	1.00	1.00	.03	0	1.00	1.00	.91	.88	1.00	1.00	1.00	.99
2 correlated	1.00	.93	0	0	1.00	.91	.66	.66	1.00	.98	1.00	.98	1.00	.95	.95	.90
σ = 9 n m																
1	.49	.47	0	0	.81	.65	.12	0	.84	.68	.55	.27	.82	.72	.72	.44
2 independent	.74	.72	0	0	.96	.88	.22	0	.97	.90	.80	.46	.97	.90	.90	.68
2 correlated	.81	.78	0	0	.99	.85	.26	.25	.99	.82	.87	.79	1.00	.90	.90	.80

$P_k = 1$

NE - No target evasion

A - Target evades away from interceptor

T - Target evades toward interceptor

A-T - Target evades either toward or away from interceptor

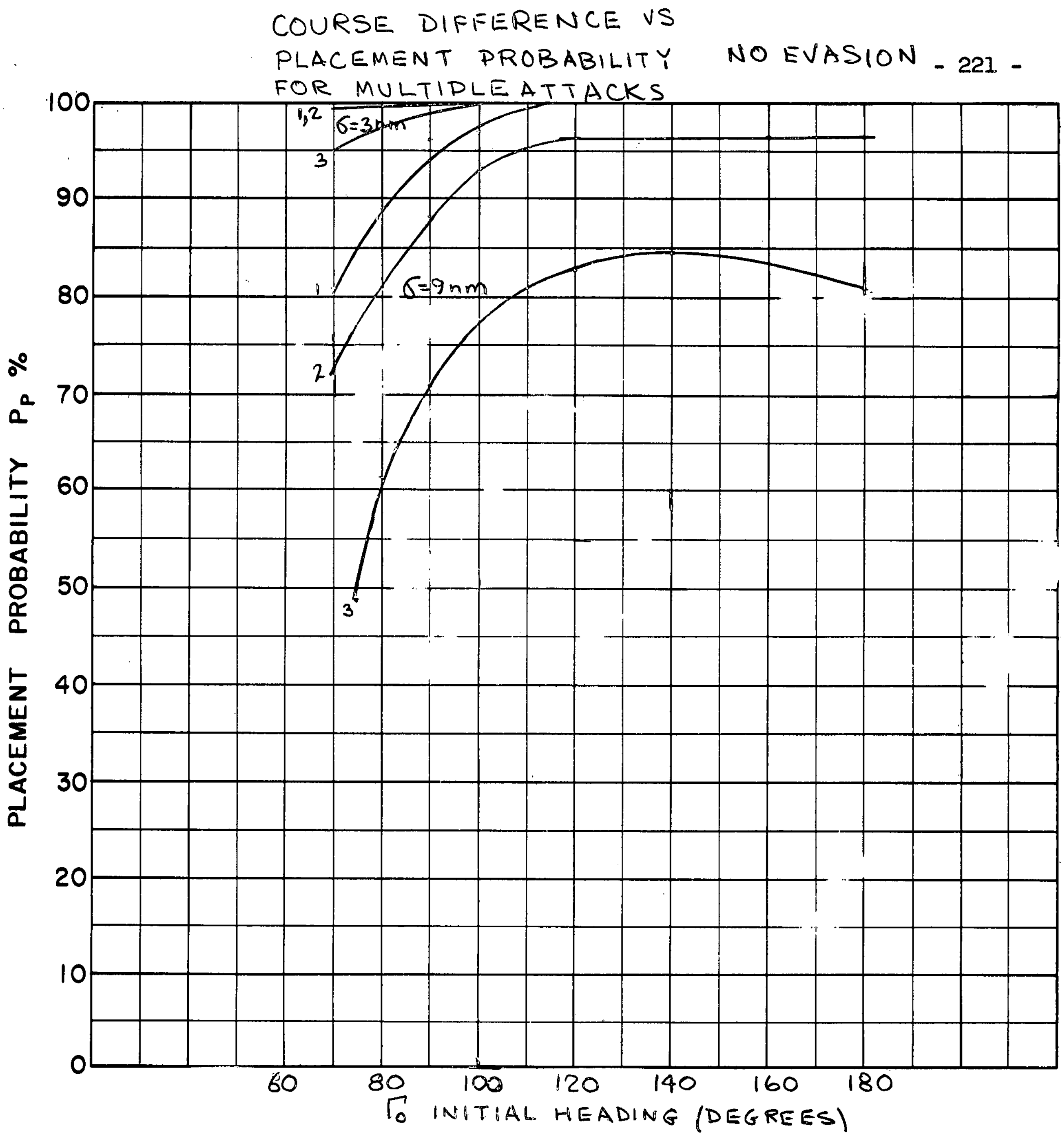

COURSE DIFFERENCE: VARIABLE
TARGET EVASION: NONE
TARGET MACH NO.: 2
INTERCEPTOR LATERAL G's:
INTERCEPTOR MACH NO.: 2
σ OF G.C.I. ACCURACY: AS INDICATED
A.I. DETECTION RANGE AS FRACTION OF SPECIFICATION RANGE, S: 1
A.I. DETECTION RANGE CONTOUR: S
ALTITUDE: 60 KFT

1 - 2 INTERCEPTORS COORDINATED AS IN TEXT
2 - 2 INTERCEPTORS INDEPENDENT $P_K = 1$
3 - SINGLE INTERCEPTOR

Figure 6

COURSE DIFFERENCE VS
PLACEMENT PROBABILITY WITH EVASION
FOR MULTIPLE ATTACKS
$\sigma = 3nm$

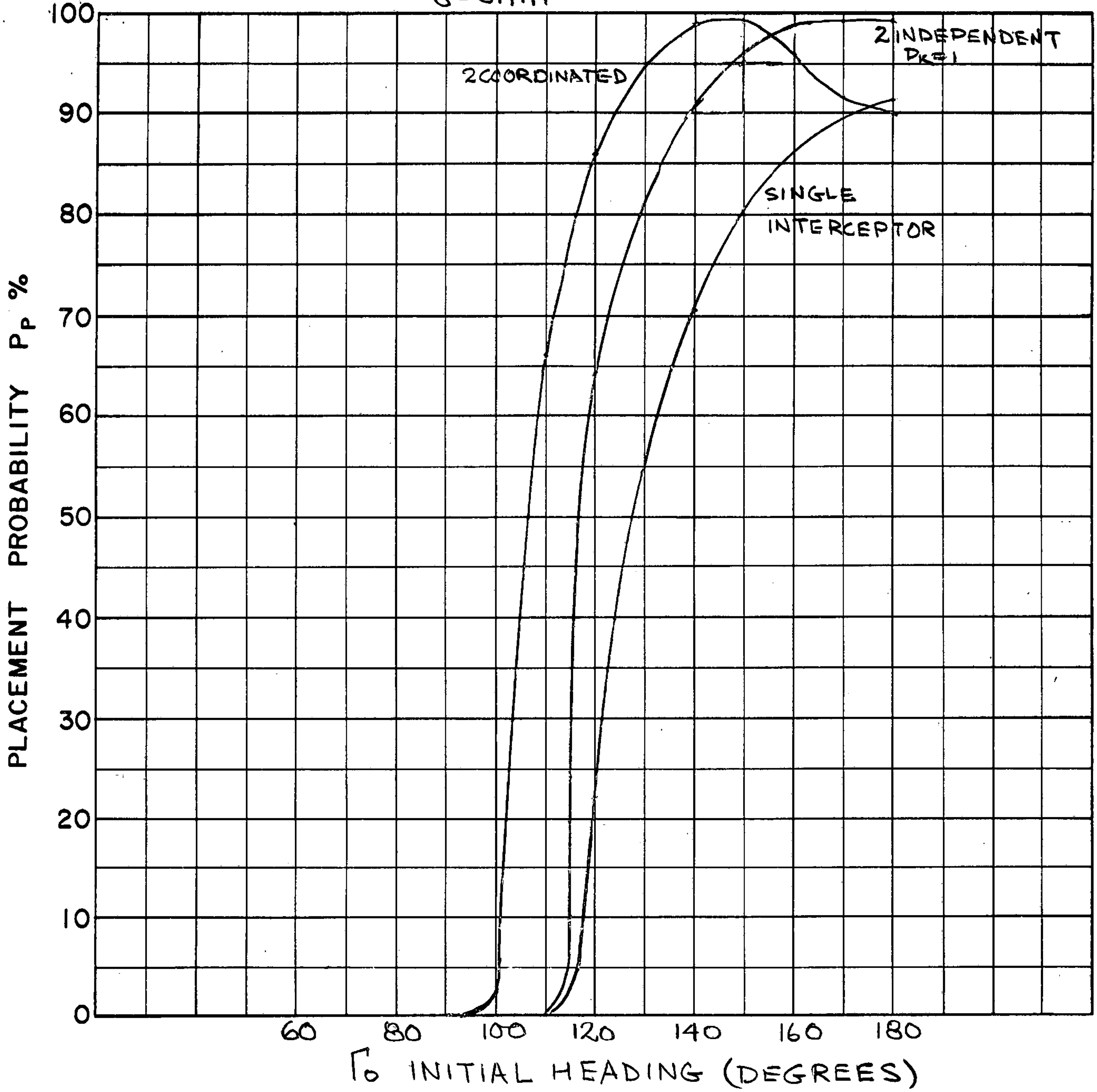

COURSE DIFFERENCE: VARIABLE
TARGET EVASION: ·75g
TARGET MACH NO.: 2
INTERCEPTOR LATERAL G's:
INTERCEPTOR MACH NO.: 2
σ OF G.C.I. ACCURACY: 3nm
A.I. DETECTION RANGE AS FRACTION OF SPECIFICATION RANGE, S: 1
A.I. DETECTION RANGE CONTOUR: S
ALTITUDE: 50KFT

Figure 7

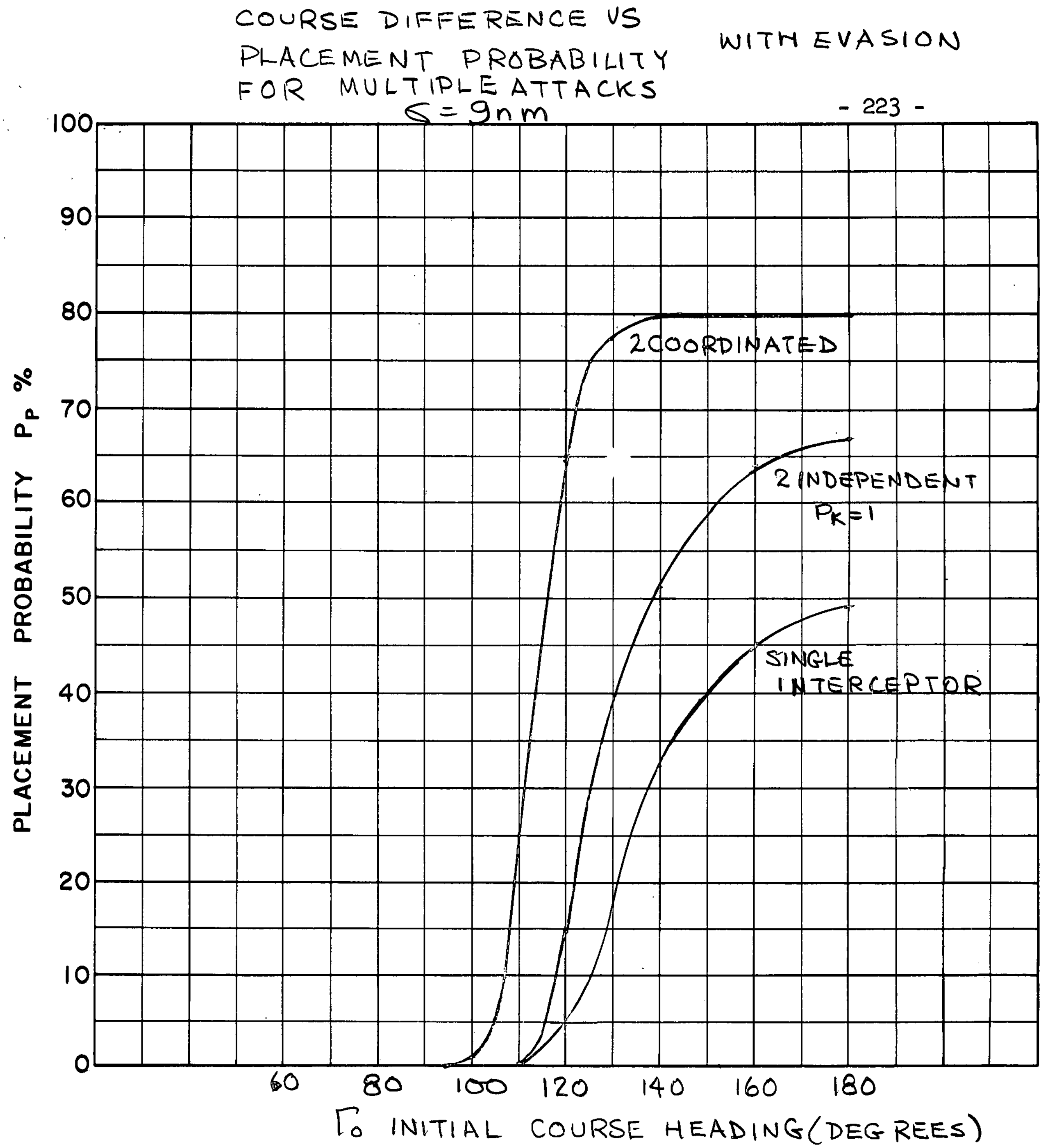

COURSE DIFFERENCE: VARIABLE
TARGET EVASION: .75g
TARGET MACH NO.: 2
INTERCEPTOR LATERAL G's:
INTERCEPTOR MACH NO.: 2
σ OF G.C.I. ACCURACY: 9nm
A.I. DETECTION RANGE AS FRACTION OF SPECIFICATION RANGE, S: 1
A.I. DETECTION RANGE CONTOUR:
ALTITUDE: 50KFT

Figure 8

The probabilities in the second table were measured at a constant angle of initial heading using four different AI acquisition contours. At each contour the ideal approach line was revised and the interceptors set a distance apart to maximize the placement probability with no target evasion. Under these conditions the placement probabilities with target evasion were measured. Figures 9 and 10 are graphs of placement probability as a function of AI acquisition range.

TABLE 2

	$\Gamma_o = 135^o$							
	0.4S		0.85S		S		1.28S	
σ = 3 n m	NE	A-T	NE	A-T	NE	A-T	NE	A-T
1	.95	.84	1.00	.87	1.00	.65	1.00	0
2 independent	1.0	.98	1.00	.98	1.00	.88	1.00	0
2 correlated	1.0	.95	1.00	.91	1.00	.98	1.00	.85
σ = 9 n m								
1	.49	.39	.75	.40	.84	.27	.94	0
2 independent	.74	.63	.94	.64	.97	.44	1.00	0
2 correlated	.81	.73	.98	.77	.99	.79	1.00	.45

$P_k = 1$

NE - No target evasion

A-T - Target evades either toward or away from interceptor

The third table lists values of P_{kmin} calculated from the probabilities of the above tables. Only in a few cases is P_{kmin} less than 0.5

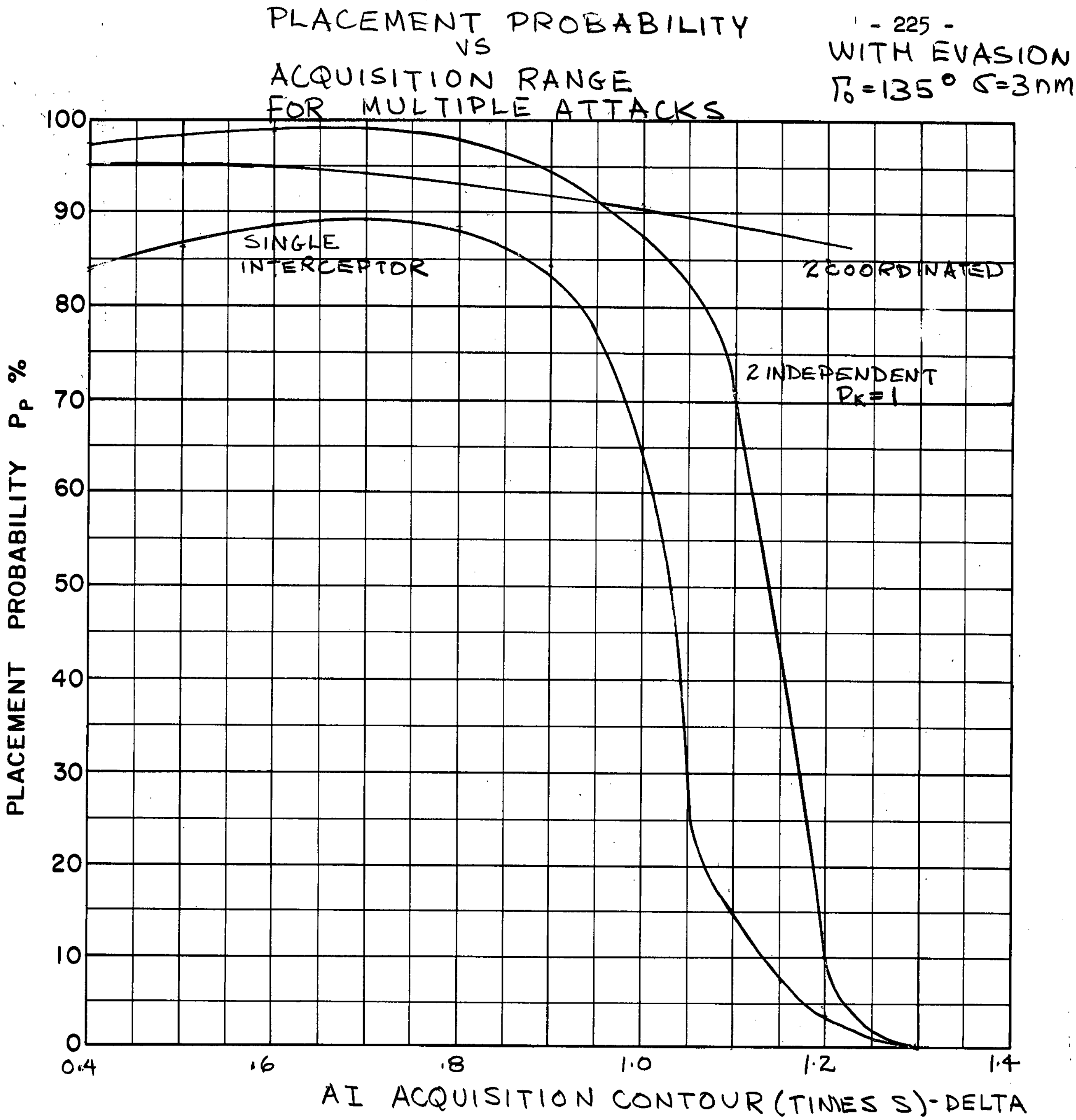

COURSE DIFFERENCE: $\Gamma_0 = 135°$
TARGET EVASION: .75g
TARGET MACH NO.: 2
INTERCEPTOR LATERAL G's:
INTERCEPTOR MACH NO.: 2
σ OF G.C.I. ACCURACY: 3nm
A.I. DETECTION RANGE AS FRACTION OF SPECIFICATION RANGE, S: VARIABLE
A.I. DETECTION RANGE CONTOUR:
ALTITUDE: 50KFT

Figure 9

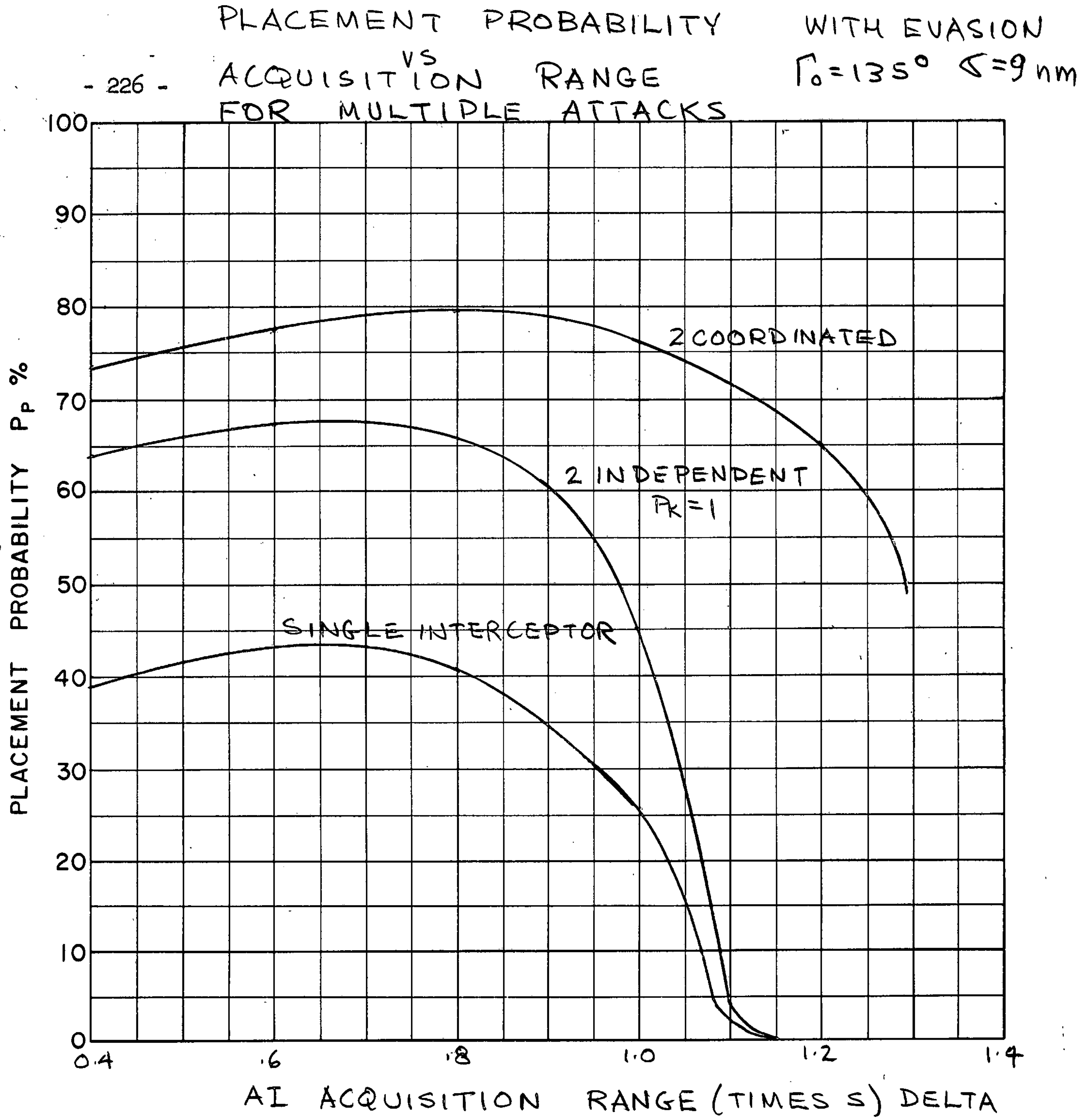

COURSE DIFFERENCE: $\Gamma_0 = 135°$
TARGET EVASION: .75g
TARGET MACH NO.: 2
INTERCEPTOR LATERAL G's:
INTERCEPTOR MACH NO.: 2
σ OF G.C.I. ACCURACY: 9 nm
A.I. DETECTION RANGE AS FRACTION OF SPECIFICATION RANGE, S: VARIABLE
A.I. DETECTION RANGE CONTOUR:
ALTITUDE: 50 KFT

Figure 10

TABLE 3

Γ_o	σ(nm)	No Evasion			Evasion		
		P_{p1}	P_{p2}	P_{kmin}	P_{p1}	P_{p2}	P_{kmin}
75°	3	.95	1.00	.99	0	0	
	9	.49	.81	.71	0		
110°	3	1.00	1.00	1.00	0	.66	-00
	9	.81	.99	.96	0	.25	-00
135°	3	1.00	1.00	1.00	.65	.98	.76
	9	.84	.99	.98	.27	.79	-3.4
180°	3	1.00	1.00	1.00	.92	.90	1.11
	9	.82	1.00	.95	.44	.80	.41

5.0 DISCUSSION

For a non-evading target with a given placement zone it has been shown that if two interceptors can be sent into the zone such that both pass through the intersections of the actual AI acquisition contour and the edges of the placement zone, the combined probability of success will be higher, in general, than that for two interceptors sent independently against the same target. This increase in the probability is higher for larger values of the standard deviation of ground control error. If the two interceptors pass either inside or outside of the intersections of the AI contour and the edges of the placement zone, the placement probability may decrease to a value lower than that for the combined placement probability of two independent interceptors. No account has been taken of the difficulties involved in the second interceptor's aligning itself in the coordinated-interceptor attack. If this be at all difficult, there is little to gain in a coordinated, two-interceptor attack over an independent, two-interceptor attack. No account has also been taken of traffic problems after lock-on has occurred. These would presumably be more difficult for the coordinated attack.

In the case of the evading target under certain conditions, there may be considerable increase in placement probability for the coordinated attack over the independent attack. This increase in placement probability appears to be larger in the cases with large values of standard deviation of ground control accuracy and smaller angles of initial course difference. Any added difficulties of performing the two-interceptor, coordinated attack would of course have to be countered against this increase.

In the calculations of the placement probabilities with target evasion the interceptors were in each case first arranged to give maximum placement probability with no evasion. Further increases in placement probability may be achieved if the interceptors be arranged to give maximum placement probability with evasion. However, in certain cases this procedure may seriously reduce the placement probability for no evasion.

6.0 CONCLUSIONS

It may be concluded that in general the two-interceptor coordinated attack is very little better than a two interceptor independent attack unless the probability of kill after lock-on P_k is very close to unity. In particular cases of a high speed evading target, the correlated attack may offer some improvement but two factors must be borne in mind.

(a) Other methods of defeating evading targets exist e.g. head-on attack with lock-on delay.

(b) Difficulty of implementing coordination are considerable and have not been considered here.

7.0 REFERENCES

1. CARDE Tech. Letter N-47-18 "Third Progress Report on CF 105 Weapon System Assessment" (SECRET)

2. Memorandum Morley to Wilson CARDES 9736-21 - 9th December 1957.

3. Memorandum Morley to Wilson CARDES 9736-21 - 10 January 1958.

4. Memorandum Analysis Group to Wilson CARDES 9736-21 - 9 Oct. 1957.

5. The CF 105 Assessment Study Summary Report 1 CARDE Technical Memorandum No. 150/57 (SECRET).

APPENDIX 'G'

RANGE FINDING METHODS

by F.W. Slingerland and C.J. Wilson

1.0 INTRODUCTION

This appendix contains two self-explanatory sections on aspects of missile launch range determination under E.C.M. conditions. It is assumed that a homing on the jammer navigational mode can be used which gives suitable interceptor heading in the launch zone region and that only range information is required to ensure successful launch.

The reader should consult the references for more complete background information. Appendix 'B' of this report contains the results of work on possible modes of navigation and also indicates how range information would be used.

2.0 MEASUREMENTS ON ANGULAR RATE NOISE IN THE APG40 RADAR

2.1 In Progress Reports 2 and 4 there have been discussions (refs. 1, 2) of the feasibility of obtaining range information on a jammer by executing programmed fighter maneuvers. The equation used is:

$$R\omega = V_F \sin \theta - V_T \sin A$$

where $V_T \sin A$ is approximated by $V_F \sin \theta_{PC}$ when the fighter is on a pure collision course, and

where ω = angular rate of the line of sight

θ = angle between fighter velocity vector and the line of sight, and

A = angle between target velocity vector and the line of sight.

The practicability of this method of range finding is critically dependent on the ability to measure accurately small ω's in the order of 1 to 5 mils/sec.

2.2 It was noted in reference 2 that if the fighter executed periodic turns on either side of a collision course, the noisy ω signal could be considerably improved by multiplying it by a unit square-wave function with period equal to the maneuver period. Integration of the resulting ω

function over integral numbers of half cycles greatly reduce the higher frequency components of ω noise, leaving the ω signal itself unchanged. However, no information was available on the amount of ω noise to be expected in a conically-scanning-pulsed radar when angle tracking a point target such as a jammer.

2.3 A contract was left with de Havilland Aircraft of Canada for angular noise measurements on an APG40 radar. A small corner reflector was set-up at a range of several hundred yards and surrounded with absorbent material to nullify extraneous reflections. The APG40 was locked on to the reflector which was then driven by a Scotch yoke drive so as to execute sinusoidul motion at frequencies of $\frac{1}{16\pi}$, $\frac{1}{8\pi}$, $\frac{1}{4\pi}$, $\frac{1}{2\pi}$ cycles per second. The output of the azimuth rate gyro was fed to a recorder, and the recorder trace was then integrated by a planimeter over periods of 1/2, 1 and 2 cycles and multiplied by a unit square wave. Each case was repeated 20 times. The results are shown in the following Table 1. σ in the following table is the rms. deviation from the mean reading.

TABLE I

APG40 Measurements of an Angular Rate

of 0.6 mils/sec.

Freq.	No. of Cycles	Average ω Max.	σ
	1/2	0.586 mil/sec	0.0338 mil/sec
$1/16\pi$	1	0.586	0.0349
	2	0.586	0.0212
	1/2	0.667	0.0510
$1/8\pi$	1	0.660	0.0414
	2	0.661	0.0298
	1/2	0.518	0.1061
$1/4\pi$	1	0.514	0.0873
	2	0.503	0.0648
	1/2	0.547	0.2269
$1/2\pi$	1	0.568	0.1808
	2	0.542	0.0861

Further measurements at ω's of 1.2 and 2.4 mils/sec are being made and will be reported later. The results show surprisingly good performance for a radar whose quoted ω accuracy is 1 mil/sec. It is noted in ref. 3 that the minimum measurable ω is approximately 2 mils/sec. for the Astra I. It is likely that a similar improvement in ω accuracy would result from application of square-wave filtering to Astra I's ω signals. This would result in greater range finding accuracy or in less severe maneuvers for the same range finding accuracy.

2.4 The de Havilland results do not include certain errors which would be present in an actual system:

(i) The square-wave must be phased precisely with the ω signal. This requires that it should be reversed in sign at the maximum bank angle when $\omega = 0$ and it may be difficult to sense this instant precisely.

(ii) Radome aberration errors will be in the order of 4 mils and this will introduce large error signals as the aircraft banks, which may not be rejected by the square-wave filter.

(iii) Rolling and pitching movements of the aircraft during maneuver will be coupled to the angular rate measurements due to imperfect angle tracking response and roll resolution.

(iv) Since only the one-way gain characteristic of the antenna is being utilized in angle tracking, the presence of multiple jamming targets will introduce considerable angular rate noise at long ranges.

However, it should be borne in mind that launch ranging errors of up to 30% can be tolerated by the Sparrow II. Hence maneuver ranging appears to be a feasible tactic worthy of hardware investigation.

2.5 Other methods of range finding are envisaged using integrating accelerometers to measure the lateral deviation from the collision course during the maneuver. This deviation forms a base line which can be used with the resulting lead angles to triangulate range. However, it appears that the base line lengths which are achievable are relatively short, and would require high angular accuracy (in the order of 1 mil) for successful triangulation. A more practicable system would be to measure the convergence angle subtended by the base line by means of integrating angular rate gyros. In this case, lead angle would be used only to obtain the base line component at right angles to the line of sight. Longitudinal accelerations could also be used to provide a triangulation base line, but the deceleration - acceleration period would be considerably longer for the same base line length than the lateral acceleration period.

3.0 THE DISTRIBUTION OF MISSILE LAUNCH RANGES

The $R/\dot{R}$ method of estimating a suitable missile launch time has been proposed and studied at CARDE (refs. 4 and 5). In analysing the effectiveness of the method it was assumed that there would be errors in the measured $R/\dot{R}$ which would be normally distributed about the true $R/\dot{R}$

value over a number of similar attacks but that the error would be constant during any particular attack. Thus, for a particular set of attacks the missile firing points would be normally distributed about the chosen firing point; this property has been used to determine the proportion of attacks where the missile would be successfully launched between the correct range limits.

There is, in fact, only a very limited knowledge of the true distribution of errors to be expected and consequently two different values for standard deviation of error were considered. It was also felt that it might be more realistic, though more difficult, to consider time varying errors rather than constant errors. The remainder of this section describes the effects which can be caused by time-varying errors, summarising the results of an analysis which is given more fully in ref. 6.

Assumptions still have to be made about the form of the noise (or time-varying error). The errors in $R/\dot{R}$ were still assumed to be normally distributed about the actual value and the form of the noise distribution was assumed to be stationary in time.

Figure G1 shows how $R/\dot{R}$ may vary with time during some particular attack. Firing occurs at the time when the measured $R/\dot{R}$ first equals $R/\dot{R}$ launch.

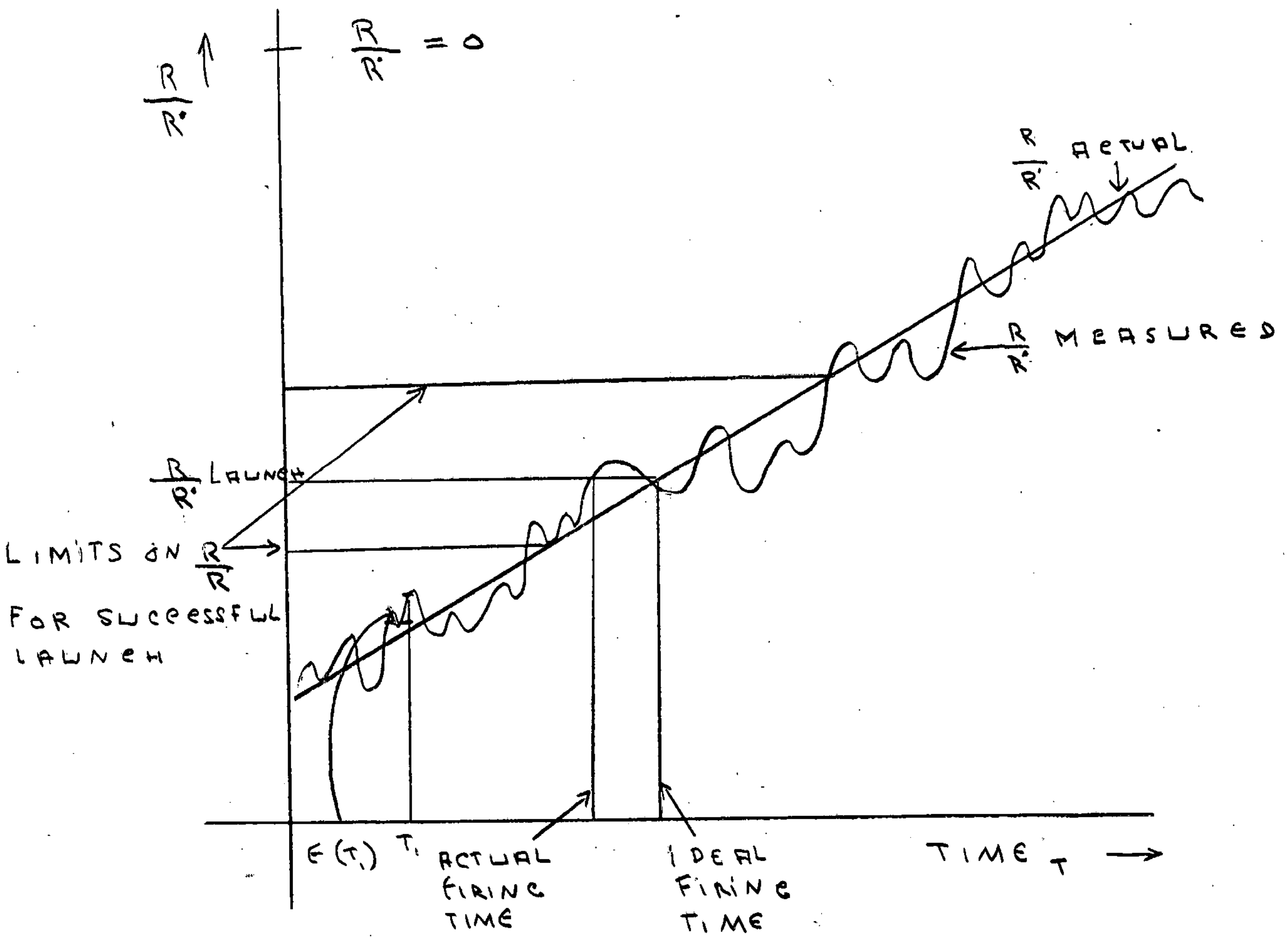

Figure G1

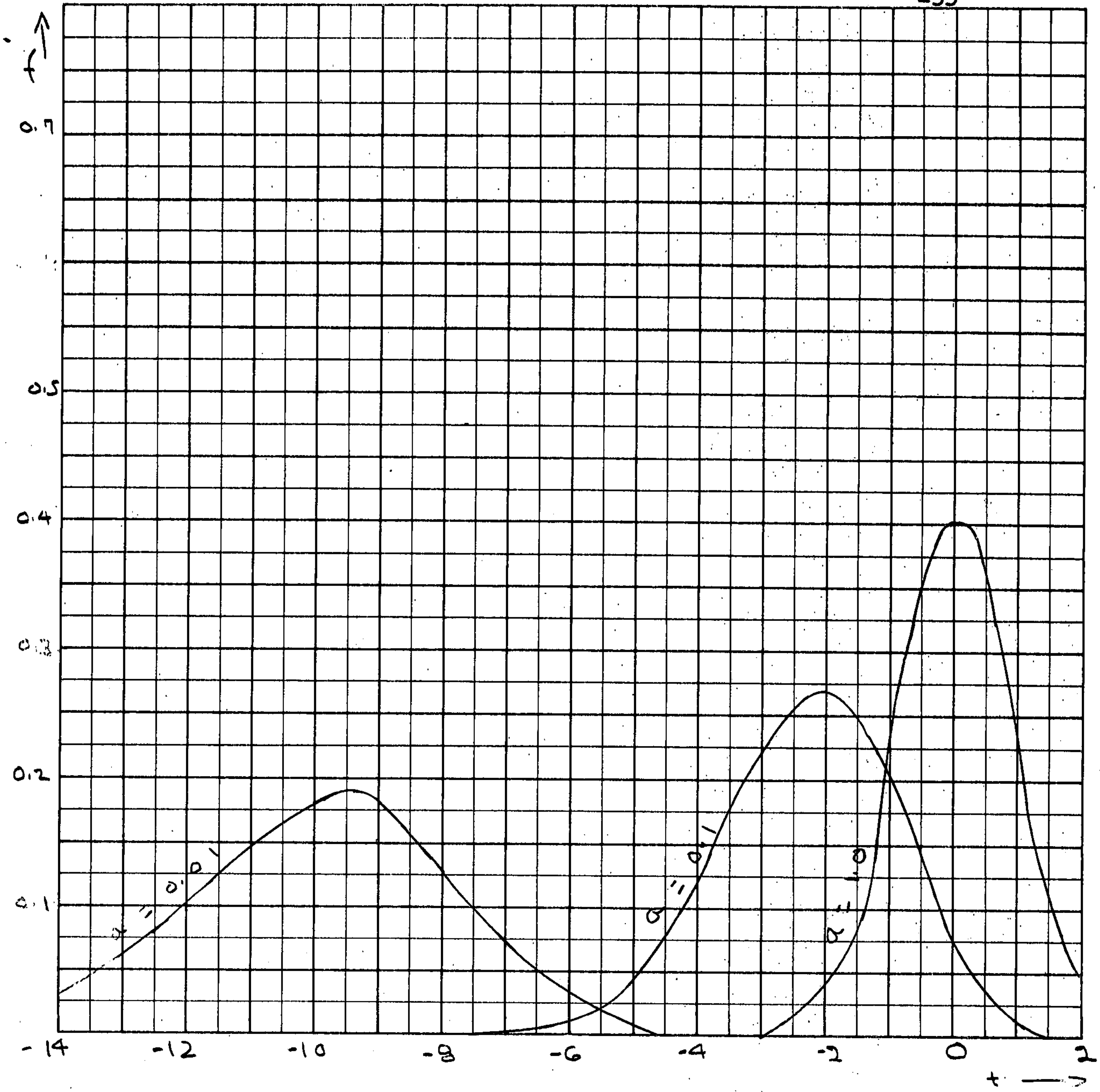

Figure G2

Figure G2 shows three possible distributions of firing point in time, the "ideal" or chosen firing time occurring at t = 0. The noise was assumed to have the same constant spectral density in each case, the bandwidth of the noise, from zero up to its cut-off frequency, being varied.

For a = 1.0 the bandwidth was small and the distribution is almost normal. This gives a very close approximation to the result obtained with the assumption of errors constant in time.

For a = 0.1 the noise bandwidth was 4.64 times the bandwidth for a = 1.0.

For a = 0.01 the noise bandwidth was 21.54 times the bandwidth for a = 1.0.

It is evident that the standard deviation of launching times about the mean increases with the noise bandwidth and that the mean occurs earlier in time as the bandwidth increases. The distributions become slightly skew but do not depart sufficiently from the normal distribution to modify the results of the minimum information study if the value of $R/\dot{R}$ launch is changed to accommodate the displacement of the mean from t = 0 in such a way that the distribution still lies symmetrically between the missile launch range limits. This compensation would have to include correction for any filter or other time delays in the system.

The analysis has been carried only to the point of showing that the assumption of constant errors which was used in obtaining placement probabilities in the minimum information study leads to the correct results. To implement an actual missile firing system would require more complete analysis to obtain optimum results, but at the same time more complete information would be available.

4.0 REFERENCES

1. "A Study of a Range-Finding Proposal in the Two Dimensions" D. Ferguson, CARDE T.L. N-47-12 (SECRET).

2. "A Study of Range-Finding by Manoeuvre" D.P. Flemming, CARDE T.L. 1012/57 (SECRET).

3. "Summary of Progress and Program of Work on a Range Computing System" E.B. Capen, RCA/ASL Report No. 588-SP7-PR211 (SECRET).

4. CARDE Tech. Letter 1012/57, Appendix 'G', Section 2.0

5. CARDE Tech. Letter 1091/58, Appendix 'B'.

6. Internal Memorandum on file CARDES 9736-21, Wilson to Slingerland, dated 25th February 1958.

DISTRIBUTION

No. of Copies	
1	Chief Supt. & Dep/Chief Supt.
1	Supt. Systems Wing
1	Supt. Aerophysics Wing
1	Supt. Explosives Wing
1	Supt. Electronics Wing
1	Supt. Mechanics Wing
1	OC, CEPE CARDE RCAF Detachment
5	Document Library
1	Author
1	R.S. Mitchell
1	J.T. MacFarlane
1	F.W. Slingerland
1	Dr. W.J. Surtees
1	C.R. Iverson
1	G.A. Morley
2	DSIS
6	DRB, HQ: to include
	2 - DWR
	1 - Ch. of Estab.
	1 - Ch. Scientist
	1 - D Eng R
	1 - D Phys R
1	Director/NAE
1	S/ORG
3	C/S DRTE to include
	1 - S/DRTE EL
	1 - S/DRTE RPL
2	DRM London
2	DRM Washington
1	DRB Liaison Officer-Lincoln Lab MIT
2	RCAF HQ: Attn. COR/DSE
3	Attn. C Arm E
1	Attn. SACAS
7	Attn. S/L Peek to be forwarded to -
	2 - TSO, RCA Camden N.J.
	2 - RCA Airborne Systems Lab., Waltham Mass. Attn. Mr. Daelhousen

#303331

UNCLASSIFIED